The geology and petrology of the pre-camhrian basement between Sirdal and Åseral, Vest Agder, Norway

Leake, R. C.

DGF - Aarhus

FORÅRSMØDE lørdag den 28. april 1973, Geologisk Institut.

Tema: Studier i Prækambrisk geologi

Formiddag: Syd-Norge

9.00-9.25 T. Falkum: Oversigt over Prekambrium indenfor kortbladet Mandal (1:250.000).

9.25-9.50 J.R. Wilson og M.P. Annis: Granites near Farsund.

9.50-10.10 J. Sten Pedersen: En geometrisk analyse af et polyfasefoldet område.

10.10-10.35 Kaffepause

10.35-10.55 R. Pontoppidan Petersen: En intrusiv pre-synkinematisk granit.

10.55-11.15 J.A. MacFadyen: The possible occurrence of Telemark supracrustal rocks in the Austad area.

11.15-11.35 H. Carstens: Om underafkøling af magmaer.

11.35-12.00 S. Pedersen: Den sveconorwegiske magmatiske periode i det nordlige Iveland - Evje område.

12.00-13.30 Frokostpause

Eftermiddag: Grønland

13.30-14.15 D. Bridgwater: The relations between the central Archean gneiss block and the surrounding proterozoic mobile belts.

14.15-14.40 K. Sørensen: Metadoleriter anvendt ved tolkningen af metamorfose og deformation i Nagssugtoqiderne.

14.40-15.10 Kaffepause

15.10-15.35 J. Bak: Strukturer i Agto-området

15.35-16.00 J. Korstgaard: Bjergarter i Inugsuk-området og deres oprindelse.

ABSTRAKTER:

Formiddag: Syd Norge

T. FALKUM: Oversigt over Prækambrium inden for kortblad Mandal (1: 250 000)

Som en introduktion til geologien i Syd Norges Prækambrium gives en oversigt over en lithostrukturel sekvens samt dennes strukturelle udvikling og metamorfose. Endvidere behandles de magmatiske intrusioner specielt med henblik på kronologisk udvikling.

J.R. WILSON & M.P. ANNIS: Granites near Farsund

A group study in progress of the granitic rocks of the Farsund area has shown that there are three distinct plutons - a dark charnockite, a light hornblende granite and a light biotite granite. These were previously considered to be a single body.

JON STEEN PETERSEN: En geometrisk analyse af et polyfase foldet område

Det strukturelle billede af et foldet, højmetamorft grundfjeldsområde ved Lyngdal, Syd Norge, hvori indgår mindst 4 makroskopiske foldefaser, præsenteres. På grundlag af en geometrisk analyse af dette antydes en kinematisk udvikling, der omfatter såvel homogen som heterogen deformation.

RENE PONTOPPIDAN PETERSEN: En intrusiv præ-synekinematisk granit.

På grundlag af feltobservationer på en granit i Bjelland-området diskuteres:

a) at granitlegemet kan tænkes at være intruderet ved en passiv intrusionsmekanisme
b) at graniten har været udsat for en kraftig deformation samtidig eller senere end granitens intrudering.

Eftermiddag: Grønland

D. BRIDGWATER: The relations between the central Archean gneiss block of Greenland and the surrounding proterozoic mobile belts

KAI SØRENSEN: Metadoleritter anvendt ved tolkning og deformation i Nagssugtoqiderne

Metamorfosen i store dele af Nagssugtoqiderne "balancerer" på grænsen mellem amfibolit- og granulitfacies. De metamorfe reaktioner, der definerer denne grænse afspejles tydeligst i basiske bjergarter. Manglende ligevægt gør det muligt at påvise reaktionernes retning og anvende dette resultat på den metamorfe historie.

Med kendskab til to gangretningers orientering før og efter deformation er det muligt at beregne deformationen forudsat, denne er homogen. Denne beregning for Nagssugtoqidernes sydgrænse demonstreres og diskuteres.

JENS BAK: Strukturer i Agto-området

Strukturelt næsten homogene parallel-bælter veksler med områder med komplicerede interferensfigurer og stærkt varierende foldeakser.

De to "strukturtyper" sammenlignes geometrisk og diskuteres i relation til homogen deformation.

JOHN KORSTGÅRD: Bjergarter i Inugsuk-området og deres oprindelse

Bjergarter i Inugsuk-området er hovedsagelig granulit-facies gnejser af varierende sammensætning. Granat-sillimanit-førende gnejsers oprindelse synes klart sedimentær. For hypersten- og biotitgnejser foreslås udfra zirkonstudier ligeledes en sedimentær oprindelse. Statistiske zirkonstudier peger i retning af, at hypersten-gnejser og biotit-gnejser har forskelligt sedimentært udgangsmateriale.

J.A. MACFADYEN: The possible occurrence of Telemark supra crustal rocks in the Austad area

In the pre Cambrian of the Austad area of southern Norway an apparently older granite gneiss is overlain by a younger banded gneiss and granite gneiss sequence. Evidence is presented suggesting that this younger sequence may be the correlative of the Telemark supra crustal complex.

H. CARSTENS: Om underafkøling af magmaer

Underkjøling i overflatenære magmaer er en meget viktig faktor som kontrollere både nukleasjon og vekst-mekanismen og derfor morfologien av det endelige krystallisasjonsprodukt. Eksempler er hentet fra permiske ganger (dykes) i Det Syd-norske grunnfjell.

SVEND PEDERSEN: Den sveconorwegiske magmatiske periode i det nordlige Iveland-Evjeområde

I det nordlige Iveland - Evjeområde kan der skelnes mellem to forskellige bjergartsgrupper, de regionale amfibolitfaciesgnejser og de yngre intrusiver (amphibolit - monzonit/granit - aplit/pegmatit). Disse sidste regnes for at være intruderet under den sveconorwegiske magmatiske periode.

Radiometriske aldersbestemmelser af granit og monzonit giver Rb/Sr - bjergartsaldre på 1038 m.å. En K/Ar alder på biotit fra graniten giver 845 m.å. Strontiumisotopforholdene viser, at bjergarterne efter alt at dømme er genereret fra kappen.

A

Thesis

entitled

The Geology and Petrology of the Pre-Cambrian Basement between Sirdal and Åseral, Vest Agder, Norway.

submitted for the degree

of

Doctor of Philosophy

at the

University of Durham

by

R.C.Leake

June 1972.

ABSTRACT.

The field relations and petrography of the rocks of the PreCambrian basement complex between Sirdal and Aseral, comprising two series of high-grade metamorphic gneisses separated by a structural discontinuity, syntectonic granites, intrusive quartz monzonites with thermal metamorphic aureoles and basic dykes, are described. During orogeny the gneisses were subjected to intense poly-phase deformation, three regional and two localised phases of which have been recognised. Minor fold relics within augen gneiss in the lower gneiss sequence suggest that this rock was involved in earlier deformation. The climax of metamorphic crystallisation occurred at the low-pressure granulite facies-amphibolite facies boundary with mineral parageneses corresponding closely with the sillimanite-cordierite-orthoclase subfacies of the Abukuma-type cordierite amphibolite facies except for the additional occurrence of orthopyroxene.

Major and trace-element X.R.F. analyses of gneissic and some igneous rocks are presented. These data reveal significant differences between basic rocks of the two gneiss series, basic gneisses with different mineral assemblages and to a lesser extent different lithostatigraphical units in the upper gneiss series.

Electron microprobe analyses of alkali feldspar, plagioclase, biotite, hornblende, clinopyroxenes, orthopyroxene,

sphene, magnetite, ilmenite, chlorite, and garnet from several rock types are presented. With the exceptions of alkali feldspar, magnetite and ilmenite all minerals are chemically homogeneous and represent original equilibrium compositions. The chemical inhomogeneity of alkali feldspar resulted from post-crystallisation leaching and redistribution of alkalies, resistance to which is related to grain size. Equilibrium during original feldspar crystallisation is indicated by the restricted composition of plagioclase coexisting with alkali feldspar.

The distribution of titanium and magnesium between coexisting silicates indicates equilibrium compositions, influenced by oxygen fugacity, the nature of the coexisting iron oxides and the tetrahedral aluminium content of the hydrous phases in addition to the rock composition. The application of several means of multicomponent paragenesis analysis reveals that the various mineral assemblages can be interpreted in terms of variations in major element rock composition and oxygen fugacity.

The widespread molybdenite mineralisation is considered to have been transported from depth in siliceous hydrothermal solutions into the gneisses, especially where the strike of the gneissic layering coincided with deep fractures. Fixing of the metal as sulphide occurred particularly in the vicinity of pre-existing fahlband sulphide due to release of sulphur in the local environment of increased oxygen fugacity.

TABLE OF CONTENTS.

	Page.
Abstract.	I
List of maps.	IX
List of plates.	X
List of figures.	XIII
List of tables.	XIX
1. Introduction	1.
a) Geographical location and accessibility	1.
b) Topography and exposure	2.
c) Glacial geology	3.
d) Previous research	4.
e) Regional geological setting	6.
f) Age	9.
2. The Sirdalsvatn Series	11.
a) The Feda augen gneiss	11.
b) The Tonstad layered feldspathic gneiss	14.
c) Basic gneisses within the Sirdalsvatn Series	15.
3. The Flekkefjord Series	17.
a) The Lervig gneiss	18.
b) The Øie gneiss	24.
c) The Lande gneiss	25.
d) The Kvinesdal gneiss	30.
e) The Knaben gneiss	31.
f) The Flofjell gneiss	33.
g) The Oddevassheii gneiss	34.
h) Gneisses to the east of the Ljosland intrusion	36.

4. The syntectonic granites 37.

a) The porphyritic gneissic granites 37.

b) The equigranular granite 38.

5. The discordant quartz monzonite intrusions 40.

6. The basic dykes. 47.

a) Amphibolite dykes exhibiting regional mineral orientation. 47.

b) Impersistent and lensoid metamorphic dykes 48.

c) Persistent dykes with metamorphic mineral assemblages. 49.

d) Persistent dykes with igneous texture and mineralogy. 50.

7. The Structure. 54.

a) Unit 1a. 55.

b) Unit 1b. 57.

c) Unit 1c. 58.

d) Unit 2a. 60.

e) Unit 2b. 61.

f) Unit 2c. 63.

g) Unit 3a. 64.

h) Unit 3b. 64.

i) Unit 4a. 65.

j) Unit 4b. 67.

k) Unit 5a. 68.

l) Unit 5b. 69.

m) Unit 5c. 69.

n) Unit 6a 70.

o) Unit 6b 71.

p) Structural synthesis and history of deformation 71.

8. Brittle deformation and retrograde metamorphism 78.

a) Early healed faults 78.

b) Mylonites 79.

c) Retrograde metamorphism 80.

d) Linear fractures and associated retrograde metamorphism. 83.

9. The molybdenite and other sulphide mineralisation 86.

a) Description of mineralisation 86.

1) Sulphides impregnated in layered and basic gneisses. 87.

2) Molybdenite associated with small quartz veins in layers and rafts of fahlband gneiss within phenoblastic granitic gneiss. 87.

3) Molybdenite associated with thick but impersistent quartz veins at the contacts of massive amphibolite horizons. 88.

4) Molybdenite and chalcopyrite associated with thin quartz veins, pegmatite and granular leucogranite layers within layered phenoblastic granitic gneiss. 89.

5) Molybdenite with a little pyrite and chalcopyrite associated with quartz and

pegmatite within faintly-layered phenoblastic granitic gneiss. 90.

6) Molybdenite associated with quartz and plagioclase-rich veins in basic gneiss. 90.

7) Molybdenite associated with discordant pegmatite veins. 91.

8) The mineralisation in the Knaben 2 workings. 92.

9) Discordant quartz chalcopyrite veins 93.

b) Sulphide textures and relationships 94.

c) Regional setting and origin of sulphide mineralisation. 96.

10. The chemistry and origin of the granitic gneisses. 103.

11. The chemistry and origin of the Feda augen gneiss. 107.

12. The chemistry of the intermediate, basic and garnet-bearing gneisses 110.

a) Biotite-hornblende gneisses with intermediate silica contents. 110.

b) Biotite-clinopyroxene gneisses 111.

c) Amphibolites. 112.

d) Pyribolites. 112.

e) Garnetiferous gneisses. 113.

f) Oxidation ratios of the intermediate and basic gneisses. 114.

g) Trace element chemistry. 115.

13. Mineral chemistry.

a) Alkali feldspar. 122.

b) Plagioclase. 126.

13. c) Biotite 127.

d) Hornblende 129.

e) Clinopyroxene 132.

f) Orthopyroxene 133.

g) Other silicates 134.

h) Oxide minerals. 135.

14. The distribution of elements between coexisting minerals. 137.

15. The analysis of mineral parageneses. 143.

16. Summary. 156.

Appendix. 162.

a) Rock chemical analysis. 162.

b) Mineral chemical analysis. 164.

1. Alkali feldspar 164.

2. Plagioclase 165.

3. Mafic minerals. 165.

c) The instrumental precision of electron microprobe analysis 166.

d) The variation in composition of minerals within a single rock specimen 167.

1. Alkali feldspar 168.

2. Plagioclase 169.

3. Mafic minerals 171.

e) Accuracy of mineral analyses. 172.

1. Alkali feldspar 174.

2. Plagioclase 175.

3. Orthopyroxene. 176.

16. 4. Clinopyroxene 177.

5. Sphene 178.

6. Biotite 179.

7. Hornblende 181.

8. Chlorite and garnet 182.

References 183.

Acknowledgements. 198.

LIST OF MAPS. (In folder)

1. Geological map of the area between Sirdal and Åseral, Vest Agder, Norway, scale 1:50,000.

2. Structural map of the area between Sirdal and Åseral, scale 1:100,000.

3. Section illustrating major features of structure.

4. Map of distribution of molybdenite and other sulphide mineralisation in area between Sirdal and Åseral, scale 1:100,000.

LIST OF PLATES.

		After page.
1.	Topographical map, scale 1:250,000, showing boundary of area surveyed.	(Folder)
2.	a) View up Sirdalsvatn from south showing joint and foliation controlled slopes.	
	b) The high plateau from Grungevasskmuten.	2.
3.	a) Flå end moraine from east slope of Anneliknuten, near Sandvatn.	
	b) Exposure of Feda augen gneiss.	3.
4.	Map, scale 1:500,000, showing geological setting of area surveyed.	7.
5.	a) Exposure showing complex relationship between Feda augen gneiss and granular leucogranite.	
	b) Healed fault separating contrasting facies of the Tonstad gneiss.	13.
6.	a) Photomicrograph in reflected light showing three size generations of exsolved hematite in ilmenite.	
	b) Photomicrograph of garnet-cordierite gneiss from Lervig gneiss.	15.

7. a) Exposure of feldspathic Lande gneiss with some basic horizons.
b) Exposure of layered basic gneiss from Lande gneiss. 27.

8. a) Exposure of deformed augen gneiss at top of Lande gneiss.
b) Photomicrograph of pyribolite from Lande gneiss. 27.

9. a) Photomicrograph of amphibolite from Lande gneiss.
b) Photomicrograph of granitic gneiss from Kvinesdal gneiss. 28.

10. a) Photomicrograph of pyribolite from contact aureole of Ljosland intrusion.
b) Exposure showing basic gneiss inclusion in Ljosland quartz monzonite. 36.

11. a) Photomicrograph of basic igneous dyke from Knabedalen.
b) Contact of basic igneous dyke and country granitic gneiss. 50.

12. Minor structures in Sirdalsvatn Series. 54.

13. Minor structures in Lervig gneiss. 61.

14. Minor structures in Lande gneiss. 66.

15. a) Photomicrograph of piemontite-bearing rock from retrograded Lande gneiss.
b) Photomicrograph of fluorite within biotite from Lande gneiss. 80.

LIST OF FIGURES.

	After page
1. Normative quartz, albite and orthoclase for analysed intrusive quartz monzonite samples.	44.
2. Total iron, magnesium and total alkalies diagram for analysed intrusive quartz monzonite samples	44.
3. Variation in silica and total alkali contents of basic dykes compared with other dykes of South Norway.	52.
4. Stereogram showing distribution of poles to foliation in tectonic subunits 1a & 1b.	57.
5. Stereogram showing distribution of poles to foliation in tectonic subunits 1c & 2a.	58.
6. Stereogram showing distribution of lineations in tectonic unit 1 & subunit 2a.	60.
7. Stereogram showing distribution of poles to foliation in tectonic subunits 2b & 2c	62.
8. Stereogram showing distribution of lineations in tectonic subunits 2b & 2c.	62.
9. Stereogram showing distribution of poles to foliation in tectonic subunits 3a & 3b.	64.
10. Stereogram showing distribution of lineations in tectonic units 3 & 4.	65.
11. Stereogram showing distribution of poles to foliation in tectonic subunits 4a & 4b.	66.
12. Stereogram showing distribution of poles to foliation in tectonic subunits 5a & 5b.	68.

13. Stereogram showing distribution of poles to foliation in tectonic subunits 5c & 6a. 70.

14. Stereogram showing distribution of lineations in tectonic units 5 & 6. 70.

15. Stereogram showing distribution of poles to foliation in tectonic subunit 6b. 71.

16. Normative quartz, albite, orthoclase and albite, orthoclase, anorthite for analysed metamorphic granitic rocks. 103.

17. Sodium and potassium contents of analysed metamorphic granitic rocks 103.

18. Variation of potassium to potassium plus sodium against magnesium to magnesium plus iron in gneissic rocks with intermediate silica contents. 110.

19. Niggli mg against c plot for analysed amphibolites and gneisses with intermediate silica contents. 111.

20. The relationship between titanium to total iron and manganese to total iron in analysed basic and intermediate gneisses. 111.

21. The relationship between the rock zinc to iron ratio and the biotite content in analysed basic and intermediate gneisses. 117.

22. Factor analysis; loadings for 15 element and ratio variables in terms of first two factors. 119.

23. Histogram of electron microprobe potassium determinations in alkali feldspar from Feda augen gneiss specimen. 122.

24. Relationship between the titanium content and negative charge balance in probe analysed biotites. 128.

25. Variation in tetrahedral aluminium and alkali contents of probe analysed amphiboles. 129.

26. Variation in titanium and total alkali content of analysed amphiboles compared with N.W. Adirondack hornblendes. 131.

27. Relationship between titanium content and negative charge balance in probe analysed amphiboles. 132.

28. Variation in titanium and iron contents of probe analysed ilmenites with the rock oxidation ratio. 136.

29. The distribution of titanium between biotite and hornblende. 138.

30. Relationship between the atomic fraction of titanium in the y site to the iron content of probe analysed biotites. 138.

31. The relationship between the sodium content of hornblende and the distribution coefficient of titanium between biotite and hornblende. 138.

32. The distribution of magnesium between hornblende and clinopyroxene. 139.

33. The distribution of magnesium between hornblende and orthopyroxene. 139.

34. The relationship between the distribution coefficient of magnesium between hornblende and clinopyroxene and the rock oxidation ratio. 139.

35. The composition in terms of calcium, magnesium and iron of coexisting clinopyroxenes and orthopyroxenes. 139.

36. The distribution of magnesium between biotite and orthopyroxene. 140.

37. The distribution of magnesium between biotite and clinopyroxene. 141.

38. The relationship between the distribution coefficient of magnesium between biotite and clinopyroxene in pyribolites and the tetrahedral aluminium content of the biotite. 141.

39. The distribution of magnesium between biotite and hornblende. 141.

40. The relationship between the distribution coefficient of magnesium between biotite and hornblende and the ratio of their tetrahedral aluminium contents. 142.

41. A C F & A'K F diagrams of the sillimanite-cordieite-orthoclase-almandine subfacies of the Abukuma type cordierite amphibolite facies. 143.

42. Projection of the Al,Ca,Fe,Mg tetrahedron through the anorthite composition onto a plane passing through Fe and Mg and parallel to the line joining Al and Ca. 144.

43. The composition of coexisting orthopyroxene, clinopyroxene and hornblende on the above projection. 144.

44. The composition of coexisting orthopyroxene, clinopyroxene and hornblende from the Granite Falls-Montevideo area, Minnesota (data from Himmelberg and Phinney 1967) on the above projection. 145.

45. The composition of coexisting orthopyroxene, clinopyroxene and hornblende from the Colton area, N.W. Adirondacks, New York (data from Engel,Engel & Havens 1964) on the above projection. 145.

46. The role of aluminium as a phase determining component illustrated by a Na+K+2Ca/Al against Fe+Mg/Al diagram. 145.

47. The relationship between the magnesium content of biotite the rock oxidation ratio. 150.

48. Comparison of wet chemical and X.R.F. determinations of iron in rocks. 163.

49. Calibration for the determination of potassium in alkali feldspar using the electron microprobe. 164.

50. Calibration for the determination of sodium in alkali feldspar using the electron microprobe. 164.

51. Calibrations for the determination of calcium and sodium in plagioclase using the electron microprobe. 165.

52. Calibration for the determination of silicon and aluminium in plagioclase using the electron microprobe. 165.

53. Variation in the composition of plagioclase grains within the same rock section as determined by electron microprobe and optically. 170.

54. Histogram of alkali feldspar molecule totals. 175.

LIST OF TABLES. (In appendix)

1. X.R.F. analyses of intrusive quartz monzonites and kindred rocks.

2. X.R.F. analyses of basic dykes.

3. Electron Probe analyses of a garnet and a chlorite.

4. Comparison of analysed retrograded rocks with similar unaltered rocks.

5. X.R.F. analyses of mineralised rocks.

6. X.R.F. analyses of granitic rocks of the Kvinesdal gneiss.

7. X.R.F. analyses of granular leucogranites.

8. X.R.F. analyses of granitic rocks of the Øie gneiss.

9. X.R.F. analyses of massive and layered Tonstad granitic gneisses.

10. X.R.F. analyses of porphyritic gneissic granites.

11. X.R.F. analyses of assorted granitic rocks.

12. X.R.F. analyses of Feda augen gneiss.

13. X.R.F. analyses of intermediate gneisses of the Lervig and Lande gneisses.

14. X.R.F. analyses of intermediate gneisses within the Kvinesdal gneiss.

15. X.R.F. analyses of intermediate gneisses within and adjacent to the Fjotland granite.

16. X.R.F. analyses of intermediate gneisses within the Sirdalsvatn Series.

17. X.R.F. analyses of biotite-clinopyroxene gneisses.

18. X.R.F. analyses of amphibolites of the Lervig gneiss.

19. X.R.F. analyses of amphibolites of the Lande gneiss.

20. X.R.F. analyses of amphibolites of the Knaben gneiss.

21. X.R.F. analyses of basic gneisses of the Oddevassheii gneiss.

22. X.R.F. analyses of pyribolites.

23. X.R.F. analyses of garnet-bearing gneisses.

24. Oxidation ratios of intermediate and basic gneisses.

25. X.R.F. trace element analyses of rocks from the Sirdalsvatn Series.

26. X.R.F. trace element analyses of rocks from the Lervig gneiss.

27. X.R.F. trace element analyses of rocks from the Lande gneiss.

28. X.R.F. trace element analyses of rocks from the Kvinesdal, Knaben and Oddevassheii gneisses.

29. Electron microprobe analyses of 37 points within a potassium feldspar megacryst from a specimen of the Feda augen gneiss.

30. Electron microprobe analyses of matrix potassium feldspar grains within the same specimen of the Feda augen gneiss.

31. Electron microprobe analyses of potassium feldspar within a further nine rocks.

32. Electron microprobe major element analyses of plagioclase in seven rocks.

33. Electron microprobe partial analyses of plagioclase from 27 rocks.

34. Electron microprobe analyses of biotite from 39 rocks.

35. Electron microprobe analyses of hornblende from 31 rocks.

36. Electron microprobe analyses of clinopyroxene from 15 rocks.

37. Electron microprobe analyses of orthopyroxene from nine rocks.

38. Electron microprobe analyses of sphene from eight rocks.

39. Normative mineral proportions for biotite-clinopyroxene gneisses in the biotite-hornblende eight-dimensional simplex.

40. Normative mineral proportions for biotite-hornblende-clinopyroxene gneisses in the biotite-hornblende eight-dimensional simplex.

41. Normative mineral proportions for pyribolites in the biotite-hornblende eight dimensional simplex.

1. INTRODUCTION

This work was instigated under the auspices of the Telemark Project, initiated by the Geologisk Museum of the University of Oslo to map and elucidate the geology of the accessible areas of the PreCambrian basement complex of Southern Norway. Field work for the present study was carried out during the summers of 1965, 1966 and 1967 and the first year of laboratory work was effected at the Geologisk Museum, Oslo. Subsequent laboratory work was carried out at the Department of Geology, Durham University.

a) Geographical location and accessibility.

The present investigation covers some 1200 square kilometres of the county of Vest Agder, stretching from Sirdalsvatn and Sirdal in the west to Ørevatn, Åseral and Ljoslandsdalen in the east. The northern boundary of the area is a line from the village of Øvre Sirdal to Ljosland and the southern is a broken line from the south end of Sirdalsvatn to the southern extremity of Ørevatn. A topographical map showing the boundaries of the area surveyed, physical features and place names is included as plate (1). The following 1 : 50,000 map sheets were used as bases during mapping :- Sheets 1311 (1) Flekkefjord, 1411 (1V) Haegebostad, 1312 (11) Tonstad, 1412 (111) Fjotland, 1412 (11) Åseral, 1312 (1) Øvre Sirdal and 1412 (1V) Kvifjorden.

Settlement within the area is largely confined to the sheltered valleys except for the community at Knaben which is centred on the molybdenum mine. The whole of the southern part of the area is easily accessible but in the north, as the few roads generally follow the major vallyes, access to some of the remote upland parts is difficult. The mapping of such districts, eg. to the north-east of Knaben, is in consequence imprecise. Aerial photographs on the scale of 1 : 50,000 for the south of the region and 1 : 30,000 for the northern parts were extensively used during the geological mapping.

b) Topography and exposure.

Topographically the area is a plateau, sloping gently southwards towards the coast. Dissection is more pronounced in the south with valleys separated by eminences, often steep-sided but flat-topped, rising to about 600 metres above sea-level. The north is a more uniform upland area with all the summits reaching about 1000 metres above sea-level. The highest point of the area, Skarve, reaches 1041 metres above sea-level and occurs in the extreme north-east. Sirdalsvatn, illustrated in plate (2a), is on the other hand only 53 metres above sea-level. The upland areas are covered with a myriad lakes, some of which are elongated in the direction of the regional gneissic layering, others along crush zones. The major valleys often have precipitous east sides, probably controlled by near vertical joint planes. The slopes of the western sides of the valleys are in contrast more gentle, frequently following

Plate 2.

Plate 2a.

View to north up Sirdalsvatn from near Ersdal. The joint-controlled precipitous east side of the lake contrasts markedly with the gentle slope of the west side, parallel to the regional gneissic-layering.

Plate 2b.

View to north-east from Grungevassnuten, to the west of Kvina mine. Bare rock predominates on this high plateau, particularly where granite gneiss is exposed. In the foreground the gentle eastward dip of the gneissic layering in predominantly granitic Kvinesdal gneiss can be seen.

a

b

Plate 2.

the gneissic layering which in many places dips to the east at about 30°. These features are well developed in the Sira valley and are illustrated in plate (2a).

Extensive forest cover is confined to the main river valleys and the broader areas of lower ground in the south. Pine is common but birch tends to replace it as dominant in the higher valleys. Most of the plateau consists of bare rock interspersed with bog and coarse grasses but in the extreme north, as illustrated in plate (2b), the vegetation becomes scanty. The Ljosland intrusion (see page 40) forms high ground but is extensively covered with dwarf shrubs and other hardy vegetation and contrasts sharply with the almost bare granitic rocks surrounding it to the north and west. Isolated basic gneiss horizons within predominantly granitic gneiss sometimes give rise to lines of more luxuriant vegetation than is prevalent upon the granitic rocks.

c) Glacial Geology.

The great Flå end-moraine, described by Andersen (1960), crosses the south-west edge of the area from west to east. It is well developed on the plateau to the east of Sandvatn, illustrated in plate (3a), where it consists of a hummocky zone some 500 metres wide at about 25 metres above the plateau surface. Here the moraine is composed chiefly of large granitic gneiss boulders.

Plate 3.

Plate 3a.

View to the east from the slopes of Anneliknuten, near Sandvatn, showing Flå end-moraine. The moraine is composed mostly of large rounded boulders of granitic gneiss. Scattered pine trees and coarse grasses cover much of the lower-level plateau top. In the background the wooded ridge is formed of layered basic Lervig gneiss which swings round into the nose of the Sandvatn synform (F 3 age) just south of the moraine.

Plate 3b.

Typical exposure of Feda augen gneiss from edge of Sirdalsvatn near Optedal. The exposure shows various sizes of alkali feldspar megacryst with some degree of parallel orientation and a thin branching sheet of fine-grain granular leucogranite.

a

b

Plate 3.

All the main valleys bear evidence of the recent presence of powerful glaciers, with steep sides, wide and flat floors and hanging tributaries. The most powerful glacier probably occupied Sirdal, excavating the deep basin now filled by Sirdalsvatn. Drift deposits of either sticky clay with abundant boulders or finely laminated sands with fewer rock fragments are plastered along the lower slopes and floors of the major vallyes. The sandy deposits are widely worked for road material. The upland areas are devoid of glacial deposits except for perched boulders but some of the flat rock surfaces have been polished and glacial striations, often orientated roughly north-south, have also been observed.

Narrow steep-sided linear depressions are a significant feature of the plateau physiography. These mark the position of crush zones which according to Holtedahl (1960) have been eroded by the process of nivation, though loose material may also have been plucked out by active ice.

d) Previous research.

The first regional survey of the PreCambrian of Norway was undertaken by Keilhau (1838-1850) and was followed by a more detailed study of the southern Norwegian rocks by Kjerulf (1879). Barth (1936) studied the intrusive bodies of southern Norway, including the anorthosite and associated rocks of the Egersund region and the farsundite of the extreme south coast. Later (1945) he compiled a general geological map of the Pre-Cambrian rocks of

southern Norway in which he showed the distribution of augen gneisses, gneiss-granite, gneisses in general and poorly foliated granite. Some indications of foliation trends and structural lines were also given.

Barth and Dons (1960) stated in a compilation of information concerning the PreCambrian rocks that " the rather highly elevated tracts between Telemark and Rogaland are made up of gneiss and granite, but very little detailed information is at hand." Barth and Reitan (1963) state in a further review that " In the district of central and western Agder, gneissose granite and granitised rocks, often of granodioritic composition, are most common. They strike usually north-south, with steep dips. In some places they are mixed with amphibolites, but in others they are nearly massive (the Holum granite) and are often marked by selvages of augen gneiss which gradually pass into the granite on one side and into darker migmatites and gneisses with bands and schlieren of amphibolite on the other."

In recent years detailed information on some segments of the PreCambrian Telemark gneiss complex has emerged. The Rogaland anorthosites and adjacent gneisses have been extensively studied by P. Michot (1956, 1957 and 1960) and J. Michot (1961). The geology of the Ørsdalen tungsten deposit and its country gneisses, which lie to the north-west of Tonstad, has been described by Heier (1955 and 1956). Early published work from the Telemark Project include a preliminary report on the geology of the country to the west of Sirdalsvatn by Tobi (1965), a similar paper on the

Flekkefjord area by Falkum (1967) and a more detailed account of the Holum granite by Smithson and Barth (1967). A preliminary interpretation of the geology of the present area appeared in abstract in R. Leake (1968). The petrology of the farsundite intrusion has been investigated by Middlemost (1968).

There have been several publications concerned with the molybdenum deposits of the area, in particular those around the present Knaben mine. C. Bugge (1907) was the first to mention these deposits which he classified into two main types, pneumatolytic quartz vein ore and impregnation ore in granite. Falkenberg, in a series of papers (1915,1917,1920 and 1936), concluded that the richest ore in the Knaben area occurred within a one kilometre broad, north-south running zone of older gneiss within granite. Schetelig (1937) in a more detailed account of the ore and associated rocks came to the conclusion that within the Knaben ore zone there was a general association between the molybdenite and thin quartz injections parallel to the foliation of the gneiss and granite. These injections occur within the older gneiss and amphibolites, along the border between these rocks and the younger granite and within the younger granite itself. A more recent comprehensive description of the Knaben and other major molybdenite occurrences has been given by J. Bugge (1963).

e) Regional geological setting.

The PreCambrian rocks of southern Norway have been divided geographically into three units. The south-east series of gneisses

which extends into Sweden is separated from the other PreCambrian rocks by the Oslo graben. West of the Oslo province are two areas of high-grade gneisses which form the Kongsberg-Bamble formation. West of these rocks and separated from them by a mylonite zone is the extensive Telemark-Rogaland province. A series of supracrustal rocks, exceeding 4,000 metres in thickness, is found in Telemark in the central part of the province. These rocks are surrounded by a vast expanse of basement gneisses and granite, stretching westwards through the Agders into Rogaland. The exact relationship between the supracrustals and basement gneisses is as yet imperfectly understood.

The area between Sirdal and Åseral which has been mapped by the present author is situated within the south-west part of the basement gneiss complex of the Telemark-Rogaland province. The immediate general geological setting of the area is illustrated in plate (4) which has been adapted from a map of Sørland geology compiled by Barth (1960). The approximate positions of other nearby areas also mapped by Telemark project geologists are also shown on this map.

The metamorphic rocks of the area which has been studied by the present author are divided into two series, separated by a discontinuity. The most distinctive component of the rocks which form the structurally lower group is an augen gneiss with large alkali feldspar crystals. As this rock is the only major constituent of the lower group of gneisses in the Flekkefjord area, Falkum (1967) has proposed the name ' Feda augen gneiss ' for the whole series. This name is unsuitable for these rocks in

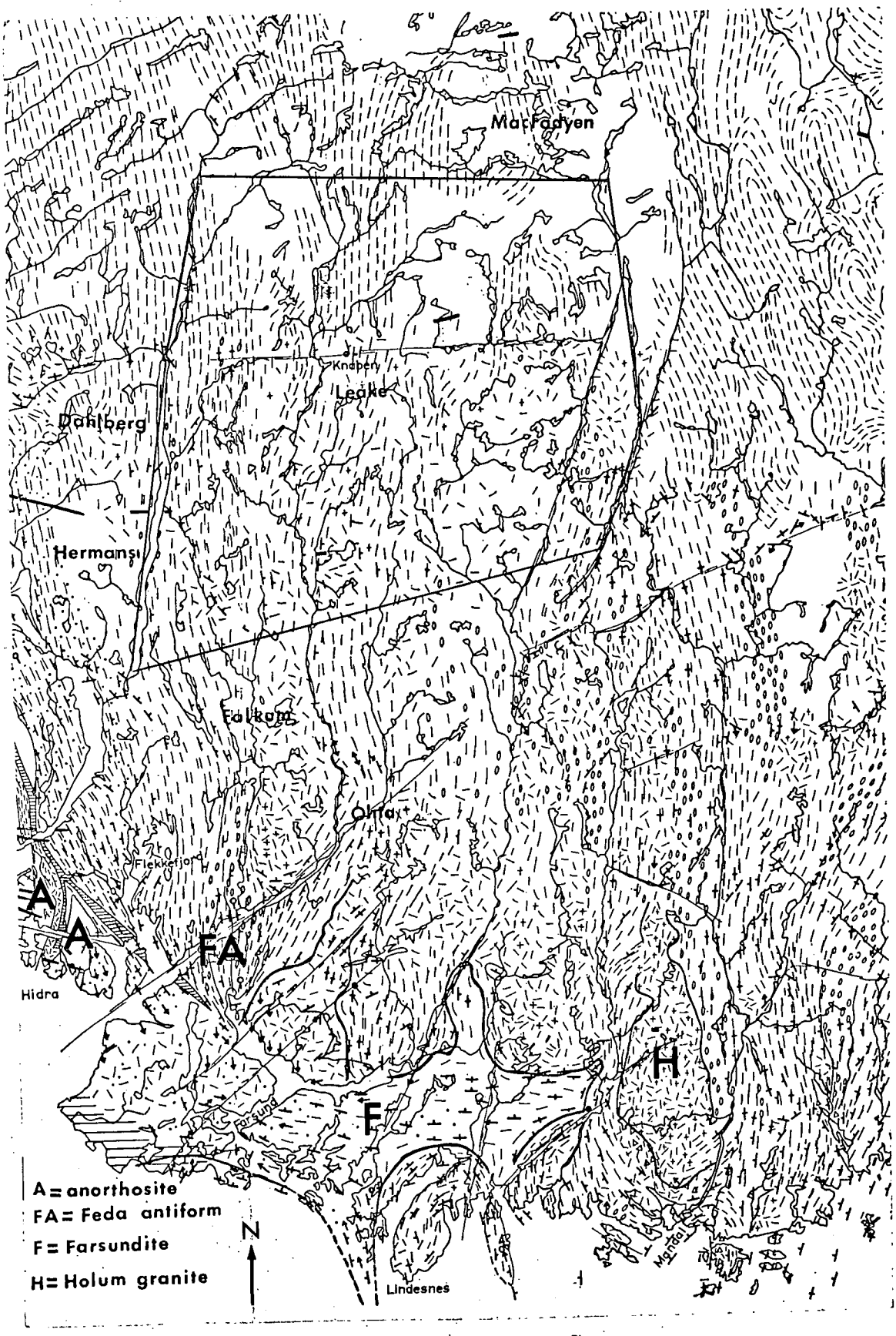

Scale 1:500,000

The geological setting of the area between Sirdal and Åseral together with boundaries of adjacent areas mapped by Telemark Project geologists. Geology after Barth (1960).

Plate 4.

the present area however as the augen gneiss becomes subordinate to layered feldspathic gneisses. The name ' Sirdalsvatn series ' is therefore proposed for the lower gneiss group. The upper series of gneisses can be correlated in many respects with the ' Flekkefjord group ' described by Falkum (op.cit.).

Three main types of acid plutonic rocks occur within the area between Sirdal and Åseral. Porphyritic granite with diffuse concordant boundaries and abundant gneissic inclusions, which closely resembles the Holum granite described by Smithson and Barth (1967), has been discovered in four areas. An equigranular granite with poor foliation occupies much of the terrain to the east and north-east of Knaben. The same type of rock has been observed by MacFadyen (personal communication) to extend some 15 kilometres northwards from the northern boundary of the present area. Three intrusions of coarse-grained granitoid rock with sharp igneous contacts and thermal metamorphic aureoles, very similar to the farsundite rocks, have also been discovered. The largest of these bodies, the Ljosland intrusion, occupies most of the north-east sector of the area and is predominantly a quartz monzonite but grades into granite particularly along its eastern border. The smaller ovoid Åseral intrusion is more dioritic in composition with many basic gneiss inclusions. The extent of the Haddeland quartz monzonite on the southern border of the area to the west of the Little Kvina valley is probably small.

f) Age.

Age dates for material from the Telemark-Rogaland province have been given by Neumann (1960), Broch (1964) and J.Michot and Posteels (1968). Potassium-argon dates for minerals from the Egersund region range from 437 m.y. for pegmatite alkali feldspar to 864 m.y. for biotite from norite. Rubidium-strontium ages of Rogaland biotites range from 820 m.y. to 900 m.y. Whole rock and alkali feldspar rubidium-strontium ages and zircon uranium to lead ages range from 1000 m.y. to 1050 m.y. The pegmatite phase of the farsundite intrusion has been dated at 825 m.y. using the potassium-argon method on a biotite and at 920 m.y. using the uranium-lead method on uraninite, euxenite and thorite. J.Michot and Posteels (op. cit.) conclude that the intrusive phase in Rogaland ended at 930 m.y. before present. The term Sveconorwegian orogeny, introduced by Magnusson (1965) to cover a period of regional high temperature rock alteration dated at 950 m.y. to 1000 m.y. in south-west Sweden and south-east Norway, can also be applied to the main metamorphism of the Telemark-Rogaland province.

Rhenium-osmium dates of several molybdenites are reported in Neumann (1960). The average age of the Telemark deposits has been calculated as 708 m.y. but the Kobberknuten deposit on the northern Setesdalheiene has a significantly greater apparent age of 862 $\pm$ 10 m.y.

The discovery of a gneiss horizon containing aggregates

of plagioclase crystals identical in composition to those of the Rogaland anorthosites by Falkum (1967) may provide some evidence of age relationships within the Telemark-Rogaland province lithostratigraphy.

2. THE SIRDALSVATN SERIES

This distinctive gneiss formation has been traced from the core of the Feda antiform (plate 4) along a continuous but sinuous outcrop northwards as far as Skredadalen, to the west of Øvre Sirdal, a distance of some 70 kilometres. Within the Sirdal-Åseral area the series can be subdivided into two lithostratigraphical units, the Feda augen gneiss and the Tonstad layered feldspathic gneiss. The Feda augen gneiss is easily identifiable in its typical form with euhedral alkali feldspar crystals, often ten centimetres in length (plate 3b). In some of the exposures north of Sirdalsvatn the augen gneiss contains smaller phenoblasts and in certain horizons is interspersed with granitic gneiss, pegmatite and basic layers. The Tonstad gneisses emerge from beneath the augen gneiss in the antiformal nose near Kleivi on the south-western boundary of the area. From there they outcrop northwards along the eastern side of Sirdalsvatn and in the Sira valley. They are predominately layered feldspathic gneisses, often porphyritic, but include more basic layers several metres thick.

a) The Feda augen gneiss.

A typical specimen of massive augen gneiss contains pale pink euhedral to subhedral potassium feldspar crystals with simple twins set in a quartz dioritic matrix. The large single crystal augen frequently exhibit some degree of preferred

orientation with their y axes perpendicular to the foliation of the matrix. The smaller phenoblasts range down to the matrix grain size and are more irregular in shape, a few consisting of mosaics rather than single crystals. The majority of both augen and matrix alkali feldspar grains are untwinned but show irregular and undulatory extinction. Careful examination of any thin section will reveal a few grains with a faint development of gridiron twinning, particularly at their margins. Other grains in the same thin section may have almost uniform extinction. Albite intergrowths in the forms classified by Andersen (1928) as film and drop perthites are common in crystals of all sizes. Inclusions of quartz, biotite and oligoclase rimmed with albite are scattered throughout the larger phenoblasts. Bulbous myrmekite projects from oligoclase grains into the larger alkali feldspar augen that they surround.

The matrix of a typical massive augen gneiss contains 20% by volume quartz, 15% alkali feldspar, 50% oligoclase, 4% biotite, 7% hornblende and 2% clinopyroxene with a few grains of ilmenite, magnetite, apatite, zircon, pyrite and chalcopyrite. The biotite shows pleochroism from straw to deep chestnut brown and the hornblende from pale yellow-green (X) to brownish green (Y) to deep green (Z). Strain extinction domains in quartz and deformed plagioclase twin lamellae are indicative of post-crystallisation stress.

The massive augen gneiss frequently contains thin concordant but irregular layers of fine granular aplite (Plate 3b) and amphibolite layers or lenses. Much of the Feda augen gneiss is more heterogeneous and may contain horizons of layered gneisses

several dekametres thick. These gneisses are mostly pink and pale grey equigranular quartzo-feldspathic rocks with some thin biotite-rich lenses and streaks. Some of the thicker pale grey gneiss layers may contain scattered phenoblastic potassium feldspar crystals similar to those in the massive augen gneiss. Coarse-grain pink feldspar-rich layers and cross-cutting veins are also widespread. The association of augen gneiss with other rocks is particularly complex to the north and west of Tonstad. Augen gneiss occurs either as irregular masses surrounded by pale pink granular aplite with quartz segregations (Plate 5a), or interlayered with other gneisses. Inclusions of basic and intermediate gneiss in the form of relic fold noses or thin lenses are widespread in both augen gneiss and adjacent feldspathic gneiss horizons. Some of the feldspathic gneiss layers also display minor folding on a larger scale.

Augen gneiss from different localities shows a substantial variation in the size of the potassium feldspar phenoblasts and in the composition of the matrix. In the Tonstad area the maximum dimension of the augen is about two cm. and the matrix is less basic than in the largest feldspar variety. Petrographically the augen gneiss from north of Tonstad differs from other types in the absence of clinopyroxene and the presence of sphene as rims to oxide mineral grains. A further variety of augen gneiss with relatively small phenoblasts from near Ersdal in the extreme south-western corner of the area has a more basic matrix with clinopyroxene in greater abundance than hornblende. The plagioclase is untwinned and antiperthitic and the alkali

Plate 5.

Plate 5a.

Exposure of Feda augen gneiss in roadside west of Tonstad. The complex relationship between the augen gneiss, here with dark relatively hornblende-rich matrix, and fine-grain granular leucogranite is apparent. Thin irregular quartz-rich layers occur in parts of the leucogranite.

Plate 5b.

Contrasting types of the Tonstad layered feldspathic gneiss separated by healed fault in roadside section just south of Tonstad. The well-layered feldspathic gneisses on the left of the photograph turn into the fault plane which is filled with a few centimetres of faintly layered granular granitic rock. The more homogeneous gneiss on the right of the photograph abuts sharply against the fault plane. Height of section is about 2 metres.

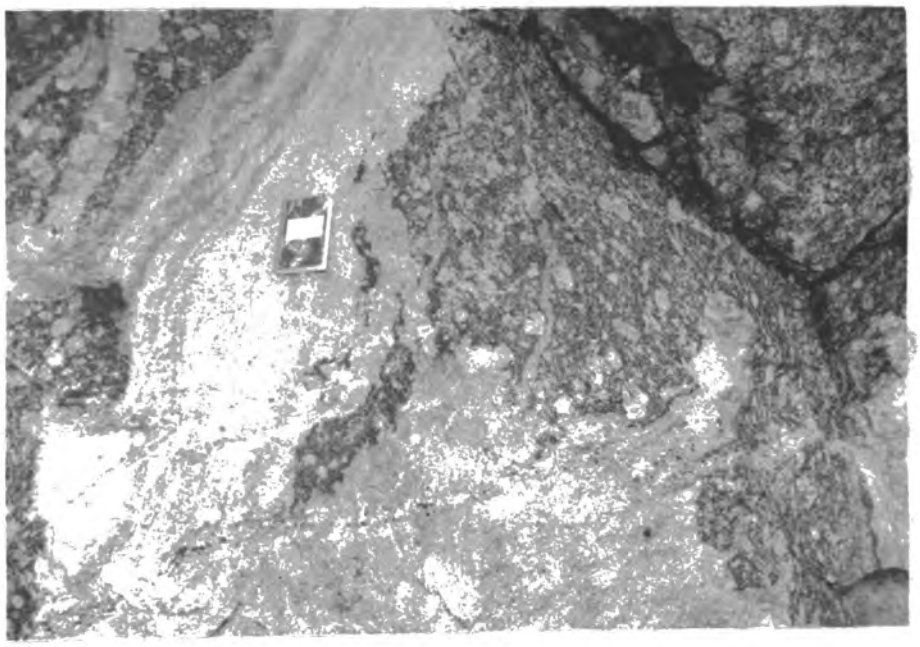

a

b

Plate 5.

feldspar also untwinned with little trace of undulatory extinction.

b) The Tonstad layered feldspathic gneiss.

The contact between the Feda augen gneiss and the Tonstad layered feldspathic gneiss is extremely diffuse. Within a wide transitional zone the matrix of augen gneiss layers gradually becomes more leucocratic and the size of phenoblasts smaller. The proportion of interlayered equigranular granite gneiss gradually increases, displacing the porphyroblastic layers until only isolated horizons persist.

Parts of the Tonstad gneiss series are sharply and regularly layered with pale grey and pale pink coloured horizons. The darker layers contain less quartz but more plagioclase, biotite and the opaque phases than the adjacent pink horizons. The proportion of alkali feldspar is only slightly less in the pale grey horizons however. In contrast other sections are more homogeneous and compositional layering is more diffuse (Plate 5b). These rocks are generally richer in alkali feldspar and contain some granular leucogranite layers and others rich in magnetite with only a little biotite. Alkali feldspar in these gneisses is perthitic with irregular and undulatory extinction but grains with gridiron twinning also exist. The larger plagioclase grains are frequently antiperthitic and rims of clear albite are abundant. Biotite is the only mafic silicate present, except in a few grey horizons with large scattered hornblende grains, and is pleochroic from pale straw yellow to chestnut brown though it is in places altered to chlorite.

c) Basic gneisses within the Sirdalsvatn series.

Both the Feda augen gneiss and Tonstad gneiss contain horizons of more basic gneiss. Hornblende-bearing gneisses of intermediate to basic composition occur either as thin and irregular layers and lenses within the predominantly quartzofeldspathic Tonstad gneisses or as thicker bodies within the Feda augen gneiss. All examples of these rocks contain some modal alkali feldspar and in the augen gneiss even the thicker amphibolites contain some irregular veins and lenses of potassium feldspar rich pegmatitic leucosome. Mineralogically the basic layers in the Tonstad gneisses differ from adjacent more siliceous horizons chiefly in the presence of hornblende as a major component. The hornblende is similar to that of the matrix of the Feda augen gneiss with a brownish-green (Z)-axial colour. The large size and relative abundance of apatite and zircon grains is also a feature of these gneisses. The opaque oxide phases consist of magnetite and ilmenite with much exsolved hematite either regularly distributed as lenses of various sizes (Plate 6a) or as larger and irregular patches. The thicker amphibolites differ from the augen gneiss matrix only in the smaller proportion of quartz and alkali feldspar and in the greater amount of hornblende present.

A further type of basic gneiss with biotite and clinopyroxene as the main mafic silicate phases is also widespread in the Sirdalsvatn series. These rocks occur in layers from a few cm. to several metres in thickness. One thick horizon of these distinctive rocks has been traced for several kilometres in the Tonstad gneisses. Though rather variable in composition, these

Plate 6.

Plate 6a.

Photomicrograph taken in reflected light of three size generations of exsolved hematite in ilmenite. Specimen is from an oxide-sulphide ore segregation in the Kvinesdal granitic gneiss near Knaben. Similar textures are found in many amphibolites and biotite-clinopyroxene gneisses throughout the area. Magnification x 250.

Plate 6b.

Photomicrograph taken in plane polarised light of garnet-cordierite gneiss from the Lervig gneiss east of Tonstad. The garnet is elongate and contains small biotite inclusions orientated parallel to the long axis of the grain. Clear areas within and adjacent to the garnet are of quartz. The two cloudy areas with low relief are partially altered cordierite. The orientation of the biotite grains within the garnet is also parallel to the planar fabric of other parts of the rock. Magnification x 50.

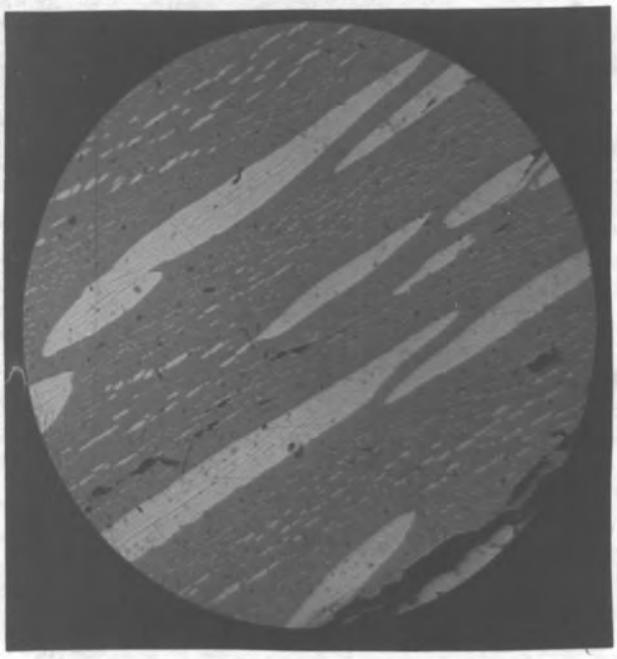

a

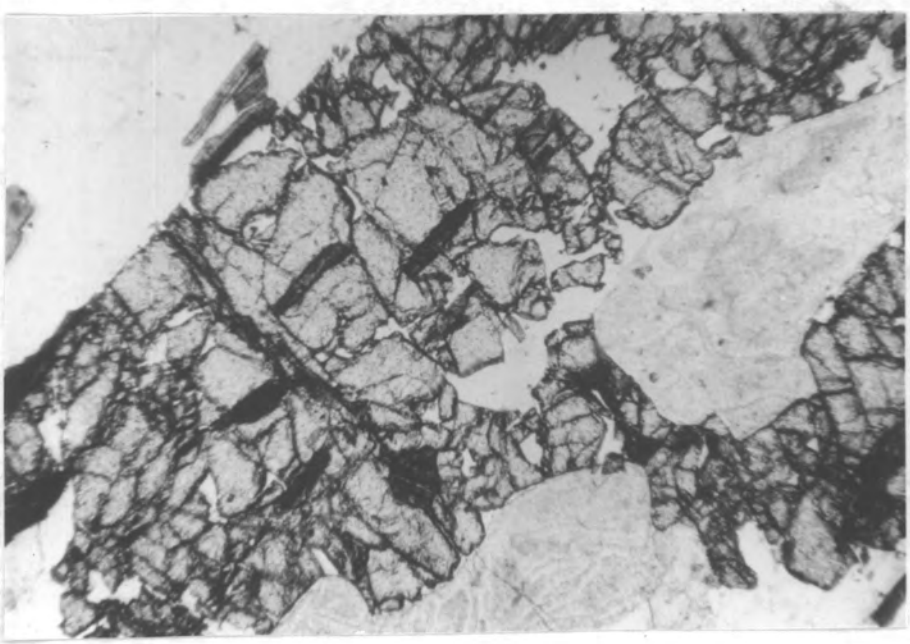

b

Plate 6.

gneisses all contain quartz, alkali feldspar, plagioclase, biotite, clinopyroxene, apatite and opaque phases. Potassium feldspar ranges as a component from an accessory to about 40 volume % of the rock and is usually untwinned with some drop perthite. Sphene is sometimes a conspicuous minor phase and the opaque minerals are typically magnetite, ilmenite with a great deal of exsolved hematite and pyrite. A few horizons may also contain a little hornblende showing a brownish- green (Z)-axial colour.

3. THE FLEKKEFJORD SERIES

All the gneisses above the Sirdalsvatn series are included in one group, the Flekkefjord series, although there is an apparent discontinuity towards the base of the sequence. The series is divided into a number of lithostratigraphical units, some of which have also been recognised by Falkum (1967) in the Flekkefjord area. The apparent stratigraphical sequence of the units is as follows :-

Oddevassheii layered basic and feldspathic gneiss

Flofjell massive quartzofeldspathic gneiss

Knaben layered basic and feldspathic gneiss

Kvinesdal massive quartzofeldspthic gneiss

Lande layered basic and feldspathis gneiss

Øie layered quartzofeldspathic gneiss

----------apparent discontinuity----------

Gyadal garnetiferous gneisses

Lervig layered basic and feldspathic gneiss

----------discontinuity----------

Sirdalsvatn Series.

The Knaben, Flofjell and Oddevassheii gneisses are all structurally above the highest unit recognised by Falkum in the Flekkefjord area. Thicknesses are almost impossible to gauge because of widespread mesoscopical folding, sometimes only evident in very fresh exposures.

A sharp contact separates the Flekkefjord series from the underlying Sirdalsvatn series. To the south-west of Sandvatn there is a sharp, roughly concordant junction between massive Feda augen gneiss and a quartzofeldspathic gneiss with faint layering which passes eastwards into more heterogeneous Lervig gneiss. Further north in the Sandvatn area, though the boundary itself is obscured, there is a pronounced discontinuity in strike between the two series. North of Espetveit the contact is often obscured by vegetation but a low angle discordance in regional foliation can often be observed on either side of the presumed junction. In the Sira valley the contact has been observed as a plane dipping to the east at a lower angle than the gneissic layering. Little of the western contact of the Sirdalsvatn series is exposed on the eastern side of the lake but where it can be observed the Feda augen gneiss is in sharp contact with layered or quartzofeldspathic gneiss with apparent conformity.

a) The Lervig gneiss

This series of rocks is extremely heterogeneous with layers exhibiting 23 different mineral assemblages neglecting accessory minerals and those produced as a result of retrograde metamorphism. The parageneses are divided into four major categories and listed below.

Quartzofeldspathic gneisses.

1) Quartz - K-feldspar - Plagioclase - Biotite.

2) Quartz - K-feldspar - Plagioclase - Biotite - Hornblende ± Sphene.

3) Quartz - K-feldspar - Plagioclase - Biotite - Orthopyroxene.

Garnet-bearing gneisses.

4) Quartz - K-feldspars - Plagioclase - Biotite - Almandine.

5) Quartz - K-feldspar - Plagioclase - Biotite - Spinel - Almandine $\pm$ Sphene.

6) Quartz - K-feldspar - Plagioclase - Biotite - Almandine Cordierite.

7) Quartz - Plagioclase - Biotite - Almandine.

8) Quartz - Plagioclase - Biotite - Almandine - Cordierite.

9) Quartz - Plagioclase - Grossular - Clinopyroxene - Scapolite - Sphene.

10) K-feldspar - Plagioclase - Biotite - Almandine.

Quartz-bearing basic gneisses.

11) K-feldspar - Plagioclase - Biotite - Hornblende - Clinopyroxene.

12) K-feldspar - Plagioclase - Biotite - Hornblende - Clinopyroxene - Orthopyroxene.

13) Plagioclase - Biotite - Hornblende.

14) Plagioclase - Hornblende - Clinopyroxene.

15) Plagioclase - Biotite - Hornblende - Clinopyroxene.

16) Plagioclase - Biotite - Hornblende - Orthopyroxene.

17) Plagioclase - Biotite - Hornblende - Clinopyroxene - Orthopyroxene.

Quartz-free basic gneisses.

18) Plagioclase - Biotite - Hornblende.

19) Plagioclase - Biotite - Orthopyroxene.

20) Plagioclase - Biotite - Hornblende - Clinopyroxene.

21) Plagioclase - Biotite - Hornblende - Orthopyroxene.

22) Plagioclase - Biotite - Hornblende - Clinopyroxene - Orthopyroxene.

23) Plagioclase - Hornblende - Clinopyroxene - Orthopyroxene.

With the exception of assemblage 9 and some examples of assemblage 7 all the gneisses also contain magnetite. Ilmenite is present in all the more basic rocks. Apatite and zircon are common accessory minerals while allanite is only noticeable in certain feldspathic gneisses of intermediate composition. Small amounts of pyrite are widespread in many of the hornblende-bearing gneisses and pyrrhotite occurs in some of the basic amphibolites. Fine sulphide is disseminated in a few thin horizons within biotite-rich quartzofeldspathic gneiss. The rusty staining of these fahlbands makes them conspicuous in weathered outcrops. Though most of the sulphide is pyrite, a few layers also contain chalcopyrite.

Assemblages 1,2,13,15,17,18,20 and 22 are by far the most abundant in the Lervig gneiss. The garnet-bearing rocks, though conspicuous, amount to a small proportion of the total sequence. Many of the other assemblages have been found only in thin isolated layers. Thick pyribolite horizons occur, particularly in the lower part of the Lervig gneiss. They often exhibit fine diffuse layering and also contain thin white plagioclase sheets, some of which are slightly discordant. Other pyribolites show sharper compositional layering and contain lensoid inclusions of more basic rock.

Amphibolites, sometimes with clinopyroxene, are more abundant in the upper Lervig gneiss where they occur either as thick horizons of layered rocks or as thin isolated bodies within predominantly feldspathic gneisses. The basic gneisses are interlayered chiefly with either a granitic rock with only faint layering or sharply layered biotite-rich feldspathic gneisses. The granitic gneiss contains a few thin concordant sheets of coarse-grained pink potassium feldspar-rich neosome. The layered biotitic and feldspathic gneisses are extremely variable in composition and may include some horizons with hornblende in addition to biotite and granular leucocratic rocks in sheets up to several metres thick. Magnetite replaces biotite as the major dark mineral in these granular horizons.

The plagioclase of the layered pyribolites is relatively sodic with an anorthite content of between 27% and 33%. The darker massive lensoid pyribolites contain more calcic plagioclase with anorthite contents of about 45%. The biotite of these rocks shows a distinctive pleochroism from pale orange to a deep red. The pleochroic scheme of the hornblende is from pale yellow (X) to greenish brown (Y) to brown (Z). Clinopyroxene is colourless but orthopyroxene shows marked pleochroism. All four mafic silicate minerals are quite fresh and occur together without reaction rims or other textural indications of disequilibrium. The ilmenite is usually without visible exsolved hematite.

A deep red-coloured biotite is also found in the ortho-

pyroxene-bearing quartzofeldspathic gneisses and many of the garnetiferous rocks. The biotite of amphibolites and other feldspathic gneisses is, in contrast, a chestnut brown. A green tinge is present in the (Z)-axial colours of hornblendes from amphibolite and intermediate gneiss horizons. The amphibolites also differ from the pyroxene-bearing gneisses in their more variable and calcic plagioclase compositions (up to An 55 %). The grains of ilmenite in the amphibolites may either be without visible exsolution or contain a little fine grain hematite. Alkali feldspar grains of the more leucocratic gneisses are untwinned and show either uniform or slightly undulatory extinction. Drop perthitic texture is common but myrmekite and albite rims to plagioclase are not as well developed as in gneisses from the Sirdalsvatn Series. Garnets are usually lensoid with inclusions of biotite parallel to the planar fabric of the matrix (Plate 6b), though some grains in the same exposure may be subhedral and sharply discordant to the matrix.

A more migmatitic facies of the Lervig gneiss is developed in areas of particularly intense and complex deformation. In the region of complex folding to the east of Espetveit basic gneiss horizons are interlayered with thick coarse-grained pegmatites. The thinner amphibolite layers are often broken up and penetrated by surrounding granitic rocks. In some layers the process has been intense enough to produce agmatic structure. Migmatite is best developed in the area north and east of Sandvatn within a domain of complex folding. Pegmatoid and aplitic leucosomes are widespread both in the form of irregular pods and lenses and concordant and discordant sheets. The alkali

feldspar of both paleosome and neosome has undulatory extinction and film perthite exsolution but unlike other similar Lervig gneiss rocks some of the grains also have diffuse cross-hatch twinning.

A series of distinctive garnet-bearing granitic gneisses overlies the typical basic layered Lervig gneiss in the Sira valley to the north of Guddal. These rocks are similar to the ' white gneisses of Ørsdalen ' described by Heier (1956) from an area to the north-west of Tonstad and remapped by Tobi (1965) as the ' Gyadal garnetiferous migmatites '. They are mostly phenoblastic quartzofeldspathic gneisses with scattered, often lensoid almandine garnets and streaks and lenses richer in biotite. Throughout these gneisses there are also small bodies of pegmatoid rock with large euhedral garnets and layers of white granular rock with small scattered garnets. Biotite and magnetite are completely absent from these rocks.

The potassium feldspar of these gneisses is a microcline perthite with sharp twinning. The included albite is abundant in the form of fine films and lenses. The intergrowth is not as intimate as in the mesoperthites of the Ørsdalen rocks however. Included potassium feldspar is common in the larger plagioclase grains. The biotite is similar in colour to the mineral in the quartzofeldspathic rocks of the Lervig gneiss.

The garnetiferous gneisses of the Sira valley have been provisionally correlated with the ' Gyadal garnetiferous migmatites ' mapped by Tobi (1965) to the west of the Sira

valley though the two outcrops have not yet been connected. None of the distinctive blueish-grey rocks with garnet, cordierite, sillimanite and graphite which are characteristic of some parts of the unit mapped by Tobi (op.cit.) have so far been discovered within the Sira valley. In the Sira valley these rocks overlie the Lervig gneiss with apparent conformity but south of Guddal they lens out against the base of the Øie gneiss. These relationships can be explained in terms of a discontinuity at the base of the Øie gneiss.

b) The Øie gneiss.

The predominant rock of this lithostratigraphical unit is a medium-grain pale grey quartzofeldspathic gneiss with a phenoblastic texture in places. In fresh exposures the rock is seen to be layered with pale pink and pale grey, more mafic horizons. Streaks and lenses richer in biotite are also frequent and as these tend to weather more readily than the more siliceous layers, the rock has a distinctive ribbed appearance in the denuded upland exposures. Other parts of the unit are more homogeneous and a pale pink colour but streaks of more biotitic rock can still be found. Sheets of fine-grained granular leucogranite and thin layers of coarse alkali feldspar rich neosome are widespread, particularly in the more uniform gneisses.

Most of the alkali feldspar of these gneisses is a microcline with coarse drop perthite inclusions but a few grains with undulatory extinction also coexist. Both quartz and plagioclase often show strain extinction and myrmekite is

frequent. Biotite shows pleochroism from pale yellow-brown to a medium brown but may also be partly altered to chlorite. Zircon, apatite, allanite and magnetite are the usual accessory minerals.

The lower contact of the Øie gneiss with the Lervig gneiss is relatively sharp and in some areas slightly discordant. The upper contact with the Lande gneiss is gradational. Within the contact zone the gneissic layering becomes more pronounced and basic gneisses appear, often in the form of schollen.

c) The Lande gneiss

This series of layered basic and feldspathic gneisses is in many respects similar to the Lervig gneiss. The 11 mineral assemblages that have been encounted in the unit are listed below.

Quartzofeldspathic gneisses.

1) Quartz - K-feldspar - Plagioclase - Biotite.

2) Quartz - K-feldspar - Plagioclase - Biotite - Hornblende ± Sphene.

3) Quartz - K-feldspar - Plagioclase - Biotite - Orthopyroxene.

Quartz-bearing basic gneisses.

4) Plagioclase - Biotite - Hornblende.

5) Plagioclase - Biotite - Hornblende - Clinopyroxene.

6) Plagioclase - Biotite - Hornblende - Orthopyroxene.

7) Plagioclase - Biotite - Hornblende - Clinopyroxene - Orthopyroxene.

Quartz-free basic gneisses.

8) Plagioclase - Biotite - Hornblende.

9) Plagioclase - Hornblende - Clinopyroxene.

10) Plagioclase - Biotite - Hornblende - Clinopyroxene Orthopyroxene.

The Lande gneiss differs from the Lervig gneiss in the presence of amphibolite and pyribolite layers with very little or no opaque iron oxide phases. Other pyribolite horizons contain either ilmenite alone or ilmenite and magnetite. The common accessory minerals are apatite, zircon, allanite and pyrite, often with a little included chalcopyrite. Fine-grain disseminated pyrite is also present in a few thin quartzofeldspathic gneiss layers but it not as widespread as in the Lervig gneiss.

No garnet-bearing rocks have been encounted by the author in the Lande gneiss, though Falkum (1965) mentions that sillimanite - cordierite - garnet gneisses are characteristic of the same unit in the Flekkefjord area. The pyribolite with anorthositic inclusions, exhibiting a texture that has been interpreted by Falkum (op.cit.) as primary graded bedding and found by him in the Lande gneiss at several localities, has not been observed by the author in the present area. Pyribolite layers are not as abundant in the Lande gneiss as in the Lervig gneiss and tend to be more intimately interlayered with amphibolites, clinopyroxene amphibolites and more siliceous gneisses. The

leucocratic components of these intimately-layered gneisses are themselves extremely variable in composition, particularly with respect to the proportion of alkali to plagioclase feldspar. Layers of fine-grained granular rock are frequent, either pink alkali feldspar-rich or less commonly of pale greenish plagioclase and quartz. Other parts of the Lande gneiss are more feldspathic with thin biotite rich streaks and lenses and few horizons of basic gneiss often penetrated by adjacent granitic rocks (Plate 7a). More massive and phenoblastic quartzofeldspathic gneiss horizons also exist.

The basic gneisses frequently contain thin layers and lenses of white plagioclase-rich neosome (Plate 7b), some of which exhibit ptygmatic folding. Other more massive basic gneisses contain thin discordant veins of basic pegmatite with isolated euhedral amphibole or pyroxene crystals. Layers and pods of pegmatoid leucosome are found in the more feldspathic facies of the gneiss but are not numerous. A few sharply discordant dilational pegmatite veins cut the more basic horizons. Some of the gneisses at the top of the sequence have been intensely deformed into augen gneiss with granular composite quartzofeldspathic eyes surrounded by a dark biotite and hornblende-rich matrix (Plate 8a).

The mineralogy of the pyribolites in very similar to that of the same rocks in the Lervig gneiss. The (z)-axial colour of the hornblende has a greenish tinge however. The four mafic silicates are also usually fresh though orthopyroxene may sometimes show slight alteration. The Lande gneiss pyribolites frequently exhibit diffuse layering into hornblende-rich and

Plate 7.

Plate 7a.

Roadside exposure of feldspathic Lande gneiss with basic horizons from Kvina valley north of Netlandsnes. The basic horizon fish-tails into and is penetrated by the adjacent granitic rock. The faint layering within the granitic gneiss is partly obscured by the weathered nature of the exposure.

Plate 7b.

Roadside exposure of layered basic and felspathic Lande gneiss from east side of Kvina river near Moland. The rock is very heterogeneous with basic gneiss lenses, some with sheets of plagioclase-rich neosome, and finely-layered more biotite-rich gneiss.

a

b

Plate 7.

Plate 8.

Plate 8a.

Deformed gneiss at top of Lande gneiss, Novassheii, near Kvinlog. Spindle-shaped composite augen of granular quartz and feldspar grains are surrounded by a dark biotite and hornblende-rich matrix.

Plate 8b.

Photomicrograph taken in plane polarised light of pyribolite from Lande gneiss near Netland showing diffuse layering into hornblende-rich and plagioclase plus pyroxene-rich components. Darker layers consist predominantly of hornblende and plagioclase with a little biotite and ilmenite. The paler layers consist predominantly of plagioclase, a little quartz, pyroxene grains, biotite and ilmenite. In the photograph the larger elongate pyroxenes are clinopyroxene and the smaller and rounded grains, orthopyroxene. Magnification x 9.

a

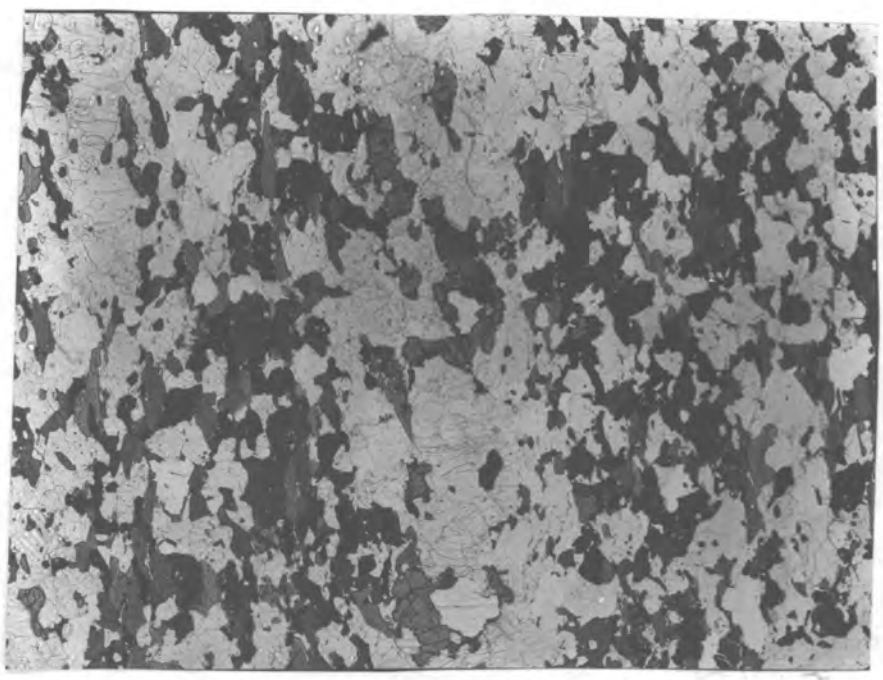

b

Plate 8.

plagioclase and pyroxene-rich components (Plate 8b). Unlike the Lervig gneiss the Lande gneiss contains several horizons of orthopyroxene-bearing basic gneiss without clinopyroxene. Mineralogically these rocks are very similar to the pyribolites.

Biotite varies in the Lande gneiss amphibolites from a major constituent to an accessory mineral in some almost pure plagioclase hornblende rocks (Plate 9a). It varies in colour from dark red to a deep brown. The (z) -axial colour of hornblende in these rocks also ranges from brown-green to green and in a few cases is blue-green. Biotites from hornblende-bearing intermediate gneisses show pleochroism from straw to dark olive brown and the amphiboles have blueish tints. The microperthitic potassium feldspar of these more siliceous gneisses exhibits straight to undulatory extinction. In the granitic gneisses this mineral is usually a microcline with included drop and film perthite, though a few grains within any section may be untwinned. The larger plagioclase grains in the quartzo-feldspathic gneisses are frequently antiperthitic and the smaller crystals are rimmed with clear albite. Biotite is a dark brown except in the orthopyroxene-bearing granitic rocks where it is distinctly red in colour. Sphene is conspicuous in many of the alkali feldspar-bearing intermediate gneisses, either rimming oxide grains or as separate crystals. Ilmenite is without visible hematite exsolution.

The Lande gneiss on the eastern limb of the Kvina valley antiform becomes more feldspathic with relatively few basic gneiss horizons as it is traced northwards. In the upper Kvina valley,

Plate 9.

Plate 9a.

Photomicrograph taken in crossed polarised light of amphibolite from the Lande gneiss. The photograph shows a mosaic of hornblende and plagioclase with one small biotite grain near the centre of the field. A few small apatite grains are visible within plagioclase crystals. Twinning is relatively scarce in the plagioclase. Magnification x 100.

Plate 9b.

Photomicrograph taken in crossed polarised light of typical Kvinesdal granitic gneiss from west of Knaben. The section shows microcine with pronounced cross-hatch twinning, often with small rounded grains of plagioclase at the centre of each crystal. Twinned and untwinned plagioclase grains are of various sizes and often with thin albite rims particularly where the crystals are in contact with alkali feldspar. There are also a few areas of clear white quartz. Magnification x 50.

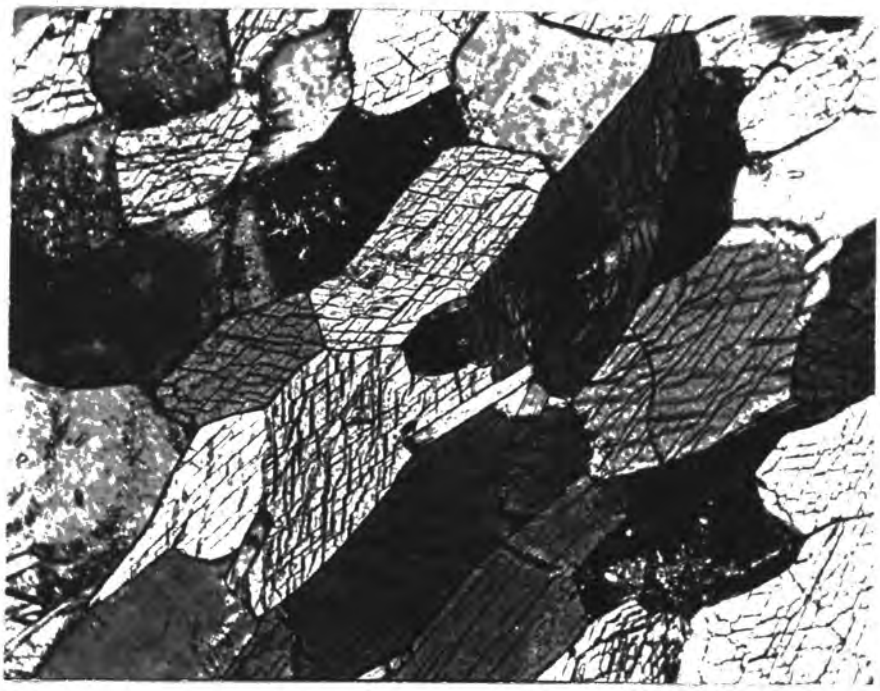

a

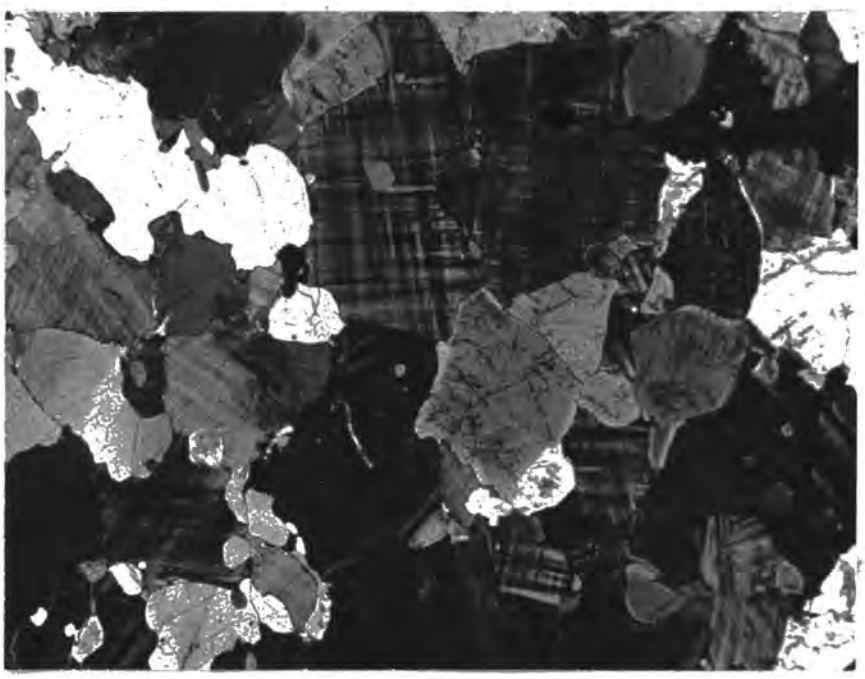

b

Plate 9.

to the north-east of Homstøl, the layered rocks have been invaded or largely replaced by a coarsely porphyritic gneissic ' granite ', varying in composition from adamellite to granodiorite and quartz monzonite. There are abundant relics of layered gneiss however, though often the minor fold hinge zones are all that is preserved. Other parts of the porphyritic gneiss exhibit diffuse compositional layering in which it is still possible to trace the outline of minor fold noses. Many of the thinner basic gneiss layers contain scattered alkali feldspar phenoblasts. More massive parts of the porphyritic gneissic 'granite' show a broad scale diffuse heterogeneity with some sectors relatively rich in hornblende. The most basic facies of these rocks contain quartz, microcline, antiperthitic oligoclase, olive-brown biotite, blue-green hornblende, magnetite and sphene. The few amphibolite horizons within these gneisses also contain hornblende with a blue tinge.

The layered basic and feldspathic gneiss which surrounds and is included in the margins of the Fjotland porphyritic gneissic granite dome have been tentatively correlated with the Lande gneiss. A thin impersistent horizon of layered feldspathic, biotitic and basic gneisses can be traced along much of the eastern limb of the fold. It is thickest to the north of Åsevatn where several layers of basic gneiss occur. The gneisses to the southwest of the dome are thicker and more feldspathic but extensively replaced by and interlayered with the porphyritic gneissic granite. Schollen of amphibolite are frequent and some thicker basic gneiss layers can be traced for some distance within the margin of the domal gneissic granite. The layered gneiss on each limb of the fold converge in the southern part of the area and are presumed to close a little way beyond the region mapped.

The basic layers of this gneiss differ from those of the typical Lande gneiss in generally containing alkali feldspar, usually in the form of microcline microperthite. True amphibolites are relatively uncommon and no orthopyroxene-bearing gneisses have been observed. There are several layers of biotite-hornblende-clinopyroxene and biotite-clinopyroxene gneisses however. The latter are in many respects similar to rocks of the Sirdalsvatn series but are less extreme in composition.

Biotites from these gneisses show pleochroism from pale yellow or orange to dark brown, sometimes with an olive tint. Hornblendes from both amphibolites and alkali feldspar-bearing gneisses have green or blue-green (z)-axial colours.

d) The Kvinesdal gneiss.

The predominant rock of this unit is a massive pink medium to coarse-grained phenoblastic granitic gneiss. Thin fine-grain layers rich in biotite and a few horizons of hornblende-bearing gneiss are scattered throughout the sequence but are never numerous. A body of finer grained granite gneiss with poorer foliation occurs within the Kvinesdal gneiss to the west of Netland but the relationship between it and the surrounding phenoblastic gneiss is uncertain. Pegmatite veins and pods are rare in the Kvinesdal gneiss but layers and veins of granular leucogranite are more numerous. Though a little variation can be discerned in the weathered outcrops of the Kvinesdal gneiss, fresh exposures in the rock demonstrate the existence of some compositional inhomogeneities. Though most of the rock is coarsely

porphyritic, there are also horizons of more leucocratic gneiss with smaller phenoblasts and biotite-rich streaks. In a few of these exposures of fresh rock faint traces of minor folds are outlined in biotite-rich layers.

The typical phenoblastic gneisses contain large and small crystals of microcline, sometimes with drop and string perthite and often with rounded inclusions of either quartz or olioclase rimmed with albite (Plate 9b). Biotite shows pleochroism from pale yellow to dark brown and coexists with accessory magnetite, apatite, zircon and sometimes allanite. The hornblende-bearing intermediate gneisses contain perthitic alkali feldspar with undulatory extinction, olive-brown biotite, blue-green hornblende, magnetite and conspicuous sphene in addition to quartz and oligoclase. Sphene occurs both in thick rims around magnetite and as separate grains. The amphibolites are similar in mineralogy except that alkali feldspar is either a minor constituent or absent.

e) The Knaben gneiss.

This series of layered gneisses has an irregular outcrop of varying width and is extensively interfingered with massive phenoblastic granite gneiss. It consists of fine-grained quartzofeldspathic gneiss with abundant biotite-rich layers and several horizons of massive amphibolite. Many of the feldspathic gneisses are impregnated with fine sulphide and are conspicuous in weathered exposures. Parts of the layered biotitic gneiss, particularly to the north of Knaben, have been

deformed into augen gneiss with eyes of granular quartz and feldspar around which the biotite rich matrix is superposed. Some of these rocks may also be impregnated with fine-grain sulphide. Complex minor folding can be observed in an outcrop of the layered gneisses some five km. south of the Knaben mine, but is rare elsewhere. Amphibolites occur either as rather persistent layers or as lenses within both layered biotite-rich feldspathic gneisses and massive phenoblastic granitic gneiss. No garnet-bearing or pyroxene-bearing gneisses have been observed within the Knaben gneiss.

To the west of the main outcrop of layered gneiss are a few scattered horizons or isolated lenses of biotitic gneiss, augen gneiss or amphibolite within the massive phenoblastic granite gneiss. These rocks are included within the Knaben gneiss as they are closely similar to components of the main gneiss horizon. Within this zone of included gneisses, there are also several horizons within the phenoblastic granite gneiss which also exhibit layering. In these rocks there are pink and pale grey granitic components, layers with scattered biotite-rich streaks and several horizons of granular leucogranite.

The main layered horizon of the Knaben gneiss varies considerably in thickness along its length. To the north of the Kvina mine it is represented by a few thin horizons of fine grain biotite-rich quartzofeldspathic gneisses which become impersistent as traced further to the north. As the same horizon is traced southwards down Litladalen it again becomes thin and impersistent but towards Eiesland, in the south of the area, it thickens again considerably and becomes more basic in composition.

The phenoblastic granite gneiss of the Knaben area is petrographically very similar to the Kvinesdal gneiss. The layered biotitic and feldspathic gneisses contain either microcline with a little drop and film perthite or more perthitic alkali feldspar with undulatory extinction. The plagioclase is calcic oligoclase often with a thin rim of albite and myrmekite growths where grains are in contact with alkali feldspar crystals. The biotite of these rocks shows pleochroism from pale yellow to a dark brown with a tinge of red and the little hornblende present has a brown-green (z)-axial colour. The amphibolites of the Knaben gneiss are the most basic rocks of the whole area and are quartz-free. The biotite content of thse gneisses varies from about 2% to about 25% in volume. Unlike other amphibolites of the Flekkefjord Series, the only oxide phase present is ilmenite, sometimes with a little exsolved hematite and sometimes accompanied by sphene. Apatite is usually a conspicuous accessory mineral and pyrite is widespread in small amounts. The biotite of the amphibolites is similar in colour to that of the layered gneisses and exhibits red brown colours while the hornblende has a brown-green (z)-axial colour.

f) The Flofjell gneiss.

The eastern contact of the Knaben gneiss is relatively sharp against the Flofjell massive phenoblastic granitic gneiss, a rock close in appearance to the Kvinesdal gneiss. The rock is monotonously uniform except for a few thin horizons of diffusely layered more biotite-rich gneiss. Some five kilometres to the

north-north-east of Knaben is a lensoid body about 600 metres wide of coarsely porphyritic granite gneiss with alkali feldspar crystals up to eight centimetres in length. It grades with a decrease in the size of the phenoblasts into the surrounding typical Flofjell gneiss. There is little difference in composition or mineralogy between the matrices of the two rock types. There are also a few thin sheets of extremely potassic microgranite with 50 volume % microcline within the Flofjell gneiss.

g) The Oddevassheii gneiss.

On the western side of the Ljosland intrusion is a thick and persistent horizon of layered basic and biotite-rich feldspathic gneisses with some granitic gneiss. The horizon is truncated against the Ljosland intrusion to the north of Skjerkedalsrindan but widens northwards to the northern boundary of the area, to the west of Kvennevatn. The western contact of the Oddevassheii gneiss is broad with rafts of folded layered biotite-rich gneiss surrounded by poorly foliated massive granite. Most of the Oddevassheii gneiss is composed of finely layered basic and feldspathic gneisses with more massive basic layers and fine granular granitic rocks with biotite-rich streaks. Many of these quartzofeldspathic rocks are impregnated with fine-grain sulphide and are stained brown in weathered outcrops. Biotite and hornblende exhibit very pronounced preferred-orientation and minor folding is very frequent within the layered rocks. The basic gneisses are similar in composition to those of the Knaben gneiss and are quartz-free but in other respects their mineralogy is completely different with the universal presence of orthopyroxene. The

following five mineral assemblages have been encounted within the unit.

1) Quartz - K-feldspar - Plagioclase - Biotite - Orthopyroxene.

2) Plagioclase - Biotite - Hornblende - Orthopyroxene.

3) Plagioclase - Biotite - Clinopyroxene - Orthopyroxene.

4) Plagioclase - Hornblende - Clinopyroxene - Orthopyroxene.

5) Plagioclase - Biotite - Hornblende - Clinopyroxene - Orthopyroxene.

Hornblende is a relatively minor constituent of these rocks and is segregated into diffuse layers separated by hornblende-free pyroxene gneiss. All the basic gneisses also contain magnetite with relatively abundant exsolved ilmenite and ilmenite without visible exsolved hematite. Basic gneiss with similar mineralogy is included in rafts in the margins of the Ljosland intrusion. Basic gneisses near the contact of the Ljosland intrusion contain thin ramifying veins of plagioclase-rich pegmatite with a little orthoclase-perthite and ortho-pyroxene. The more feldspathic rocks adjacent to the intrusion are finely granular but contain large biotites with random orientation. Many of these rocks contain very little alkali feldspar and are impregnated with fine grain nickeliferous pyrrhotite.

The biotites of the Oddevassheii gneiss differ from those of the Knaben gneiss in their pleochroic scheme which is from pale orange to deep red in the Oddevassheii gneiss. As in Lervig gneiss pyribolites the hornblende has a deep brown (z)-axial

colour. Alkali feldspar is untwinned but contains broad lamellae of exsolved albite which are themselves antiperthitic. The pyroxenes of the basic gneisses are fresh and rather granular (Plate 10a).

h) Gneisses to the east of the Ljosland intrusion.

To the east of the Ljosland intrusion are a series of layered biotitic and feldspathic gneiss with a few more basic horizons alternating with granitic gneiss. Similar rocks extend several kilometres to the east of the present area. The granitic gneiss is either massive and phenoblastic or faintly layered into pale grey and pink components. The basic layers contain quartz, microcline, plagioclase, deep brown biotite, brown-green hornblende, sphene and ore. The few massive amphibolites are similar to those of the Knaben gneiss with no quartz and little biotite. The mineralogy of the gneisses changes as the contact of the Ljosland intrusion is approached and hypersthene becomes abundant. A few garnet-bearing orthopyroxene gneisses have also been observed close to the igneous contact.

These gneisses are tentatively correlated with the Knaben gneiss as they can be traced southwards into the nose of the complex synformal fold discovered by Ohta (1966) at Kvinesheii, some 15 km. south of the present area. The layered gneiss on the western limb of this fold can probably be traced northwards up the eastern side of the valley of the Little Kvina river to tie up with the Knaben gneiss just south of Eiesland. There is evidence that the gneisses to the south east of the Ljosland intrusion are thickened by isoclinal folding.

Plate 10.

Plate 10a.

Photomicrograph in plane polarised light of a specimen of basic Oddevassheii gneiss from the contact aureole of the Ljosland quartz monzonite intrusion. The section contains dark biotite showing striking parallel orientation and two pyroxenes. In the photograph the orthopyroxeneis is darker, more cracked and less regular in shape than the clinopyroxene. Opaque phases are also frequently associated with the orthopyroxene. The colourless areas represent plagioclase grains. Magnification x 100.

Plate 10b.

Inclusion of basic gneiss within the Ljosland quartz monzonite from west-north-west of Rossevatn. The inclusion measures about 50 cm. across.

a

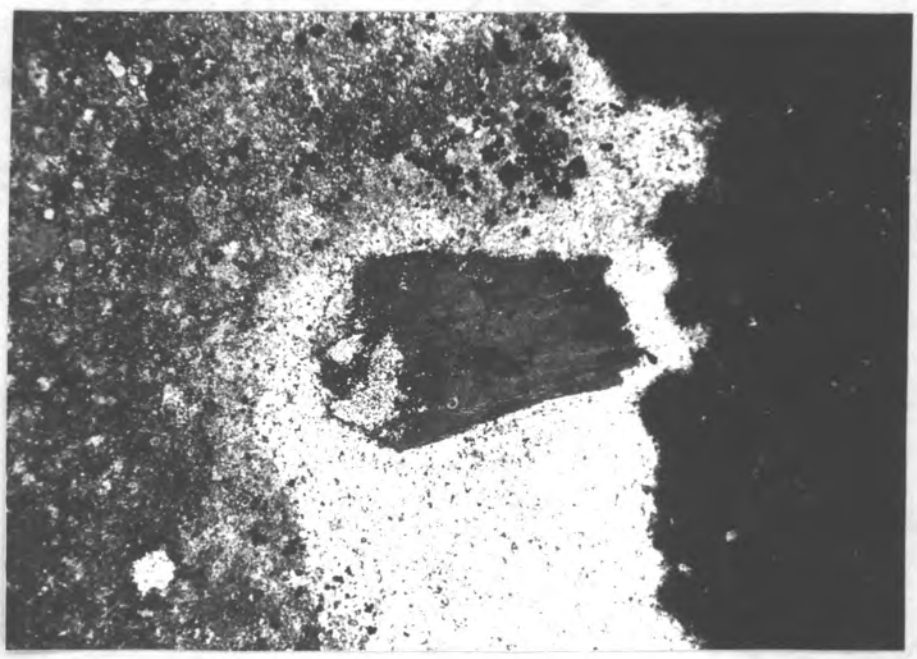

b

Plate 10.

4. THE SYNTECTONIC GRANITES.

a) The porphyritic gneissic granites.

The core of the Fjotland dome is occupied by a coarse-grained porphyritic adamellite with a pale grey matrix similar to the Holum granite described by Smithson and Barth (1967). The predominant rock of the Fjotland granite is distinctly more basic than the Kvinesdal and other granitic gneisses and is similar to parts of the Feda augen gneiss. Foliation is not as pronounced as in the country gneisses but the contacts of the granite are extremely gradational, particularly in the north where the matrix becomes progressively more siliceous and passes insensibly into phenoblastic granite gneiss. Though most of the granite is massive, there are horizons with faint compositional layering often with traces of minor folding and basic gneiss inclusions, similar in mineralogy to the gneisses enveloping the intrusion.

A typical specimen of the Fjotland adamellite contains by volume 21% quartz, 40% alkali feldspar, 29% plagioclase, 4% biotite, 5% hornblende and a little magnetite, sphene, apatite, zircon and allanite. The alkali feldspar megacrysts reach 3 cm. in length and display prominent cross-hatch twinning and inclusions of drop, film and patch perthite. In some sectors of these large crystals the twinning is coarser and more diffuse. Some megacrysts also contain isolated rounded inclusions of

either quartz or oligiclase rimmed with albite. The matrix grains of alkali feldspar are much smaller and show sharp, fine twinning and a little film and drop perthite. The plagioclase, a calcic oligoclase, is mostly untwinned with antiperthite developed in a few of the largest grains. The pleochroic scheme of the biotite is from straw-yellow to dark olive brown and the (z)-axial colour of the hornblende is green or blue green. Sphene, both as separate grains and rimming magnetite, is relatively abundant. Apatite and allanite are also conspicuous accesory minerals.

A triangular outcrop of similar porphyritic adamellite is centred on Haddeland, some 8 kilometres to the east of Fjotland. This body is probably a small offshoot of a much larger volume of the rock to the south of the area mapped. It is surrounded by phenoblastic granite gneiss into which it grades. A further body of similar rock outcrops to the east of Linland in Sirdal. It occupies the core of an antiform and is surrounded by layered basic and feldspathic gneisses with a narrow transition zone. The porphyritic granite of the upper Kvina valley (see page 29) is similar in texture to the Fjotland granite but is more basic and heterogeneous and contains many more gneiss inclusions.

b) The equigranular granite.

This rock is exposed in a large elongate area to the west of the Ljosland intrusion. Its western contact is concordant

and relatively sharp with a transitional zone of a few metres into massive phenoblastic Flofjell granitic gneiss. On the eastern side there is a wider contact zone with rafts of the Oddevassheii gneiss included in the margins of the granite. The granite is homogeneous over large areas but biotite-rich streaks and faint layering can sometimes be observed.

A typical specimen of the granite contains abundant quartz, alkali feldspar with undulatory extinction, oligoclase and myrmekite, a little greenish-brown biotite, magnetite and a few grains of tourmaline. Some of the marginal granite is slightly darker and more biotite-rich.

5. THE DISCORDANT QUARTZ MONZONITE INTRUSIONS.

Three intrusions of this type have been discovered within the area surveyed. The Ljosland intrusion extends over a vast uninhabited region in the east and north-east sector. It is roughly oval in shape with a long axis over 27 km long trending just east of north and a short axis of 12 km. It therefore covers rather more area than that occupied by the Farsundite, a star-shaped intrusion along the south coast between Flekkefjord and Lindesnes which it resembles closely. In some of the most inaccessible areas the contact of the intrusion has had to be inferred from aerial photographs. Just east of the Ljosland intrusion is a much smaller avoid igneous body centred on Åseral. A very small area of similar rock has also been found in the extreme south of the area surveyed, to the west of Haddeland in the Little Kvina valley.

The predominant rock of the Ljosland intrusion is a pale grey coarse-grained equigranular granoblastic quartz monzonite. It exhibits a very weak foliation particularly at its margins. A typical specimen of this rock contains by volume 18% quartz, 35% microcline perthite, 35% plagioclase, 4% biotite, 5% hornblende and a little magnetite, ilmenite, sphene and apatite. Though the predominant alkali feldspar is microcline, it often coexists with a few grains of more disordered potassium feldspar with undulatory extinction. The plagioclase is unzoned but varies slightly about An30 % in composition. The biotite is pleochroic from a pale yellow orange to a dark orange brown

and the hornblende usually has a blue-green (z)-axial colour. The mafic silicates tend to occur in clumps together with oxide grains surrounded by sphene and large apatite crystals.

Fresh exposures in the Ljosland intrusion reveal that there are zones where the rock is much less uniform and contains lenses of more basic and feldspathic rocks. The leucocratic lenses approach alkali granite in composition and are without hornblende and porphyritic in texture. The melanocratic lenses are similar both in mineralogy and texture to the normal quartz monzonite but are much richer in the mafic silicates. Much of the north-eastern part of the intrusion is composed of a porphyritic variety of quartz monzonite with large pink microcline crystals and a few tourmaline grains but in other respects similar to the equigranular facies.

The Åseral intrusion differs from the Ljosland intrusion is being rather more basic and variable in composition and richer in gneiss inclusions. The alkali feldspar is usually of intermediate triclinicity with undulatory extinction. In other mineralogical respects, except for the presence of allanite as a widespread accessory mineral, the Åseral rocks are very similar to those of the Ljosland intrusion. Diorite in the form of scattered lenses represents the most basic component of this igneous complex. These diorites have little potassium feldspar but contain clinopyroxene in addition to hornblende and biotite.

The rocks of the Haddeland intrusion are slightly more

basic than those of the Ljosland igneous complex and are also slightly porphyritic. The alkali feldspar has rather diffuse cross-hatch twinning but in other respects the rocks are similar mineralogically to the typical Ljosland quartz monzonite. As in the Åseral intrusion, allanite is a conspicuous accesory mineral. The chemical compositions of the coexisting minerals of one specimen from the Haddeland intrusion have been determined using the electron microprobe (see appendix). Both biotite and hornblende are significantly more iron-rich than any of the minerals from the gneissic rocks of the area. The sphene is also significantly richer in aluminium than any mineral from the regional gneisses. The magnetite of the intrusive rock is both more titanium-rich and contains more exsolved ilmenite than is encounted in any of the regionally metamorphosed gneisses. Both magnetite and ilmenite, which is usually without visible exsolved hematite, are rimmed with a thick but irregular layer of sphene, separate grains of which also occur.

Both pegmatite and quartz veins have been observed within the Ljosland and Åseral intrusions but they are never abundant. No complex or rare-element minerals have been discovered in any of the veins, though they are known in the Farsundite intrusion. Thin aplite layers are also found in parts of both intrusions.

The nature of the country rocks influences the external contacts of the intrusions. Where the Ljosland intrusion is in contact with the basic Oddevassheii layered gneiss the boundary is relatively sharp with a narrow zone in which tongues of

intrusive rock separate lenses of basic gneiss. Inclusions of these gneisses persist further into the intrusion and are sharply bounded (Plate 10b). Examination of several of these rafts reveals that they are randomly orientated. The mineralogy of these inclusions is similar to that of the basic gneisses in the contact aureole (see page 35). Barth (1960) mentions that amphibolite inclusions, often with a reaction rim of diopsidic augite are common within the margins of the Farsundite. These inclusions are distinct from coarse-grained basic segregations with a similar mineralogy to the intrusive rocks which are frequent in other parts of the intrusion. These probably represent basic gneiss inclusions that have been partially assimilated and have recrystallised after permeation by magmatic fluid. Along the southern contact of the Ljosland intrusion the country rocks are phenoblastic granitic gneisses. These have been assimilated into the margins of the intrusion to produce a more feldspathic rock with pink alkali feldspar crystals similar in appearance to the megacrysts of the gneisses. Furthermore the granitic rocks adjacent to the intrusion have been remelted in places to a rock similar in texture to the margins of the intrusion. In these areas the contact becomes difficult to define precisely.

Rafts of both basic gneiss and finely layered biotitic and feldspathic gneisses up to 20 metres wide occur at the margins of the Åseral intrusion. Inclusions in various stages of assimilation of both basic and feldspathic gneisses are abundant throughout the main body of the complex, particularly in the west and north sectors. The surface exposed at present may therefore be close to the roof of the intrusion.

The farsundite has been described by Barth (1960) as varying chemically from a monzonite to a quartz monzonite to an alkali granite. In the north-western part of the mass the rock becomes schistose and orthopyroxene and clinopyroxene take the place of hornblende. Middlemost (1968) in a reappraisal of the intrusion, recognises a dark, charnockitic or M-type farsundite and a light or L-type farsundite on the basis of feldspar colour. He also recognises a mixed border facies of farsundite and microgranite. None of the M-type rocks, similar to the acid rocks of the charnockite series of Madras, have been discovered in the three intrusions surveyed by the present author.

Chemical analyses of the intrusive rocks are given in table 1. A plot of normative quartz, orthoclase and albite for these rocks, calculated by the method of Barth (1959), is shown in figure 1 with ten farsundite analyses in Barth (1960). These normative compositions plot on the triangular diagram in a similar field to other granitic rocks of magmatic origin. The rocks of the Ljosland intrusion are noticeably richer in calcium and aluminium and poorer in iron and titanium than the L-type farsundite. The predominant rock of the Åseral intrusion is similar in composition to Ljosland intrusion rocks but the dioritic facies is much more basic. The rocks of the Haddeland intrusion are much closer in composition to the L-type farsundite, a fact illustrated in figure 2, a triangular plot of total iron, alkalies and magnesium.

The genesis of the farsundite is considered by

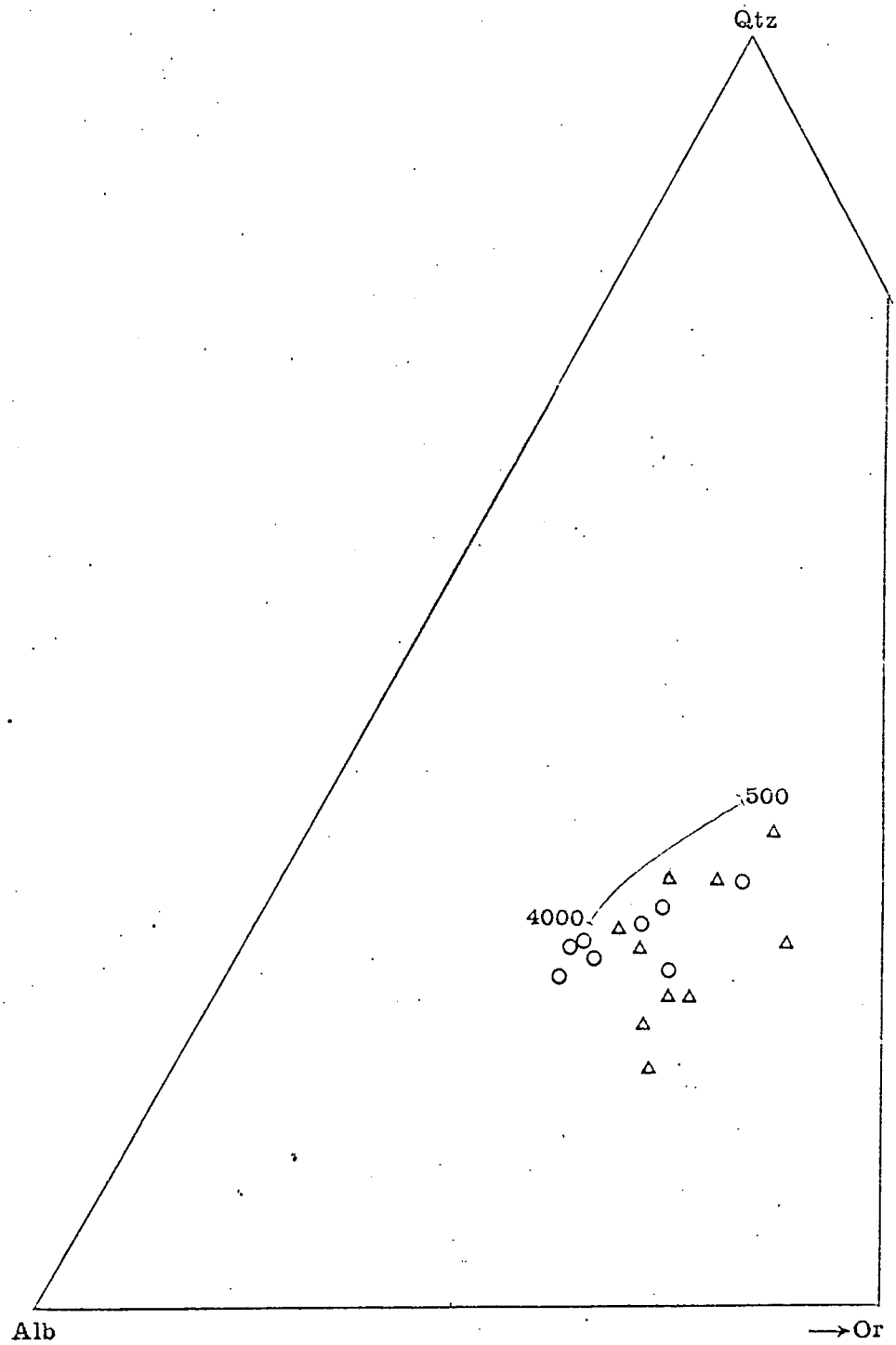

Normative quartz, albite, orthoclase diagram for △ farsundite & ○ Sirdal-Åseral intrusions. The variation in minimum melting composition with water pressure in Bars is also shown. Diagram and farsundite analyses after Barth (1960).

Figure 1.

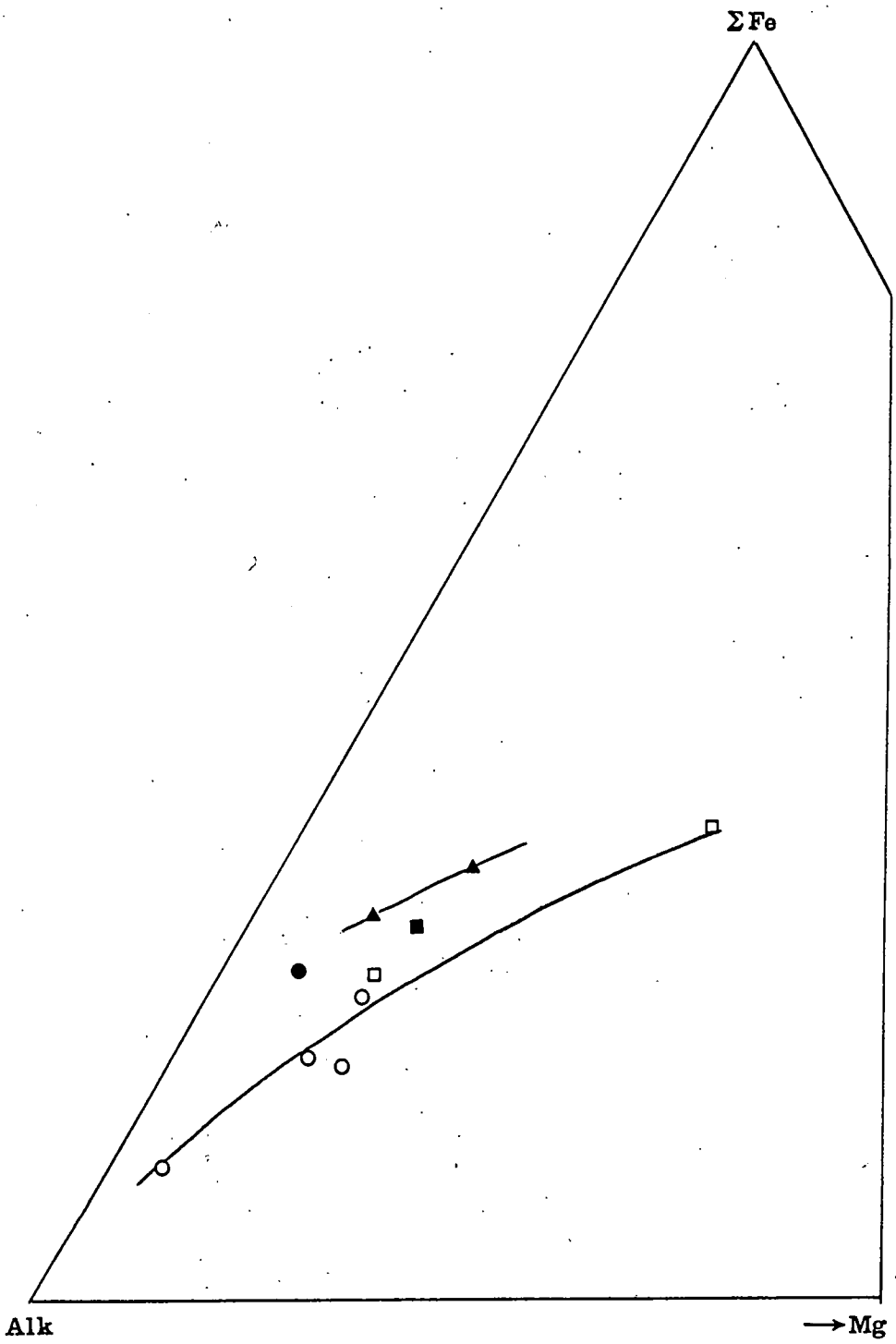

Variation in composition of Ljosland ○ , Åseral □ ,& Haddeland ▲ intrusions together with Barth's (1960) average L-farsundite ■ & average M-farsundite ● .

Figure 2

Middlemost (1968) to be linked with the other rocks of the anorthosite kindred in south-west Norway. He postulates that the whole complex originated from a gabbroic-dioritic magma by a process of seismically assisted 'magma-mush-sieving' below a relatively rigid upper crustal layer. He envisages that this process would result in the downward migration of mafic phases and the upward movement of the more volatile elements leaving a residuum of essentially interlocking feldspar crystals. The granitic differentiate at the top of the magma chamber then migrated along planes of weakness with significant lateral as well as upward movement, assimilating some of the predominantly granitic country rocks. The south-eastern part of the intrusion, the most mafic in composition is considered by the above author to have been emplaced first with subsequent fractions being progressively enriched in silicon and potassium towards the north.

The resemblance between the Ljosland, Åseral and Haddeland intrusions and the farsundite is so marked that a common origin must be considered. This implies on the above petrogenetic model the existence of rocks of the anorthosite kindred beneath the gneisses of the area surveyed by the present author.

Abundant mafic gneiss xenoliths are found both in the Ljoland and Åseral intrusions and farsundite, the majority with sharp contacts as in plate 10b, but some in more advanced stages of assimilation. Granitic gneiss inclusions are much less common than the basic rocks even though the amount of granitic gneiss in the country rock far outweighs the amount of amphibolite. A few

exposures of the Ljosland intrusion exhibit considerable heterogeneity, though clearly recogniseable partially assimilated granitic gneiss has not been observed. A quantitative estimate of the amount of country rock assimilated by the intrusions is thus not feasible.

6. THE BASIC DYKES.

Basic dykes of the area are divided into four groups on the basis of their texture and mineralogy. These are a) thin discordant bodies of amphibolite with mineral orientation parallel to the regional structure ; b) impersistent dykes of irregular shape with a metamorphic mineral assemblage but without well developed mineral orientation ; c) thicker linear persistent dykes with a metamorphic mineral assemblage and a fine-grain granular texture with a few lath-shaped plagioclase megacrysts and d) persistent linear dykes with igneous mineral assemblages and textures upon which is superimposed a later phase of mineral growth.

a) Amphibolite dykes exhibiting regional mineral orientation.

A few thin discordant amphibolite dykes have been observed within the massive phenoblastic granitic gneisses, particularly at the head of Litladalen, to the south of Knaben. These dykes are irregular in shape and thickness with bulges that fish-tail along foliation planes into the surrounding granitic gneisses. They are also penetrated by feldspathic veins of various grain-sizes. Biotite in the dykes is orientated parallel to the regional foliation of the country gneisses. Mineralogically the rocks resemble amphibolite horizons within the Knaben gneiss.

b) Impersistent and lensoid metamorphic dykes.

The majority of these dykes are less than two metres wide but a few thicker bodies have also been found. A relatively thick dyke of this type is exposed in the road cut just south of Tonstad. It is without much internal mineral orientation except for a few shear planes and is sharply discordant to the layered granitic gneisses into which it was emplaced. The dyke has also been invaded by thin feldspathic veins from the surrounding granitic gneiss so that both rocks intrude each other. The dyke rock contains a little quartz, andesine, reddish biotite, clino-pyroxene and orthopyroxene and bears strong resemblance to pyribolite horizons in the Lervig gneiss. This dyke must therefore have been emplaced before the end of the metamorphic episode that produced the regional gneisses, the waning stages of which saw the production of pegmatitic fractions in the granitic gneisses. Several thinner dykes within the Lervig gneiss show a very strong mineralogical resemblance to the pyribolites of that unit with the presence of hornblende with a brown (z)-axial colour in addition to biotite and the two pyroxenes. Other dykes similar in form have retrograde mineral assemblages with altered plagioclase, chlorite, epidote and iron oxide. All of these dykes can only be traced for a few metres along the strike.

A few examples of biotite-rich dyke rock also occur. Within the migmatitic gneiss at Sandvatn is an irregular lensoid body of a dark biotite-rich rock with subordinate quartz, andesine, hornblende and orthopyroxene. The biotite tends to show some orientation parallel to the boundary of the dyke. Bugge

(1963) mentions a similar biotite-rich dyke some ten metres wide within the Knaben mine workings. This rock is not exposed at the surface and consists of biotite and plagioclase with a little clinopyroxene, sphene, apatite and ore with accessory hornblende and quartz.

c) Persistent dykes with metamorphic mineral assemblages.

Two examples of these linear dykes have been discovered. One can be traced for some four kilometres to the west of Stakkeland. This dyke contains abundant lath-shaped strained but unzoned plagioclase together with granular hornblende, clinopyroxene and orthopyroxene. A similar dyke can be traced for some eight kilometres to the east-north-east from a point about three kilometres to the north of Knaben. This dyke has a fine grain margin consisting of a granular aggregate of plagioclase and hornblende and a coarser-grain central rock containing biotite, opaque minerals and orthopyroxene in addition. A few large euhedral plagioclase crystals are scattered throughout the dyke. Feldspathic veins from the surrounding granitic gneiss also penetrate the margins of this dyke. These rocks must have been emplaced at approximately the same time as the less persistent dykes of the previous group.

Antun (1962) describes two subvertical east-west dykes from the Ørsdalen area very similar in appearance to the above intrusion. They also carry a few large plagioclase phenocrysts and a fine granular margin with plagioclase, orthopyroxene and

ore. The central part of the dyke contains biotite, hornblende and clinopyroxene in addition.

d) Persistent dykes with igneous texture and mineralogy.

Three examples of these dykes have been discovered in the present area. The longest can be traced from south of Tonstad a distance of 27 kilometres to the east-north-east. A typical specimen of this intrusion consists of an aggregate of zoned lath-shaped plagioclase crystals with moderately fresh highly-pleochroic orthopyroxene. Some of these grains are mantled with rather altered clinopyroxene. Between the feldspar laths are also a few small granular grains of fresh clinopyroxene. Scattered tabular crystals of ilmenite, often surrounded by clusters of rather dusty brown biotite and a little chlorite, also occur. Parts of the dyke are more altered, particularly in the eastern part of its outcrop. A specimen from Knabedalen (Plate 11a) illustrates this rock type with more altered pyroxenes, particularly the orthopyroxene cores which are shot through with iron oxide grains. In this specimen the small granular pyroxenes are also rather more abundant as are the sheaves of biotite round the ilmenite and larger pyroxene grains.

The contacts of the dyke are well exposed in Knabedalen. The margin of the dyke is much finer in grain than the central portion and contains a few plagioclase phenocrysts set in a fine granular matrix of plagioclase, epidote and chlorite. The dyke is in contact with massive phenoblastic granitic gneiss (Plate 11b)

Plate 11.

Plate 11a.

Photomicrograph in plane polarised light of Knaben dyke from lower part of Knabedalen. The section contains zoned lath-shaped plagioclase grains, dark cloudy aggregates of orthopyroxene and a few clearer granules of clinopyroxene, thin plates of ilmenite and small dark biotite grains which on the photograph are almost black. A clump of biotite surrounds the large ilmenite grain in the upper left corner of the section. Magnification x 8.

Plate 11b.

Polished slab measuring 6cm. by 8cm. of the contact of the Knaben dyke with granitic gneiss from the lower part of Knabedalen. The central layer of the specimen consists of lensoid fragments of the coarse-grain feldspathic gneiss set in a matrix of altered dyke rock consisting mostly of epidote with a little chlorite. The boundary of the epidotisation can be discerned in the fine-grain chilled marginal dyke-rock.

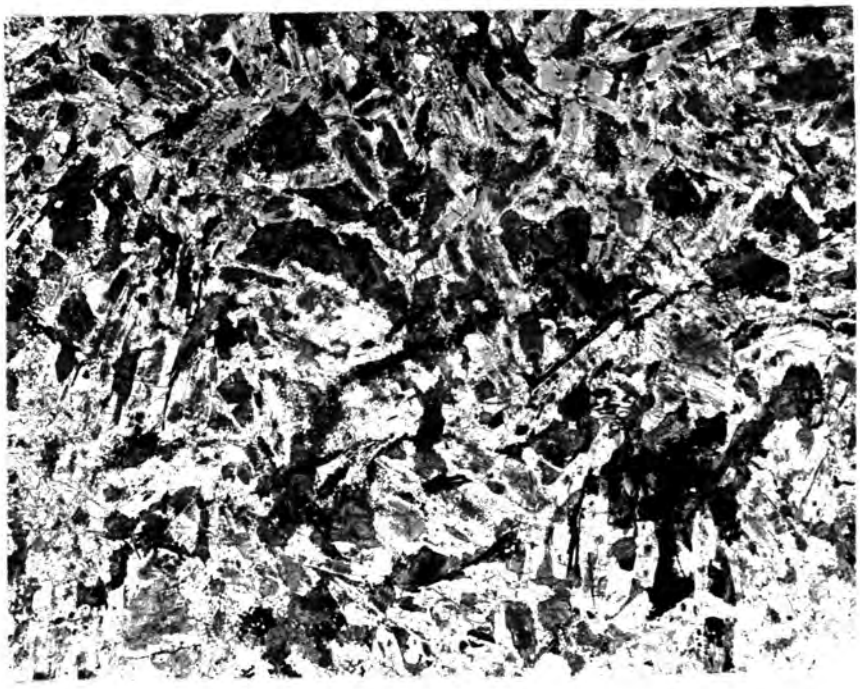

a

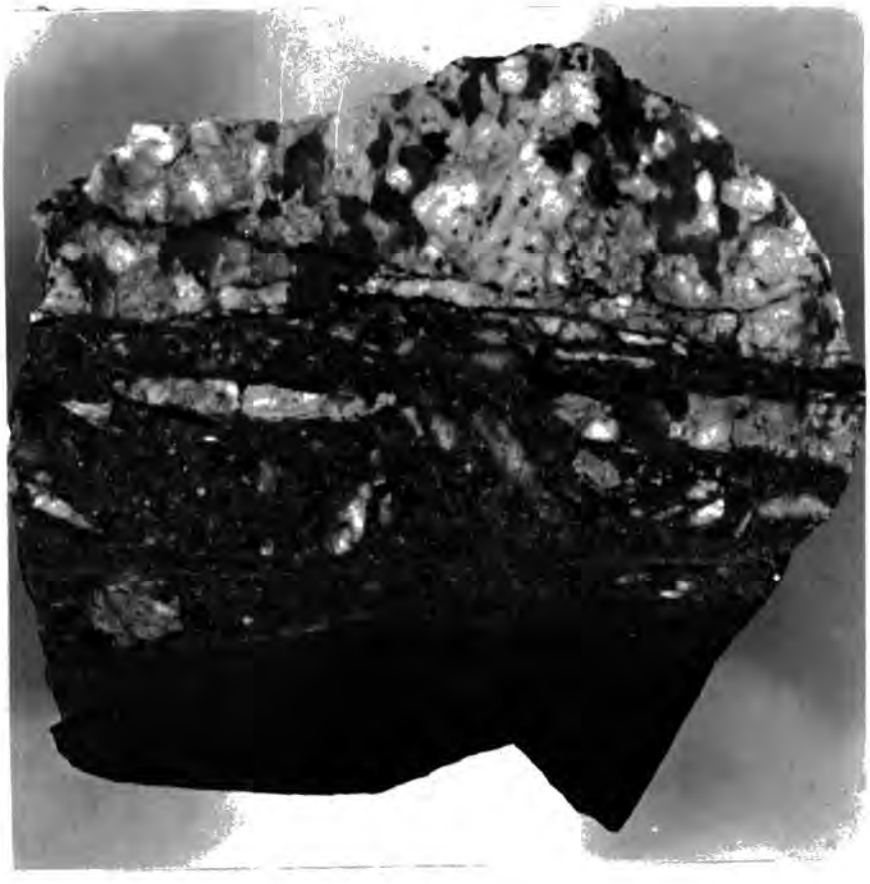

b

Plate 11.

with a thin zone of mixed rock between. The mixed rock consists of rounded aggregates of quartz and feldspar in a matrix of epidote and a little chlorite. Some of these quartzofeldspathic inclusions have recrystallised into fine granular crystals. The margin of the granitic gneiss is rather altered with a few patches of epidote and chlorite and a few veinlets of fine granular feldspathic rock.

The chemical composition of the coexisting minerals in a similar specimen of dyke rock from just north of Knaben have been analysed with the electron microprobe. The plagioclase is zoned from rim to core from An 30 % to An 42 %. The fresher parts of the orthopyroxene cores of the larger grains are ferrohypersthene with a composition of (Mg_{39-42} Ca_3) though this does not represent the primary composition because of the widespread unmixing of iron oxide during the second phase of mineral growth. The fresher clinopyroxene rims are augite with an atomic composition of (Fe_{24} Mg_{35} Ca_{41}). The small granular pyroxene grains are similar in composition except that the orthopyroxene is less calcic. The biotite of this dyke rock is about 2% richer in aluminium and correspondingly poorer in silicon than most of the biotites from the regional metamorphic rocks.

The northernmost dyke is very similar mineralogically to the southernmost dyke described above. The central dyke differs from the other two in the presence of olivine, fresh except for iron oxide-filled cracks. The plagioclase shows well-developed compositional zoning of the same order as the southern dyke. Both clinopyroxene and orthopyroxene are also present and similar in appearance to the Knaben dyke minerals.

Clusters of fresh red-brown biotite are also present. A specimen of intermediate gneiss in contact with this dyke contains a micrographic intergrowth of quartz and orthoclase formed probably after partial remelting of the rock.

Barth (1960), quoting from Antun (1956), states that there are several dolerite dykes with chilled margins in the Rogaland anorthosite province. The dykes are often multiple and vary in composition from olivine dolerite to trachydolerite. On the silica - total alkalies diagram, in figure 3, two groups can be distinguished on alkali content. Carstens (1959) describes lamprophyres in close association with diabases along the coast to the west of Kristiansand and near Arendal. The lamprophyres contain anorthoclase, hornblende, clinopyroxene and chlorite as dominant silicate phases. Associated with these rocks are diabases of two types, one with labradorite, clinopyroxene and chlorite, the other with quartz, oligoclase and perthitic orthoclase with trachytic texture and rather altered clinopyroxene. There are chemical similarities between the igneous dyke analyses in table 2 and the lamprophyre analyses quoted by Carstens (op. cit.) viz. high titanium, sodium and potassium contents. The similarity in alkali contents is illustrated in figure 3.

Carstens (1959) postulates that the lamprophyres originated as volatile-rich differentiates of a basic magma which accumulated at the top of the magma chamber. In addition to being alkali-rich the differentiate has a high content of carbon dioxide. Oftedahl (1957) on the other hand proposes that lamprophyres are formed after assimilative reactions between normal basic magma and

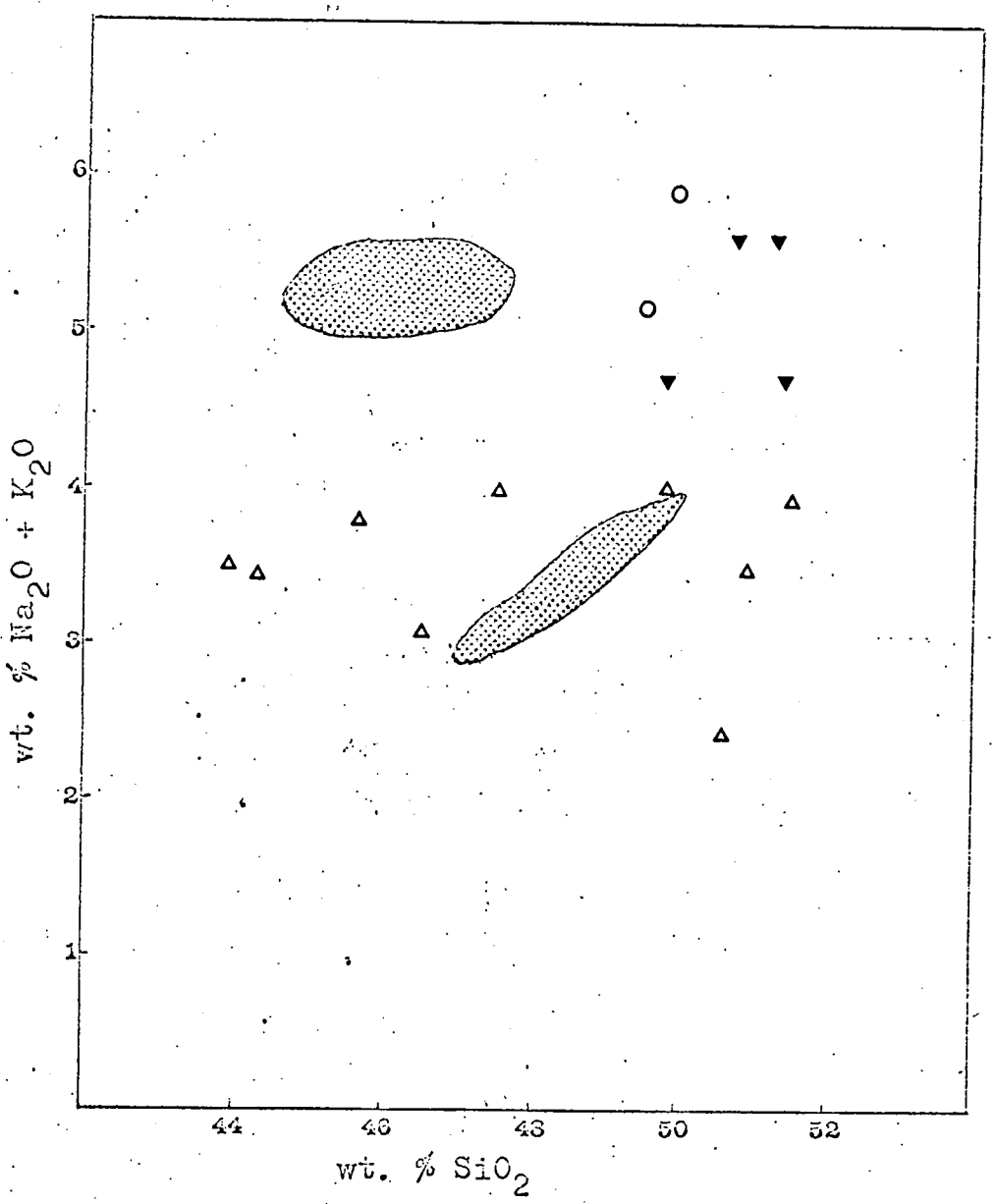

Variation in silica and total alkali contents of basic dykes in the PreCambrian of S.Norway. Shaded areas represent two conjugate groups of olivine dolerite from Rogaland, △ = labradorite diabases, ○ = lamprophyres and ▼ = author's dykes. (Modified after Barth 1960).

Figure 3.

granitic and pelitic wall rocks.

Though the texture of the three dykes encounted by the present author is predominantly doleritic, the chemistry, the presence of two generations of pyroxene and the relatively high biotite content, particularly of the easternmost specimen of the Knaben dyke, indicate some similarity with lamprophyres. The graphic quartz-feldspar intergrowth observed at localities along the contact of the dyke with granitic gneiss suggest that some alkalies may have been assimilated into the dyke from the country rock though the magnitude of the process would appear small in the observed environment of high-grade gneisses.

7. THE STRUCTURE.

Prior to this work, the area between Sirdal and Åseral had been cursorily examined by Barth (1945) as part of a general survey of the PreCambrian of southern Norway. This sector was considered by him to consist predominantly of north-south-striking gneisses dipping monotonously to the east. The present author's research has revealed that this apparent uniformity conceals great structural complexities which can only be unravelled by detailed mapping, especially by following marker horizons along their strike. Basic gneiss horizons form convenient markers as do the thinner granitic gneisses in a predominantly layered gneiss sequence. On a mesoscopic scale it has proved impossible to follow individual gneiss layers in a heterogeneous sequence for more than a few metres.

The planar elements of the fabric of the gneisses are lithological layering and a foliation produced by parallel orientation of biotite flakes and sometimes flattened feldspar and quartz grains. These two features are always parallel except for the early 'arrowhead folds' (Plate 12). These structures have sheared limbs and an axial plane foliation. The gneissic layering and foliation can be traced round the noses of all other folds and secondary planar structures have not developed. It cannot be assumed that the lithological layering necessarily represents original sedimentary stratification, particularly as no definite primary structures have been recognised. Falkum (1967), on the other hand, has found a gneiss horizon at several places in the Flekkefjord area with a structure that he interprets as original graded bedding.

Plate 12.

Plate 12a & b.

Arrowhead fold relics of mafic gneiss in leucocratic Feda augen gneiss from road sections to north of Haughom.

Plate 12c.

Arrowhead relic of feldspathic rock in basic gneiss layer within Feda augen gneiss from west of Tonstad.

Plate 12d.

Granitic gneiss with thin spindles of basic rock showing parallel orientation from within Feda augen gneiss in road section north of Haughom.

Plate 12e.

Relic minor folds in layered biotitic and feldspathic gneiss horizon within Feda augen gneiss near Sporkland.

Plate 12f.

Crenulated minor folding shown by thin feldspathic gneiss layer within Feda augen gneiss near Haughom. The type of fold is similar to structures of F 2 age in the Flekkefjord Series (see plate 14).

Plate 12g.

Intrafolial fold within the Tonstad gneiss to the south of Tonstad with axis oblique to the regional foliation.

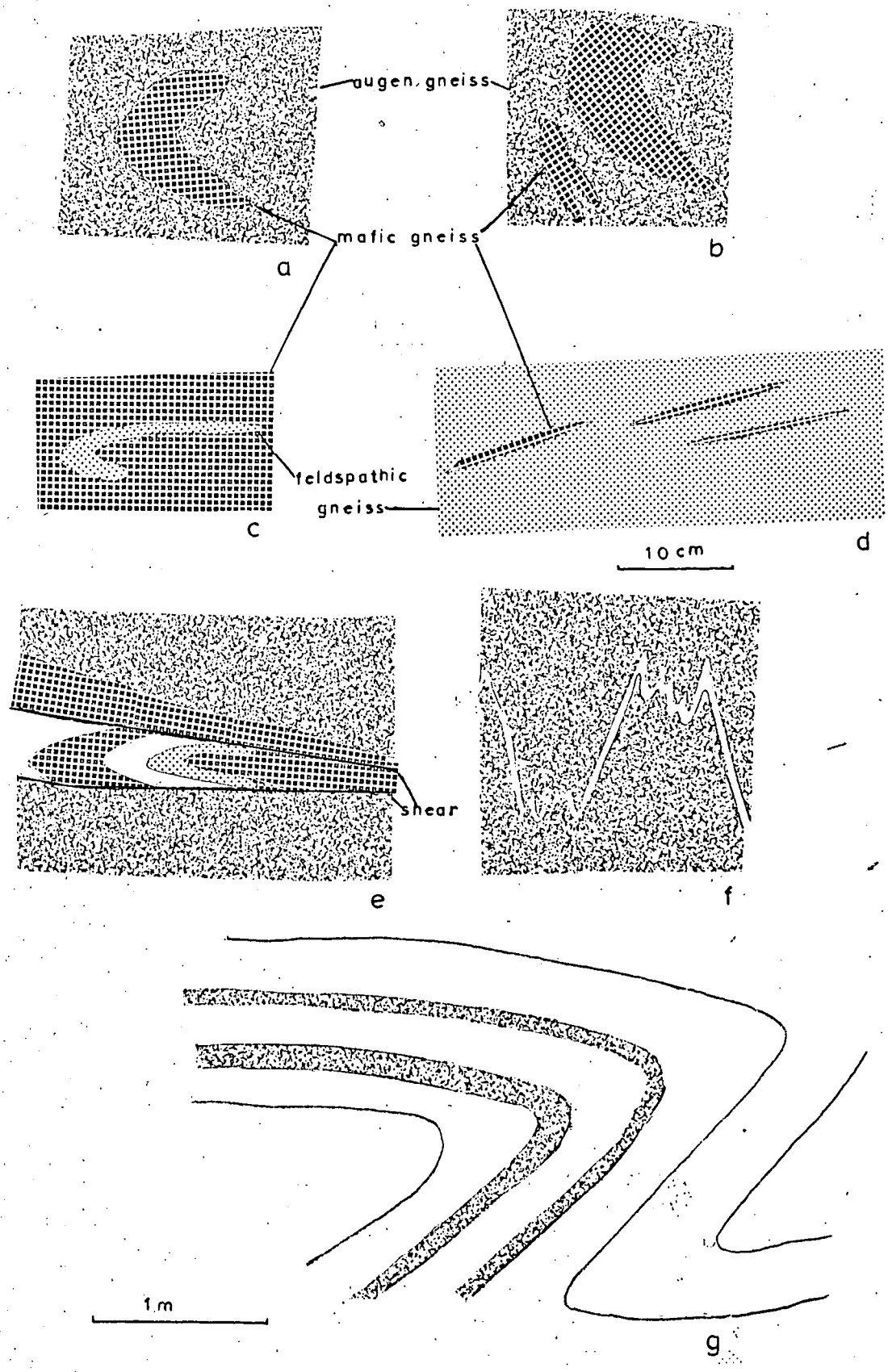

Minor structures in Sirdalsvatn Series

Plate 12.

The linear elements of the gneiss fabrics are minor fold axes and parallel orientation of prismatic minerals like hornblende. Measurement of these lineations is often difficult on the flat and rounded weathered outcrops of the upland regions. Statistical plots of linear structures are generally more random than for the planar structures but maxima and partial girdles have been recognised. Minor folds are rare in many of the more siliceous gneisses but are usually frequent in the more basic layered gneisses. The great complexity of this folding is often only apparent in the larger fresh roadside exposures.

The PreCambrian gneiss complex between Sirdal and Åseral has been divided into 6 tectonic units and 15 subunits on the basis of major structures. The boundaries of these subunits are shown on the accompanying structural map. The major structures of each subunit together with any noteable minor structures are described in sequence below.

a) Unit 1a.

This unit comprises the extreme south-west of the area, adjacent to Sirdalsvatn. A synform, the core of which is occupied by the small feldspar facies of the Feda augen gneiss,and an antiformal nose in the surrounding layered basic and feldspathic gneisses are the major structures. These layered gneisses on the western side of the main outcrop of the Feda augen gneiss can be correlated with the Lervig layered gneiss on the evidence of Falkum (1967) in the Flekkefjord area. They have been traced round the antiformal closure of the augen gneiss on the south coast near Feda. Only part of the

antiformal closure of the Lervig layered gneiss is exposed on the eastern side of Sirdalsvatn. Information supplied by the Telemark Project geologists Dahlberg and Hermans (personal communication) indicates that a thin outcrop of basic layered gneiss outcrops on the western shore of the lake and closes towards the east. Furthermore the outcrop of augen gneiss in the synformal core widens on the western side of Sirdalsvatn and then swings round the antiformal nose to join with the main outcrop of the Feda augen gneiss on the eastern side of the lake.

The axis of the antiform trends roughly north-north-west and plunges gently (5-10°) in the same direction. The axial plane of the fold dips about 35° to the east. The axis of the augen gneiss synform trends roughly parallel to the antiform at the closure but further north it swings round to the east, round the antiformal closure into the main outcrop of the Feda augen gneiss. The synformal axis plunges at a slightly steeper angle (15-20°) than the antiformal axis.

It is concluded that the augen gneiss synform represents an original isoclinal fold refolded around the antiformal axis in the Lervig gneiss. It is apparent from the work of other Telemark Project geologists, in particular Dahlberg (personal communication), that the Feda augen gneiss is refolded around other folds in the surrounding gneisses to the west of its main outcrop. The refolded augen gneiss on the north-western side of Sirdalsvatn, mapped by Dahlberg appears to be a tongue rather than an isoclinal fold however.

There is little sign of minor folding within the Feda augen gneiss within this unit, though some broader fluctuations in strike direction are apparent. The potassium feldspar crystals are randomly orientated as are other prismatic minerals. There is abundant minor folding in the surrounding Lervig layered gneiss however, generally with rather open U-shaped noses. These folds mostly trend parallel to the major antiform and plunge gently either north or south. The plot of foliation poles from the unit shows a maximum with a suggestion of two partial girdles.

b) Unit 1b.

This unit comprises the main outcrop of the Feda augen gneiss and Tonstad gneiss to the south of Haughom. The main structure in the unit is a tight, isoclinal, flat-lying antiform, the core of which is occupied by granitic Tonstad gneiss. The axis of the fold trends roughly to the north-north-west just north of the closure but just west of Sandvatn it swings round to a more northerly direction. The axial plane of the fold is roughly parallel to the regional foliation in the unit and dips to the east at about 40°. Figure 4 shows the plot of foliation poles in this tectonic subunit which are concentrated in a maximum but also extend into a girdle with a very flat B-axis trending north at a very low angle. The stereogram also shows the elongation of the maximum into a partial girdle trending about N 30° E and plunging at about 35°.

Minor-scale folding in the Sirdalsvatn Series in this unit is relatively rare though the strike of the foliation fluctuates considerably. A few folds with open U-shaped closures and flat axes

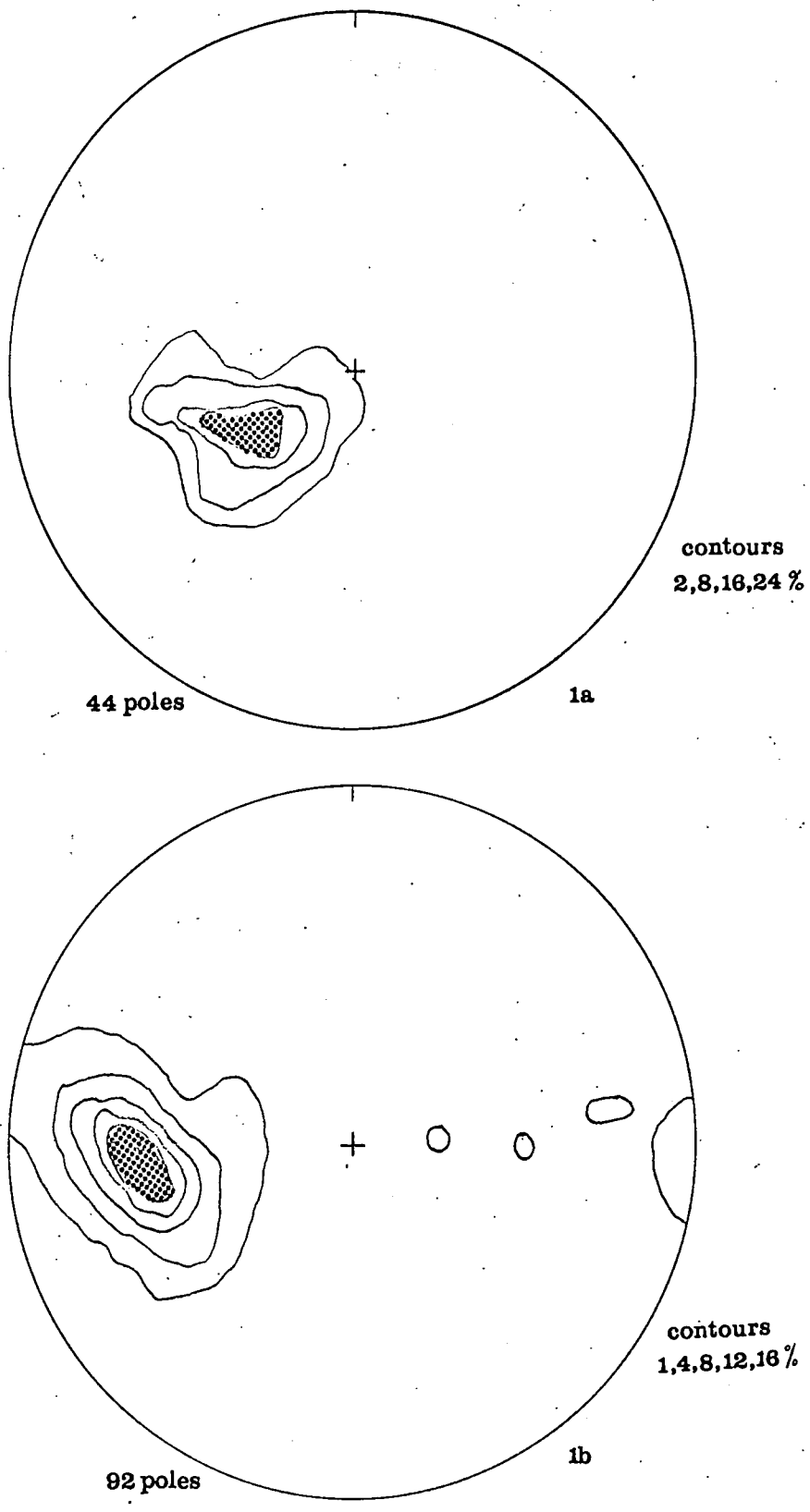

Stereograms showing distribution of poles to foliation in tectonic sub-units 1a & 1b.

Figure 4

trending roughly parallel to the regional foliation have been observed but more obvious are a series of folds and S-shaped flexures with axes trending to the north-east. The axes of these folds plunge at about 30° to the north-east and they can be correlated with the major S-fold in unit 2a.

At fresh exposures of heterogeneous and layered Feda augen gneiss remnant arrowhead folds can often be observed. Plate 12 illustrates these structures in the Feda augen gneiss to the east of Sporkland. A thin layer of finely banded biotite-rich gneiss contains a thin arrowhead nose of more feldspathic rock. An adjacent more feldspathic gneiss layer contains a similar nose outlined by a thin biotitic horizon. An incipient axial plane foliation is developed through the more mafic parts of these noses. These structures represent remnants of the earliest recognisable isoclinal folding on a minor scale within the Sirdalsvatn Series and have been designated F 0 minor folds.

c) Unit 1c.

This unit comprises the main outcrop of the Sirdalsvatn Series to the north of Haughom. There are no major fold noses exposed though the outcrop of the Sirdalsvatn Series may represent the western limb of the continuation of the antiform in tectonic subunit 1b. The plot of foliation poles in this unit in figure 5 shows a clear maximum but also the trace of a great circle girdle with a B-axis trending about south 15° east with a very gentle dip to the south.

The Sirdalsvatn Series is well exposed in fresh road cuts both

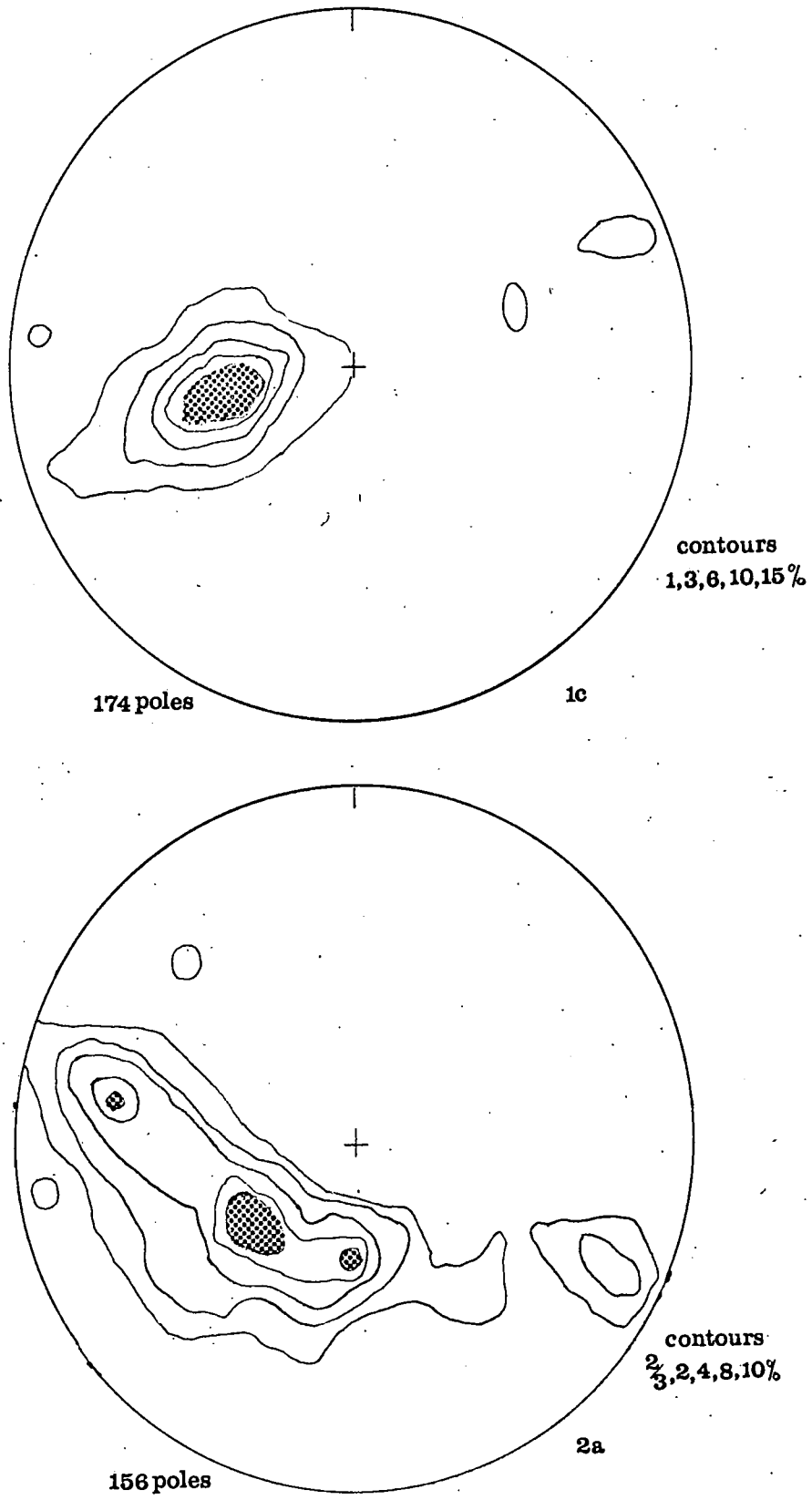

Stereograms showing distribution of poles to foliation in tectonic sub-units 1c & 2a.

Figure 5

between Haughom and Tonstad and west of Tonstad. Relic arrowhead fold noses with sheared limbs are widespread but never abundant and frequently take the form of an inclusion of mafic gneiss surrounded by more feldspathic rock. Very rarely a more extensive fold relic can be observed within the more heterogeneous parts of the Feda augen gneiss. At Haughom a series of V-shaped folds with many smaller scale corrugations along the hinges occurs in a body of augen gneiss surrounded by more mafic gneiss (see plate 12). These folds have almost horizontal axes and vertical axial planes striking parallel to the regional foliation of the gneiss. Isoclinal U-shaped minor folds occur in thin feldspathic layers within some of the more basic horizons of the Sirdalsvatn Series. They have flat-lying axes and steeply east-dipping axial planes striking parallel to the regional foliation and are probably of later age than the V-shaped folds. An isolated example of a further type of minor fold occurs in the Tonstad gneisses just south of Tonstad and is illustrated in plate 12. The fold is an S-shaped flexure with an axis oblique to regional foliation, plunging gently to the south-east. This is of later origin still and may be related to the movement producing the Sandvatn S-fold. Broad east-west-trending flexures with an easterly plunge are widespread on both the minor and mesoscopic scales.

Hornblende shows almost horizontal linear orientation in some of the basic gneisses of the Sirdalsvatn Series in this unit and trends roughly north-south. Within some of these basic gneisses there are also spindles of feldspathic rock, also with roughly horizontal linear orientation. In addition to arrowhead fold relics some of the more layered parts of the Feda augen gneiss contain thin spindles of mafic gneiss orientated parallel to the foliation of the

rock and close to horizontal. The measured lineations from all three subunits of the tectonic unit 1 are grouped together in stereographic projection in figure 6 because of the paucity of data for each subunit. The plot shows concentrations trending just west of north and plunging either gently to the north or south and roughly parallel to the B axis of the Sandvatn S-fold at N 30 E and a plunge of about 30-20° to the north-east. Other lineations are scattered over the stereogram.

d) Unit 2a.

This unit comprises the complementary antiform and synform which form the Sandvatn S-fold. The synform is the most obvious major structure in the whole area and is clearly visible on aerial photographs. The reclined nature of the two folds in this tectonic subunit distinguishes them from all other major structures in the area. Associated with this structure are well developed mineral orientation, crinkle and minor fold-axis lineations, particularly in the Lervig gneiss. The plot of poles to foliation in the subunit, shown in figure 5, shows a well developed great circle girdle. The plot of the lineations in the subunit is shown in figure 6 and shows a strong maximum coinciding with the B-axis derived from the great circle girdle of foliation poles.

The Lervig gneiss in the nose of the antiform is well exposed in the Sandvatn area. Minor folding is both abundant and complex and three major varieties have been recognised. A few tight isoclinal folds with axial planes parallel to the regional foliation occur but these have often been refolded in the same way as the gneissic

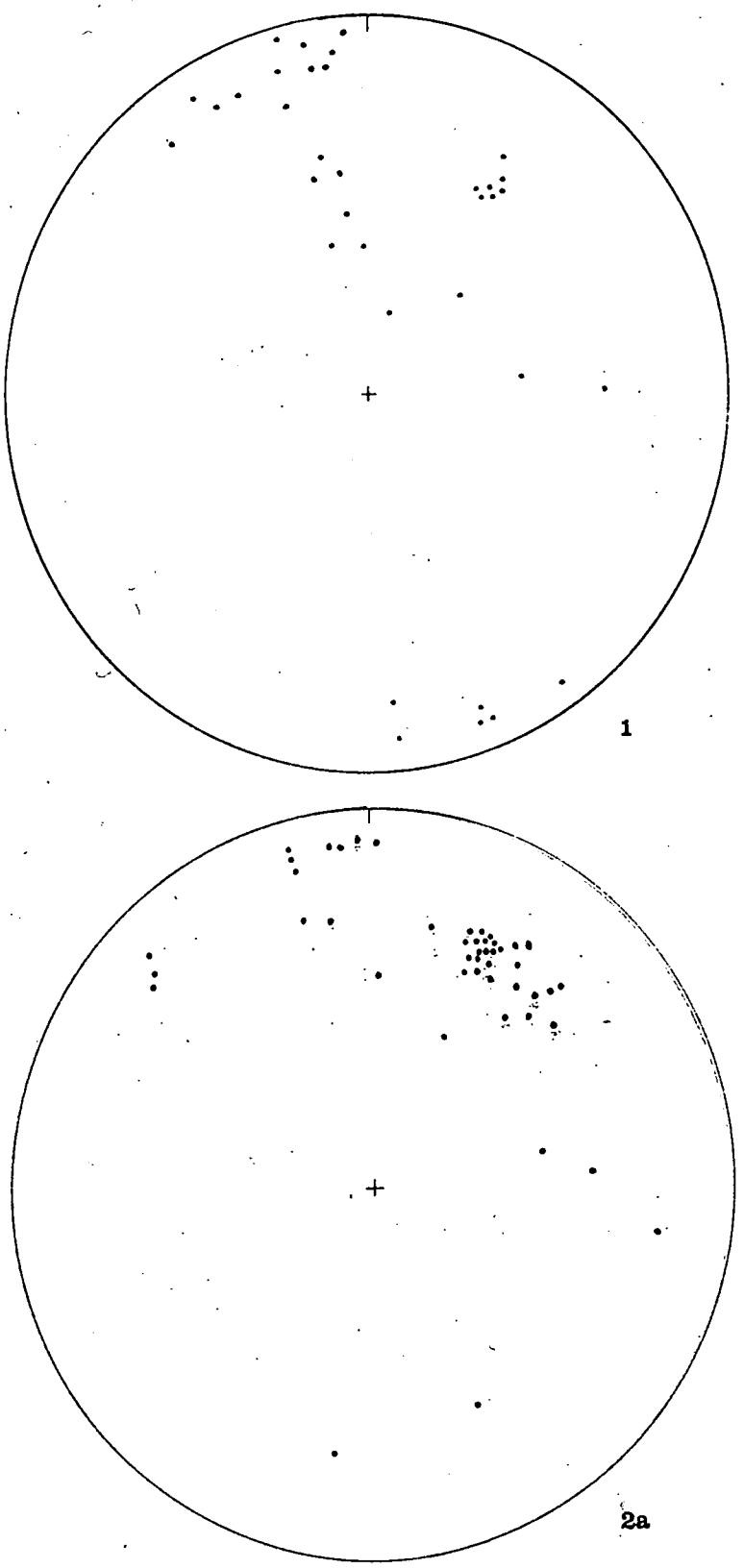

Stereograms showing distribution of lineations in tectonic units 1 & 2a.

Figure 6

layering. Closely spaced isoclinal v-shaped folds, showing considerable variations in axial plane orientation from exposure to exposure, are numerous and sometimes refold the tighter isoclines though there is little divergence in fold axes between the two. Of clearly different origin and age are a series of small scale flexures, often isolated, with roughly constant fold axes parallel to that of the major folding. The interference of these folds with the other varieties produces complex geometrical patterns some of which, together with the normal fold styles, are illustrated in plate 13. More irregular styles of folding also occur particularly in the coarser grain neosomal layers which are abundant in the antiformal core.

Much of the nose of the synform in this subunit is obscured by the end moraine (plate 3) so that few minor structures have been observed, though north-east plunging flexures are widespread.

e) Unit 2b.

This unit comprises the main complex of the Lervig gneiss, stretching from north of the S-fold in unit 2a to the Råtagangen crush zone, west of Tonstad. Granitic gneiss horizons in the predominantly basic layered Lervig gneiss have been used as marker horizons in the elucidation of the structure of this tectonic unit. A major antiform occurs on the eastern side of the unit with an axis trending just west of north and plunging gently to the north. The axial plane of this fold strikes parallel to the regional foliation in the area and dips to the east at 40^{o}. West of this fold there are several other parallel folds of smaller amplitude within the

Plate 13.

Plate 13a.

Refolded isocline in layered garnetiferous, biotitic and feldspathic gneisses from the Lervig gneiss near Sandvatn. The garnetiferous gneiss occupies the core of a presumed F1 isoclinal fold and is surrounded by layered biotitic gneiss. Superimposed on this fold are a series of V-shaped isoclines with steep dipping axial planes of F 2 age. The axes of the two fold types appear very similar.

Plate 13b.

Near vertical section of two feldspathic horizons in finely-layered biotitic Lervig gneiss near Sandvatn showing F 2 folding. The axial surfaces are near horizontal.

Plate 13c.

Outcrop pattern of south-plunging, mesoscopic F 2 folds in Lervig gneiss north-east of Espetveit.

Plate 13d.

Outline of quartzofeldspathic gneiss layer within garnetiferous Lervig gneiss in near-horizontal outcrop north-east of Optedal, showing sharp similar F 2 minor folds.

Plate 13e.

Sketch of thin gneiss layer showing F 3 flexure superimposed upon flat F 2 isocline in Lervig gneiss near Sandvatn.

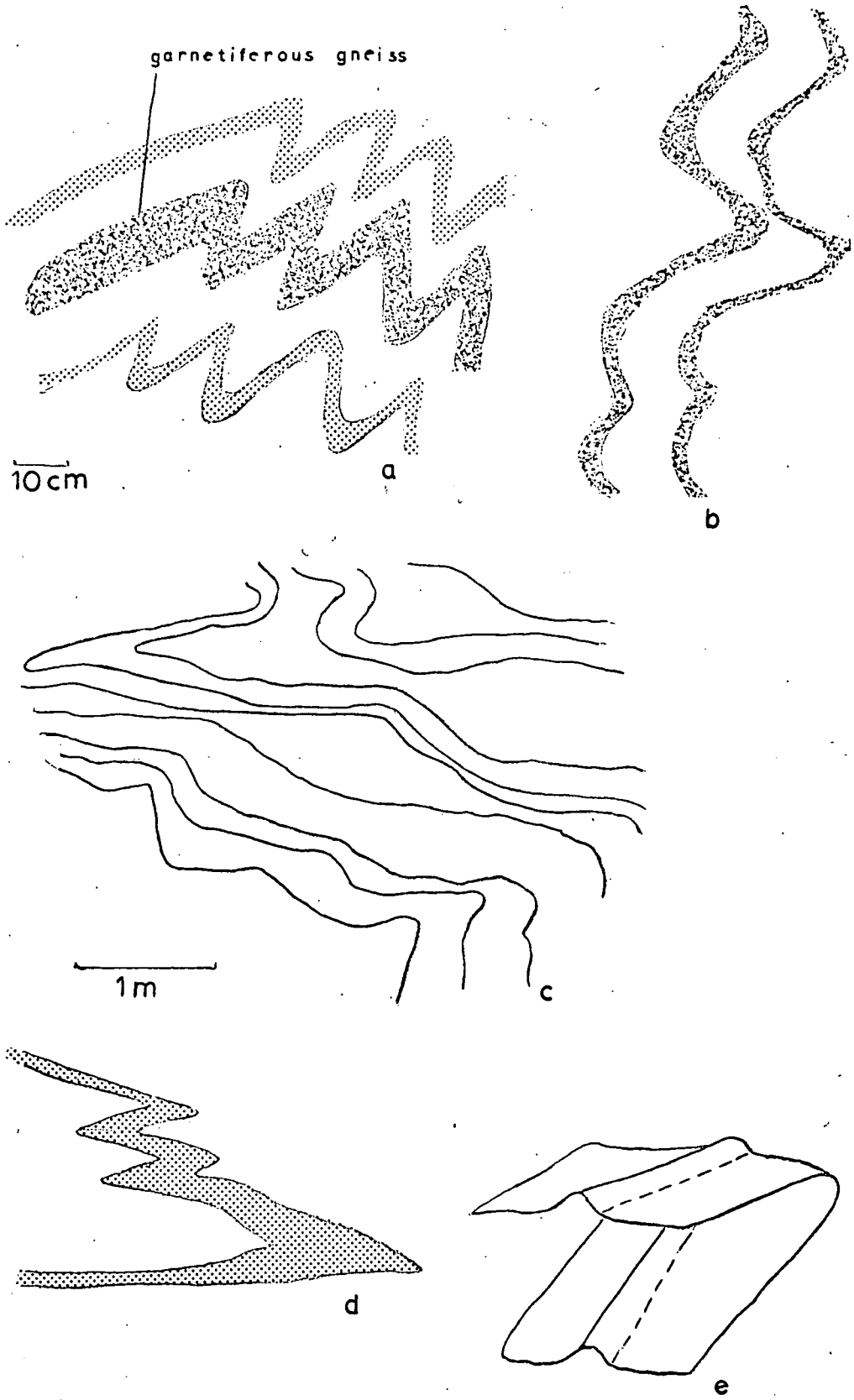

Minor structures in the Lervig gneiss.

Plate 13.

layered gneiss, though absence of any persistent marker horizon makes their precise delineation impossible. Granitic gneiss occupies the core of an antiformal fold of this category to the north-west of Kleivatn. Three bodies of granitic gneiss separated by thin layered gneiss horizons outcrop in the hinge zone of the antiform along the eastern edge of the subunit. A tight, flat-lying, mesoscopical isoclinal fold can be delineated in one of these bodies with an axis which swings round the main antiformal closure. It is possible that detailed structural analysis of this tectonic subunit may reveal other similar tight isoclinal folds which have been subsequently refolded. The plot of poles to foliation in the unit is shown in figure 7. It shows a prominant elongate maximum extending into a diffuse girdle with an almost horizontal roughly north-trending axis and a further great circle girdle of similar pattern to that for unit 2a. A plot of lineations from the area, shown in figure 8, includes concentrations trending just west of north with gentle plunges to north or south but is otherwise scattered.

Minor folding is both abundant and complex in the Lervig gneiss of this unit but in many parts of the area the flat or rounded exposures make precise geometrical measurements difficult. Both broad U-shaped folds and closer-spaced V-shaped folds are widespread. The garnetiferous gneisses on the western side of the area frequently exhibit sharp V-shaped folds of various amplitudes. The garnets of these rocks are mostly euhedral or subhedral and sharply discordant to the foliation defined by biotite orientation though a few lensoid grains surrounded by biotite also occur in the same exposures.

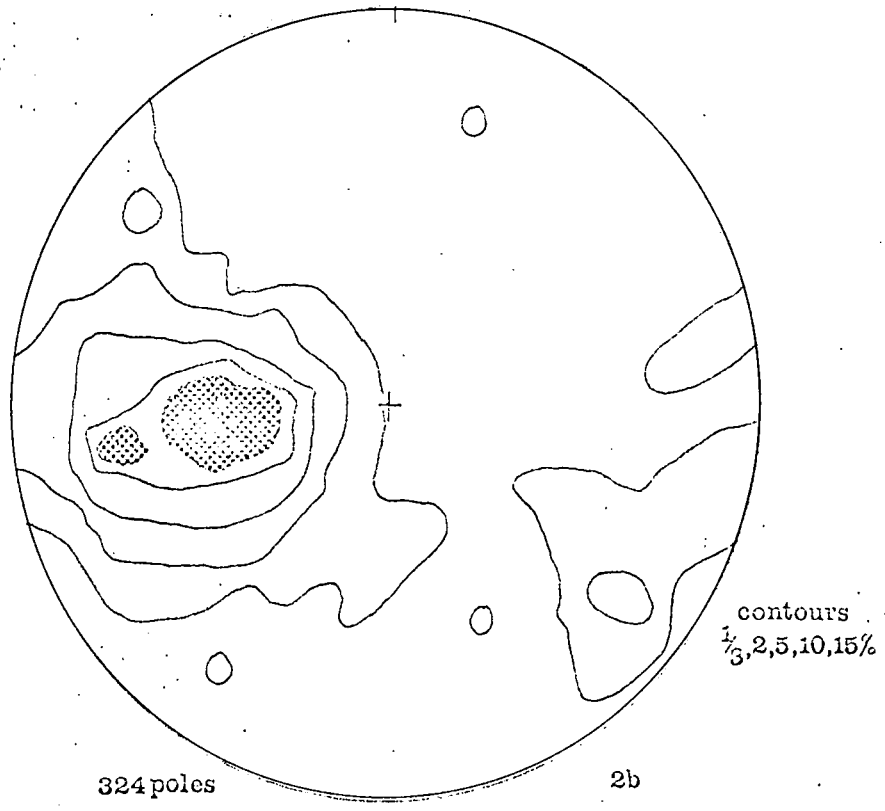

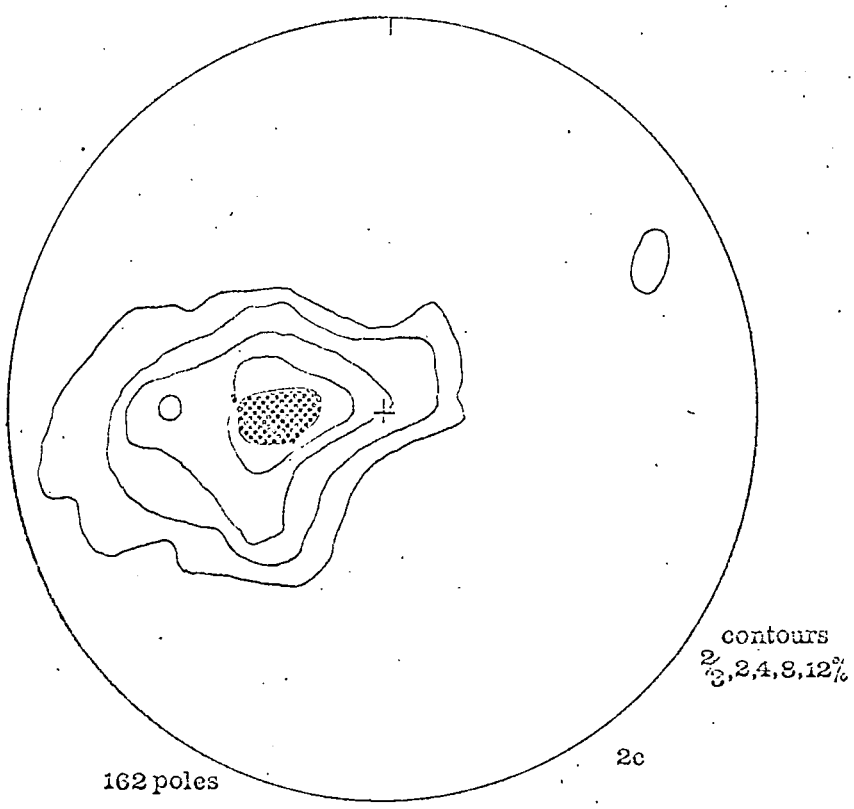

Stereograms showing distribution of poles to foliation in tectonic sub-units 2b & 2c.

Figure 7.

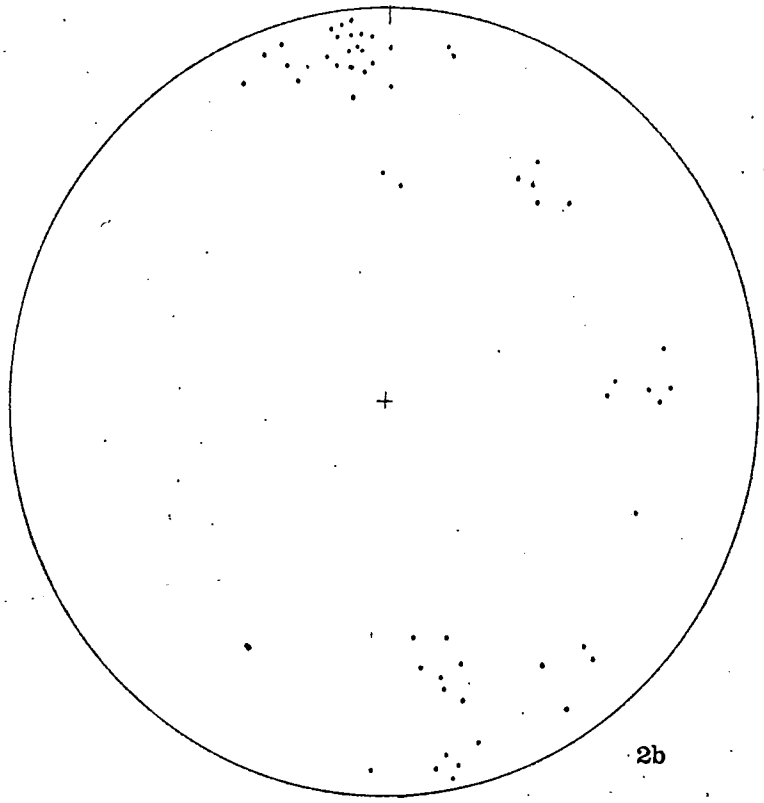

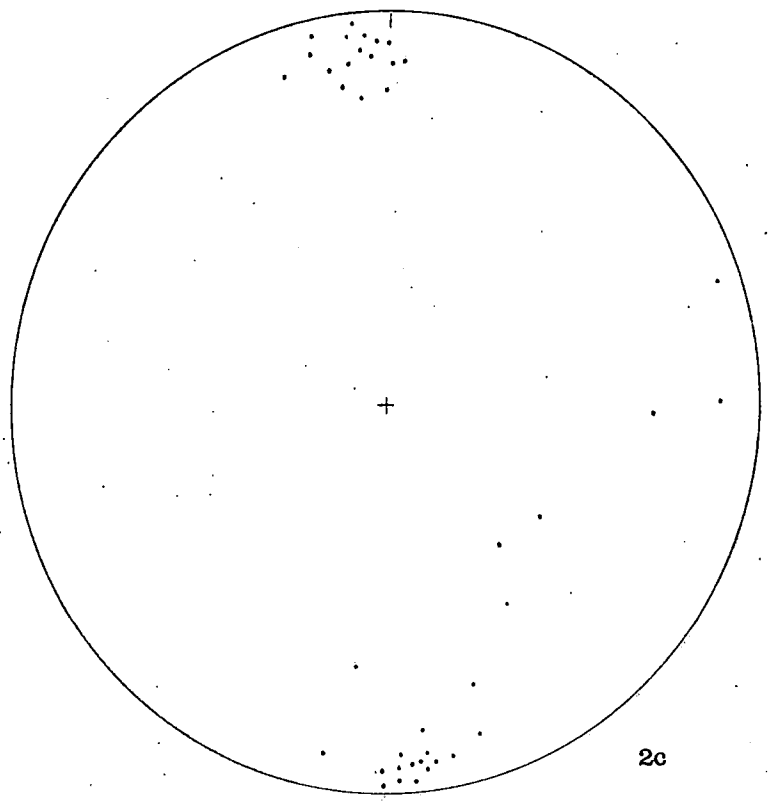

Stereograms showing distribution of lineations in tectonic units 2b & 2c.

Figure 8

f) Unit 2c.

This unit comprises the outcrop of the Lervig and Øie gneisses north of the Råtagangen crush zone. Within this area is a major antiformal fold, the core of which is occupied by a porphyritic gneissic granite surrounded by a layered basic gneiss horizon which has been provisionally correlated with the Lervig gneiss. The southern part of this fold is a very tight isoclinal structure with a very gentle plunge to the south on a north-south trending axis. North of the Guddal valley the core of the fold broadens considerably to accomodate the porphyritic gneissic granite. The axial plane of the fold dips eastwards at about 40° in the south but decreases to 15° in the northern sector of the subunit. The plot of foliation poles for this unit, in figure 7, shows a maximum and associated elongate area equivalent to a partial great circle girdle with a B-axis trending roughly south and almost horizontal. The plot of lineations in figure 8 shows a concentration of points trending just west of north on either side of horizontal.

The basic layered gneiss in the core of the antiform differs from the Lervig gneiss outcrop in the Sira valley in that the feldspathic component of the sequence is pegmatitic. The more basic layered horizons in the gneiss tend to occur as rafts or isolated layers within the granitic material and minor folding is infrequently observed. A few traces of rounded U-shaped folds in flat exposures of the adjacent Øie gneiss can also be seen. A few isoclinal minor folds with steep easterly-dipping axial planes and more irregular convoluted folds occur in the Lervig gneiss in the Sira valley. Thin biotitic layers within the garnetiferous granitic gneisses also show

traces of complex minor folding but these are too faint to reveal geometrical patterns.

g) Unit 3a.

This unit comprises the outcrop of the massive Kvinesdal granitic gneiss to the south of Netland together with the Lande gneiss to the west. This tectonic subunit contains no major fold closures but the plot of foliation poles for the area shows a maximum, elongated to suggest a partial great circle girdle with a B-axis plunging at a moderate angle to the east. This pattern, illustrated in figure 9, is an expression of the gentle, open east-west undulations on both major and minor scales observable throughout most of the area. An isolated north-east trending flexure occurs in the south of the area together with several minor folds with similarly orientated axes.

Minor folding is absent in the Kvinesdal granitic gneiss but can be observed in the adjacent layered Lande gneiss. Most of the folds are isoclinal with axial planes parallel to the regional foliation but a few flat S-shaped flexures with axes oblique to the regional strike have also been observed. Ptygmatic folds and other irregular convolutions occur in thin feldspathic sheets within the more basic horizons.of the Lande gneiss.

h) Unit 3b.

This unit comprises the outcrop of the Kvinesdal and Lande gneisses to the north of Netland. An open synform with an axis trending 15^{o} west of north and plunging gently to the south closes

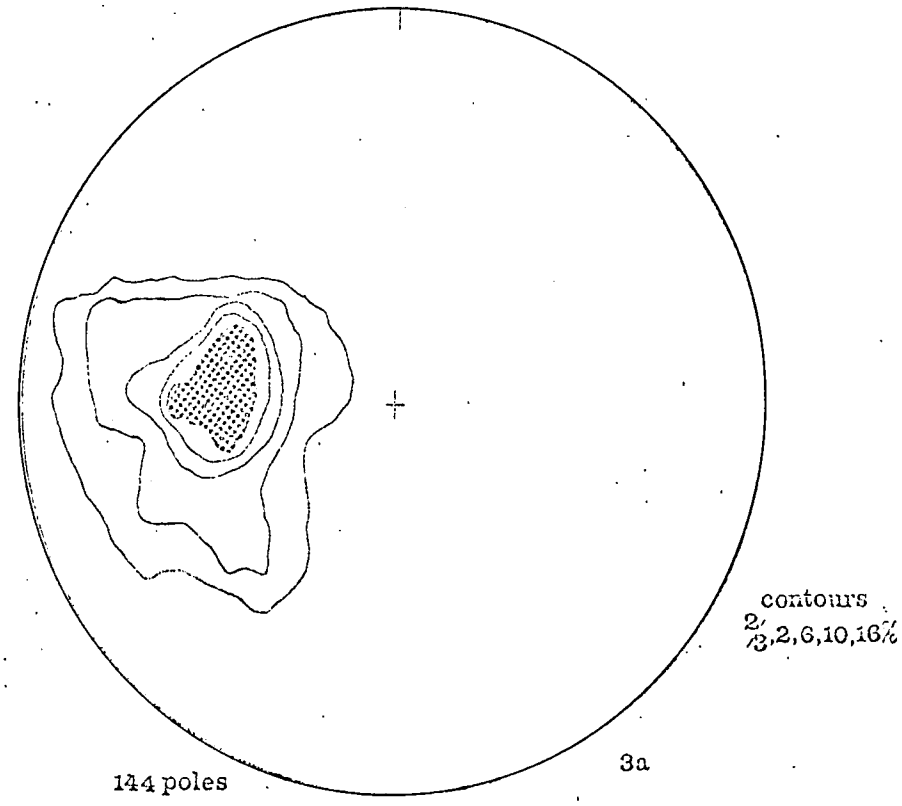

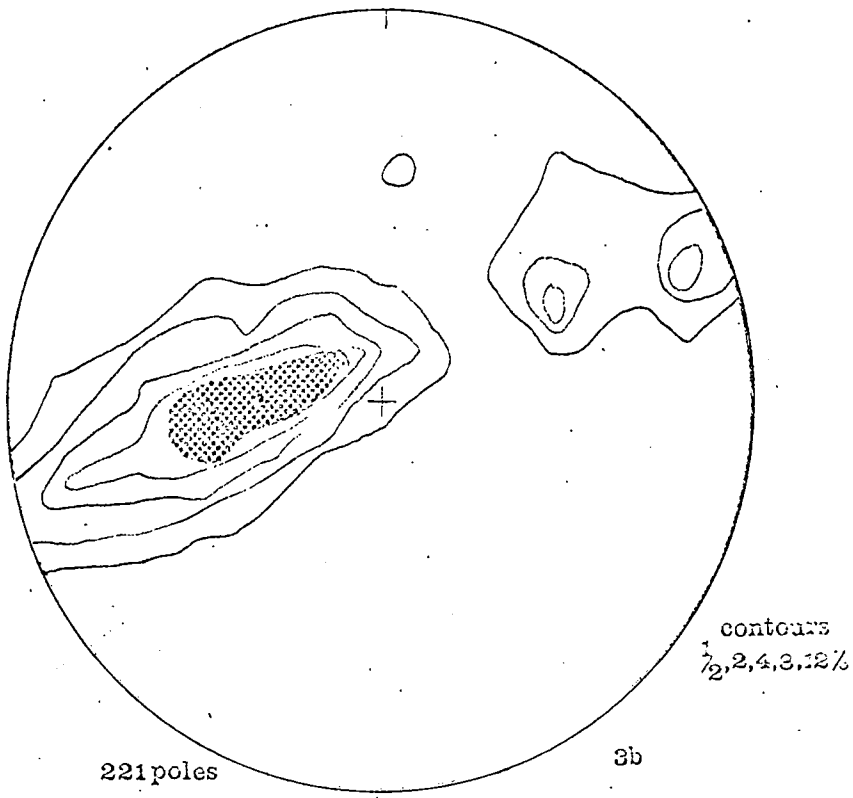

Stereograms showing distribution of poles to foliation in tectonic sub-units 3a & 3b.

Figure 9.

the two gneiss horizons in the northern part of the area. The axial plane of this fold follows the regional foliation strike and dips at a moderate angle to the east. The plot of the poles to foliation in the unit in figure 9 shows an elongate maximum extending into a great circle girdle with a B-axis trending about 20° west of north and plunging to the south-south-east at about 10°.

The granitic gneiss in the core of this fold shows poorly-developed foliation and little other fabric. The surrounding Lande gneiss exhibits a little minor folding in the form of tight isoclines with U-shaped noses. A plot of fold axes and some mineral orientations from both subunits 3a and 3b is shown in figure 10. This diagram shows a considerable scatter but concentrations close to both poles with gentle plunges and a few with an easterly plunge representing the gentle cross folds.

i) Unit 4a.

This unit comprises the outcrop of the Lande gneiss and associated rocks in the Kvina valley to the south of Netland. The Lande gneiss outcrop represents the core of a tight isoclinal antiform that closes a little to the south of the area surveyed by the present author. Ohta (1966) has traced this antiform further down the valley of the Kvina from where the Lande gneiss disappears beneath the Kvinesdal granitic gneiss in a tight closure as far as the south coast. In the southern part of the valley the antiform is an open fold with an axis trending to the north-north-east. As the fold is traced further up the valley however, the western limb gradually becomes overturned, a geometry it maintains throughout the present

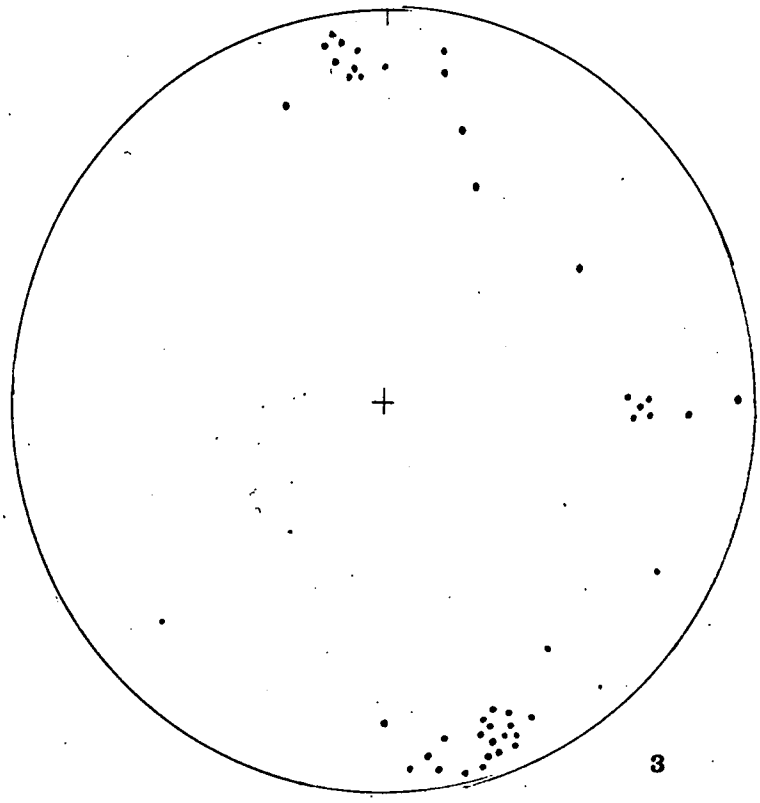

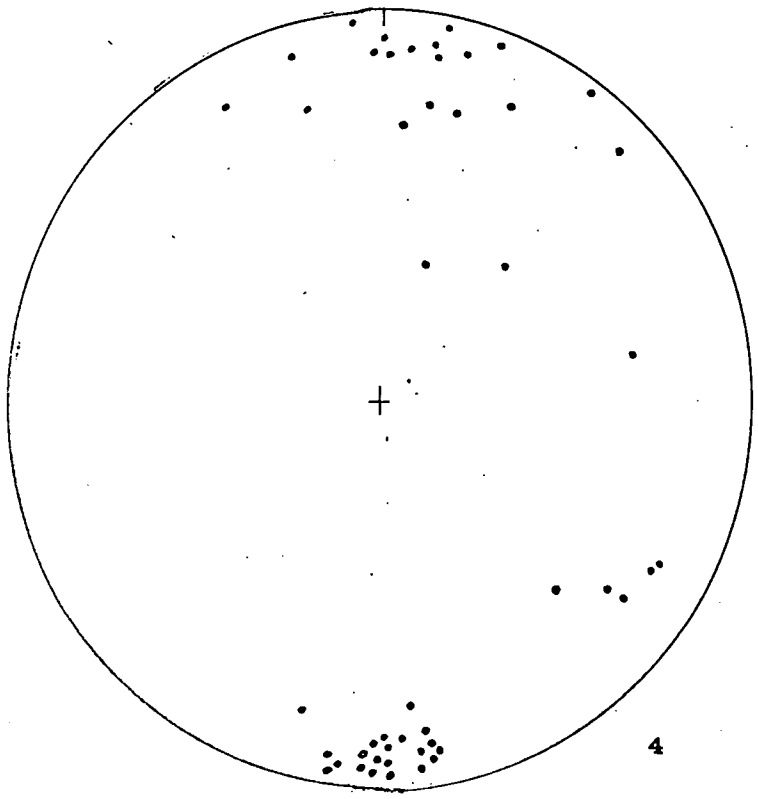

Stereograms showing distribution of lineations in tectonic units 3 & 4.

Figure 10

area. In the southern part of its outcrop surveyed by the present author, the fold has an axis which trends north-south and plunges very gently to the south. North of Lindefjell the axis swings to north-north-east again. The plot of foliation poles in the subunit, in figure 11, shows an elongate maximum and a partial great circle girdle, the pole of which plunges at a low angle to the south.

Minor folding is both abundant and complex within the Lande gneiss in this tectonic subunit. Five styles of fold have been recognised and these are illustrated in plate 14. Tight isoclinal linear noses with axial planes parallel to the gneissic layering represent the result of the earliest recognisable phase of folding. In some instances these folds have been flexured in a subsequent folding phase. The most abundant folds are isoclinal V-shaped folds with steeply-dipping to vertical axial planes. Particularly in the feldspathic horizons in the Lande gneiss there are broad U-shaped folds with convoluted hinges and near vertical axial planes. The trace of the fold is only obvious in fresh exposures when thin biotite-rich layers can be followed. The wavelength of the major component of these folds is several metres but the convolutions, which resemble some ammonite suture traces, have wavelengths of only a few centimetres. In addition to these folds, some of the feldspathic gneiss exhibits irregular flow folding of extremely complex geometry. There are also a few isolated S-shaped flexures in the more granitic sectors of the limb of the fold. In the northern part of the unit there are several linear masses of granitic gneiss interfingered with the more heterogeneous Lande gneiss. These rocks are the transitional facies of the underlying Øie layered granitic gneiss rising to the surface in the cores of tight isoclinal antiforms

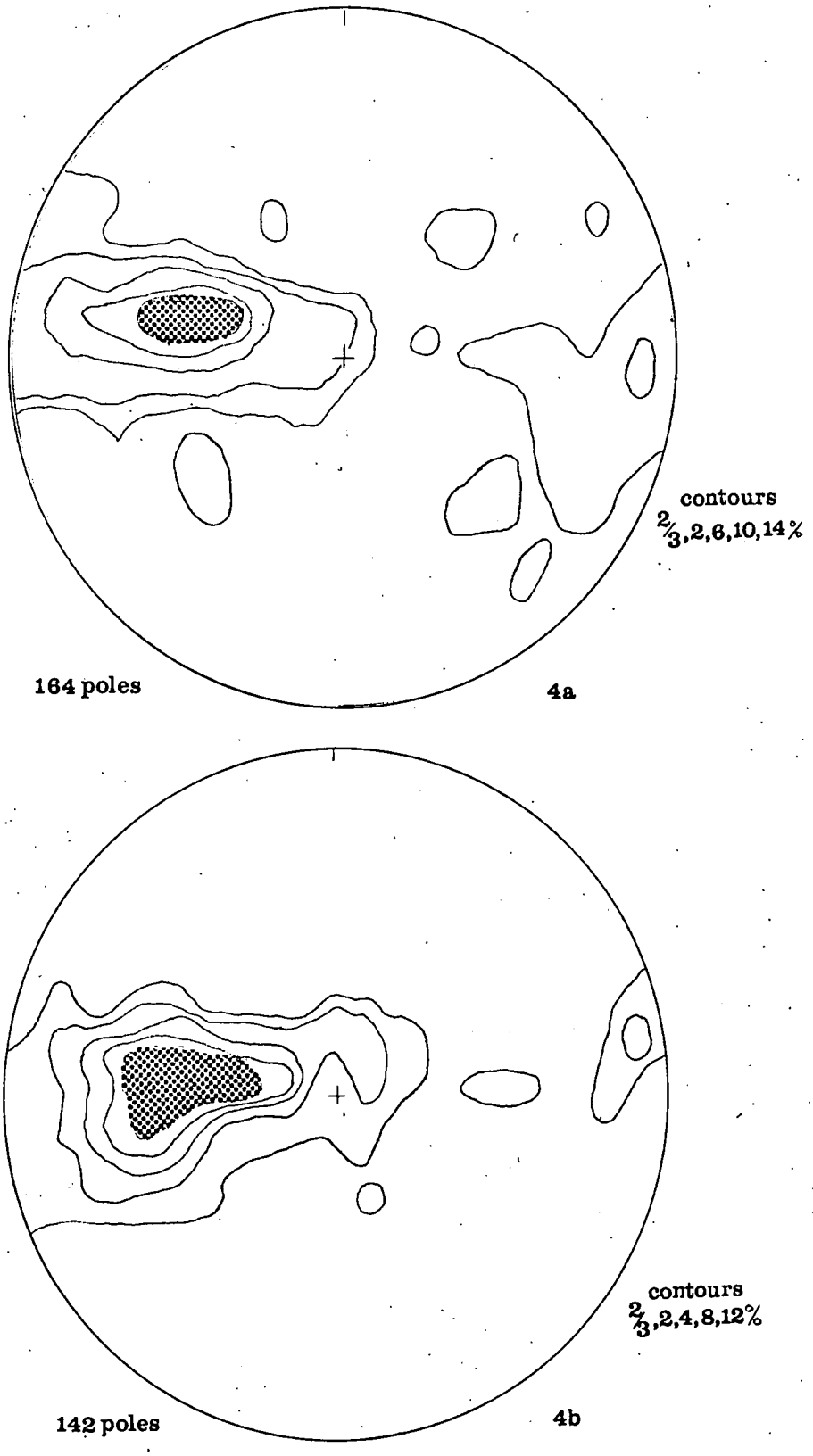

Stereograms showing distribution of poles to foliation in tectonic sub-units 4a & 4b.

Figure 11

Plate 14.

Plate 14a.

Vertical section of refolded tight isocline of biotitic gneiss within layered feldspathic Lande gneiss, south of Kvinlog. The V-shaped isoclines with near vertical axial planes are F 2 structures.

Plate 14b.

Outcrop pattern of complex-folded feldspathic gneiss horizon within layered biotitic Lande gneiss, south of Kvinlog.

Plate 14c.

Vertical section of ptygmatic folding within granular feldspathic rock within basic Lande gneiss north of Urddal.

Plate 14d.

Vertical section of complex F 2 minor folding in faintly layered granitic gneiss of Lande gneiss north of Urddal.

Plate 14d.

Vertical section of complex F 2 minor folding in faintly layered granitic gneiss of Lande gneiss west of Stakkeland.

Plate 14e.

Vertical section of isoclinal F 2 minor folding in layered biotitic and feldspathic Lande gneiss near Solham.

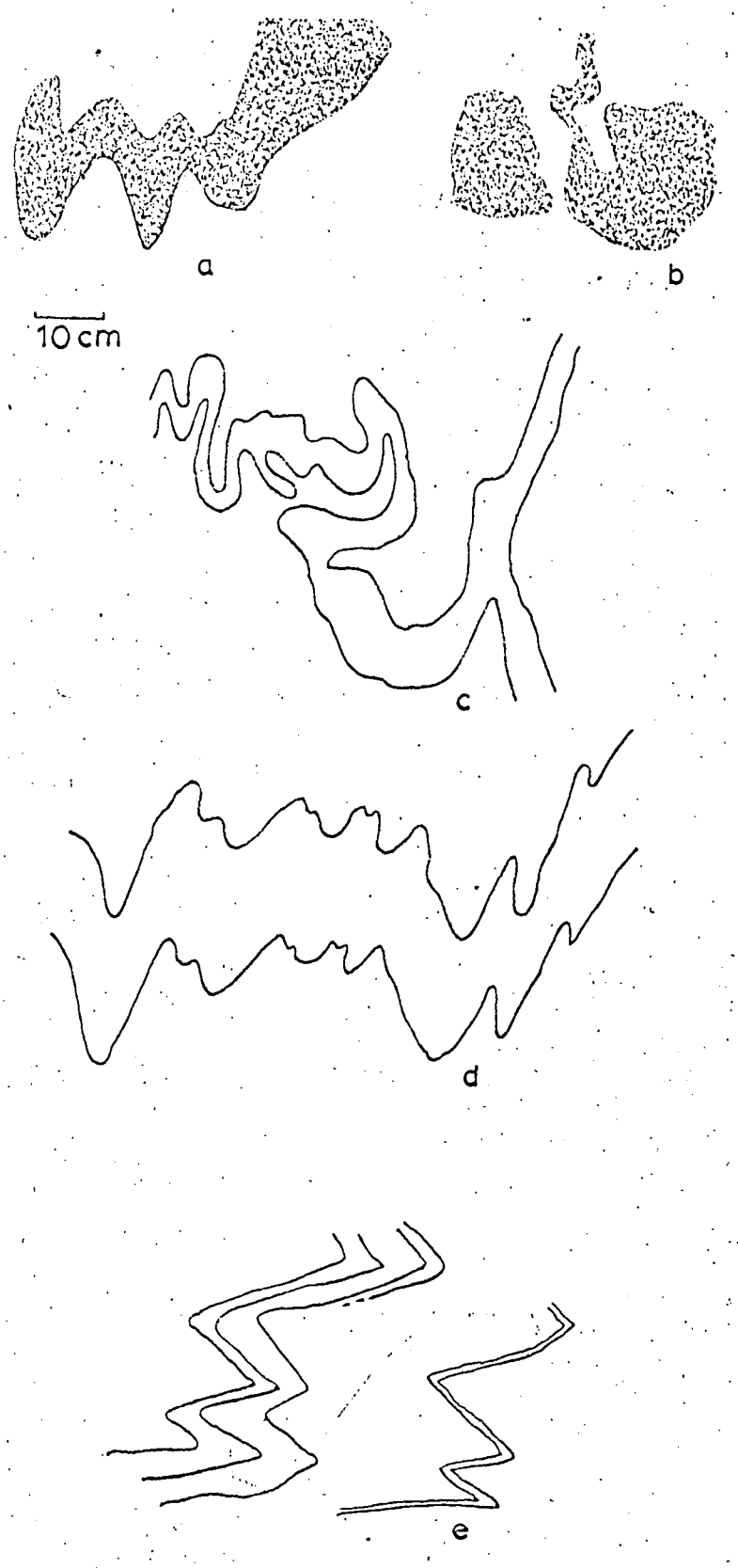

Minor structures in the Lande gneiss.

Plate 14.

parasitic on the major fold. There also appears to be some lateral replacement of the basic layered Lande gneiss by more granitic rocks in this northern sector.

j) Unit 4b.

This unit comprises the outcrop of the Lande and Øie gneisses in the Kvina valley and surrounding area to the north of Netland. The major structure of this unit is a continuation of the tight overturned antiform encountered in unit 4a with a series of smaller-scale parasitic folds. North of Risnes the axial trend of this fold swings from north-north-east to approximately north. In the extreme north of the unit the typical Øie layered granitic gneisses occupy the core of the fold surrounded by more heterogeneous but predominately feldspathic gneisses transitional into the more basic Lande gneiss. Outcrops of basic gneiss horizons are rare except on the western limb of the fold. In the extreme north of the unit much of the eastern limb of the fold is occupied by porphyritic gneissic granite of granodioritic composition containing many gneiss inclusions. The plot of poles to foliation from the subunit is included in figure 11 and contains an elongate maximum extending into a girdle, the pole of which trends approximately north-south and plunges gently to the south.

Many of the gneiss rafts on the eastern limb of the antiform in this subunit display minor folding. The predominant type is a set of closely-spaced isoclinal V-shaped folds with axial planes dipping a moderate angles to the east, parallel to the regional planar fabric in the area. Potassium feldspar megacrysts, similar in appearance

to the mineral grains in the adjacent porphyritic gneissic granodiorite, occur within some of the folded gneiss layers. The plot of lineations in figure 10 for both subunits 4a and 4b shows a cluster of points around the south pole of the diagram and a more scattered distribution at the opposite pole.

k) Unit 5a.

This unit comprises the outcrop of the massive Kvinesdal granitic gneiss, thin horizons of the Lande layered gneiss and the porphyritic gneissic granite in the core of the elongate Fjotland antiform to the south of Åsevatn. This antiform which provides the major structure of the subunit is presumed to close a little to the south of the boundary of the area surveyed by the present author. The structure is therefore domal with an axis plunging very gently to the south in its southern sector. The plot of the distribution of poles to foliation in unit 5a is illustrated in figure 12 and shows an elongate area with two maxima. The distribution can be partly explained in terms of the influence of an axis trending 10° east of north and plunging very slightly to the south.

Minor folding is relatively infrequent within this tectonic subunit. Intrafolial S-shaped folds with near horizontal axes and axial planes are the most abundant type of structure. These folds are particularly noticeable when outlined by relic gneissic layering within the central porphyritic granite. Isoclinal V-shaped folds with steep east-dipping axial planes are encountered within layered gneiss horizons. A few more open U-shaped folds occur in the most heterogeneous horizons of the Kvinesdal gneiss on the fold limbs.

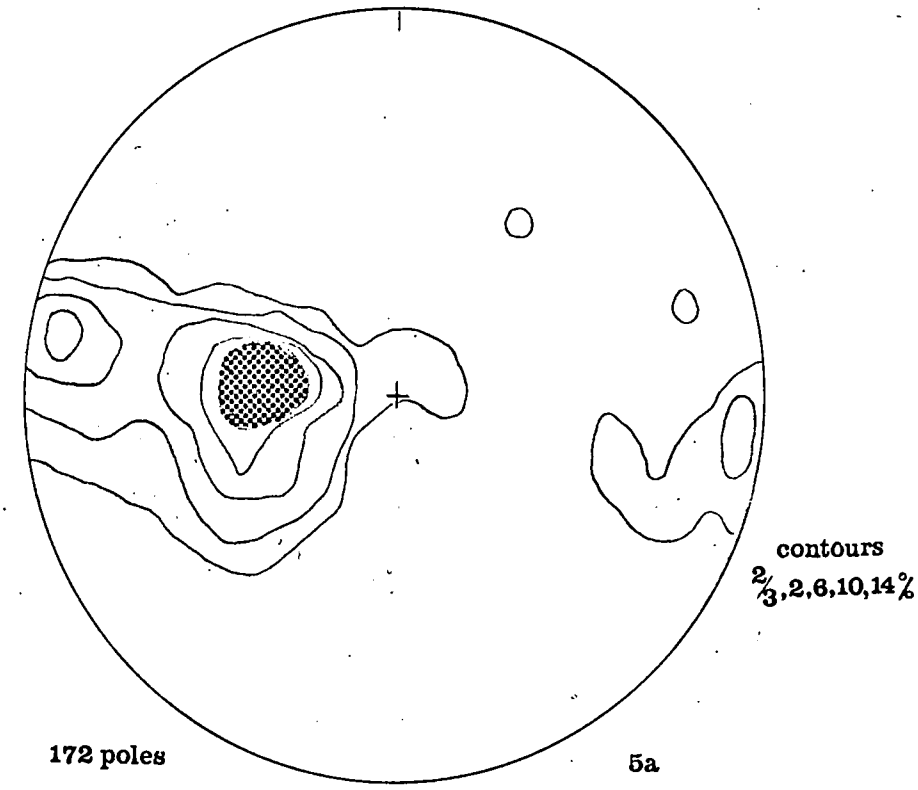

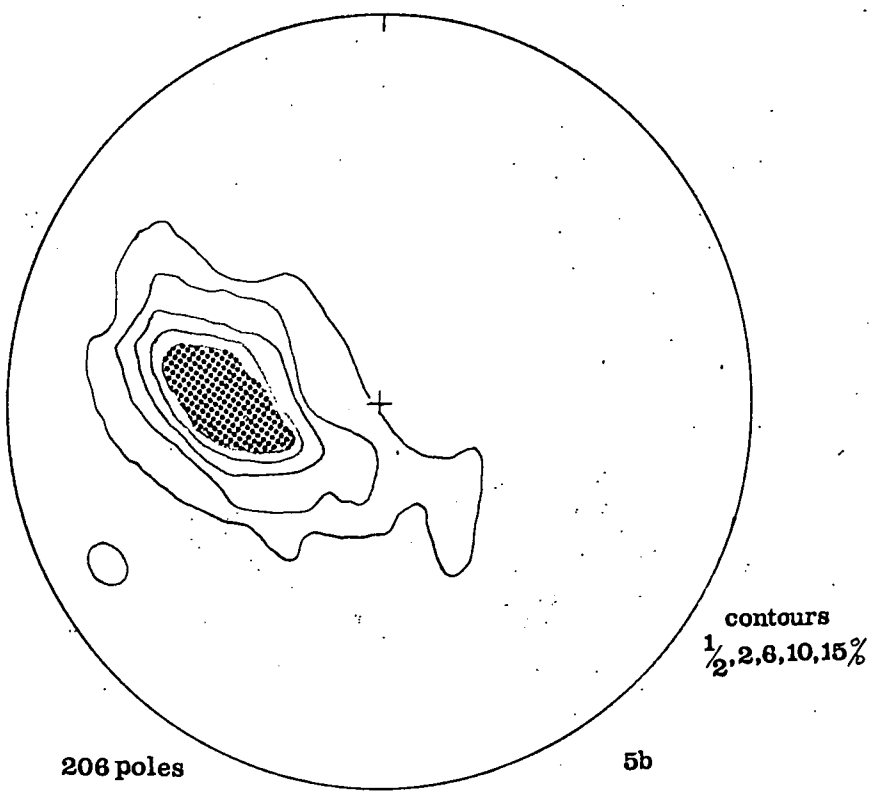

Stereograms showing distribution of poles to foliation in tectonic sub-units 5a & 5b.

Figure 12

Some thin biotite-rich layers are crenulated into very small sharp folds with near vertical axial planes.

l) Unit 5b.

This unit comprises the northern part of the Fjotland antiform from Åsevatn to Knabedalen and the main outcrop of the massive Kvinesdal granitic gneiss around it. A thin horizon of basic and feldspathic layered gneiss can be traced round a north-plunging antiformal nose to the south of Håland. Here the axis of the major fold trends north-20°-east and plunges at about 15°. The plot of foliation poles for the unit shows a maximum elongated into a partial great circle girdle the pole of which trends at north 30° east and plunges at about 20° to the north-north-east. The southern boundary of this unit is provided by a linear flexure and disturbance zone running in a north-easterly direction up Åsevatn. The layered gneisses on the north-west side of Åsevatn take on an almost east-west strike as they swing into this structure. This fold is probably continuous with the similar flexure in the southern part of unit 3a.

The few minor folds that have been observed in this unit are either isoclinal with axial planes parallel to the regional foliation, or gentle east-west trending flexures.

m) Unit 5c.

This unit comprises the outcrop of the massive Kvinesdal granitic gneiss to the north of the valley of the Knabenelva. The gneisses all dip monotonously to the east and no major structures have been

recognised. The plot of poles to foliation, in figure 13, shows a roughly circular concentration of points and very little scatter. Few minor folds have been observed within the rocks of this unit. Traces of isoclinal V-shaped folds and a few S-shaped flexures are brought out by thin biotite-rich layers within the more heterogeneous parts of the granitic gneiss however. A small number of isolated flexures trending between north-north-east and north-east have also been observed.

The plot of lineations for the three subunits, 5a, 5b and 5c, in figure 14 shows a considerable scatter of points with diffuse concentrations about both poles of the diagram.

n) Unit 6a.

This unit comprises the outcrop of the Knaben, Flofjell and Oddevassheii gneisses to the west of the Ljosland intrusion. These gneisses are presumed to occur on the western limb of a large synform, the core of which has been largely replaced by the Ljosland intrusion. This structure is possibly continuous with the large synformal complex discovered by Ohta (1966) on Kvinesheii (see plate 4). The plot of poles to foliation in the unit is illustrated in figure 13 and shows a circle of maximum density with elongate areas projecting in two directions, one of which could be a partial girdle with an axis trending to the north-north-east and plunging at a low angle in this same direction.

Minor folding is abundant in the Oddevassheii gneiss but less so in the Knaben gneiss. Most of these folds are simple V-shaped

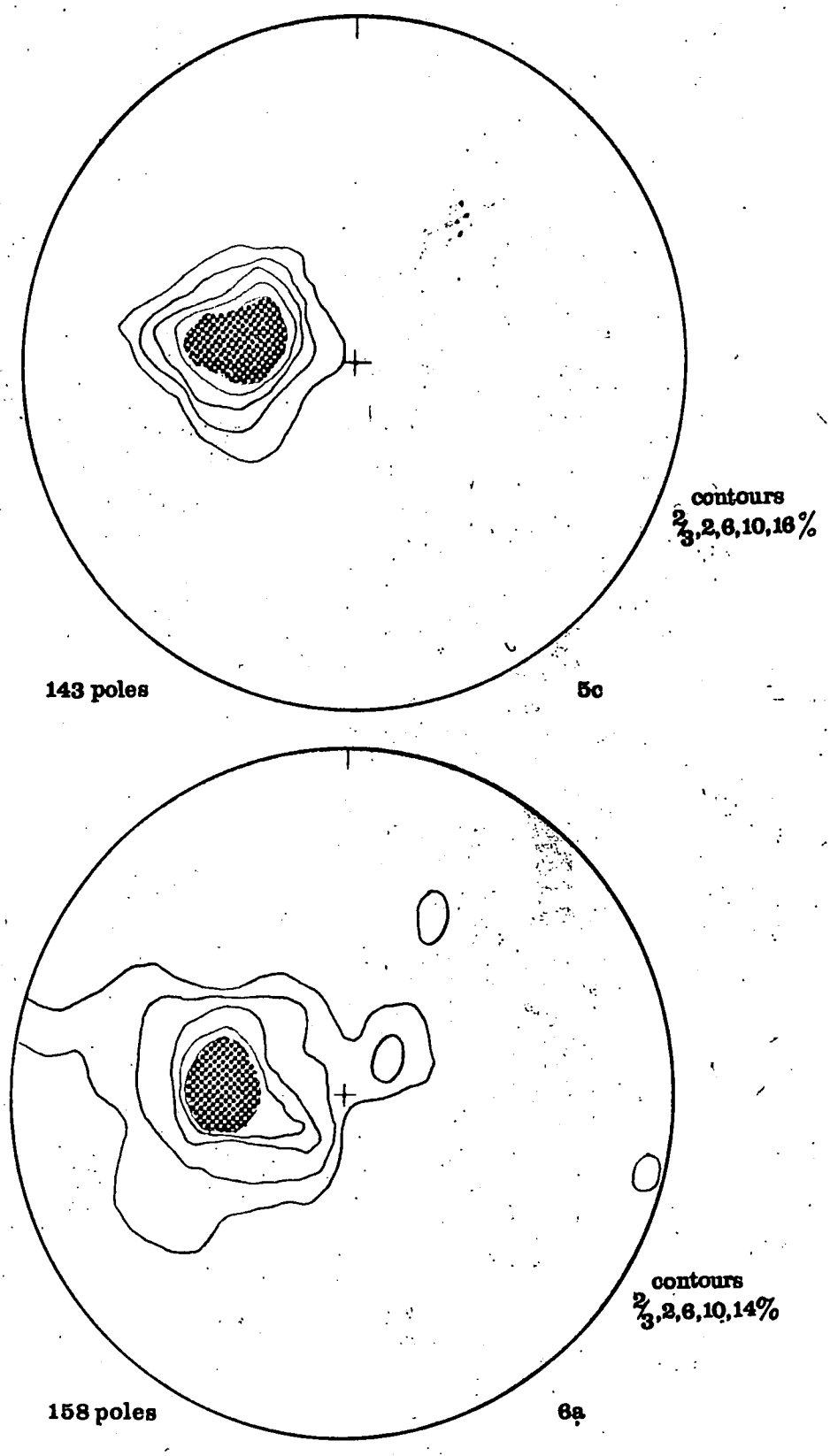

Stereograms showing distribution of poles to foliation in tectonic sub-units 5c & 6a.

Figure 13.

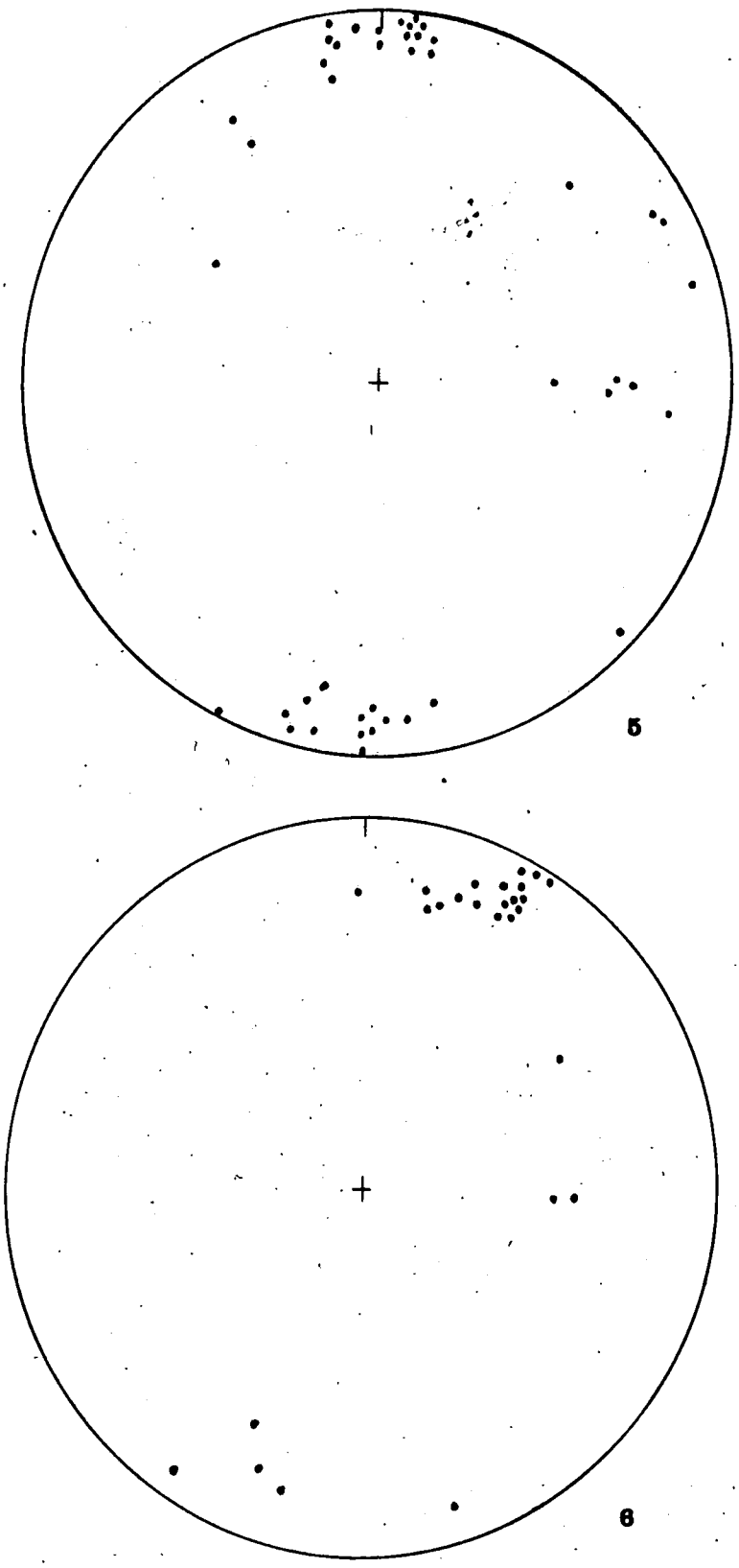

Stereograms showing distribution of lineations in tectonic units 5 & 6.

Figure 14.

isoclines with axial planes close to the orientation of the regional foliation of the gneisses, though some more complex structures with curved axial traces have also been observed.

o) Unit 6b.

This unit comprises the outcrop of the alternating layered biotitic and basic gneisses and the massive granitic gneiss to the east of the Ljosland intrusion. These rocks are presumed to lie on the eastern limb of the major synform extending from Kvinesheii. The detailed mapping of a small area of similar gneisses around the Flottorp molybdenum field, just to the south east of the present area, by Zeppernick (1966) has revealed several isoclinal folds with wavelengths of a few hundred metres. These folds are tight isoclines with axial planes parallel to the regional foliation. The plot of poles to foliation of the gneisses in this subunit, in figure 15, exhibits a well defined great circle girdle with an axis trending north 20^{o} east and plunging gently in this direction. It is noticeable that westerly-dipping foliation is more abundant than in other units.

Most of the minor folding within the layered gneiss of this unit is isoclinal with axial planes close to the regional foliation. A few isolated U-shaped folds also occur. The plot of the lineations from subunits 6a and 6b, in figure 14, shows a concentration of points with gentle plunge trending to the north-north-east.

p) Structural Synthesis and history of deformation.

The structural evolution of the high-grade basement gneisses

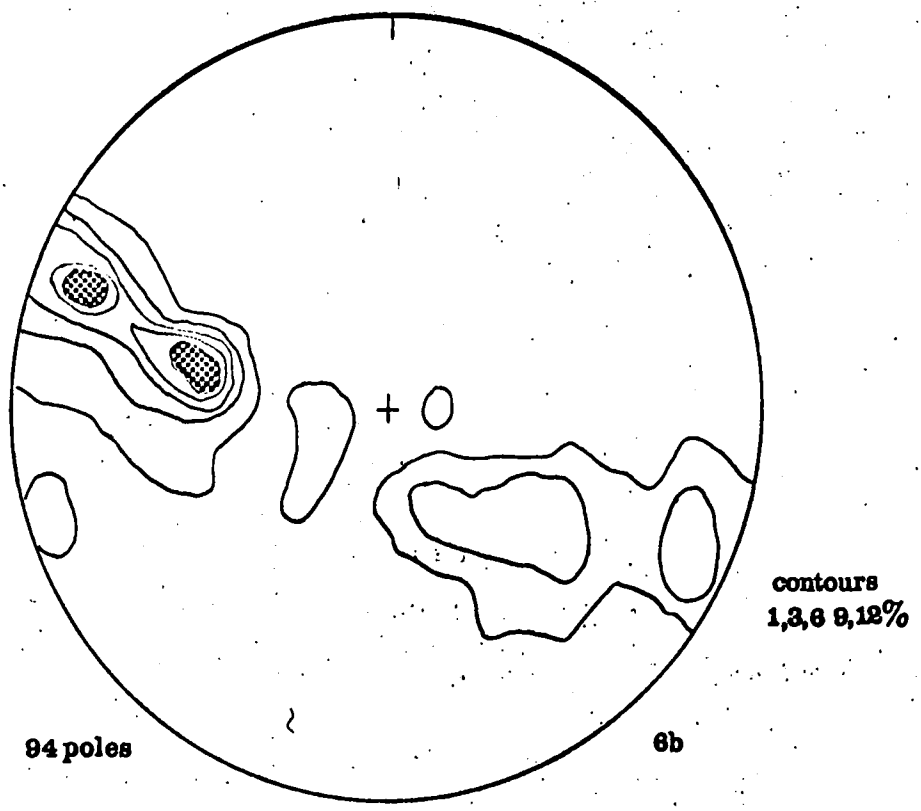

Stereogram showing distribution of poles to foliation in tectonic sub-unit 6b.

Figure 15.

of this area is both complex and difficult to elucidate. The early-formed fabric of the rocks has been largely or completely obiliterated by the recrystallisation and deformation during the climax of the orogeny. The geometrical analysis of the structures produced under the high temperatures to which these rocks were subjected is complicated by the possibility of continuous flow deformation. Such a process may produce intricate patterns of folding within one stress field. The evaluation of the tectonics of this sector of the PreCambrian of Southern Norway is therefore necessarily incomplete and perfunctory.

The structural interpretation of the area is based primarily on the analysis of major fold structures and to a lesser extent on minor folding. Five deformation phases or styles have been recognised within the rocks of the Flekkefjord Series. The development of the gneissic layering and foliation marks the first recognisable event in the evolution of the tectonic fabric of the rocks. The isolated S-shaped intrafolial flexures in otherwise unfolded rocks may also have originated during these early stages of orogenesis. During the initial period of tectonism the rocks were also deformed into a series of tight isoclinal folds with parallel limbs and U-shaped noses. Only one example of this F 1 folding has been clearly recognised on a major scale. This F 1 fold, the core of which is occupied by granitic gneiss occurs within the Lervig gneiss complex in tectonic subunit 2b. The axis of this fold has been refolded round an isoclinal antiform which originated during the subsequent F 2 deformation episode. Detailed structural analysis of the complex isoclinal folding in the layered gneiss horizons would probably reveal further early folds though these are largely

eclipsed by F 2 structures. A few possible examples of F 1 isoclines refolded by subsequent deformation have also been observed on a minor scale, particularly in fresh road sections in subunits 2a and 4a (see plates 13 and 14).

The major folded structures that determine the outcrop pattern of the rocks of the area originated during the F 2 deformation phase. These folds are normal isoclines, overturned to the east with gently-plunging axes. They trend from just west of north in the western sector to north-north-east in the eastern sector of the area. Several styles of minor folding, the main types of which are illustrated in plates 13 and 14, originated within this deformation episode. Axial planes of these folds usually dip at moderate angles to the east in common with the major structures.

The reclined complementary antiform and synform of tectonic subunit 2a originated during a third and localised phase of deformation. The axial planes of these folds trend in a north-north-westerly direction but the fold axes plunge at a moderate angle to the north-east. The interrelationship of these folds with the major F 2 structures in the Lervig gneiss is difficult to decipher, particularly as exposure is very poor in the core of the F 3 synform (see plate 3a). A strong crinkle and minor fold axis lineation parallel to the major F 3 fold axes is developed in the core of the anti-form and in the adjacent rocks. These F 3 structures interfere with and refold F 2 minor folds (see plate 13).

The isolated north-east trending flexures, often associated with linear weakness zones eg. Åsevatn, are assigned to a fourth phase of deformation, in the waning stage of orogeny. Similar isolated small scale flexures occur throughout the whole area but are most abundant in the north-east.

Throughout the region there are also some very broad, gentle, east-west-trending flexures which cause undulations in the strike of the major F 2 structures. Similar small-scale flexures are widespread, sometimes in otherwise unfolded rocks. These gentle cross-folds are assigned to a fifth phase of deformation, though in many cases they could be contemporaneous with the F 2 structures.

Six phases or styles of deformation have been recognised within the Sirdalsvatn Series. The arrow-head minor fold relicts within the Feda augen gneiss are indicative of a phase of folding prior to the development of the gneissic layering and regional foliation. These structures have been assigned to an F 0 deformation, confined to the Sirdalsvatn Series. The rocks were then thrown into a series of tight isoclinal folds possibly contemporaneous with the F 1 phase of folding which affected the Flekkefjord Series. Only in a few of the freshest exposures of the Feda augen gneiss are there indications of complex structures which probably originated at this time.

The Sirdalsvatn Series was refolded during the main F 2 deformation essentially as one large unit but minor structures dating from this deformation are relatively rare. Some flexures of F 3 age can be seen in the Sirdalsvatn series adjacent to the Sandvatn antiform and F 5 type cross-folds occur on both major and minor scales.

In recent years several authors have proposed sequences of deformations to explain structural complexity in several sectors of the PreCambrian of southern Norway. P. Michot (1957 and 1960) proposed that the gneisses to the north of the Rogaland anorthosite complex were thrown into complex plastic folds and nappes during two tectonic phases in the deep catazone. These two deformations produced structures trending north-south and east-west respectively. A later deformation then largely obliterated traces of the earlier structures.

Wegmann (1960) recognised three distinct periods of deformation in the Kongsberg-Bamble formation. The first occurred when the rocks were at medium depths within the crust and was contemporaneous with the formation of granodioritic gneisses. The second phase took place when the rocks were at a deeper level and the twisting and refolding of the earlier folds produced structures of great complexity. Deformation became cataclastic at the end of this period. A third deformation produced extensive zones of mylonite in a high-level brittle basement. Barth (1963) developed this interpretation for the whole south Norwegian PreCambrian and dated the end of the second period of deformation at 1000 m.y. He considered that the first

deformation was common to all sectors and the second began after the deposition of the Telemark supracrustals with an orogeny with extensive migmatisation and was followed by the intrusion of the anorthosite complex, hyperites and finally the farsundite and other diapir granites. Fissuring, mylonitisation, brecciation, dyke intrusion and mineralisation occurred within the third period of deformation.

Tobi (1965) postulated that the gneisses between Sirdalsvatn and the anorthosite complex were subjected to three phases of deformation. He considered that early tight isoclinal folds were refolded by more open isoclines during the second phase and then the whole area was block-faulted. Falkum (1966) interpreted the structure of an area of gneisses near Kristiansand in terms of two fold phases. The first of these produced structures trending to the north-north-east and the second a gentle doming trending east or south-east. The distribution of lineation orientations was explained in terms of a combination of the later folding and the large scale block tilting that affected the area. Smithson and Barth (1967) recognise three phases of folding in the gneisses surrounding the Holum granite based on the study of minor fold styles, but admit that the detailed structure is probably more complex. The earliest folds transposed the original layering but were largely obliterated by the F 2 chevron folds with north-trending axes. The axes of these folds show broad east-west undulations which are classified as F 3 folds.

Falkum (1967) has given a summary of a detailed structural

synthesis of the Flekkefjord area based primarily on the analysis of major fold structures. Four phases of folding with the possibility of a fifth are postulated. In this interpretation large isoclinal folds were produced in the initial deformation period and subsequently refolded about north-north-west to north-trending axes. These structures were locally refolded about north-east trending F 3 folds with steeper axial surfaces. The gentle east-west undulations are assigned to fourth phase folding.

The complexity of the geometry of the earlier folding of the gneisses has now been recognised within several sectors of the Rogaland-Telemark basement. East-west cross folds have also been widely identified. The approach to the elucidation of the basement structure in the above works and the present study has been essentially analytical and geometrical. A dynamic interpretation of the structure of the Rogaland-Telemark province will be possible from a synthesis of the work of the Telemark Project.

8. BRITTLE DEFORMATION AND RETROGRADE METAMORPHISM

Four types of brittle fracture have been distinguished within the present area, the latter three of which are associated with some alteration or retrograde metamorphism.

a) Early Healed Faults

In these structures both sides of the movement plane have been cemented together so that no break occurs in the rocks. These planes are therefore very difficult to see except in fresh exposures. An example is exposed in the roadside to the south of Tonstad and is illustrated in plate 5. There is a clear distinction between the rocks on either side of the fault but it has not been possible to estimate the throw of this break. The fault plane trends between north-north-east and north east and hades at about 65° to the south-east. The layered feldspathic Tonstad gneiss to the north of the plane is folded plastically until the layering is parallel to the fault plane, in the space of a few centimetres. The fault plane is occupied by a few centimetres of layered coarse-grain granitic rock which is sharply truncated against the pinker granitic gneiss to the south of the fault. A few other similar but less well defined faults are exposed further south along the road.

Healed faults have also been observed within the Feda augen gneiss, the Lervig gneiss and the Kvinesdal gneiss. The material filling these fault planes is either fine-grain granular leucogranite

or coarser pegmatite. The fault line at Ornehommen near Knaben has been filled with two generations of vein rock, an earlier dark quartz vein with chalcopyrite and pyrrhotite and a later white quartz pegmatite. Invariably the gneisses on one side of the break turn into the fault plane while on the other there is a sharp discordance. Low angle faults with small displacements also occur in some layered feldspathic gneiss horizons.

These faults probably originated by plastic deformation followed by rupture as a result of relatively rapid application of stress. The structures therefore exhibit features of both brittle and ductile deformation. After the initial release of stress the fracture was slowly healed in response to the still present regional stress. Before this process was completed these breaks represented lines of weakness into which pegmatite and other mobilisates were intruded.

b) Mylonites

Within the Flofjell gneiss to the east of Knaben there are several north-south mylonite zones. They are usually of the order of a metre in thickness and are filled with a fine-grain schistose rock which contrasts sharply with the surrounding phenoblastic granitic gneiss. Though narrow, these fractures are often visible on aerial photographs as they give rise to sharp steps in otherwise rounded exposures. A typical specimen of the mylonite rock contains elongate sutured quartz and feldspar fragments set in a fine micaceous groundmass which wraps round the larger grains. The few

plagioclase grains present exhibit deformed twin lamellae. The matrix consists mostly of small rounded grains of quartz, biotite partially altered to chlorite and secondary sericite. Sphene, apatite, allanite and a little hematite are the main accessories. All the fractures that have been examined dip towards the east at relatively low angles. The strong adherence of the mylonite rock to the adjacent rocks and the lack of extensive retrograde metamorphism indicate that the fractures originated while the rock was still under considerable load stress, probably during the waning stages of the orogeny.

c) Retrograde metamorphism

Retrograded rocks are widespread but confined to definite linear zones. Intense retrograde metamorphism has transformed the rocks at the base of the Lervig gneiss to the south of Optedal into quartz-piemontite and epidote-chlorite rocks. In the centre of the section is a horizon of bright pink piemontite-quartz rock, several metres in thickness, which has replaced original quartzofeldspathic gneiss. Most of the rock has a fine granular texture but some lenses and veins with quartz and large piemontite prismatic crystals also occur. A typical section of the rock, illustrated in plate 15a, consists of a fine aggregate of pale green epidote with patches showing the intense colouration of piemontite, interspersed with relatively large quartz grains. At the contact with the quartz grains are coarser euhedral crystals. Some of these crystals are pale green, slightly pleochroic, optically positive, iron-poor epidote while others contain cores or sharp zones of piemontite with

Plate 15.

Plate 15a.

Photomicrograph taken in plane polarised light of piemontite-bearing rock from retrograded Lervig gneiss, south-east of Optedal. The section consists of a mass of epidote-piemontite grains which exhibit euhedral form within and bordering the associated quartz grains. Zonation in colouration in the euhedral grains is clear in the photograph. A chlorite grain occupies the lower left corner of the photograph. Magnification x 40.

Plate 15b.

Photomicrograph taken in plane polarised light of fluorite within biotite in biotite-plagioclase gneiss from the Lande gneiss near Nordbø in the Kvina valley. The biotite is unaltered except for a thin layer of chlorite around the fluorite. The section contains a little clear quartz and cloudy plagioclase. Magnification x 100.

a

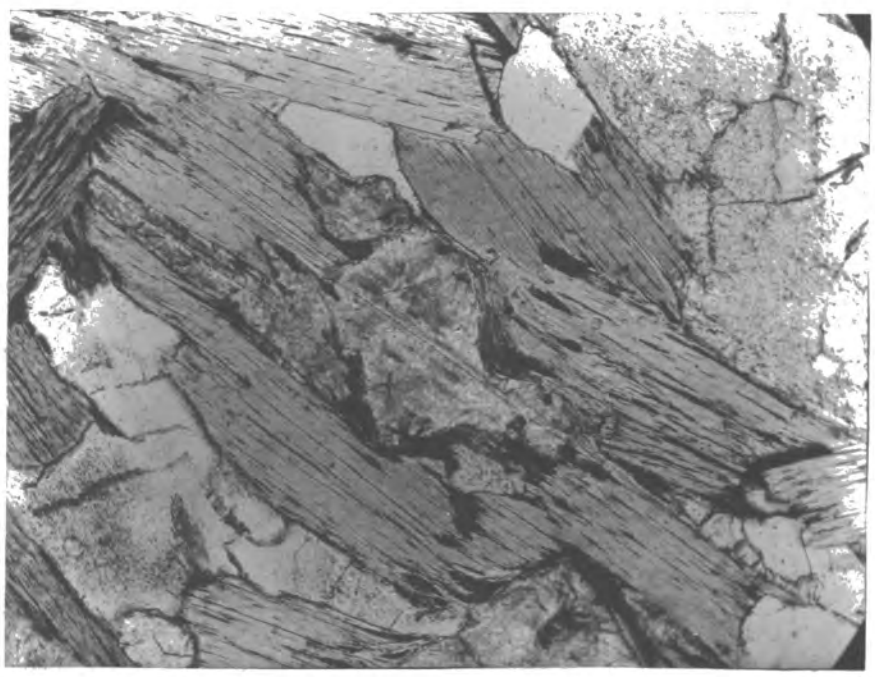

b

Plate 15.

the pleochroic scheme, (a) yellow, (b) violet and (c) rich purple-red. A little chlorite, sphene and hematite are usual minor constituents.

Morton and Carter (1963) have described some Norwegian occurrences of piemontite and withamite. They recognised withamite by its relatively low manganese content and optically negative character. They concluded that all the specimens examined except one were withamites with Mn_2O_3 contents ranging from 0.21% to 3.17%. The piemontite exhibited well defined but irregular optical zoning and contained on average 2.76% MnO plus Mn_2O_3. Several euhedral crystals of both pale green and zoned epidotes in a specimen of the quartz piemontite rock were analysed for manganese on the electron microprobe for comparison. The manganese content of pale green grains was found to vary from 0.1% Mn_2O_3 to 0.3% Mn_2O_3 but for the intensely pleochroic areas a range of from 1.1% Mn_2O_3 to 5.6% Mn_2O_3 was discovered. Within the pleochroic areas no relationship between the intensity of colouration and the manganese content was apparent. There is therefore some similarity between the manganese epidote analysed and the piemontite from Furenes in chemical composition. Manganese contents considerably in excess of the above range have frequently been reported for piemontites in the literature. Miyashiro and Seki (1958) have related the manganese contents of piemontites with their temperatures of formation. High temperature minerals are considered to contain more manganese than specimens that crystallised in the low greenschist facies. This simple relationship does not hold for the Norwegian minerals as they exhibit considerable and irregular variations in manganese content in different parts of the same grain. These fluctuations in composition probably

reflect variations in the amount of available manganese during crystallisation and lack of equilibrium.

Most of the manganese must have been externally derived though this may have been by the leaching of mafic minerals in basic rocks through which the hydrothermal solutions passed. Hutton (1938) considered that adequate manganese for the formation of the Glen Coe withamite could have been derived by the breakdown and leaching of mafic minerals in the Glen Coe lavas. An indication of the oxidising nature of the hydrothermal solutions associated with the Optedal piemontite deposition is provided by the abundance of hematite both in the retrograded rocks and nearby quartz veins.

Basic gneisses near the piemontite-bearing rocks have been retrograded to an assemblage consisting of pale to emerald green chlorite with included lenses of sphene and pale yellow ferruginous epidote, partially altered plagioclase with included zoisite prisms, magnetite rimmed with sphene and scattered grains of pale green pleochroic epidote. A pegmatite cutting these basic rocks contains quartz, red altered microcline, epidote and a few grains of chalcopyrite and bornite. The degree of alteration of the gneisses decreases a few dekametres from the piemontite rocks. The granitic rocks are bleached and contain patches of piemontite grains. The potassium feldspar is brown and turbid and the plagioclase has stepped and fractured twins and is moderately altered with a few included zoisite grains. Chlorite with associated yellow pleochroic epidote is the only mafic phase. The presence of fractured grains of plagioclase indicate a period of brittle fracture prior to the retrograde metamorphism.

Less intense but similar retrograde metamorphism is developed adjacent to Krågelandsvatn in the south of tectonic subunit 3a. The mineral assemblages of the retrograded granitic rocks are similar to the margins of the Optedal alteration zone. Epidote and piemontite are widespread but minor constituents of the rocks. Epidote segregations occur in the cores of some of the minor folds on the shores of the lake. Thin milky quartz veins with specular hematite and a little calcite are conspicuous in the most altered rocks.

d) Linear fractures and associated retrograde metamorphism

Subvertical fractures and crush zones are extremely abundant throughout the area and on the higher ground these are marked by deep depressions formed after the ice had removed preferentially the less resistent shattered and altered rocks. In no place has it been possible to demonstrate significant movements along this type of fracture. The predominant trends of the wider and more persistent crush zones are about east-west and less frequently north-west to north-north-west and north-east to east-north-east.

The rocks within and adjacent to the main crush zones are often retrograded. The rocks within the Råtagangen fracture zone which stretches across the entire area from Tonstad to Røyseland, near Åseral, contain bright red feldspars. The plagioclase of the retrograded granitic rocks in the crush zone near Knaben are heavily saussitised and the biotite is partially or completely altered to a pale green pleochroic chlorite. The electron microprobe analysis

of chlorite from one of these rocks is given in table 3. On the basis of the classification of Hey (1954), this mineral falls into the ripidolite field. Some of the chlorite grains contain small elongate to round zircon grains surrounded by pleochroic haloes and are associated with large clear grains of sphene and a few concentrically zoned allanite crystals.

Chlorite in some of the granitic gneisses adjacent to the Råtagangen crush zone in the Knaben area contains lenses or euhedral cubes of deep blue fluorite (see plate 15b). Fluorite occurs in partly chloritised biotites in otherwise unaltered granitic gneisses to the south-west of Knaben and in the Kvina valley near Nordbø. In the Kvina valley occurrence the fluorite is rimmed with a very thin layer of chlorite in otherwise unaltered biotite. The fluorite must therefore have been deposited from the hydrothermal solutions that invaded parts of the area and altered the biotite to chlorite adjacent to the major crush zones and many small fractures.

The Råtagangen crush zone cuts the east-west igneous dyke near Knaben Gård. Where the dyke is exposed near the intersection the contact rocks are altered with the development of chlorite and epidote in the dyke rock and the degradation of feldspars and biotite in the adjacent granite gneisses. The hydrothermal solutions that percolated through the crush zone were also able to move some way along the contacts of the dyke.

A comparison of the major element chemistry of retrograded rocks and unaltered similar material is illustrated in table 4. The main difference between the two granitic rocks is the high sodium and low potassium content of the altered rock in comparison to the fresh gneiss. The more basic altered gneiss is richer both in sodium and aluminium than a corresponding unaltered rock, but slightly richer in potassium also. These differences are reflected in the presence of muscovite in the altered rock.

Isolated alteration of some mafic silicates with no regional significance also occur. Cordierite invariably shows some alteration particularly along the grain boundaries. Orthopyroxene sometimes shows alteration along cracks to iron oxides and an orange brown material. Clinopyroxene is sometimes partially altered to hornblende or chlorite, iron ore and calcite.

The final event in the structural history of the area was the opening up of tension fractures and joints as the rocks were raised to a high level in the crust and residual strain was released. The predominant joint directions are east-west and roughly north-south.

9. THE MOLYBDENITE AND OTHER SULPHIDE MINERALISATION.

The aim of this study is to assess the relationship of the mineralisation with the broad regional geology. Bugge (1963) has given an account of the history of mining activity together with some geological details of the main deposits and most of the old workings within the area.

a) Description of mineralisation.

Bugge's classification of the molybdenite deposits of Norway is based on occurrences in the Knaben area and makes a primary distinction between molybdenite associated with quartz veins and molybdenite associated with pegmatite and aplite veins. The term aplite is applied by Bugge to fine or medium grain granular feldspathic rocks without visible foliation, following local nomenclature in the Knaben mine. As most of this rock is interlayered concordantly with foliated granitic and biotitic gneisses and probably resulted from in situ recrystallisation rather than introduction from depth, the term granular leucogranite is preferred by the present author. As mineralisation associated with quartz veins, pegmatite and granular leucogranite frequently occur in close association at the same locality, a classification of the deposits in terms of the geological environment is considered more instructive than the morphological classification used by Bugge. A brief description of the mineralisation

types in these terms follows.

1) Sulphides impregnated in layered and basic gneisses.

Within some of the layered feldspathic gneisses, particularly in the Knaben area, are thin horizons rich in fine grain iron and copper sulphides. In natural exposures these rocks are conspicuous because of rusty staining, though sulphide grains are only conspicuous when surface rock is removed. These fahlbands are similar to those described by Gammon (1966) from the Kongsberg-Bamble formation of the PreCambrian of south Norway. Pyrite is the most abundant sulphide though a little chalcopyrite also occurs. Significant fahlbands observed outside the Knaben area are shown on the accompanying map of mineralisation. Some biotite-rich basic gneiss layers are also impregnated with small amounts of pyrite and chalcopyrite, particularly to the north-east of Guddal.

2) Molybdenite associated with small quartz veins in layers and rafts of fahlband-containing gneiss within phenoblastic granitic gneiss.

This type of mineralisation is well developed in the Knaben area mineralisation ' midzone ' and its extension south into Litladalen. The molybdenite occurs along the margins of the quartz veins or in the adjacent gneiss. In

weathered exposures these veins are stained a bright red. To the west of the main outcrop of the Knaben gneiss these rocks occur as isolated lenses and rafts within the phenoblastic Kvinesdal gneiss and frequently exhibit flaser structure with biotite wrapped round lenses of granular quartz and feldspar. The amount of molybdenite associated with this type of deposit is generally small.

3) Molybdenite associated with thick but impersistent quartz veins at the contacts of massive amphibolite horizons.

Molybdenite has been worked at the old Knaben 1 mine in lensoid quartz veins up to 10 metres thick at the contact of an amphibolite horizon with the surrounding phenoblastic granitic gneiss. The quartz veins depart slightly from the exact contact at the margins of the deposit and in depth where the amphibolite boundary diverges from the regional foliation. The molybdenite is especially enriched along the quartz vein-amphibolite boundary and in isolated clumps within the vein. The granitic gneiss on the other side of the vein is also impregnated with a small amount of sulphide. The mineralised vein stretches about 100 metres along the strike. Similar but less extensive deposits are associated with the margins of basic gneiss horizons on the western side of Bergetjern, one kilometre to the south of the Knaben 1 mine. Clumps of molybdenite, 2 or 3 cm. in diameter, with coarse-grain biotite are associated with quartz lenses containing a little white

feldspar.

4) Molybdenite and chalcopyrite associated with thin quartz veins, pegmatite and granular leucogranite layers within layered phenoblastic granitic gneiss.

This type of mineralisation is found in a series of north-south zones within the Kvinesdal gneiss west of the Knaben gneiss. One of these zones runs from the western side of Litladalen northwards as far as the Knabenelva and is well exposed at the south-eastern side of Skjerlevatn, five kilometres to the south-west of Knaben. Though most of the rocks are quartzofeldspathic, a few layers of biotite-rich rock also occur. Thin concordant quartz veins with chalcopyrite and a little pyrite are found within both phenoblastic granitic gneiss and granular leucogranite layers. These sulphides together with a little molybdenite are also disseminated up to 3 cm. from the vein margin in the adjacent gneiss, frequently along the margins of the larger feldspar crystals. Molybdenite is also found in clumps with large biotite grains in medium-grain granular pegmatite and in adjacent biotite-rich gneisses. The ore is also associated with discontinuous lensoid quartz in granular leucogranite layers. In contrast to these concordant sulphide deposits there are also a few thin impersistent quartz veins with chalcopyrite sharply discordant to the regional gneissic layering.

5) Molybdenite with a little pyrite and chalcopyrite associated with quartz and pegmatite within faintly-layered phenoblastic granitic gneiss.

The geological environment of this type of mineralisation is similar to the preceding class except that the gneissic layering is faint and biotite-rich layers are absent. Mineralisation outside the Knaben area is frequently of this type. At the Vordal old workings, some 15 kilometres to the south of Knaben, molybdenite is associated with quartz veins up to one metre in thickness and a few pink feldspar pegmatite sheets. The richest ore occurs along the vein-gneiss boundary and in a few planes within the surrounding granitic gneiss. Both in the Kvina valley and eastern slopes above Sirdalsvatn, molybdenite is often found at the finer margins of concordant pegmatites and with lensoid quartz segregations in phenoblastic granitic gneiss with diffuse layering. It is significant that no sulphide deposits have been discovered in the massive homogeneous granitic gneiss horizons.

6) Molybdenite associated with quartz and plagioclase-rich veins in basic gneiss.

Small amounts of molybdenite are associated with irregular dark quartz veins which cut basic horizons in the Lande gneiss of the Kvina valley. A little pyrite and chalcopyrite is also

associated with thin plagioclase-pyroxene pegmatite veins within these rocks. Within the basic Oddevassheii gneiss adjacent to the western contact of the Ljosland intrusion are thin ramifying plagioclase-rich veins with coarse biotite crystals. A little molybdenite occurs in these veins and along their contacts. Fine-grain feldspathic gneisses immediately adjacent to the intrusion are impregnated with fine nickeliferous pyrrhotite.

7) Molybdenite associated with discordant pegmatite veins.

Discordant pegmatites are much less frequent than concordant sheets of this rock. Accessory molybdenite has been observed in a few examples, eg. in a 30 cm. wide dyke cutting the Tonstad gneiss near Skibeli. Bugge (1963) records that a late pegmatite in the Knaben 2 mine is barren of sulphide where it cuts massive granitic gneiss but contains molybdenite at its margins where it cuts a mineralised quartz vein zone. Furthermore the ore is especially enriched in the gneisses of the vein zone in the vicinity of the pegmatite vein.

The molybdenite mineralisation at the Kvina mine is associated with a thick pegmatite lens enveloped by a layer of vein quartz. The whole complex is flattened parallel to the regional foliation. Ore is particularly rich along the contact between the quartz and pegmatite and in the surrounding gneiss. Ore in linear zones within the country gneiss is also

enriched in the vicinity of the pegmatite-quartz lens.

8) The mineralisation in the Knaben 2 workings.

In the northern part of the mine and nearby opencast workings molybdenite with some chalcopyrite and pyrite is impregnated in a grey-coloured phenoblastic gneiss of granitic composition containing many thin quartz veins and lenses. This grey rock, termed ' gangfjell ' by Bugge, occurs as a lens within typical pink phenoblastic granitic gneiss. The lens is some 80 metres thick at the surface but decreases in depth until it has disappeared at 124 metres below the surface. The gangfjell lens is elongated in the plane of the regional gneissic foliation and also contains some relatively thick ore-bearing quartz veins and many layers of granular leucogranite. Molybdenite is often impregnated in these rocks and particularly enriched along their boundaries. The leucogranite layers frequently contain quartz segregations orientated parallel to the regional foliation of the surrounding gneisses. Thin envelopes of quartz which project into the gneiss as thin veins from where the leucogranite lens pinches out are often rich in molybdenite. A tendency for the granular leucogranite layers to coalesce and increase in grain-size has been noticed in the deeper levels of the mine workings. Close association between vein quartz and pegmatite with both sharp and gradational contacts has also been observed. At a typical exposure feldspar crystals appear at the edge of a

quartz vein and in the space of a few metres these increase into a pegmatite. Molybdenite is found at the contact with the surrounding gneisses of both the quartz and pegmatite sections of the vein.

The impregnation gangfjell lens is replaced in the southern part of the mine by a system of molybdenite-bearing quartz veins within phenoblastic granitic gneiss. Immediately adjacent to the veins the granitic gneiss is grey rather than pink, similar in appearance to the gangfjell rock. The quartz veins increase in frequency in depth to a network between 30 and 80 metres broad with very variable molybdenite content. In the deepest workings two sets of veins have been recognised, one type dipping between 10^{o} and 20 degrees to the east and the other with steeper dip in the same direction. Vokes (personal communication) has suggested that these veins are en echelon fracture fillings connected with a deep crustal penetrative movement.

9) Discordant quartz chalcopyrite veins.

A thick lensoid quartz vein with massive pyrite and chalcopyrite has been worked to the east of the Kvina molybdenum mine. The sulphides also occur between silicate grains in adjacent basic gneiss. A further vein with chalcopyrite, pyrrhotite, a little pyrite and molybdenite occupies the healed north-east trending fault at Ornehommen,

north of Knaben. The surrounding gneisses are enriched in molybdenite compared with other points along their strike. The hydrothermal solutions from which these copper-bearing veins were deposited were locally able to remobilise the molybdenite.

b)Sulphide textures and relationships.

The textural features of a few polished specimens of ore minerals, particularly from the Knaben, Kvina and Skjerlevatn areas, have been examined under reflected light to provide evidence of the sequence of sulphide crystallisation and the environment of deposition.

Pyrrhotite is a relatively local sulphide phase but where present is invariably the oldest mineral. The pyrrhotite from a concordant quartz vein near the Kvina mine is ovoid in section with the long axes of the grains parallel to the foliation strike in the surrounding rocks. A thin partial rim of chalcopyrite envelops some of these grains and a further rim of subhedral pyrite grains covers this. In other occurrences the intermediate chalcopyrite layer is absent. Molybdenite grains are seldom found in contact with the other sulphides but a specimen of mineralised gneiss from the vicinity of the Kvina mine contains undeformed molybdenite within a mass of chalcopyrite. The same specimen also contains a few interstitial grains of copper sulphide between a sheaf of molybdenite plates. Pyrrhotite and

molybdenite have never been observed in contact. A few marcasite grains sometimes occur at the edge of pyrite masses and covellite may mantle chalcopyrite grains in a few specimens.

A general sequence of sulphide phase crystallisation can be deduced from textural evidence in the gneissic rocks. This sequence in order of crystallisation is :-
a) pyrrhotite, b) molybdenite, c) chalcopyrite, d) pyrite e) marcasite and f) covellite. Heier (1955) concluded on the other hand that the sequence of sulphide deposition at the Ørsdalen tungsten deposit was a) molybdenite and wolframite, b) pyrite, c) pyrrhotite and d) scheelite.

In some of the gneisses of the Kvina mine area there are intergrowths of chalcopyrite and magnetite that can be interpreted as resulting from the simultaneous growth of the two minerals, possibly after pre-existing pyrrhotite. Pyrite and magnetite occur in close association elsewhere in the Knaben area but their interrelationships could equally well be explained in terms of separate crystallisation phases.

Some evidence of the temperature of crystallisation of the sulphide phases is provided by the frequent presence of small irregular inclusions of sphalerite containing blebs of exsolved chalcopyrite in several large chalcopyrite grains. The solid solution of sphalerite in chalcopyrite is strictly limited and estimates by Edwards (1954) place the temperature

of unmixing at about 550°C. The exsolved sphalerite itself contained appreciable copper in solution which was subsequently exsolved on further cooling. No discrete sphalerite grains have been observed within the mineralised rocks. The fact can be explained either by the low zinc content of the mineralising solutions or by the unsuitability of the physical and chemical environment for the precipitation of a zinc phase.

c) Regional setting and origin of the sulphide mineralisation.

A significant feature of the regional distribution of the molybdenite mineralisation is the tendency for the sulphide to be confined to zones parallel to the regional foliation. Though the immediate host rock of the mineralisation varies from amphibolite to phenoblastic granitic gneiss, all the ore zones lie within or adjacent to heterogeneous gneiss horizons. According to Bugge (1963) similar criteria apply to the other main molybdenite localities of south-west Norway. The stratigraphical site of the mineralised horizons varies from the Feda augen gneiss up the sequence to the Oddevassheii gneiss. Feldspathic gneisses within the four main basic layered gneiss units are the most favourable sites however.

Three possible controls can be advanced to explain the distribution of mineralisation. Sulphide occurrences may be related to the proximity of igneous intrusions in depth.

Molybdenite does occur in the Oddevassheii gneiss adjacent to the Ljosland intrusion but the amount of ore is small. Here the sulphide is associated with diorite pegmatite veins that have probably been sweated out of the basic gneiss. No appreciable sulphide has been observed in other parts of the contact aureole or associated with the other intrusions. Bugge (op. cit.) mentions that molybdenite is impregnated in an anorthosite dyke offshoot of the large Sokndal intrusion at Gullvann, to the south-west of Sirdalsvatn. There is therefore little evidence for a primary association between the sulphide mineralisation and any of the intrusions exposed at the surface.

There is some evidence of a structural control to the mineralisation though there are no obvious faults or other planes of weakness that could have served as conduits for ascending mineralising solutions except for the gneissic layering. The rafts of layered gneiss with flaser texture within the phenoblastic granitic gneiss in the Knaben area suggest a period of relatively high stress before the final recrystallisation of the gneiss. Other evidence that the Knaben area may be located over a deep fracture or weakness comes from the en-echelon form of quartz veins in the lower part of the Knaben 2 workings. A regional feature of the mineralisation is the parallelism of the strike of the gneissic layering within the areas of richest mineralisation. This direction of strike, trending a few degrees to the east of north, is prevalent in the Knaben area, from Lindefjell to

Netland in the Kvina valley and from Skibeli to Åvedal on the east side of Sirdalsvatn. Where the regional strike swings away from this direction the mineralisation dissappears or is much reduced. Significant molybdenum mineralisation reappears in the Kvina valley south of the area investigated by the present author where the strike again swings to just east of north. The upward movement of mineralising solution wasfacilitated where the direction of strike of the gneissic layering is coincidental with a deep basement fracture pattern.

The tendency for molybdenite enrichments within the north-south zones adjacent to local north-east-trending flexures has been observed in the Knaben area. These features can be explained if the mineralisation is contemporaneous with the F 4 deformation phase or was partially remobilised on a small scale during this episode. Favourable sites for the crystallisation of material from the mineralising solutions develop in the hinges of small folds as a result of the release of strain by plastic deformation.

The apparent lithostratigraphical control of much of the mineralisation can be interpreted in terms of a local origin of the metals as has been suggested by Borchert (1961) with subsequent mobilisation and redeposition with quartz and feldspathic veins and sheets. Sedimentary enrichments of metallic elements including molybdenum and copper are frequent in black organic-rich sulphidic shales. The relatively simple

trace element chemistry of the mineralised gneisses, illustrated in table 5, does not compare closely with these rocks however, but resembles deposits of undoubted epigenetic origin.

The location of the molybdenite deposits was nevertheless probably greatly influenced by the presence of sulphide-rich fahlband horizons within the layered feldspathic gneisses. According to the stability diagrams in the iron, sulphur, oxygen system, of Holland (1959) an increase in the oxygen fugacity can bring about the decomposition of pyrrhotite into magnetite. Assuming the fahlband sulphide after high-grade metamorphism to be mostly pyrrhotite, the upward-percolating hydrous mineralising solutions could cause the oxygen fugacity to rise sufficiently for the decomposition of the sulphide with the release of sulphur. This sulphur would then cause the precipitation of sulphides of any metals carried as complex ions, like the silicomolybdate complex, in the hydrous solutions if the stability fields of the sulphides extended to higher oxidation levels than that of iron. Thus copper and molybdenum sulphides would be produced by reactions of the form of :-

$$6\ FeS + 3Cu + 4O = 3CuFeS_2 + Fe_3O_4 \text{ - - - - - (1)}$$

$$6\ FeS + 3Mo + 8O = 3MoS_2 + 2Fe_3O_4 \text{ --------- (2)}$$

The textural evidence of sulphide phase interrelationships is compatible with the operation of the above reactions.

Similar arguments have been used by MacLean (1969) to explain the separation of sulphide from crystallising magma. Pyrite would then crystallise as temperature and oxygen fugacity decreased. Gammon (1966) records that both the Kongsberg silver deposits and the Modum cobalt mineralisation show close association with older fahlband zones in the PreCambrian Kongsberg-Bamble formation. The silver-bearing veins are thought to be of Permian age while the age of the cobalt mineralisation is uncertain.

Little can be deduced about the nature of the mineralising solutions as the alteration of adjacent silicate rocks is slight. The only significant difference between the impregnated gangfjell rock and the adjacent granitic gneiss is that the colour of the potassium feldspar megacrysts in the former are grey in colour rather than pink. Large clinopyroxene grains within the basic gneiss adjacent to mineralised rocks at Åvedal are altered to hornblende and calcite, the reaction possibly having occurred when the rocks were invaded by the mineralising solutions.

An interesting feature of many of the molybdenite deposits is the close association of the sulphides, often within a small volume of rock, with quartz veins, pegmatite and granular leucogranite. Krauskopf (1967), in a review of the relationships of mineralising solutions with the end stage products of magmatism, comments on the scarcity of sulphides associated with pegmatites and the " absence, or at least great

scarcity of observed transitions between pegmatites and quartz-sulphide veins ". Jahns and Burham (1957) suggest that a quartz, alkali feldspar melt, slightly undersaturated with water, can crystallise as an early aplite phase followed after the ' second boiling ' by a pegmatite phase. Quartz-sulphide veins must have crystallised from solutions with considerably more water, a solution of silica in water rather than a silicate melt saturated with water. The separation of a water-rich phase from the end stages of a crystallising magma, as the water content of the residual liquid increases, is quite feasible. The majority of field evidence would suggest that if a water-rich and a water-poor phase were formed at the end of magmatic crystallisation, there is a great tendency for them to separate because of the much greater mobility of the hydrous phase. The closeness of the association of the three phases in the Knaben area therefore points to a local origin of the silicate-rich phases.

In view of the absence of nearby magmatic rocks, it is concluded that the silicate-rich phases were produced by the partial melting of the surrounding gneissic rocks. Partial metling of high grade gneissic rocks is impossible after the climax of metamorphism unless water is supplied from outside the system. It is possible that the ascending siliceous mineralising solutions provided water for the local remelting of the gneisses through which they passed so producing pegmatite and granular leucogranite intimately associated with

the quartz sulphide veins if the rocks were still at a high temperature. San Miguel (1969) is of the opinion that aplite or granular leucogranite can be formed by the cataclasis and microgranulation of granitic rock under differential tectonic movements. Pegmatite can then be produced by synkinematic or postkinematic recrystallisation and feldspathization. Assuming that the Knaben granular leucogranite layers were formed in this way, the invading hydrothermal solutions could cause partial recrystallisation and mobilisation of these rocks to produce pegmatite associated with the quartz veins.

The molybdenite mineralisation is considered to have originated from siliceous hydrothermal mineralising solutions, formed in depth, which ascended through the gneisses particularly where the direction of the gneissic layering coincided with that of the basement fracture pattern. Deposition of molybdenite often occurred in the vicinity of prexisting fahlband sulphide.

10. THE CHEMISTRY AND ORIGIN OF THE GRANITIC GNEISSES.

Major element analyses of metamorphic granitic rocks are shown in tables 6 to 11. Normative quartz, albite, orthoclase and albite, orthoclase, anorthite contents of these rocks are plotted in figure 16. On the quartz, albite, orthoclase diagram virtually all the rocks plot within the field occupied by 53% of 1190 granitic rocks examined by Winkler and von Platen (1961).

The majority of the Kvinesdal gneiss is a leucocratic granitic rock relatively rich both in sodium and potassium as shown in figure 17. Heterogeneities are represented by faint layering into pink and grey components and diffuse biotite schlieren. These features are consistent with the development of a nebulitic migmatite during high-grade metamorphism from a sedimentary sequence rich in feldspathic greywacke by a process of almost complete homogenisation. Mehnert (1968) argues that in view of the granitic nature of the early PreCambrian crust, feldspathic sediments were probably common on the flanks of the early continents. The same author also favours the formation of granitic plutonic migmatites by homogenisation involving the redistribution of alkalies rather than external addition of material.

The granular leucogranite horizons within the Kvinesdal gneiss are more siliceous and depleted in the ferromagnesian

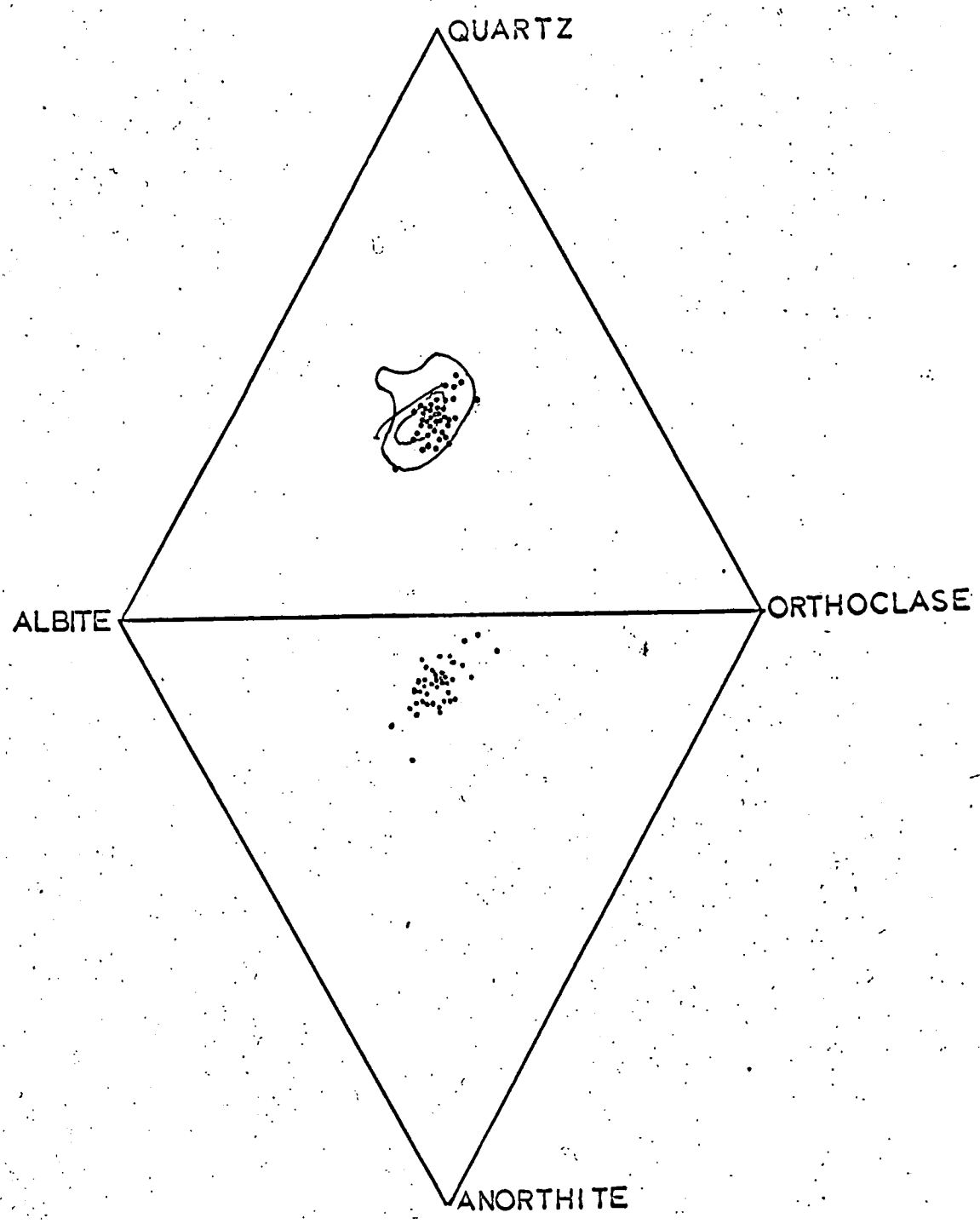

Normative mineral contents of granitic gneisses. The fields of 14% & 53% of 1190 granitic rocks from Winkler and von Platen (1961) are also shown.

Figure 16.

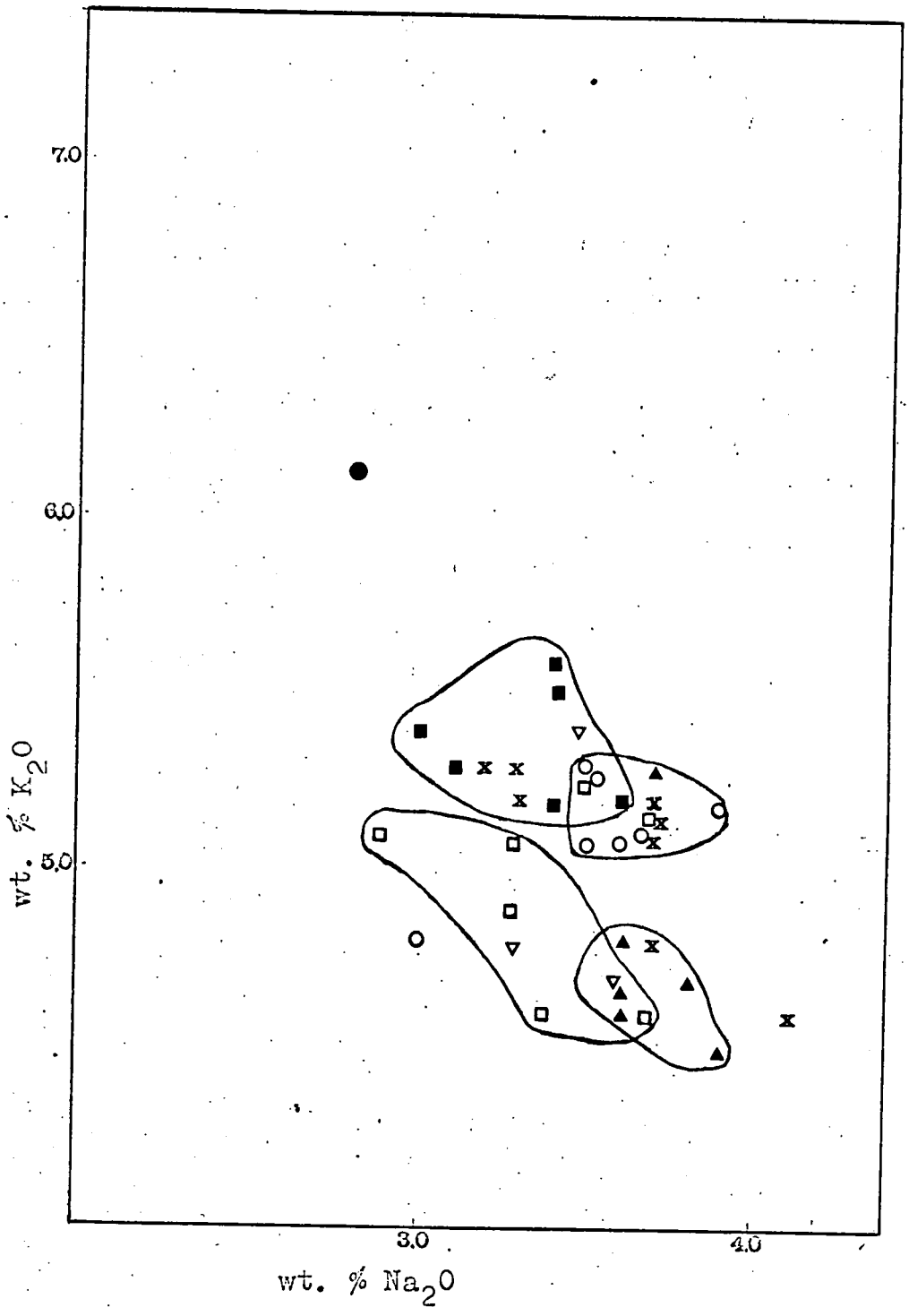

Sodium and potassium contents of microgranite ● , granular leucogranites ■ , Kvinesdal gneiss ○ , Fjotland granite ▲ , Tonstad gneiss □ , Øie gneiss x , and granitic rocks of Lervig gneiss ▽ .

Figure 17.

elements than the granitic gneisses in which they occur. Inspection of figure 17 reveals that the majority of the granular leucogranites are poorer in sodium and slightly richer in potassium than typical Kvinesdal gneiss specimens. These characteristics are features of other neosomal rocks in migmatite complexes, eg. the Finnish migmatites described by Härme (1965). In view of the small proportion of these rocks in the Kvinesdal gneiss, their derivation from the granitic gneiss at a relatively late stage of the metamorphic episode under locally increased water activity is feasible.

A slightly lower silicon content and corresponding higher iron, magnesium and calcium contents serve to distinguish chemically the rocks of the Øie gneiss from those of the Kvinesdal gneiss. In figure 17 rocks from this unit plot within the Kvinesdal gneiss field, the granular leucogranite field and also in the relatively potassium-depleted, sodium-enriched field occupied by the specimens of Fjotland granite. The chemical analyses of the Øie gneiss specimens illustrate the more heterogeneous and basic character of the unit compared with the Kvinesdal gneiss.

The granitic rocks of the Tonstad gneiss can be divided into layered and more massive varieties. The layered rocks are significantly poorer in potassium than the majority of both the Kvinesdal and Øie gneiss specimens. The homogeneous granitic rocks are similar in composition to petrographically

similar rocks in the Kvinesdal and Øie gneisses. Specimens 768p and 768d represent adjacent paler and darker layers respectively. The darker layer is significantly richer in iron, magnesium, calcium, potassium and titanium than the paler layer and correspondingly poorer in silicon and sodium. This is expressed in a much greater content of iron oxide and to a lesser extent of biotite in the darker layer, together with more calcic plagioclase. Neosomal rock in the Tonstad gneiss unlike the Kvinesdal gneiss is mostly in the form of layers of relatively coarse-grained pink potassium feldspar-rich material and pegmatite layers and pods. The layered facies of the gneiss probably represents original sedimentary compositional differences little modified by subsequent metamorphism.

The analyses of three granitic gneisses from within the basic gneiss horizons, in table 10, are similar to the layered rocks of the Tonstad gneiss and in one case to the granular leucogranite or Kvinesdal gneiss. Specimen 115, of a granitic layer within the Lervig gneiss at Sandvatn, is particularly rich in iron and magnesium compared with other granitic rocks.

The porphyritic gneissic granites are in general slightly less siliceous than the Kvinesdal gneiss. They are similar in sodium content but much poorer in potassium. The more basic varieties, of which specimen 1163 is represent-

ative, are much richer in magnesium and calcium, and hornblende-bearing. Stratigraphically the porphyritic gneissic granites at Fjotland and the north Kvina valley are equivalent to the Lande and Øie gneisses but compositionally there is a closer correspondence to the layered granitic rocks of the Tonstad gneiss. In view of these considerations and the distinctive potassium-rich nature of the basic rocks within the Fjotland porphyritic gneissic granite, this body may represent a cupola of basement Sirdalsvatn Series rock. Alternatively and more probably the Fjotland and particularly the upper Kvina valley porphyritic gneissic granites were formed by the redistribution of alkalies and the partial homogenisation of the gneiss complex by potassium feldspar blastesis. This process could have been initiated during the later stages of metamorphism by the local increase of water and oxygen fugacities as hydrous fluid migrated from depth.

The microgranite dyke specimen from within the Flofjell gneisses to the east of Knaben is considerable enriched in potassium comparednwith the granitic gneisses. These rocks are uncommon and of problematical origin. The specimen of the unfoliated granite body to the east of Knaben is slightly poorer in potassium than the Kvinesdal gneiss and also less calcic.

11. THE CHEMISTRY AND ORIGIN OF THE FEDA AUGEN GNEISS.

The study of the whole-rock chemistry of the Feda augen gneiss is hampered by the extremely large quantity of this coarse-grain rock required to obtain a representative sample. Only two samples of this rock have therefore been analysed (see table 12). Of these, specimen 1246 is representative of the relatively fine-grained marginal facies and specimen 123a of the matrix of the coarsely phenoblastic rock. Compared with intermediate gneisses with similar silica contents from the Flekkefjord Series, specimen 1246 is relatively calcium rich. This is expressed both in the presence of normative and modal clinopyroxene in addition to hornblende and biotite. When allowance is made for the absence of potassium feldspar megacrysts in specimen 123a, the chemistry of this rock resembles that of the marginal variety except for a greater proportion of iron and particularly magnesium. This composition gives rise to a greater hornblende content. The alkali element contents of specimen 1246 are very similar to those of the porphyritic gneissic granite specimens in table 11.

The detailed field relationships within the Feda augen gneiss outcrop (see page 13) suggest that the rock originated from a pre-existing layered gneiss complex. This complex differs from the Flekkefjord Series in chemistry and particularly in the nature of the included basic rocks. Furthermore the

relict arrow head minor folds are restricted to the Sirdalsvatn Series. These differences can be explained if the Sirdalsvatn Series is regarded as part of a basement complex which was caught up in the orogeny which deformed and metamorphosed the Flekkefjord Series. During this later orogeny the rocks of this complex were subjected to an intense phase of potassium feldspar blastesis and homogenisation. The above processes would be facilitated if the original basement rocks were more hydrous and oxidised than the overlying Flekkefjord Series as is suggested by the chemistry of the basic gneiss horizons within the Sirdalsvatn Series. It is unnecessary to invoke an external supply of potassium as redistribution of the element over relatively short distances between adjacent gneiss layers is sufficient to explain the growth of alkali feldspar megacrysts in sites favoured by the local stress field. The number and size of the megacrysts varies considerably from layer to layer in parts of the sequence which indicates that some sites were more favoured than others.

Touret (1967) concludes that the augen gneiss of the Vegårsheii-Gjerstad region along the great breccia between the Telemark and Kongsberg-Bamble provinces, developed by the replacement of a banded gneiss and amphibolite sequence. Smithson and Barth (1967) found small zones of augen gneiss interlayered with other gneisses and large lenses up to two kilometres in width parallel to the margin of the Holum granite. They found field evidence that banded gneiss was

converted into augen gneiss in the cores of mesoscopic folds. They consider that the Holum granite itself developed by recrystallisation from these augen gneisses.

12. THE CHEMISTRY OF THE INTERMEDIATE, BASIC AND GARNET-BEARING GNEISSES.

a) Biotite-hornblende gneisses with intermediate silica contents.

The chemical analyses of biotite-hornblende gneisses with intermediate silica contents within the Lervig and Lande gneisses, the Kvinesdal gneiss, the Fjotland granite and the Sirdalsvatn Series are shown in tables 13, 14, 15 and 16 respectively. In table 13 specimen 820 is representative of the feldspar-rich gneiss horizons with accessory amphibole which form a minor part of the Lervig gneiss. The chemistry of the scattered intermediate gneiss layers within the Kvinesdal gneiss resembles that of rocks with similar silica contents in the Lervig and Lande gneisses, except for slightly greater sodium contents. Though two of the analysed gneisses from within the Fjotland granite contain clinopyroxene in addition to biotite and hornblende, they resemble chemically other intermediate gneisses from the Flekkefjord Series. Specimen 220, on the other hand, is markedly dissimilar with proportionally greater contents of magnesium and potassium.

The hornblende-bearing intermediate gneisses from the Sirdalsvatn Series in table 16 can be divided chemically into three groups. Specimens 159 and 1040 are representative of one group, distinguished in figure 18 from similar gneisses of the Flekkefjord Series by higher magnesium to iron ratios. The

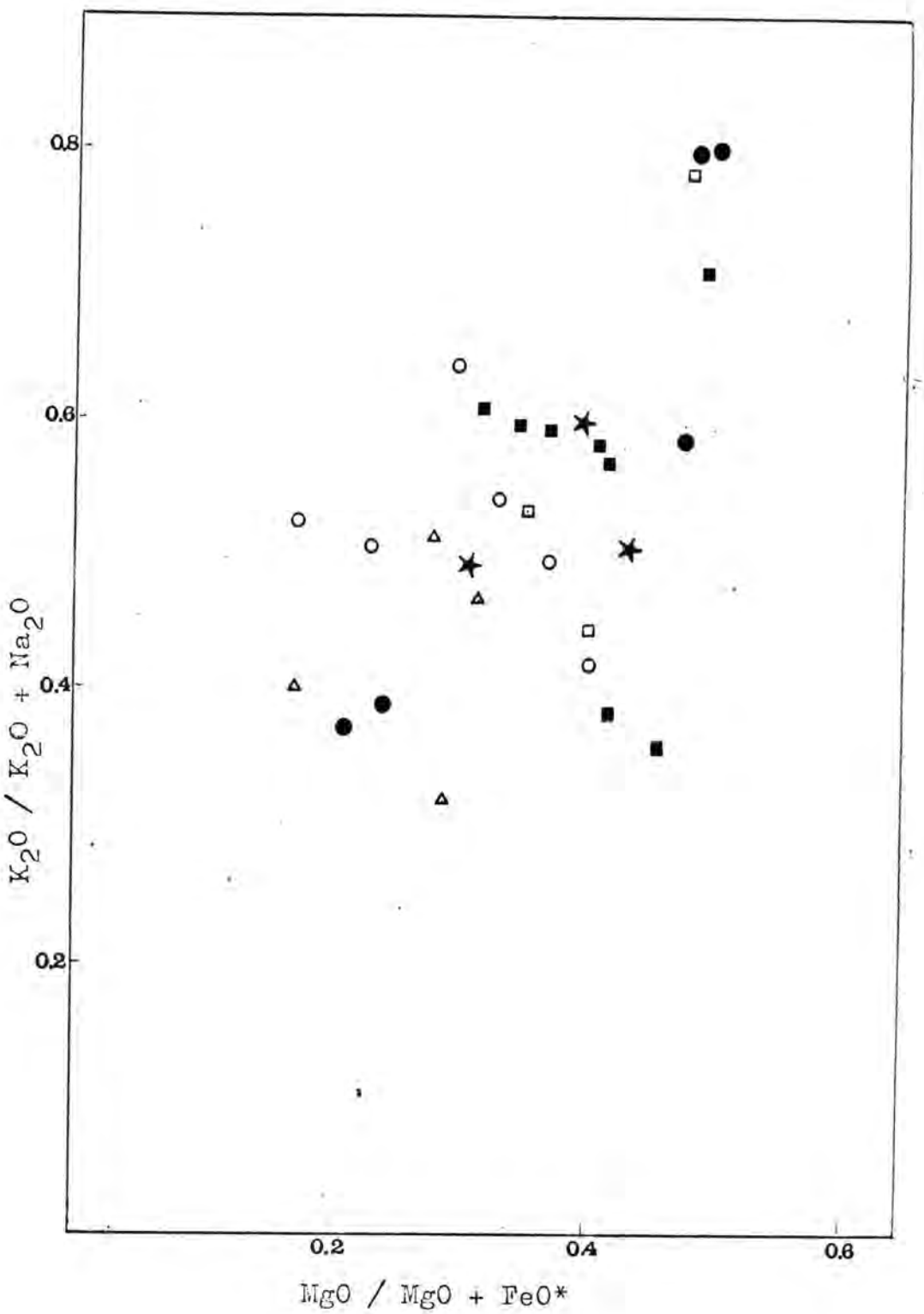

Variation of K_2O to (K_2O + Na_2O) ratio against MgO to (MgO + total Fe as FeO) ratio in intermediate hornblende-bearing rocks of Lervig and Lande gneiss ○ , Kvinesdal gneiss △ , Fjotland granite □ , and Sirdalsvatn Series ■ , together with biotite-clinopyroxene gneisses of Fjotland granite ★ , and Sirdalsvatn Series ● .

Figure 18.

remainder of the analysed rocks of the Sirdalsvatn Series can be distinguished from other groups of intermediate and basic gneisses by their high potassium to sodium ratios. Specimen 1247, which forms the third group is particularly enriched in both potassium and magnesium and contains clinopyroxene as a dominant phase.

The above gneisses have also been plotted on the Niggli mg against c graph in figure 19, a diagram used by Leake (1964) to demonstrate differences between chemical trends in igneous and sedimentary rock sequences. A trend similar to that shown by the Karroo dolerites, and considered by Leake (op. cit.) to typify igneous rocks, is apparent.

b) Biotite-clinopyroxene gneisses.

Analyses of selected examples of this rock type, occurring both within the Sirdalsvatn Series and adjacent to the Fjotland porphyritic granite are shown in table 17. Two groups with high and low potassium to sodium and magnesium to iron ratios respectively are apparent in figure 18. The specimens from the environs of the Fjotland granite have potassium to sodium and magnesium to iron ratios intermediate between the two groups of Sirdalsvatn Series gneisses. A plot of the titanium to iron ratio against the manganese to iron ratio of all the analysed intermediate and basic gneisses in figure 20 reveals that, like the hornblende-bearing gneisses of the

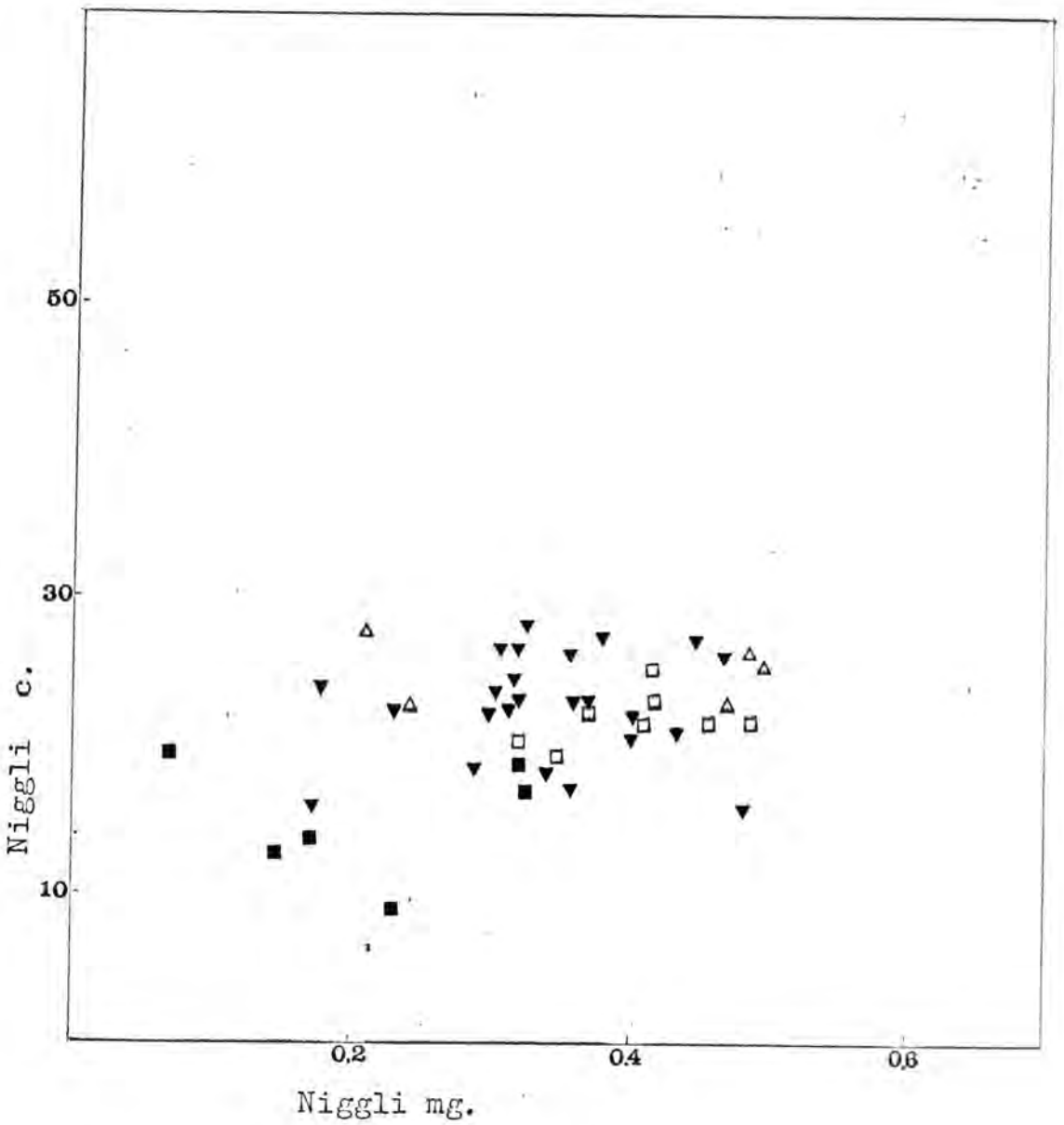

Niggli mg against c plot for hornblende-bearing Flekkefjord Series gneisses ▼ , hornblende-bearing Sirdalsvatn Series gneisses □ , biotite-clinopyroxene gneisses of the Sirdalsvatn Series △ and garnet-bearing gneisses ■ .

Figure 19.

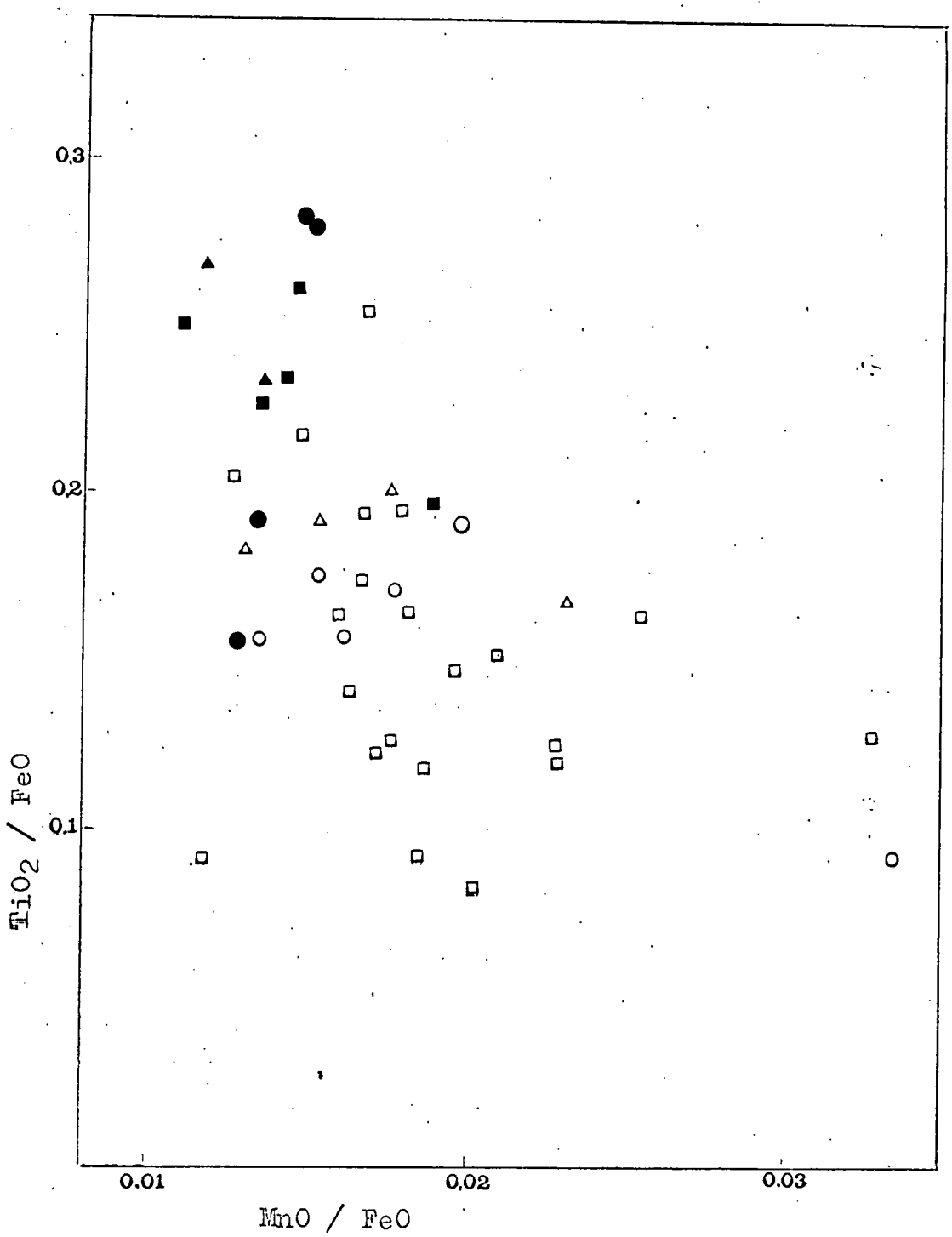

The relationship between the titanium to total iron ratio and the manganese to total iron ratio in amphibolites from the Flekkefjord Series □ , amphibole-bearing gneisses from the Fjotland granite △ , pyribolites ○ , amphibole-bearing gneisses from the Sirdalsvatn Series ■ , biotite-clinopyroxene gneisses from the Sirdalsvatn Series ● and Fjotland granite ▲ .

Figure 20.

Sirdalsvatn Series, the biotite-clinopyroxene gneisses are enriched in titanium and depleted in manganese compared with other rock groups. Other chemical characteristics of the biotite-clinopyroxene gneisses, particularly of the Sirdalsvatn Series, are their relative enrichment in phosphorous and barium compared with other rocks.

c) Amphibolites.

The composition of amphibolites and other hornblende-rich basic gneisses from the Lervig gneiss, the Lande gneiss and the Knaben gneiss are shown in tables 18, 19 and 20 respectively. The range in composition of the Lervig and Lande gneiss rocks is very similar in spite of a greater frequency of clinopyroxene in the Lervig gneiss specimens. The basic rocks of the Knaben gneiss tend to be richer in iron and magnesium and possibly phosporous and poorer in silicon and calcium than the majority of the rocks in either table 18 or 19. Some of the Knaben gneiss rocks are also relatively potassium rich and in consequence biotite rich. The analysed basic gneisses of the Oddevassheii gneiss in table 21, though pyribolites by virtue of their proximity to the Ljosland intrusion, show chemical resemblences to rocks of the Knaben gneiss.

d) Pyribolites.

The major element analyses of seven pyribolites, from both

the Lervig and Lande gneisses, are shown in table 22. With the exception of specimen 743 which represents a metamorphosed dyke rock, all the pyribolites are more siliceous than the amphibolites of the Lervig and Knaben gneisses. The range shown by most of the other elements is wide and similar to that of the other basic rocks. The range of the magnesium to iron ratios of the pyribolites is significantly lower than that of the amphibolites. Furthermore figure 20 reveals that, with the exception of specimen 149b, the two-pyroxene gneisses are richer in titanium and poorer in manganese than the majority of amphibolites. The barium to potassium ratios and phosphorous contents of several pyribolites are also in excess of the amphibolites.

e) Garnetiferous gneisses.

The analyses of six garnet-bearing rocks are shown in table 23. The compositional range covered by these rocks is extremely large. Specimens 1067 and 1063 are a garnet-bearing leucogranite and a phenoblastic feldspathic gneiss of quartz monzonite composition with some garnet in addition to biotite respectively. In major element composition these rocks are very similar to other non-garnetiferous granitic rocks. The presence of garnet is therefore indicative of an environment of lower oxygen and water fugacities during crystallisation than for the other granitic gneisses. Specimens 818d and 818e are two similar calcium-rich intermediate

gneisses from the Lervig gneiss with a close chemical resemblance to the hornblende-bearing intermediate gneisses except for lower potassium contents. The garnet of these rocks also probably originated as a result of low ambient oxygen and water fugacities.

Specimen 615b and particularly specimen 511b, on the other hand, are both rocks with pelitic affinities. They are both relatively aluminous and have low magnesium to iron ratios. Specimen 615b is also depleted in potassium and specimen 511b in calcium.

f) Oxidation ratios of the intermediate and basic gneisses.

The oxidation ratio of selected examples of the above rock types has been determined wet chemically as described in the appendix and the results are shown in table 24. The majority of the gneisses from the Flekkefjord Series have oxidation ratios between 38.0 and 42.0, whereas those from both the margins of the Fjotland granite and the Sirdalsvatn Series are much higher. The lowest oxidation ratio is shown by the biotite garnet gneiss from the Lervig gneiss, specimen 815, though two pyribolites from the Lande gneiss have only slightly higher values. The two relatively oxidised rocks from the Flekkefjord Series, specimens 551c and 24m are from the intensely migmatised Lervig gneiss in the core of the Sandvatn antiform and from within a great thickness of

granitic gneiss respectively. The four specimens of basic gneiss layers within the Tonstad gneiss, specimens 133, 832a, 835 and 1247, though exhibiting different parageneses, have very similar oxidation ratios which suggests a close original environmental relationship.

Chinner (1960) concluded that the considerable variation in oxygen contents of the Glen Clova pelitic gneisses was of premetamorphic origin and that during metamorphism the system was essentially closed to oxygen. The same conclusion can be applied to the majority of the gneisses considered in this present study. The rocks within and adjacent to the Fjotland granite may on the other hand have been oxidised as a result of interaction with the ascending hydrothermal solutions which facilitated the recrystallisation of the granite.

g) Trace element chemistry.

Analyses of the elements sulphur, chlorine, nickel, copper, zinc, gallium, rubidium, strontium, yttrium, zirconium, cerium, lead and thorium in intermediate and basic rocks of the Sirdalsvatn Series, the Lervig gneiss, the Lande gneiss and the Kvinesdal, Knaben and Oddevassheii gneisses are shown in tables 25, 26, 27 and 28 respectively.

Examination of the sulphur contents of the rocks reveals

that clinopyroxene amphibolites, with the exception of specimen 207d, are relatively depleted in sulphur. Furthermore the rocks of the Sirdalsvatn exhibit as a group the greatest enrichment in this element. A moderate but significant correlation between sulphur and copper is also apparent from the data.

A significant but moderate correlation between chlorine and phosphorous exists, particularly within rocks of the Sirdalsvatn Series which can readily be interpreted in terms of a significant chlorine content of apatite. Little correlation between the two elements is evident within many of the amphibolites and pyribolites however, Chloride contamination of natural origin or introduced during samples preparation cannot be ruled out, even though care was exercised to collect fresh samples.

Nickel shows a significant moderate correlation with magnesium and iron and is generally enriched in the most basic gneisses. The nickel content of the hornblende of specimen 56 which contains little sulphide, biotite or oxide phases can be estimated as 200ppm, a value slightly higher than the average of amphibolite facies hornblendes quoted by DeVore (1955).

Chalcopyrite has been recognised in several of the analysed rocks, usually in association with pyrite but only a moderate

correlation between the copper content of the rocks and the modal pyrite exists. Little correlation between copper and elements other than sulphur is apparent.

Zinc shows a moderate correlation with iron. There is also a regular relationship between the zince to iron oxide ratio and the modal biotite content of several of the rocks as illustrated in figure 21. Three groups of rocks can be recognised on this diagram, one consisting predominantly of biotite clinopyroxene gneisses, a second of amphibolites and biotite amphibolites and a third with the lowest gradient containing clinopyroxene amphibolites and amphibolites without oxide phases and two hornblende-bearing gneisses of the Sirdalsvatn Series. The zinc content of the hornblende of specimen 56 can be estimated as about 240ppm, an amount similar to the average zinc content of hornblendes from the granulite facies quoted by DeVore (1955).

Gallium shows a strong positive correlation with aluminium. Significant depletion in gallium is shown by the majority of the clinopyroxene amphibolites and by amphibolites from the Lande gneiss.

Rubidium exhibits a strong positive correlation with potassium but compared with all other basic gneisses the rocks of the Knaben and Oddevassheii gneisses are all significantly enriched in the element. The rubidium content of the biotite

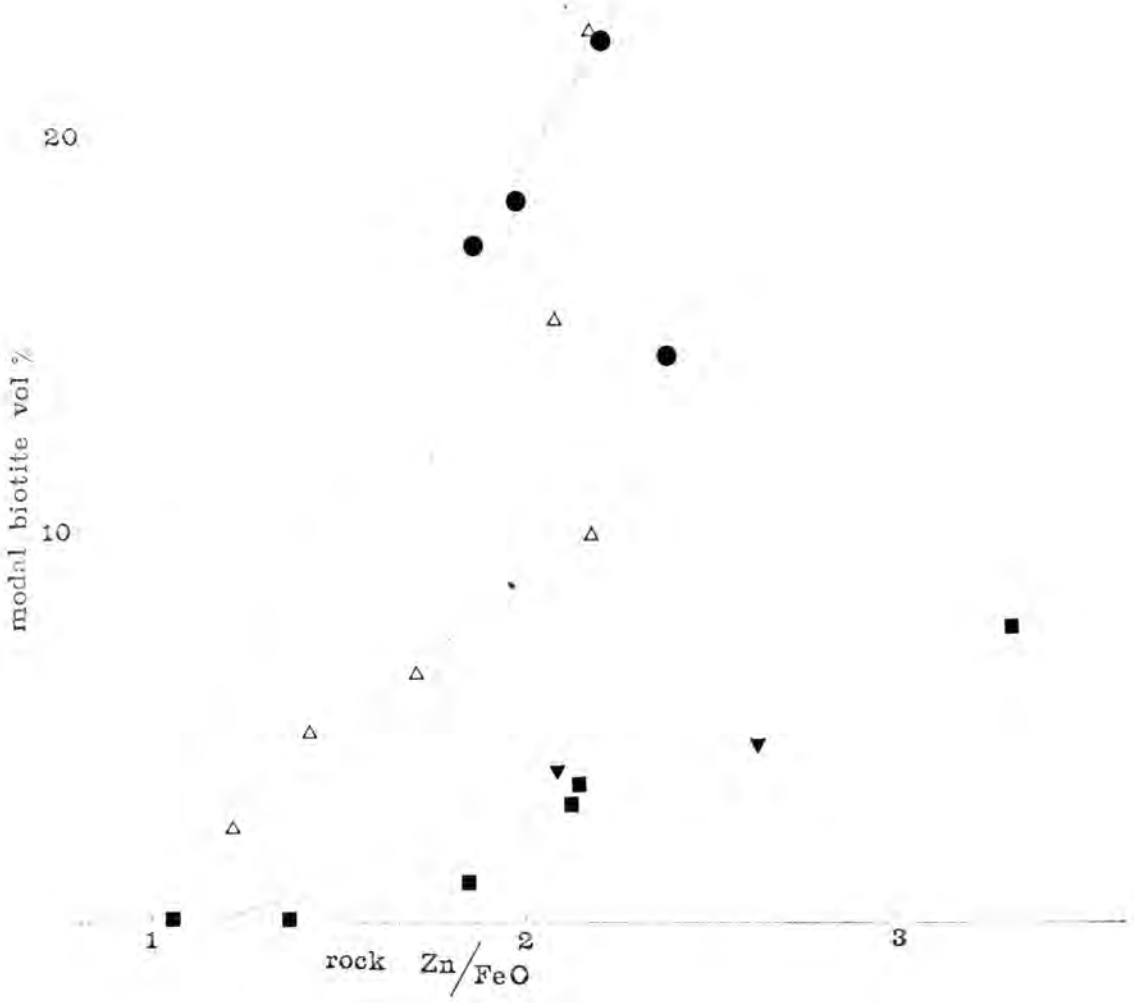

The relationship between biotite content and the rock Zn/FeO ratio for biotite-clinopyroxene gneisses ● , oxide-phase-bearing amphibolites △ , amphibolites and clinopyroxene amphibolites without oxide phases ■ and hornblende-bearing gneisses from Sirdalsvatn Series ▼ .

Figure 21.

of these rocks can be estimated at about 1700ppm, in contrast to a range of from 1200ppm to 1400ppm for biotites from other basic gneisses. The rubidium content of alkali feldspar can be estimated from the rock analyses as about 800ppm.

Strontium shows a significant moderate positive correlation with phosphorous, zirconium and barium and higher correlation with cerium and lead. Relatively high strontium contents is a feature of the rocks of the Sirdalsvatn Series and to a lesser extent of the pyribolites.

Yttrium shows significant moderate positive correlation with phosphorous, zirconium and cerium and relative enrichment in rocks of the Sirdalsvatn Series and some pyribolites.

Zirconium contents of the analysed rocks display moderate positive correlation with phosphorous, strontium, yttrium, barium and lead and high positive correlation with cerium. The lowest amount of zirconium occurs in clinopyroxene-bearing amphibolites and biotite-poor amphibolites.

In the analysed rocks cerium exhibits moderate positive correlation with phosphorous, yttrium and barium and high positive correlation with strontium, zirconium and lead. The rocks of the Sirdalsvatn Series contain both the highest cerium contents and the greatest cerium to yttrium ratios.

The lead content of the majority of analysed basic gneisses is less than 25ppm. For the intermediate gneisses there is a strong positive correlation between lead contents and the modal potassium feldspar contents. The lead within alkali feldspar can be computed as about 120ppm from this relationship.

Only three of the analysed rocks contains thorium in excess of 6ppm. Of these, the rock with the highest content, 17ppm, also contains a relatively large amount of cerium which suggests the presence of an appreciable quantity of thorium-bearing allanite.

Factor analysis with orthogonal rotation of factor axes was carried out for the 15 variables Mg/Fe, P, Ca/Fe, Ti/Fe, Mn/Fe, Ni/Fe, Zn/Fe, Ga/al, Rb/K, Sr, Y, Zr, Ba/K, Ce and Pb on an I.B.M. 1130 computer with an 8K stone in the 26 rocks for which trace element analyses were available. Ratios between minor and major elements showing significant correlation were preferred to the absolute elemental concentrations in order to reduce variations in trace elements related primarily to the variation of the major element for which they substitute in the major mineral phases present. Four factors with eigen values greater than 1.0 accounting for 81% of the total variation were indicated. The factor loadings of each variable in the first two factors, accounting for 65% of the total variation, are shown in figure 22.

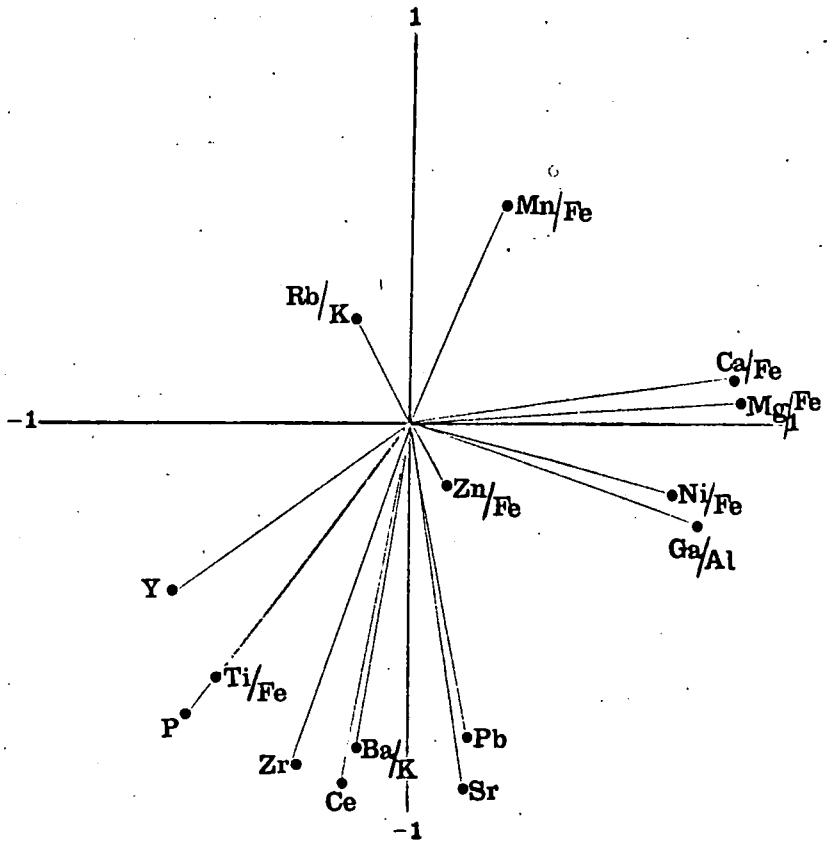

Factor analysis with orthogonal rotation of axes. Loadings for 15 element and ratio variables in terms of first two factors (1st factor vertical axis).

Figure 22.

The grouping of Pb, Sr, Ba/K, Ce, Zr and to a lesser extent Ti/Fe, P and - Mn/Fe about one factor axis is manefest. The major contributent to this factor is the difference in composition between Sirdalsvatn Series rocks and those of the Flekkefjord Series. The Sirdalsvatn series rocks are typified by barium-rich alkali feldspar and the relative abundance of the accessory minerals, apatite, zircon and allanite. These features which are most developed in the chemistry of the biotite-clinopyroxene gneisses are in many respects similar to those of potassic volcanic rocks of continental areas, such as have been described by Carmichael (1967) from Wyoming and by Coombs and Wilkinson (1969) from Otago, New Zealand.

The variables Ca/Fe, Mg/FE, Ni/Fe and Ga/Al are closely grouped around the second factor axis. This factor is interpreted as the result of the variation in composition within the Flekkefjord Series towards the most basic gneisses, rich in both hornblende and clinopyroxene and best developed within the Lande Gneiss.

The third factor comprises almost all the variation of the variable Zn/Fe and half the variation of Mn/Fe and on the basis of figure 21 is probably related to the biotite content, particularly of the gneisses without iron-titanium oxide phases.

The fourth factor comprises most of the variation in Rb/K and little else. The major contributant to this factor is the high Rb/K ratios shown by the basic gneisses of the Knaben and Oddevassheii gneisses.

The chemical study of the intermediate and basic gneisses of the area surveyed has revealed significant differences between rocks of the Sirdalsvatn Series and those of the Flekkefjord Series. Geochemical evidence thus supports the structural hypothesis of a fundamental discordance between the two gneiss series. The apparent geochemical differences between basic rocks of the Knaben and Oddevassheii gneisses and similar rocks of other parts of the Flekkefjord Series may also be useful as aids to correlation and structural interpretation of gneisses in other sectors of the Telemark-Rogaland Province. The above data also provides evidence of chemical differences between pyribolites and amphibolites with which they are associated.

13. MINERAL CHEMISTRY.

a) Alkali feldspar.

38 small areas of a potassium feldspar megacryst from a specimen of the Feda augen gneiss were analysed for sodium and potassium by means of the electron microprobe (see appendix). The spots were selected to cover the whole of the grain and were optically clear and without visible perthite. A few spots were also analysed for calcium and barium. The results of these determinations are shown in table 29 recalculated to molecular percentages. The results show a considerable spread, from Or. 71% to Or. 84% for potassium, from Ab. 12% to Ab. 27% for sodium, from An. 0.6% to An. 1.1% for calcium and from Cn. 1.7% to Cn. 2.5% for barium. A histogram of the distribution of potassium contents is shown in figure 23. A tendency for the margins of the crystal to be poorer in sodium than the centre was noticed though the variation was by no means regular.

Ohta (1969) has measured the optic axial angle at several hundred points within large potassium feldspar augen by means of the universal stage and concluded that the degree of ordering varied considerably from point to point. He regarded that this inhomogeneity was a common feature in augen gneisses and resulted from porphyroblastic growth by the coalescence of several granular crystals. As the optic

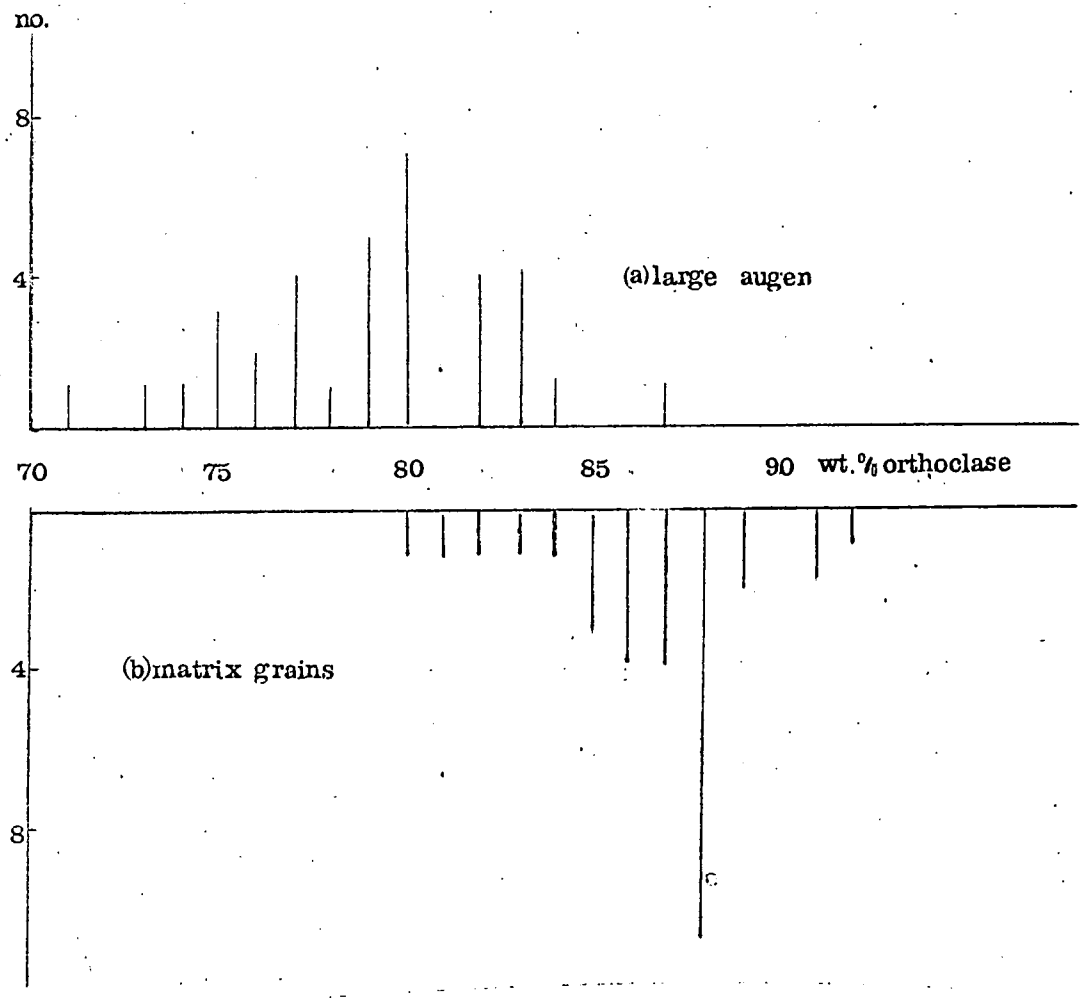

HISTOGRAM OF ALKALI FELDSPAR ANALYSES FROM AUGEN GNEISS 123a

Figure 23.

axial angle is both a function of the chemical composition and the structural state, some of the variation measured by Ohta could be the result of chemical inhomogeneity. Smithson (1962) in an X-ray powder diffraction study of Norwegian alkali feldspars found that the feldspars of augen gneisses showed either low or very variable obliquity and Touret (1967b) found similar results for augen gneisses in the Vegåsheii-Gjerstad region. Twinning is also a gross indication of differences in degree of ordering. In the feldspar megacryst analysed by the present author the twinning varies from the sharp gridiron type to a very faint and diffuse variety. It can be concluded therefore that the potassium feldspar megacrysts of the Feda augen gneiss are markedly out of both structural and chemical equilibrium.

35 matrix alkali feldspar grains from the same specimen of Feda augen gneiss were also analysed with the electron microprobe. The results of these determinations are shown in table 30. These also show a considerable spread, from Or 80% to Or. 92% for potassium, from Ab. 5% to Ab. 16% for sodium, from An. 0.6% to An. 0.8% for calcium and from Cn. 2.1% to Cn. 2.7% for barium. Figure 23 also shows a histogram of the distribution of potassium contents for these grains. It is immediately evident that the mean potassium content of the matrix grains is significantly greater than that of the megacryst. On the basis of the two feldspar geothermometer described by Barth (1956) and

developed in a series of later papers (eg. Barth , 1968) a difference in temperature of formation of the megacryst and matrix grains is implied. There is considerable textural evidence within the Feda augen gneiss of mobility and redistribution of sodium during the cooling phase of the metamorphism. The occurrence of rims of clear albite around the plagioclase grains of the rock and the widespread development of myrmekite along alkali feldspar - plagioclase interfaces is particularly suggestive of post crystallisation sodium mobility. The leaching of sodium by supercritical water has been demonstrated experimentally by Adams (1968). The operation of such a process would explain the lower sodium content of the margins of the megacryst and by virtue of the much larger surface area to volume ratio of the matrix grains, the tendency for these crystals to be poorer in sodium than the megacrysts as a whole. The large variation in apparent temperature of crystallisation for the various components of the PreCambrian of Southern Norway obtained by Barth (1956b), using the two feldspar geothermometer, could also be explained, at least in part, in terms of the size of the feldspar grains and hence their resistence to subsequent leaching. Barth obtained the highest temperatures of formation in augen gneisses, slightly lower temperatures for pegmatites and porphyritic diapir granites, much lower temperatures for regional gneisses and even lower temperatures for aplites.

Several alkali feldspar grains in a further nine rocks were also analysed for sodium and potassium, and in a few cases for calcium and barium, using the electron microprobe. The results of the analyses are shown in table 31. The rocks analysed consisted of several intermediate hornblende-bearing gneisses with varying proportions of modal potassium feldspar, biotite-clinopyroxene gneisses and a specimen of the Haddeland quartz monzonite intrusion. In five of the rocks a variation in alkali feldspar composition comparable with that in the Feda augen gneiss was obtained. In two specimens of intermediate gneiss, both with relatively low modal alkali feldspar, and a biotite-clinopyroxene gneiss from the margins of the Fjotland granite the variation in composition from grain to grain was much less. A small variation in potassium feldspar composition was also found in the retrograded piemontite, chlorite-bearing rock 52. The temperature at which this rock crystallised was probably too low for any significant subsequent movement of sodium. It is evident from table 31 that the barium content of alkali feldspar in biotite-clinopyroxene gneiss from the Sirdalsvatn Series is considerably higher than that of the Feda augen gneiss feldspars, though there is unfortunately no corresponding data for Flekkefjord Series rocks with which further comparisons can be made.

b) Plagioclase.

The major element electron probe analyses of seven plagioclases are shown in table 32. The results of electron microprobe calcium analyses of a further 25 minerals is shown in table 33. The compositions range from 21% by weight anorthite to 52% by weight anorthite. The plagioclases from alkali feldspar-containing intermediate and basic gneisses have a restricted compositional range, from 21% anorthite to 24% anorthite by weight. This implies that in the presence of alkali feldspar the plagioclase composition is independant of rock composition but probably related to external factors, of which the most important is temperature. This is the basis of the Barth (1956a) two feldspar geothermometer. If the maximum sodium content of the alkali feldspar megacrysts from the Feda augen gneiss, the crystals least affected by subsequent sodium leaching, and the composition of the coexisting plagioclase are compared with the calibrations given by Barth (1968), a temperature of formation of 580°C is obtained. This temperature is compatible with estimates from other data, eg. coexisting iron and titanium oxide compositions. Barth (1956b) presents two analyses of alkali feldspar and coexisting plagioclases from the Feda augen gneiss near Haughom. A temperature of formation of about 590°C can be deduced from these compositions using the latest calibration. For the biotite clinopyroxene gneiss 832b from the Sirdalsvatn Series a crystallisation temperature of 610°C is suggested from

the maximum sodium content of the alkali feldspar and the albite content of the coexisting plagioclase. In the other rocks where alkali feldspar compositions have been determined the temperatures obtained using the two feldspar geothermometer are much lower as a result of redistribution of sodium while the rocks were cooling.

c) Biotite.

The analyses of 39 biotites determined by means of the electron microprobe, as described in the appendix, together with their recalculations with respect to 22 oxygen atoms are shown in table 34. The majority of these compositions are richer in silicon and poorer in aluminium than most of the classical analyses of metamorphic biotites quoted by Deer, Howie and Zussman (1962). Nine of the present biotite analyses recalculate with insufficient silicon and aluminium to fill the z site. It is undoubtedly significant that the two minerals with the lowest z site totals are from the highest temperature environment of metamorphism, in the contact aureole of the Ljosland intrusion. The two biotites which coexist with garnet, specimens 818d and 818e, are significantly richer in aluminium than all the other analysed minerals.

The y site totals of the biotites range from 5.50 to 6.00 atoms per formula unit and the x site totals from 1.71 to 1.88

atoms per formula unit. A plot of the number of titanium atoms per biotite unit against the negative charge balance calculated from the ideal phlogopite-annite formula is shown in figure 24. A close approach to linearity is apparent, particularly when vacencies in the z site are also included in the charge balance assessment where appropriate. Extra positive charge due to the presence of ferric iron would cause the biotites to plot to the right of the line with gradient o.5. As there is a close approach to this line, except for the specimen with the lowest titanium content, it is concluded that the ferric content of the rest of the biotites is constant and allowing for any bias in the analytical results, probably small. The most iron-rich biotites must therefore have the lowest ferric iron to ferrous iron ratios. Furthermore the titanium content is inversely related to the ferric to ferrous ratio of the biotites by virtue of the [illegible] correlation between total iron and titanium shown by the analyses. Dahl (1970) has explained a correlation between the titanium content and a comparable valency balance to that used by the present author, in metamorphic biotites from the Swedish PreCambrian, in terms of a tendency for the size of the octahedral layer to remain constant. Thus an increase in the iron content of a biotite tends to expand the octahedral layer and this can be counted by the introduction of more titanium and aluminium with the simultaneous creation of vacancies.

The colour of the biotites that have been analysed in

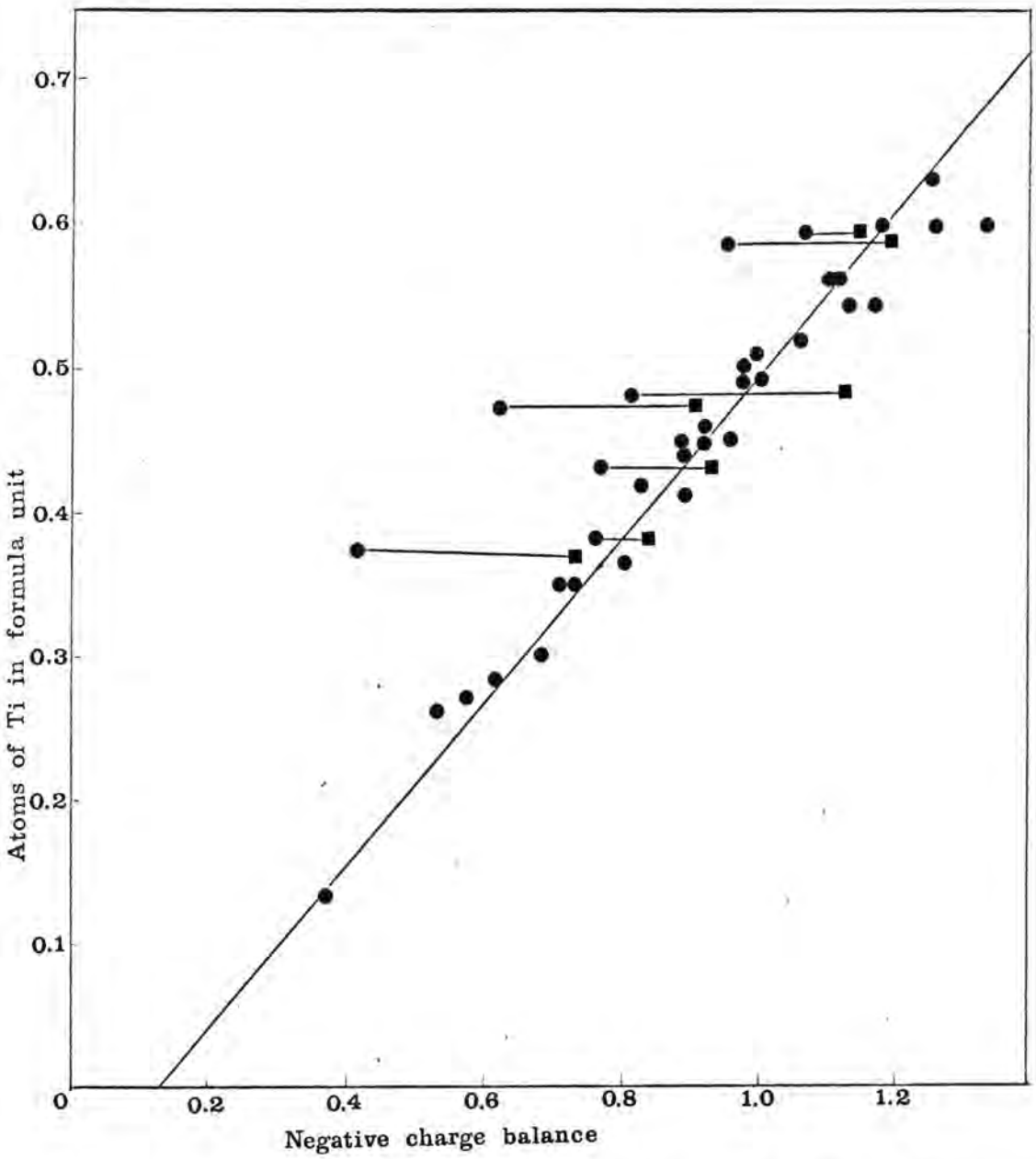

● Negative charge balance given by Al in z site - 2 - Al in y site + 2 x vacancies in y site + vacancies in x site.

■ Negative charge balance as above + 4 x vacancies in z site.

Relationship between Ti content and negative charge balance in biotites.

Figure 24.

the present study are at least in part related to the titanium content. The minerals with the highest titanium contents are a distinctive deep brown-red colour while those with less of this element are various shades of deep brown and chestnut brown.

d) Hornblende.

The electron microprobe analyses of 31 hornblendes together with their recalculations with respect to 23 oxygen atoms are shown in table 35. The y-site totals range from 4.98 to 5.34 atoms per formula unit, a deviation from the ideal from the ideal five atoms per formula unit, which according to Phillips (1963), suggests some analytical error. Many chemical analyses of amphiboles show similar or even greater deviations from this ideal and have been accepted by Shido (1958) as indicative of a cummingtonite substitution in which magnesium enters the x site in place of calcium. In figure 25 the hornblendes are plotted on a diagram of Deer, Howie and Zussman (1963) of aluminium in the tetrahedral site against the total sodium and potassium contents. The minerals occupy a position between the point arbitrarily termed hornblende and the pargasite-ferrohastingsite end-member in common with many other metamorphic hornblendes. The tetrahedral aluminium contents range from 1.19 to 1.60 per formula unit and the total alkali content from 0.49 to 0.82 per formula unit. The hornblende from the metamorphosed

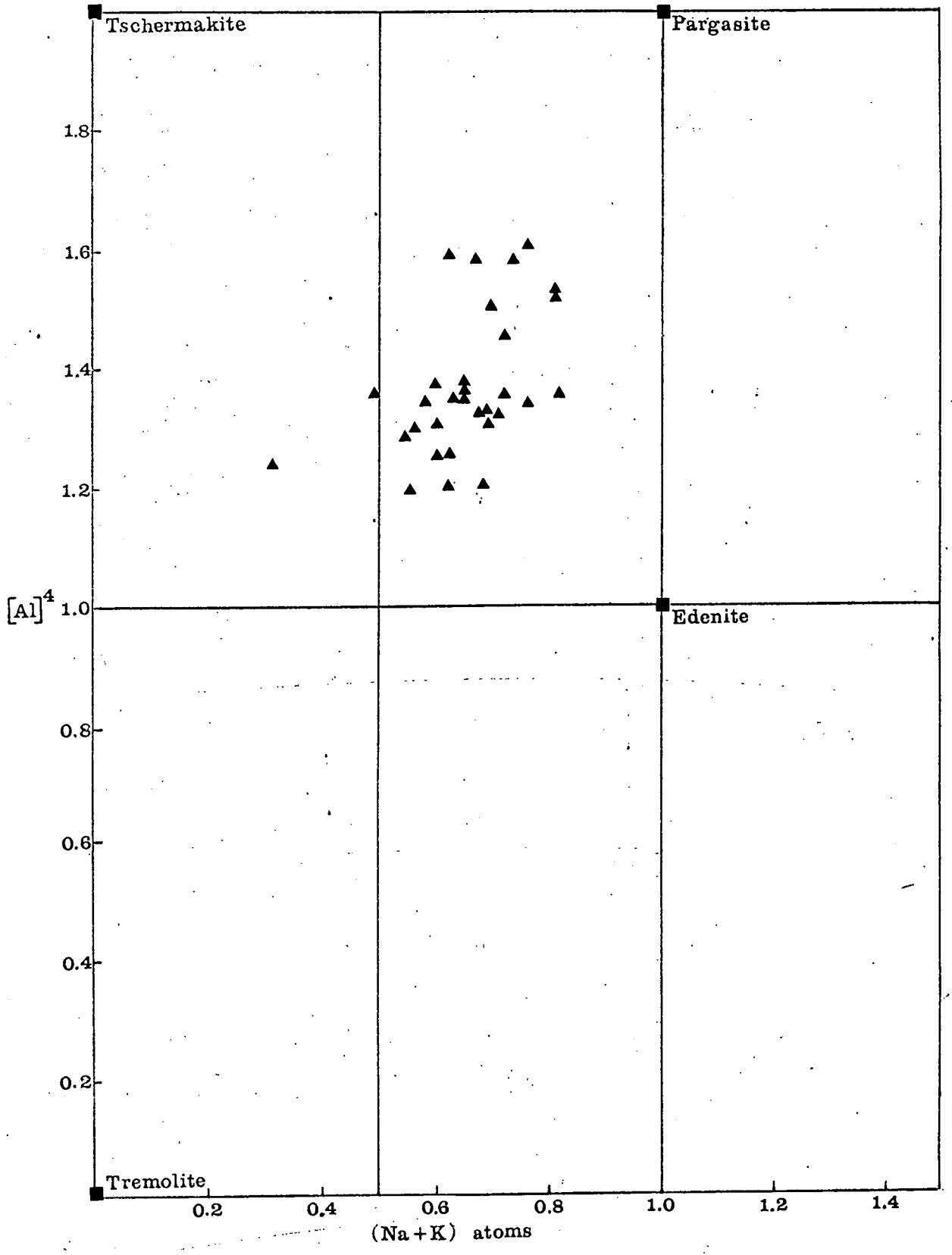

Variation in composition of Sirdal - Åseral amphiboles
(diagram after Deer,Howie and Zussman,1962)

Figure 25.

basic dyke specimen 114q is significantly poorer in alkalies than the rest of the minerals.

The chemical complexity of amphiboles makes their classification and comparison difficult. Simple graphical analysis of selected components has been used by Deer, Howie and Zussman (op. cit.)min comparative compositional studies. Phillips (1965) has extended this approach into three dimensions and on his classification the majority of the present hornblendes would lie in the field of edenite sensu extenso. Shido (1958) developed the work of Hallimond (1943) and Sundius (1956) and proposed the recalculation of calciferous amphibole compositions in terms of eight end members, some of which are arbitrarily defined, by means of computations resembling norm calculations. This method of approach has been further pursued by Perry (1968) using computer techniques. He attempted to explain the variation of some 200 well analysed amphiboles and found that even 19 end-members, chosen on the basis of possible atomic substitutions, adequately define only 25% of the amphiboles considered.

In spite of the obvious inadequacies of graphical representation of such complex minerals, some informative relationships can be demonstrated. A plot of the alkali content against the titanium content of the north-west Adirondack hornblendes, studied by Engel and Engel (1962a),

in Leake (1965) distinguishes between the amphibolite and granulite grade minerals. The present hornblende compositions are superimposed on this diagram in figure 26. The Norwegian minerals occupy a field between the two Adirondack groups but show a considerable spread at right angles to the Adirondack trend. This indicates that the composition of the present amphiboles is influenced by factors in addition to temperature. A plot of tetrahedral aluminium against octahedral aluminium in hornblendes is also informative but, as pointed out by Leake (1965b), is also relatively sensitive to analytical error. Kostyuk and Sobolev (1969) have used this diagram in order statistically to separate paragenetic types of hornblendes. The granulite facies minerals are distinguished from those formed within the amphibolite facies by virtue of their higher tetrahedral aluminium content. They recognise a further group of hornblendes which coexist with orthopyroxene that are much closer to amphibolite facies composition however. None of the present hornblendes have aluminium contents comparable with the granulite facies field of Kostyuk and Sobolev. They plot within or near to the amphibolite facies range but with relatively low octahedral aluminium. This may reflect the different analytical techniques used by the author and the Russian workers.

A plot of the titanium content against the negative charge balance calculated with respect to the ideal tremolite-

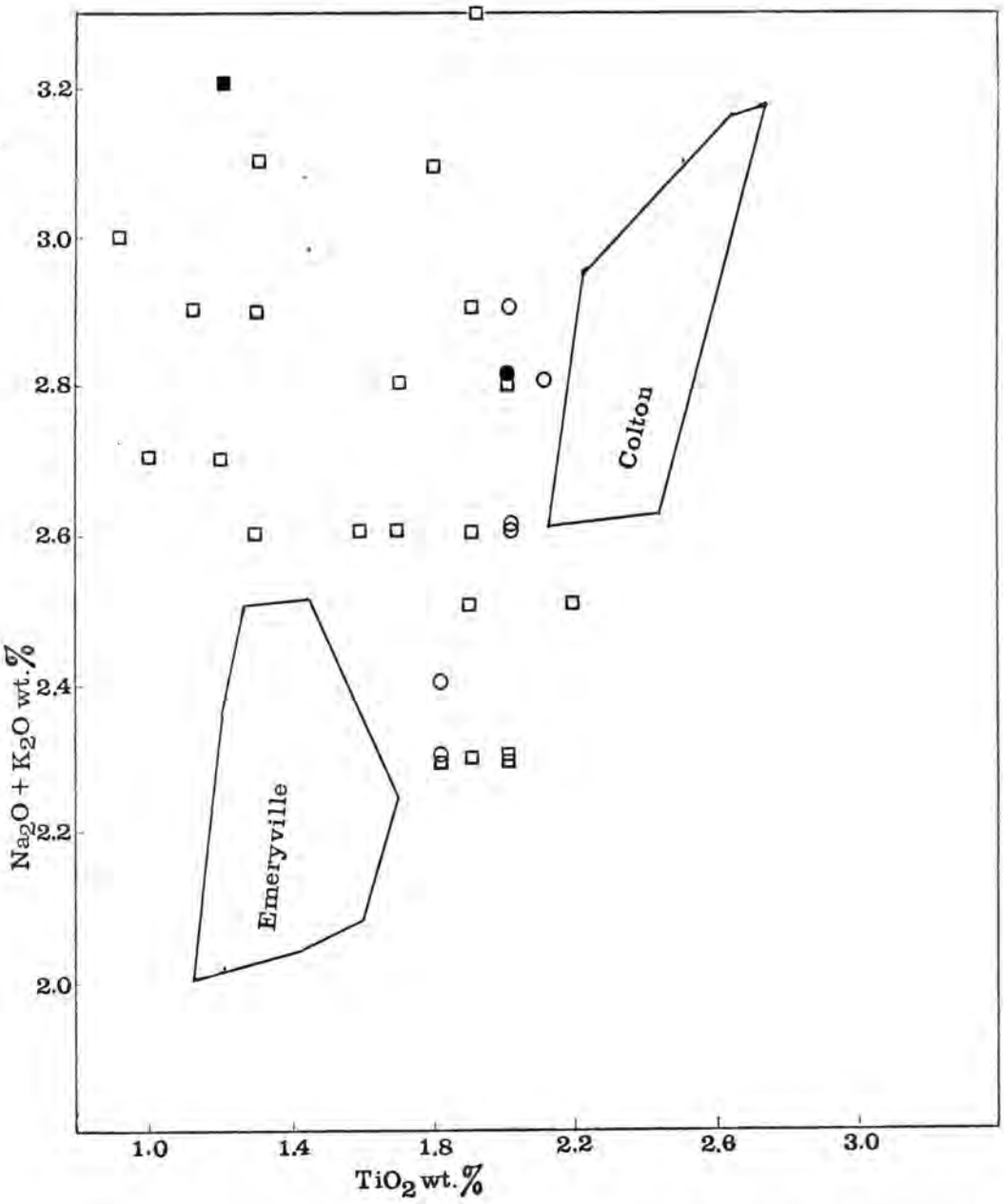

Variation in amphibole composition from amphibolites □ , pyribolites ○ , monzonitic intrusion ■ , and its contact aureole ● , compared with N.W. Adirondack hornblendes from amphibolite facies (Emeryville) and granulite facies (Colton). Diagram from Leake (1965) incorporating data from Engel and Engel (1962a).

Figure 26.

actinolite formula is shown in figure 27. As in the case of the analysed biotites, the majority of the minerals fall close to the line with gradient 0.5 but a few minerals show significantly greater negative charge balances. The ferric content of these amphiboles must therefore be appreciably greater than those that plot close to the line in figure 27. The relationships are therefore more complex than in the biotites though for the majority the ferric content must be relatively constant.

The colour of hornblendes has been used by Shido (1958) and Shido and Miyashiro (1959) as a general indication of metamorphic grade. The hornblendes from the present area exhibit a range of colours from green with a blue-green component to brown with a green component though there is evidence to suppose that the maximum temperature was roughly constant during metamorphism over the whole region. Brownish and green hornblendes occur in rocks separated by only a few metres in the Lervig and Lande gneisses. There does appear to be some correlation between colour and titanium content, as those minerals with the least amount of this element all have a blue-green component and those with the highest titanium contents are distinctly brown.

e) Clinopyroxene.

The electron microprobe analyses of fifteen

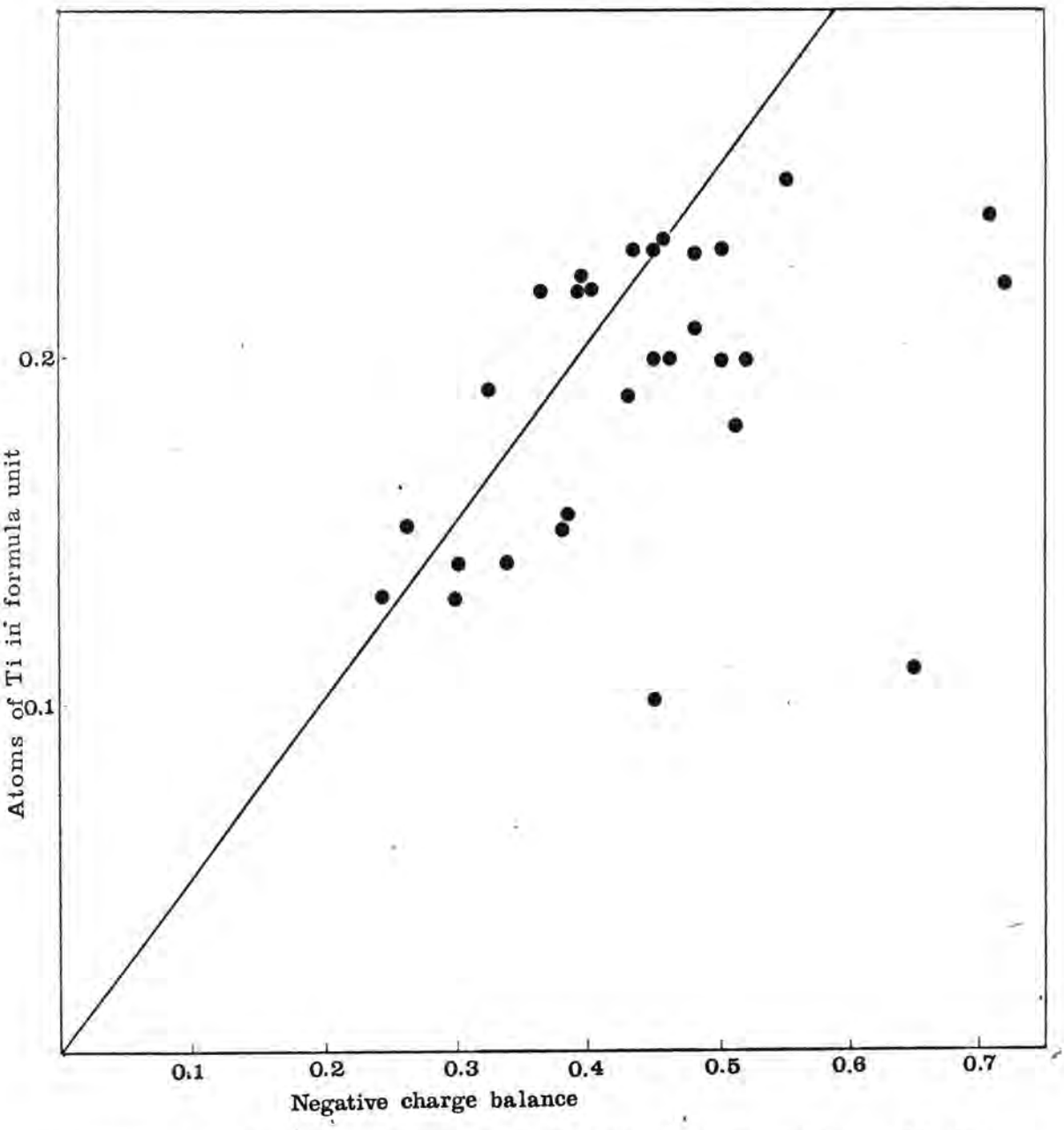

Negative charge balance given by Al in z site - Al in y site + Na in x site -(Na + K) in a site - twice (Fe + Mg - 5) in y site.

Relationship between Ti content and negative charge balance in hornblendes.

Figure 27

clinopyroxenes, together with their recalculations with respect to six oxygen atoms, are shown in table 36. Following the nomenclature of Poldervaart and Hess (1951), only three of the minerals belong to the diopside-hedenbergite series. The others have just insufficient calcium contents and therefore fall into the augite-ferroaugite field. Shido (1958) found an increase in the magnesium plus iron to calcium ratio with inceasing grade of metamorphism in the Abukuma plateau, Japan. It is therefore probably significant that the clinopyroxene with the lowest calcium content, specimen 359d, is from the contact aureole of the Ljosland intrusion. Among the analysed regional clinopyroxenes there is a tendency for those coexisting with orthopyroxene to be less calcic than those coexisting with biotite alone. The magnesium-rich clinopyroxenes from the biotite-clinopyroxene gneisses with relatively high rock oxidation ratios are also richest in sodium. This relationship can be interpreted in terms of increased aegirine substitution at greater oxygen fugacity.

f) Orthopyroxene.

The electron microprobe analyses of nine orthopyroxenes and their recalculations with respect to six oxygen atoms are shown in table 37. All the minerals can be classified as ferrohypersthenes, with the exception of specimen 2000 which is a hypersthene. Although the calcium contents of the

minerals are roughly constant, the aluminium contents of the three minerals from the contact aureoles of the monzonite intrusions, specimens 145, 359d and 2000, are significantly higher than those of the regionally metamorphosed minerals. This may reflect a higher temperature environment in the contact aureoles, as suggested by the experimental work of Boyd and England (1960).

g) Other silicates.

The analyses of eight sphenes and their recalculations with respect to $19\frac{1}{2}$ oxygen atoms are shown in table 38. The sphene from the Haddeland intrusion, specimen 306c, is noticeably richer in aluminium than the minerals from the gneissic rocks. As the rare earths and other minor elements have not been determined, it is impossible to evaluate the significance of variations in iron and aluminium contents of the sphenes from the regionally metamorphosed rocks in terms of environmental factors.

The electron microprobe analysis of one garnet together with its recalculation with respect to 24 oxygen atoms is shown in table 3. No trace of compositional zoning was found in this mineral after several electron microprobe scans. The garnet composition can also be recalculated into end-member percentages of 70.0% by weight almandine, 21.0% pyrope, 5.2% grossularite and 3.8% spessartine, proportions typical of high-grade metamorphic minerals.

h) Oxide minerals.

The determination of the original composition of many of the oxide minerals by means of the electron microprobe is frequently impossible because of widespread unmixing during the waning stages of metamorphism. Where hematite occurs in the form of coarse and irregular growths within the ilmenite host, bulk separation and analysis would also be difficult. The occurrence of sphene rims round magnetite or ilmenite also precludes the accurate determination of the original oxide composition. Nevertheless the iron and titanium contents of 8 ilmenites were determined semiquantitatively with reference to fused titanium dioxide and ferric oxide standards respectively. The ilmenites chosen for analysis showed either no or regular fine-grain hematite exsolution. The titanium content of the coexisting magnetite was also determined in 6 of the rocks. The analyses are included in table 39.

The titanium content of 5 of the analysed magnetites is very small, equivalent to only 1% of the ulvospinel molecule. According to Buddington and Lindsley (1964), an estimate of the temperature and the oxygen fugacity which prevailed during crystallisation can be made from the chemical composition of the coexisting magnetite and ilmenite. Reference to figure 5 in this work shows that the likely temperatures indicated from the present magnetite analyses

are much lower than would be expected from other evidence. This apparent discrepency can be explained by the exsolution of ulvöspinel during cooling, which then either recrystallised as discrete layers of ilmenite within the magnetite host or reacted to produce a rim of sphene. The magnetite compositions therefore reflect the temperatures at which exsolution ceased.

The satisfactory recalculation of ilmenite analyses is impossible without both ferrous and ferric iron determinations. The graph of total iron as FeO and TiO_2 in the analysed ilmenites against the rock oxidation ratio, in figure 28, approximates nevertheless to linearity, particularly in the case of titanium. A difference in iron content equivalent to 6.7% Fe_2O_3 is apparent in the ilmenites from the most reduced and oxidised rocks. If this is assumed to be equivalent to hematite originally in solid solution within the ilmenite host, reference to the temperature-oxygen fugacity diagram of Buddington and Lindsley (1964) at an assumed temperature of about 600°C. reveals a probable range of oxygen fugacity from 10^{-21} to 10^{-18} bars. This range can probably be extended by a further order upwards when visible estimates of the amount of exsolved hematite in ilmenites of the most oxidised rocks is made.

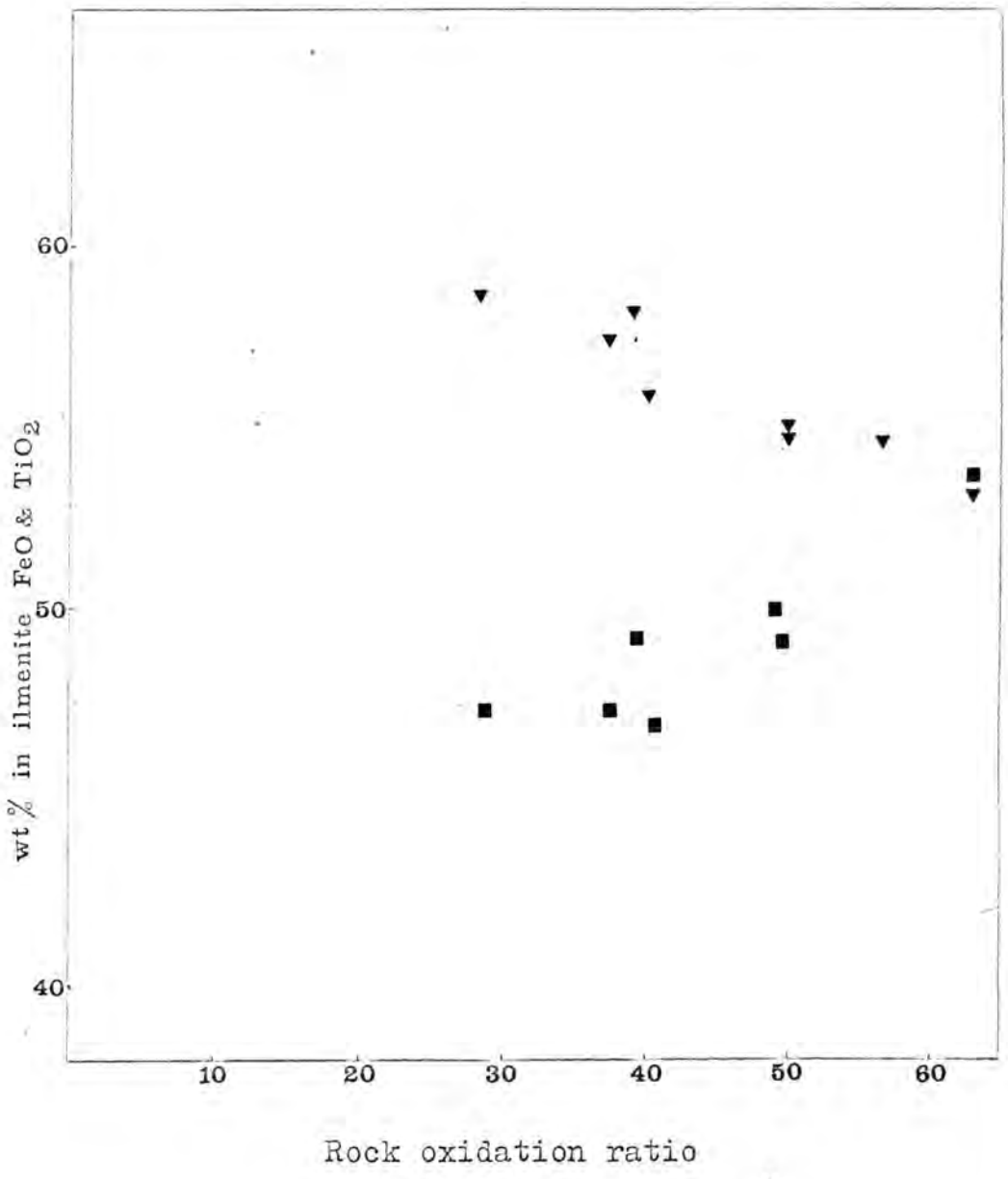

Variation in TiO_2 ▼ and total iron as FeO ■ (uncorrected) in ilmenites with rock oxidation ratio.

Figure 28.

14. THE DISTRIBUTION OF ELEMENTS BETWEEN COEXISTING MINERALS.

Ramberg and DeVore (1951) and Kretz (1959) applied thermodynamics to the distribution of elements between coexisting complex minerals and developed the equation :-

$$\frac{Xa^{\alpha}}{1 - Xa^{\alpha}} \cdot \frac{1 - Xa^{\beta}}{Xa^{\beta}} = \exp (\Delta F / R T) - - - (1)$$

where Xa^{α} is the atomic fraction of element a in the phase α and Xa^{β} is the atomic fraction in the phase β . The complete expression on the left of the equation represents the distribution coefficient of the element a between the two phases. On the right of the equation ΔF is an energy term, R is the gas constant and T the absolute temperature. The equation applies only if the two phases are ideal mixtures so that at constant temperature and pressure the graphical relationship between Xa^{α} and Xa^{β} is a characteristic curve. If the two phases are not ideal mixtures the equation becomes :-

$$\frac{Xa^{\alpha}}{1 - Xa^{\alpha}} \cdot \frac{1 - Xa^{\beta}}{Xa^{\beta}} = Kf \exp (\Delta F / R T) - - - (2)$$

where Kf is a function of Xa^{α} and Xa^{β} . The distribution coefficient at constant temperature and pressure is then not constant and a plot of Xa^{α} against Xa^{β} produces an irregular curve. If one of the elements is present in small amounts in both phases, both equations reduce to the Nernst distribution law ie.

$$\frac{Xa^{\alpha}}{1 - Xa^{\alpha}} \cdot \frac{1 - Xa^{\beta}}{Xa^{\beta}} \simeq \frac{Xa^{\alpha}}{Xa^{\beta}} = \text{constant} \quad (3)$$

The presence of further elements in either of the phases may also influence the distribution coefficient.

A plot of Xa^{α} against Xa on a Roozeboom diagram has been used by Kretz (op. cit.) and others in the investigation of element relationships within coexisting natural minerals. A smooth curve or straight line on such a diagram indicates that either equation (1) or (3) is applicable but if the points are scattered a further influencing factor can be assumed. A regular relationship between a distribution coefficient and the content of another element in either phase is still therefore indicative of chemical equilibrium.

The distribution of titanium between biotite and hornblende is graphically expressed on a Roozeboom diagram in figure 29. A linear relationship with some scatter is apparent. Figure 30 indicates that there is a moderate correlation between the iron and titanium contents of biotite coexisting with magnetite and ilmenite and very little correlation between the iron and titanium contents of biotite coexisting with ilmenite alone. At least part of the scatter in figure 29 can be explained in terms of an inverse relationship between the titanium distribution coefficient and the sodium content of the amphibole as shown in figure 31. Such a relationship was suspected by

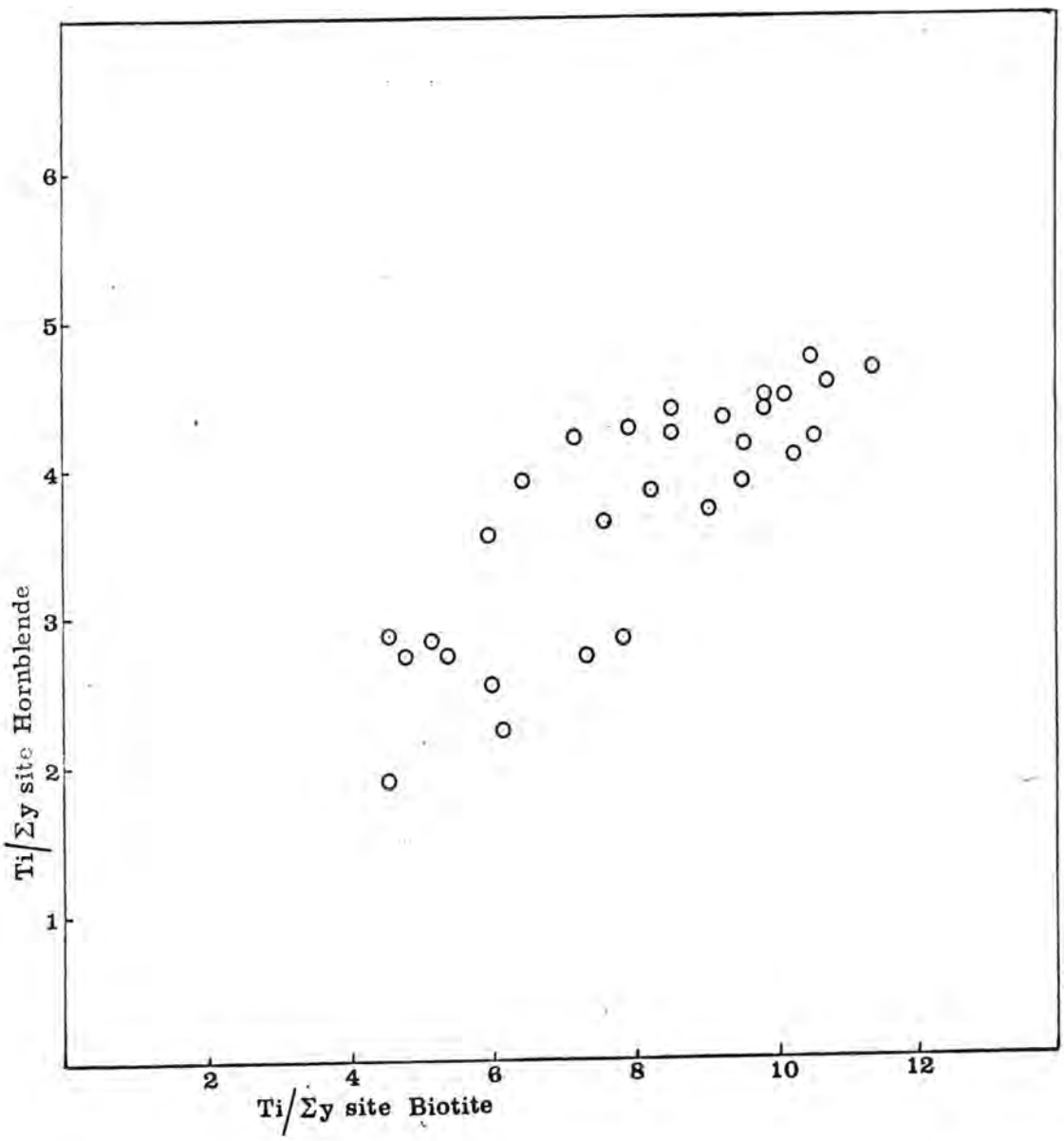

The distribution of titanium between biotite and hornblende.

Figure 29.

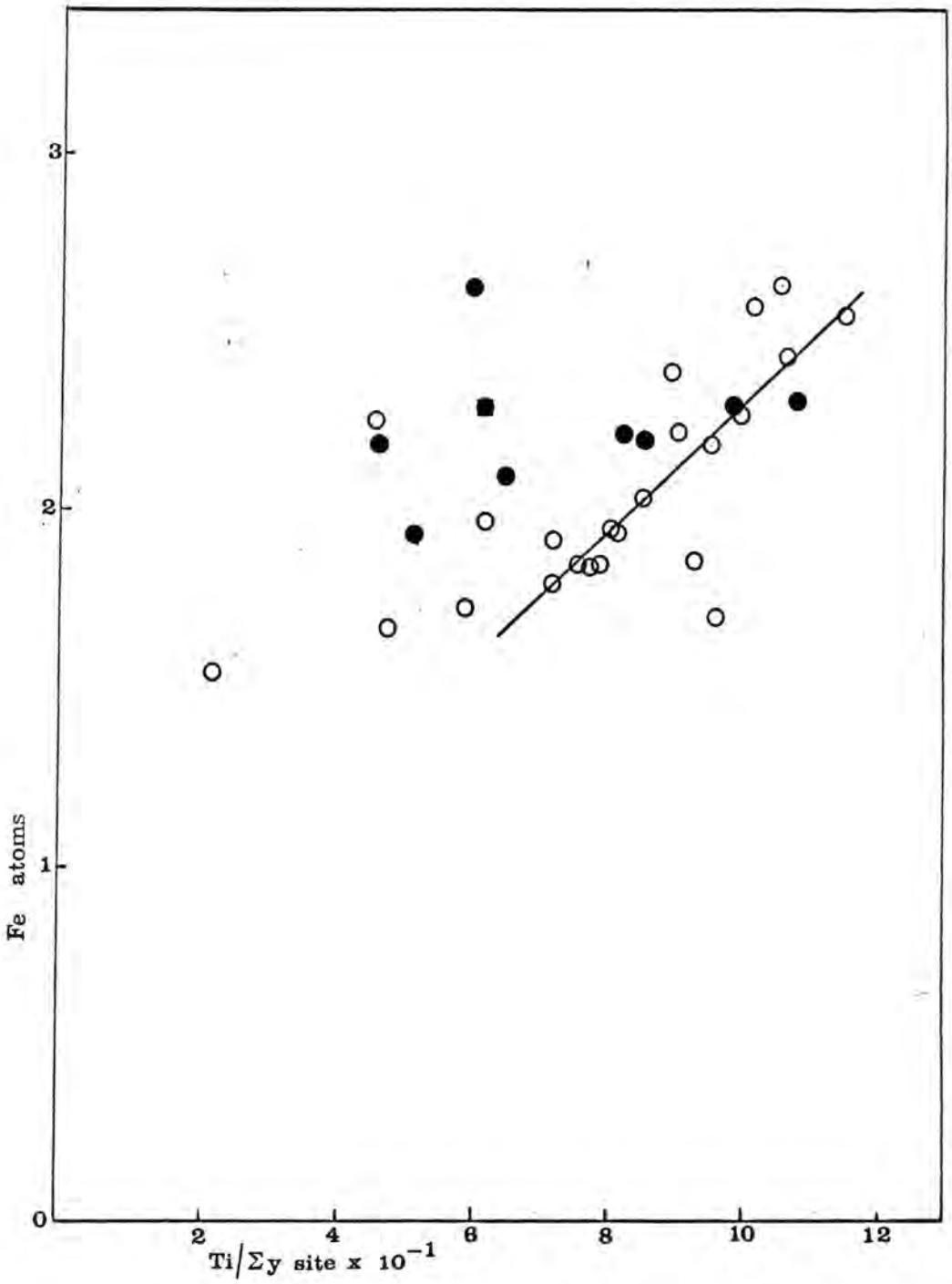

The relationship between the atomic fraction of titanium in the y site against the iron content of biotites from ■ granitic gneiss, ● ilmenite bearing gneisses and ○ gneisses with magnetite and ilmenite.

Figure 30.

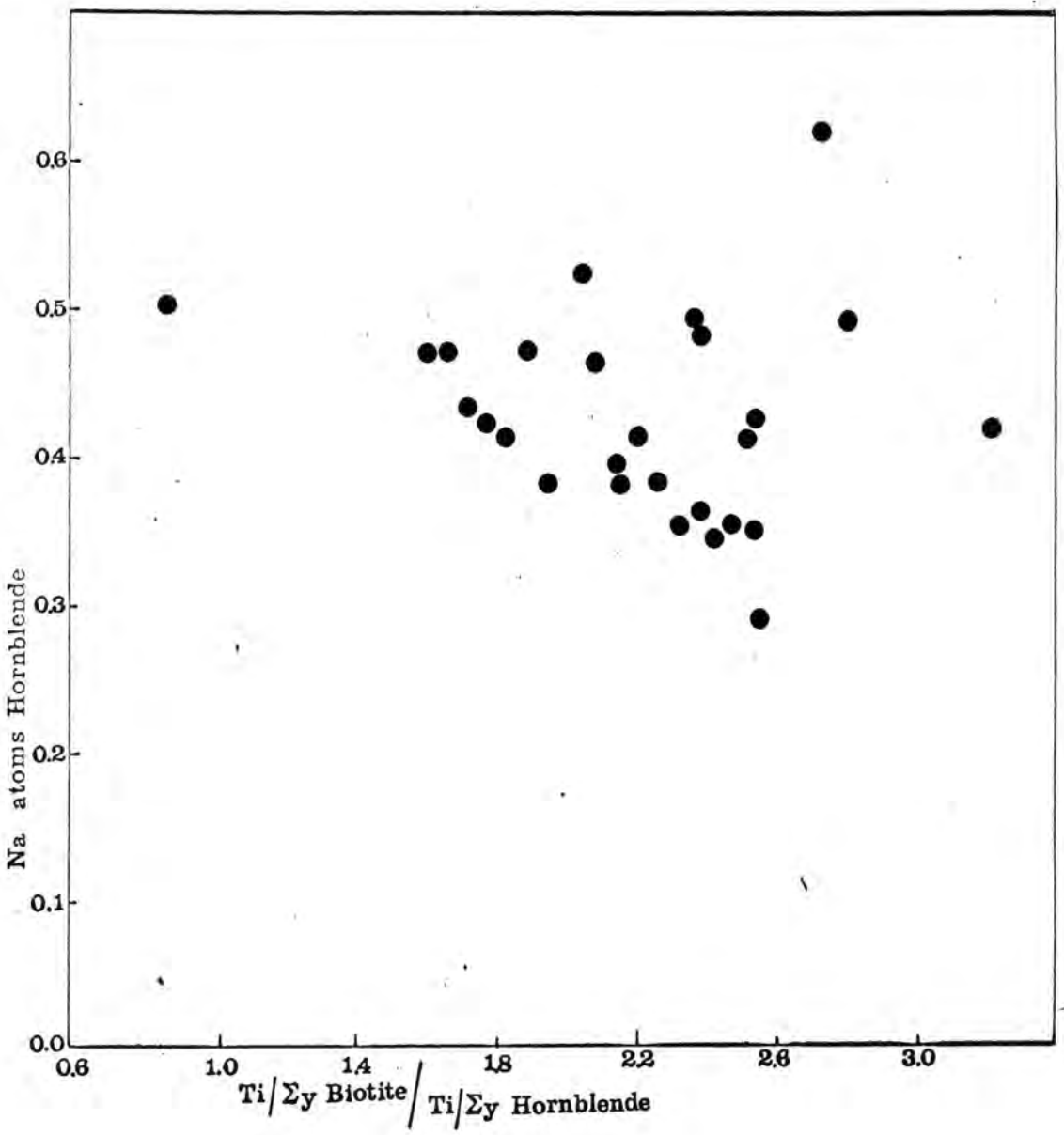

The relationship between the sodium content of hornblende and the distribution coefficient of titanium between biotite and hornblende.

Figure 31.

Kretz (1960) in a study of the chemistry of coexisting skarn minerals. An increase in sodium substitution in the amphibole may therefore increase its affinity for titanium as in the rare amphibole kaersutite which is enriched in both elements. There appears to be no correlation between the titanium content of either biotite and hornblende and the total titanium content of the rock.

The distribution of magnesium between hornblende and clinopyroxene and hornblende and orthopyroxene are shown in figures 32 and 33 respectively. Both graphs exhibit a linear or gently curved relationship with some scatter. Similar relationships were found by Himmelberg and Phinney (1967) for granulite facies gneisses and by Saxena (1968) for 'so-called' charnockites. No factor has been found to explain the scatter on the hornblende-orthopyroxene distribution diagram. There is, however, an inverse relation between the distribution coefficient of magnesium between hornblende and clinopyroxene and the tock oxidation ratio as shown in figure 34. The correlation between the magnesium distribution coefficients and the tetrahedral aluminium content of the amphibole illustrated by Saxena (op. cit.) is not apparent in the present data.

The composition of the coexisting pyroxenes are plotted on a calcium, magnesium and iron triangular diagram in figure 35. The crossing tie lines indicate that there is

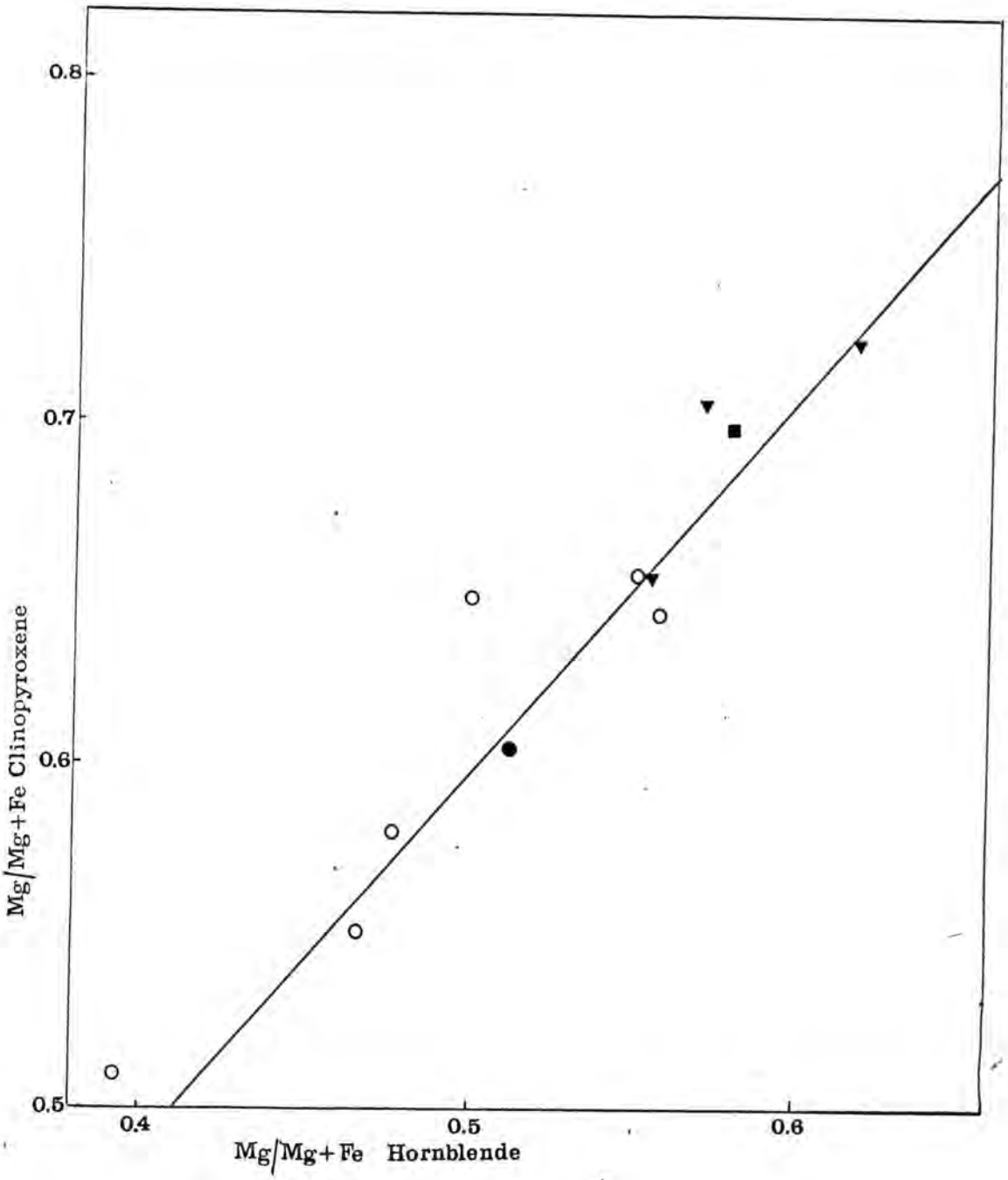

The distribution of magnesium between hornblende and clinopyroxene in ○ pyribolites, ● contact aureole pyribolite, biotite-hornblende-clinopyroxene gneisses ▼ , and ■ hornblende-clinopyroxene gneiss.

Figure 32.

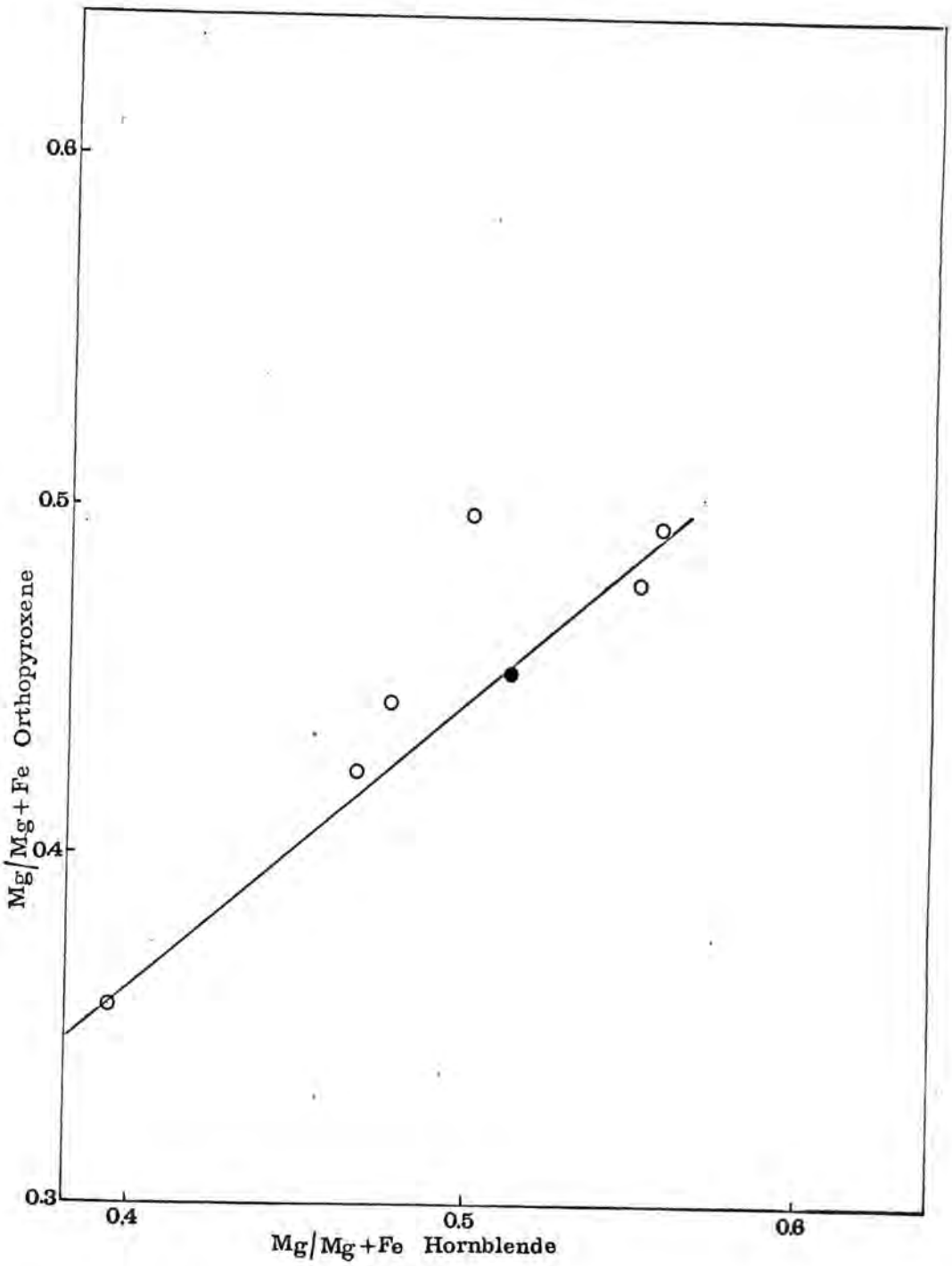

The distribution of magnesium between hornblende and orthopyroxene in o pyribolites and ● contact aureole pyribolite.

Figure 33.

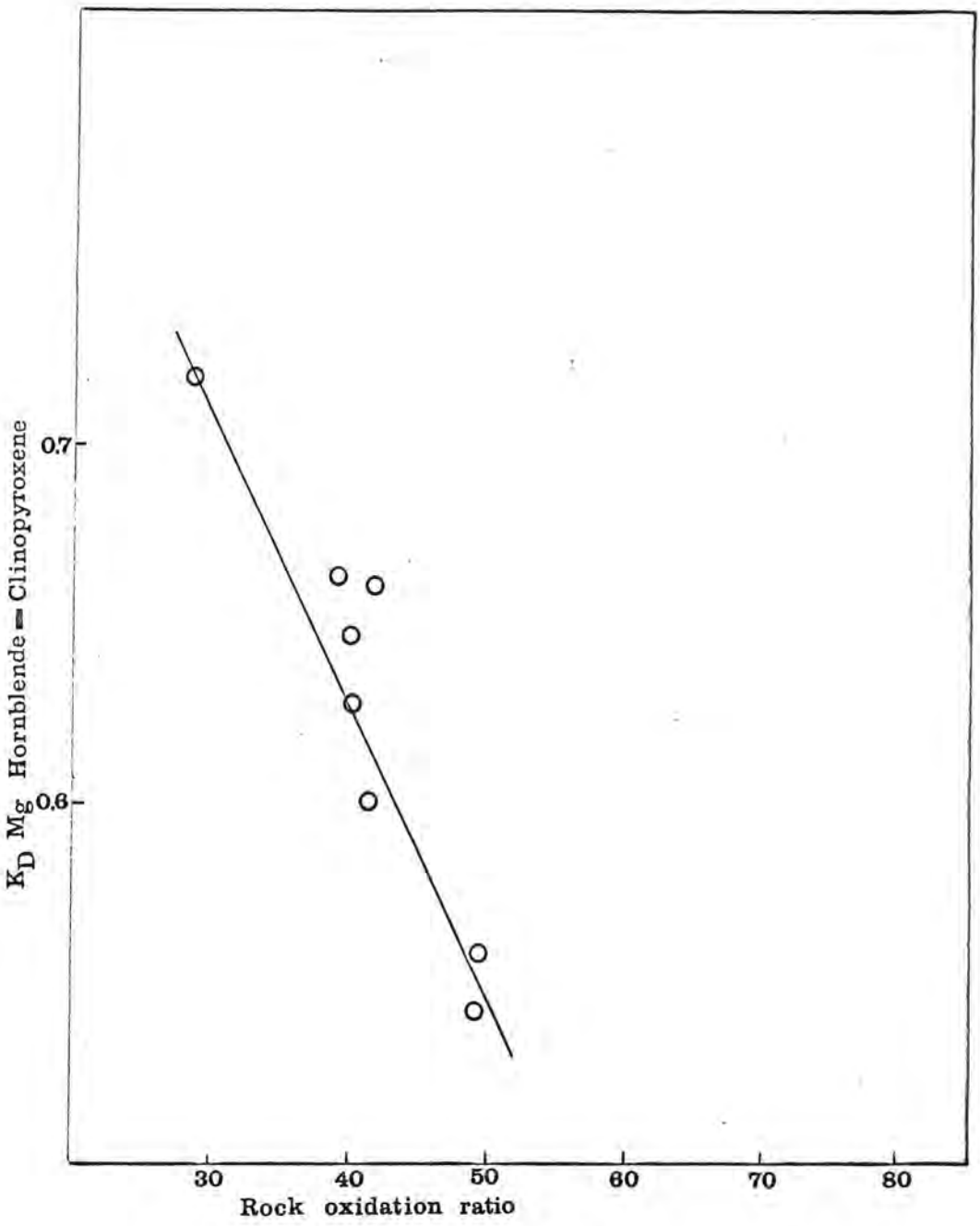

The variation of the distribution coefficient of magnesium between hornblende and clinopyroxene with respect to rock oxidation ratio.

Figure 34.

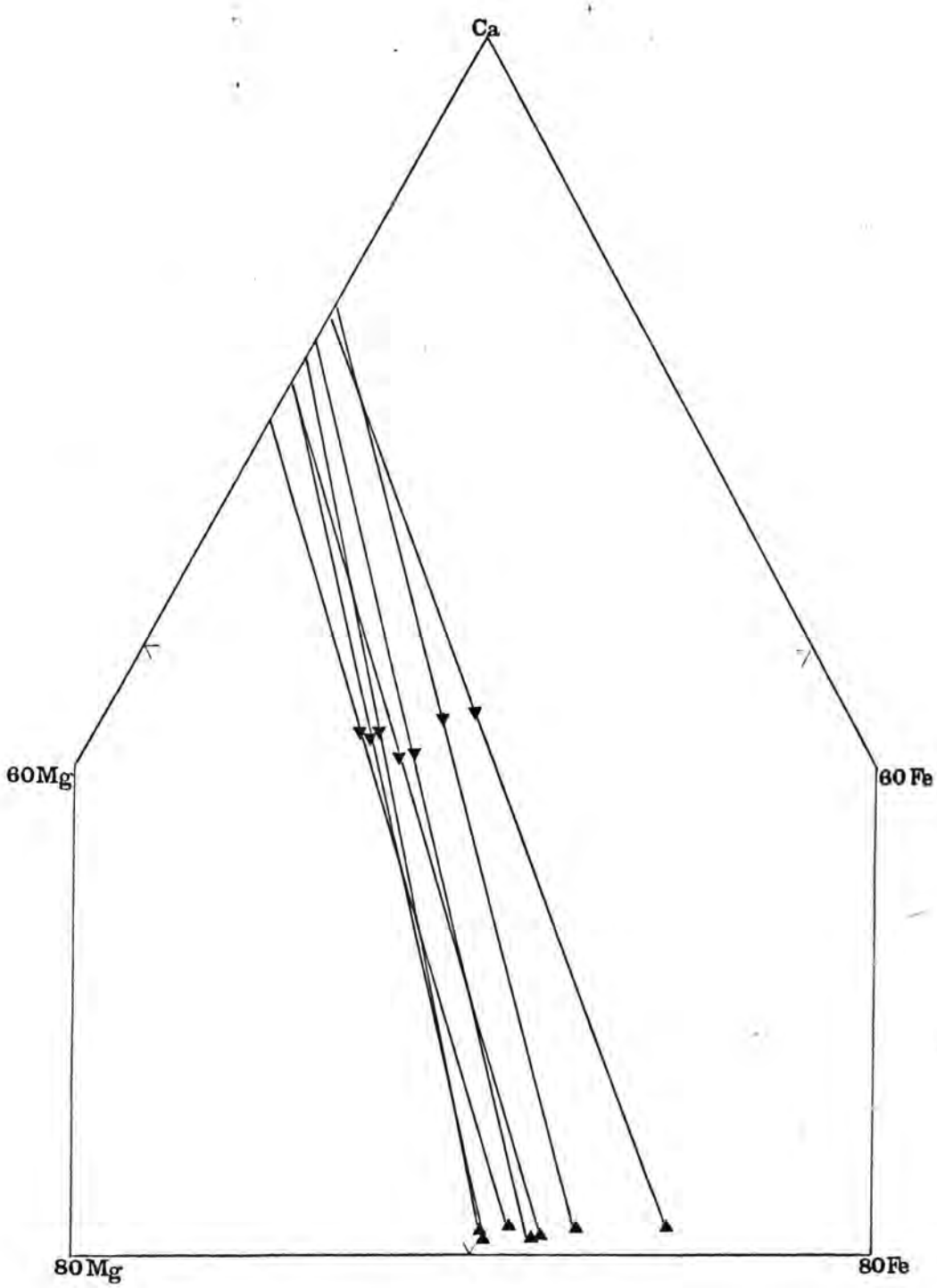

The composition of coexisting clinopyroxenes and orthopyroxenes in pyribolites.

Figure 35.

some departure from a regular relationship, a feature that can also be demonstrated by scatter on a Roozeboom diagram. Four of the pyroxene pairs plot on the curve on the Roozeboom diagram with a distribution coefficient of 0.54 that has been shown by Kretz (1963) to apply to the majority of metamorphic mineral pairs. The cause of the divergence from this relationship of the other three pairs is obscure, particularly as the greatest range of coefficient is exhibited by two samples collected a few dekametres apart. The rock oxidation ratios of these two samples are also almost identical. The pyroxene pairs of Himmelberg and Phinney (1967) also show some scattering of magnesium distribution coefficients, particularly among the less iron-rich minerals. There is no suggestion in the present pyroxene data that a regular relationship exists between the magnesium distribution coefficient and the iron content of the orthopyroxene as has been found by Binns (1962) and Davidson (1969).

The Roozeboom diagram of the distribution of magnesium between biotite and orthopyroxene is shown in figure 36. Scatter is considerable with the distribution coefficient varying from 0.865 to 1.805. Saxena (1968) also found significant scatter in the distribution of iron between biotite and orthopyroxene from Swedish PreCambrian charnockites. No simple factors have emerged to explain this scatter.

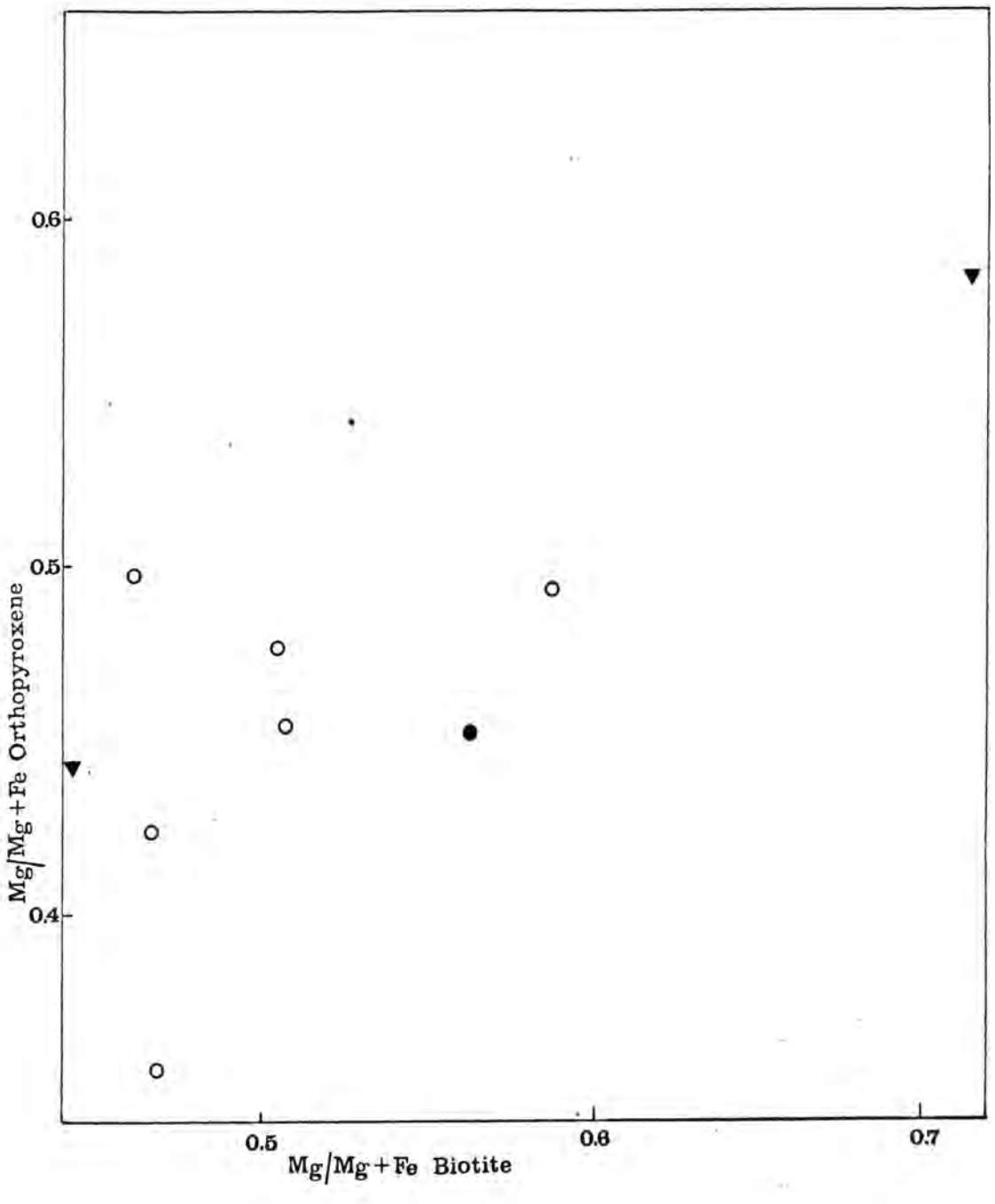

The distribution of magnesium between biotite and orthopyroxene in o pyribolites, contact aureole pyribolite ● and ▼ felsic aureole rocks.

Figure 36.

The distribution of magnesium between biotite and clinopyroxene is illustrated in figure 37. The graph is linear or gently curved with some significant scatter and a range of distribution coefficients from 0.463 to 0.846. Kretz (1960) tentatively related the scatter in iron distribution between biotite and clinopyroxene from Grenville skarns to the aluminium content of the pyroxene. Saxena (1968) related similar scatter in Swedish charnockites to the tetrahedral aluminium content of the biotite. In the present pyribolites there is a suggestion of a similar relationship as shown in figure 38. The scatter in magnesium distribution coefficients in the amphibolites and biotite-clinopyroxene gneisses is directly related to variations in rock oxidation ratio.

The distribution diagram of magnesium between biotite and hornblende, in figure 39. shows considerable scatter with distribution coefficients ranging from 0.825 to 1.740. Similar relationships have been observed in high grade gneisses by Kretz (1959), Saxena (1966) and Hollander (1970). The distribution figured by Annersten (1968). on the other hand, shows a close approach to linearity. Kretz (1960) found that iron distribution between the two minerals in skarn rocks was influenced by the aluminium, sodium and potassium contents of the amphibole. The regular relationship between the magnesium distribution in biotite and hornblende and the ratio of tetrahedral aluminium in each

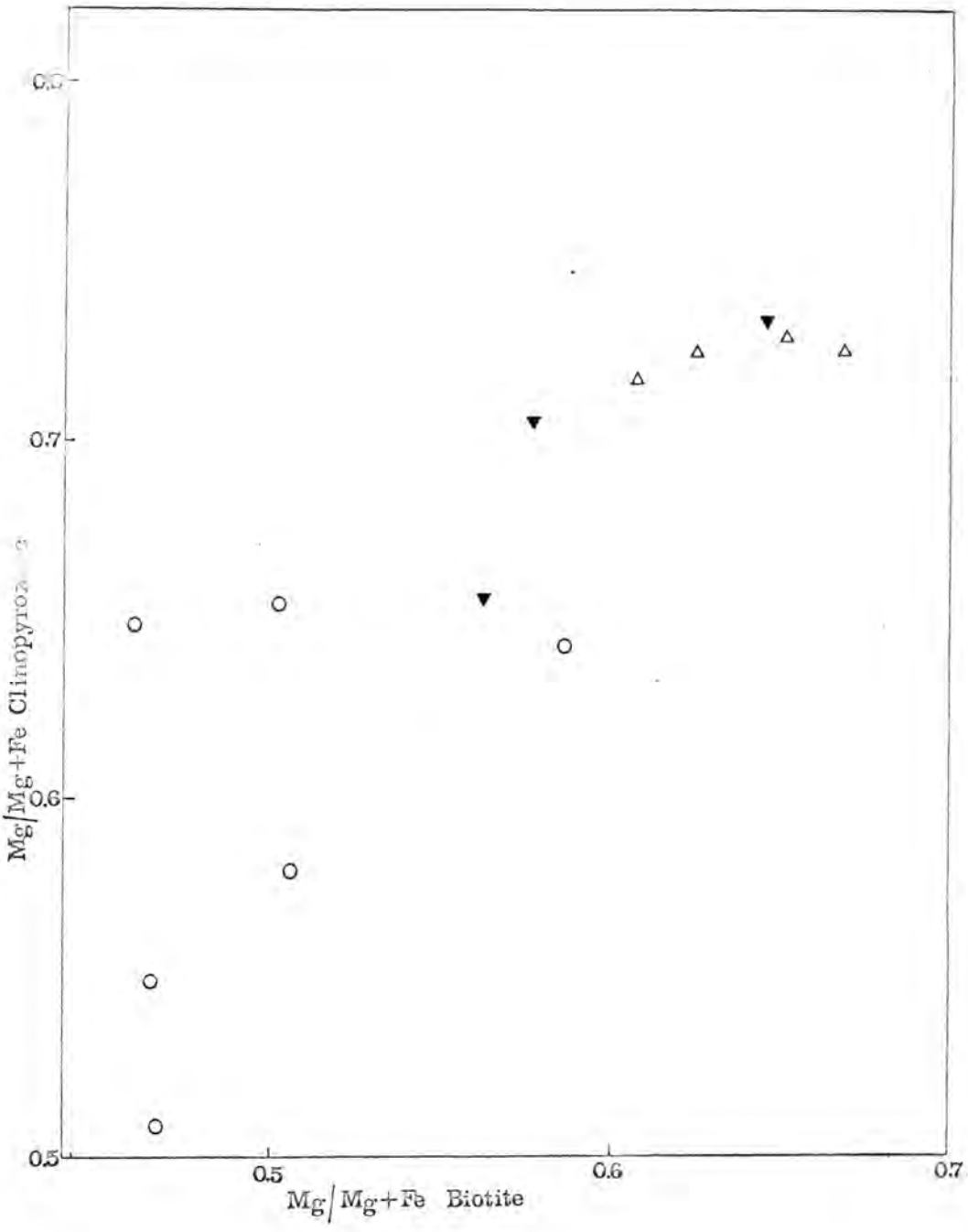

The distribution of magnesium between biotite and clinopyroxene in ○ pyribolites, ▼ biotite-hornblende-clinopyroxene gneisses and △ biotite-clinopyroxene gneisses.

Figure 37.

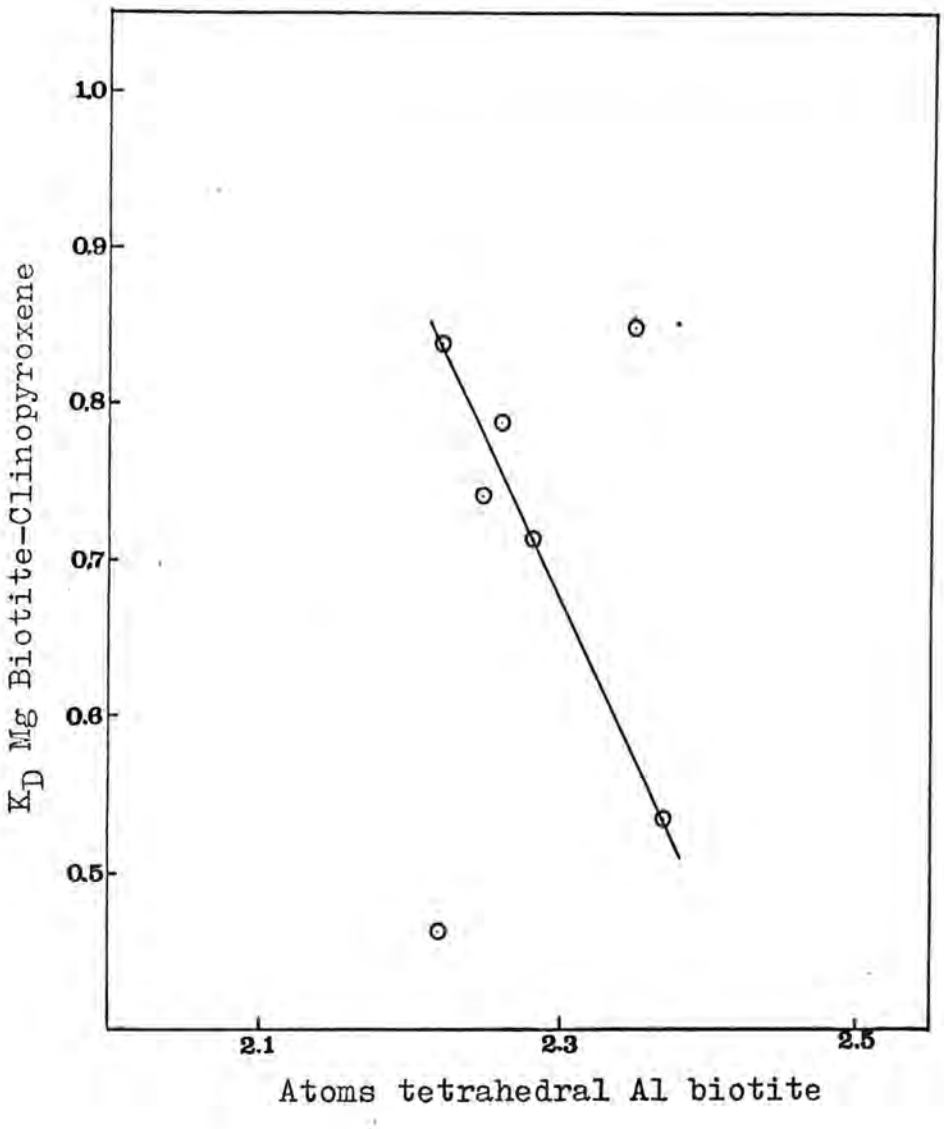

The relationship between the distribution coefficient of magnesium between biotite and clinopyroxene and the tetrahedral aluminium content of the biotite in pyribolites.

Figure 38.

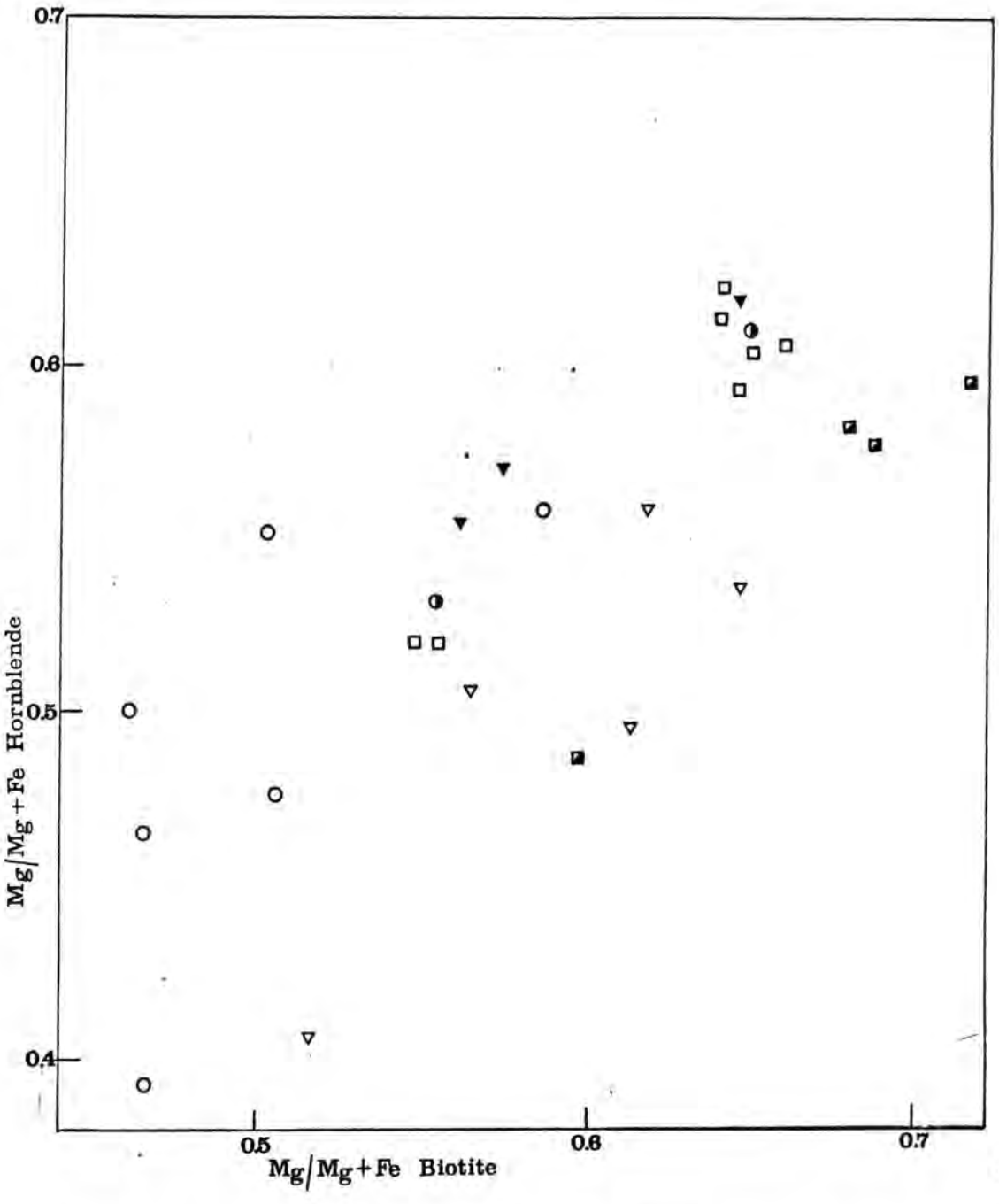

The distribution of magnesium between biotite and hornblende in ○ pyribolites, ▼ biotite-hornblende-clinopyroxene gneisses, □ amphibolites with magnetite and ilmenite, ▽ amphibolites with ilmenite, ◪ amphibolites with magnetite and sphene and ◑ amphibolites with no oxide phases.

Figure 39.

mineral found by Saxena (1968) and Hollander (1970) is also apparent in figure 40, but only for the rocks containing both magnetite and ilmenite and with comparable oxidation ratios, of about 40. The gneisses with oxidation ratios significantly greater than this figure, the pyribolites and amphibolites with ilmenite alone all show significant deviations from this relationship.

A comparison of the magnesium distribution diagrams reveals that the greatest scatter occurs where biotite is included. Much of this scatter has been related to the tetrahedral aluminium content and to the rock oxidation ratio. The latter appears to exert a considerable influence upon the magnesium partition between biotite and hornblende. Crystallisation under relatively high oxygen fugacity favours the entrance of ferric iron into the amphibole lattice, thus affecting the iron-magnesium distribution.

The partition of titanium and magnesium between the mafic silicates, though showing some irregularity, can for the most part be interpreted in terms of a complex of chemical and mineralogical factors. These include substitution of other elements into the lattice, particularly of the complex hydrous phases, the oxygen fugacity during crystallisation and the nature of the coexisting iron-titanium oxide phases. These conclusions support the validity of the occurrence of conditions of chemical equilibrium during crystallisation, and important prerequisite for the analysis of the rock paragenesis relations.

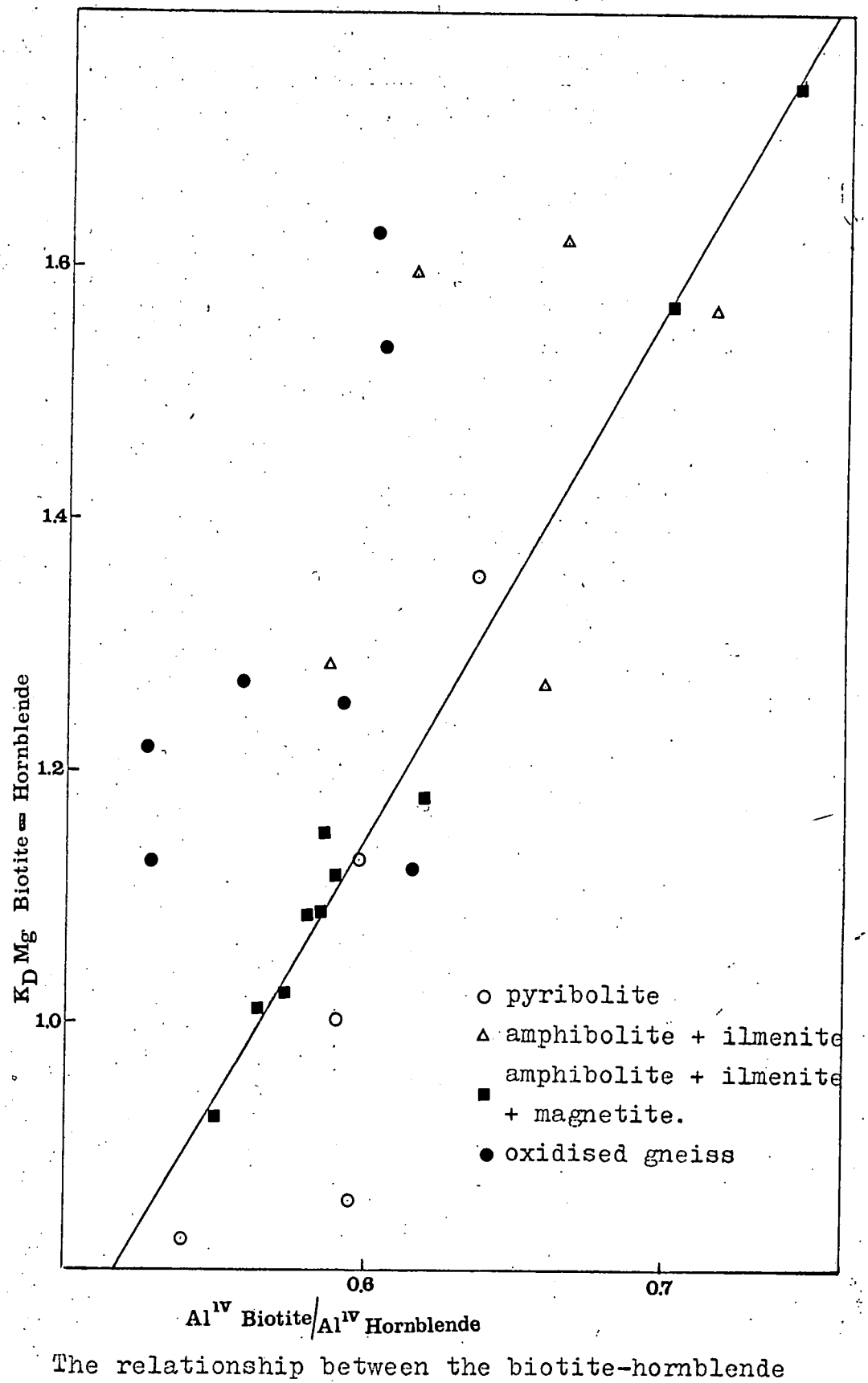

The relationship between the biotite-hornblende magnesium distribution coefficient and the ratio of tetrahedral aluminium in biotite to tetrahedral aluminium in hornblende.

Figure 40.

15. THE ANALYSIS OF THE MINERAL PARAGENESES.

The most frequently used method of representing variations in mineral parageneses with metamorphic grade is the Eskola triangular ACF and A'KF diagram. The original diagrams of Eskola (1936) have been greatly developed and extended by several authors, notably Turner (1948) and Winkler (1965). The paragenesis diagram that shows the closest approach to the mineral assemblages that have been observed in the present area is shown by Winkler (op. cit.) to represent the sillimanite - cordierite - orthoclase subfacies of the Abukuma - type cordierite amphibolite facies. This diagram is reproduced in figure 41. All the minerals that have been observed to coexist with quartz with the exception of orthopyroxene are represented on this diagram. The presence of orthopyroxene has often been considered as indicative of the granulite facies but recent work has indicated that a transitional zone can be recognised between the amphibolite and granulite facies in which the hydrous mafic silicates can coexist with the anhydrous pyroxenes. This zone has been termed the hornblende granulite or low pressure granulite facies. The five phase assemblage anorthite, biotite, hornblende, clinopyroxene and orthopyroxene which is characteristic of this subfacies cannot be represented on the ACF and A'KF diagram as the number of permissible phases is exceeded. This limitation of the ACF and A'KF diagram is imposed by

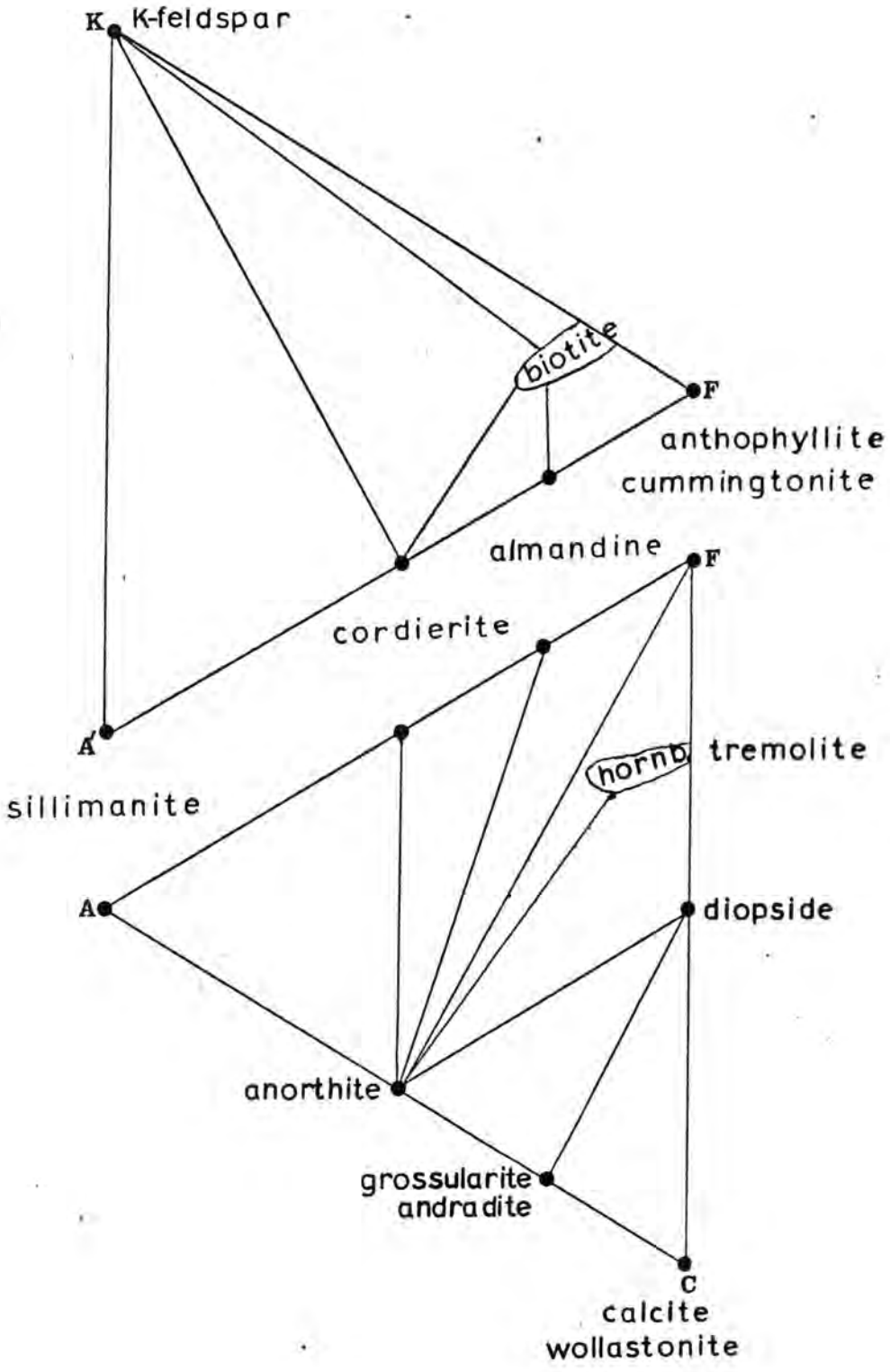

A C F & A'K F diagram of the sillimanite-cordierite-orthoclase-almandine subfacies of the Abukuma type cordierite amphibolite facies (after Winkler, 1965)

Figure 41.

the assumption that iron and magnesium can be regarded as a single component which is not strictly valid. Turner (1968) has used crossing tie lines on ACF diagrams to represent these type of assemblages but this makes the diagrams difficult to interpret.

The representation of the above five phases and their stability fields is possible on the two tetrahedral diagrams Al, Ca, Fe^{2+} and Mg and Al', K, Fe^{2+} and Mg. Graphical representation of three dimensions is difficult but effective projection onto a plane is possible. A projection of the Al_2O_3,K_2O, FeO,MgO tetrahedron through the ideal muscovite composition has been successfully utilised by Thompson (1957) in the analysis of parageneses of pelitic gneisses. The use of a projection in the manner described by Thompson (op. cit.) of the aluminium, calcium, ferrous iron and magnesium tetrahedron through the anorthite composition onto a plane parallel to the edges Al to Ca and Mg to Fe, as shown in figure 42, in the analysis of paragenesis relationships within the pyroxene bearing gneisses has been investigated. The compositions of the coexisting orthopyroxenes, clinopyroxenes and hornblendes of the pyribolites and clinopyroxene-bearing amphibolites that have been obtained during this present study are shown in this diagram in figure 43. It is also possible to show the composition of garnet and cordierite on the same diagram. The hornblende compositions are displaced to the

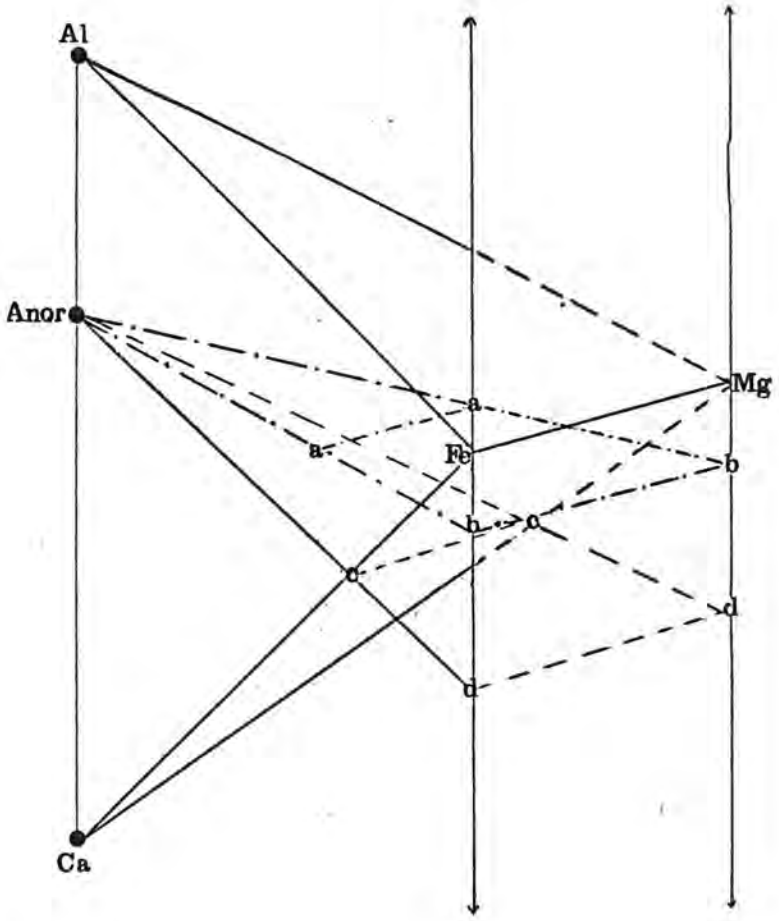

Key

a-a = approximate hornblende composition.

b-b = projection of a-a.

c-c = approximate clinopyroxene composition.

d-d = projection of c-c.

The tetrahedron Al,Ca,Fe and Mg and its projection through the anorthite composition onto a plane passing through Fe and Mg and parallel to the line Al-Ca.

Figure 42.

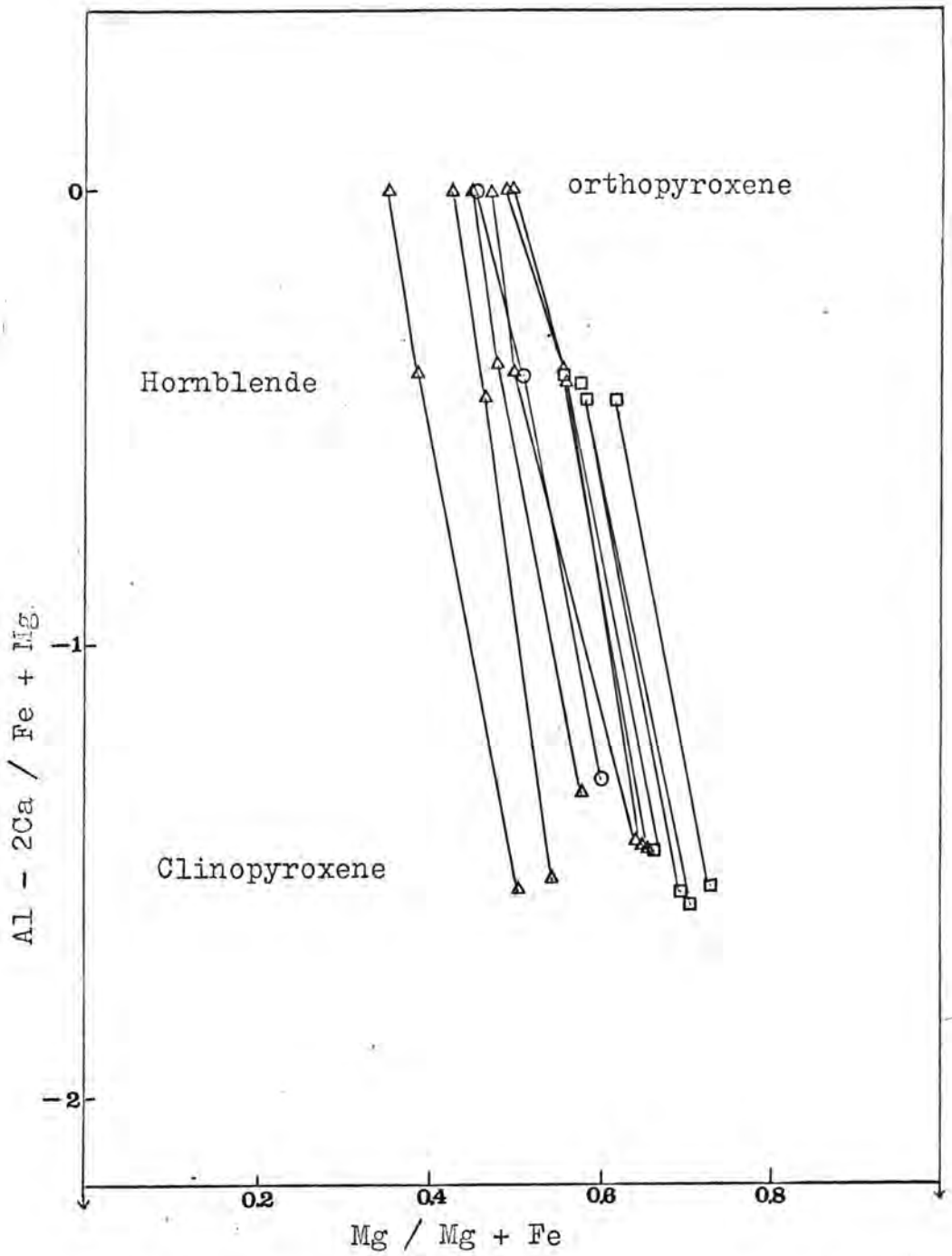

The composition of coexisting orthopyroxene, hornblende and clinopyroxene from pyribolites △ , contact aureole pyribolite ○ and clinopyroxene amphibolites □ .

Figure 43.

left in figure 43 as all the iron has been assumed to be in the ferrous state. After allowance for the estimated ferric iron content of the hornblende, it is apparent that the area enclosed by the three mineral compositions is relatively small and varies considerably in its coordinates for the different pyribolites. It must be concluded that a factor in addition to the elements considered is influencing the composition of the coexisting phases. A similar relationship applies to the chemistry of the coexisting minerals from granulite facies rocks in the Granite Falls - Montevideo area, Minnesota, studied by Himmelberg and Phinney (1967), as shown in figure 44. In contrast, the compositions of the two pyroxenes and hornblende from granulite facies rocks of the Colton area in the north-west Adirondacks, studied by Engel and Engel (1962b), as shown in figure 45, are very similar.

The reduction of the major phase determining components to four and their tetrahedral representation, though adequate for pelitic rocks, is manefestly unsuitable for the more complex basic rocks.

Chemical relationships involving more than four components can be investigated using groupings and ratios. Figure 46 illustrates the role of aluminium as a determinative inert component with respect to mafic silicate phases in a graph of $(Na + K + 2Ca) / Al$ against $(Fe + Mg)/ Al$. As the variation in the content of the above elements and the iron, magnesium

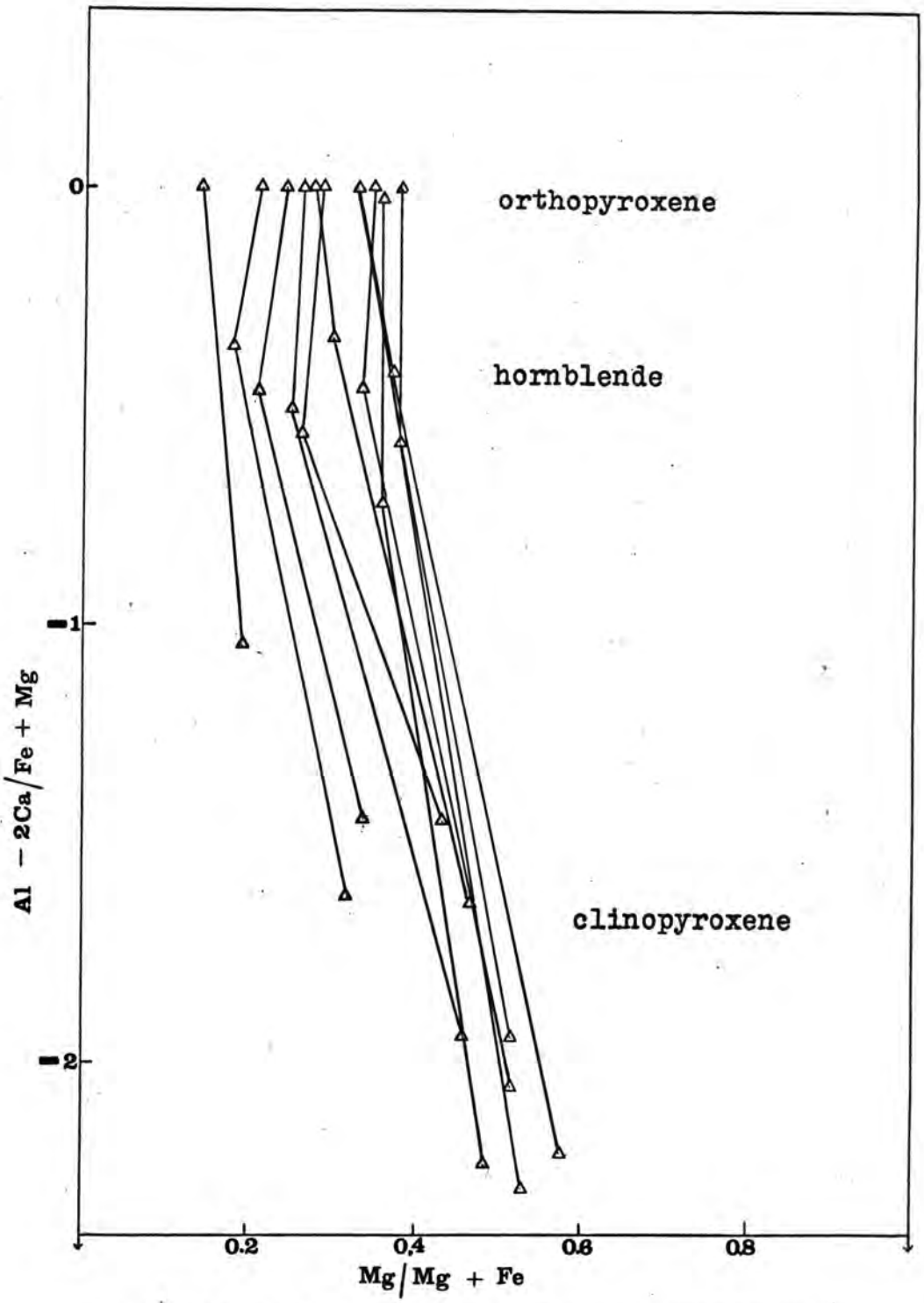

The composition of coexisting orthopyroxene, hornblende and clinopyroxene from granulite-facies rocks of the Granite Falls-Montevideo area, Minnesota. Data after Himmelberg and Phinney (1967).

Figure 44.

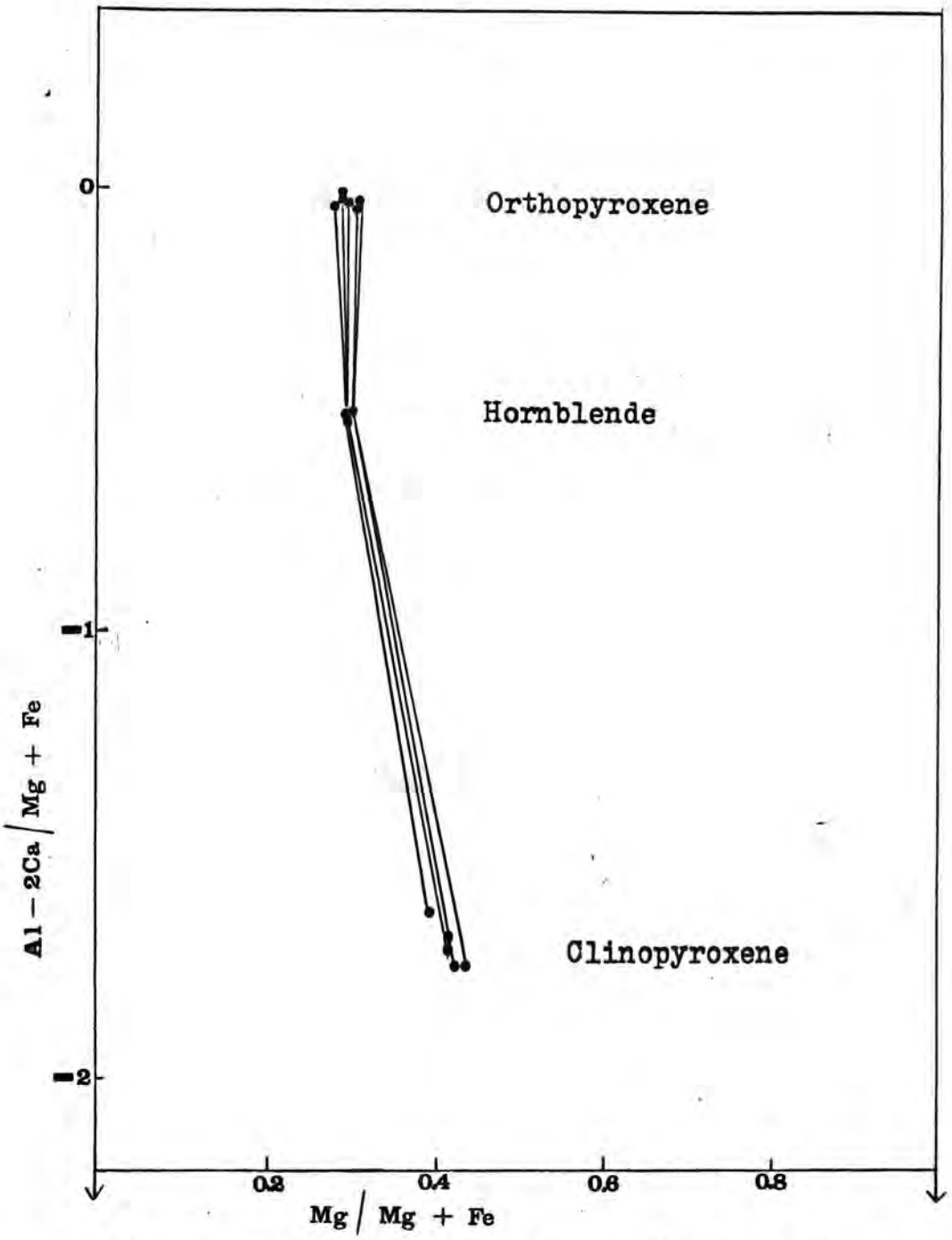

The composition of coexisting orthopyroxene, hornblende and clinopyroxene from granulite-facies rocks of the Colton area, northwest Adirondacks, New York. Data from Engel, Engel & Havens (1964).

Figure 45.

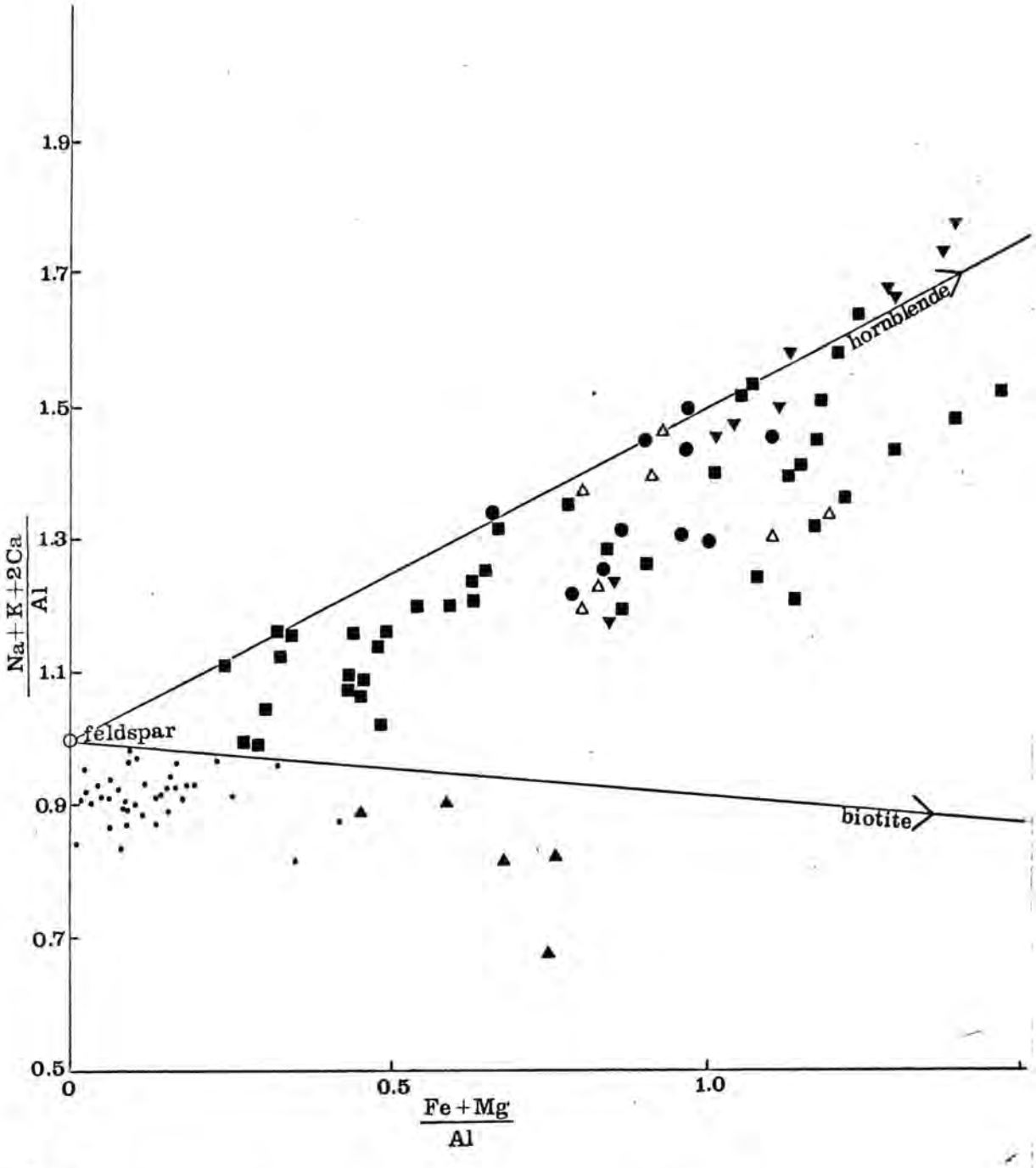

Key

• : granitic gneiss, ▲ : garnetiferous gneiss,

■ : hornblende ± biotite gneiss, ● : biotite clinopyroxene gneiss, ▼ : hornblende clinopyroxene ± biotite gneiss,

△ : biotite, hornblende, clinopyroxene orthopyroxene gneiss.

Ratio plot of whole rock compositions to illustrate the role of aluminium in determining phase assemblages.

Figure 46.

sum in both biotites and hornblendes compared with that of the iron to magnesium ratio is small, an average composition of each mineral can be plotted on this diagram. Lines between the feldspar composition and the biotite and hornblende compositions delineate three areas in which biotite coexists with a more aluminous mafic phase,eg. garnet, biotite coexists with hornblende and hornblende coexists with a less aluminous phase,eg. clinopyroxene.

The compositions of the analysed rocks are plotted on this diagram in figure 46. The iron content of the opaque phases has been neglected. The granitic rocks are clustered below the feldspar - biotite tie line near to the feldspar end-point. The fact that they are concentrated just below the tie line may indicate analytical bias in the X-ray determinations possibly in the aluminium contents. All the hornblende-bearing gneisses are clearly less aluminous than the most mafic granitic gneisses. The majority of the clinopyroxene-bearing amphibolites plot close to or above the feldspar - hornblende tie line. Several of the biotite - clinopyroxene gneisses, the pyribolites and the more siliceous clinopyroxene amphibolites plot well within the biotite - feldspar - hornblende area however. The operation or influence of other factors or components is therefore required to explain the presence of pyroxene in these rocks.

In order to explain the occurrence of pyroxenes in the

above rocks it is therefore necessary to consider systems with more than four components, the interelationships of which cannot be expressed graphically. Korzhinskii (1959) has described a method developed from Lodochnikov for the representation of four to seven component systems by means of vectors or tied vectors. Hounslow and Moore (1967) have used this method to show variations in the composition of mica schists from the staurolite zone. These diagrams are complex and difficult to interpret quantitatively. Comparable conclusions can be obtained by the careful comparison of the analyses of each rock type and the application of significance tests. Using this approach it is apparent that the pyribolites as a whole are low in potassium, high in calcium and have high iron to magnesium ratios when compared with the majority of other basic rocks. The majority of the biotite - clinopyroxene gneisses on the other hand have exactly the opposite characteristics. Some amphibolites show a close approach in composition to both these rock types however.

Paragenesis relationships can also be investigated in complex systems by the calculation of modes in terms of average mineral compositions with simultaneous equations. Ferrous iron and magnesium can be treated together as one component so that the largest source of variation in mineral composition is eliminated. The method is approximate as several smaller but significant variations in mineral compositions must be neglected. The following eight

equations can be assembled for hornblende - bearing intermediate and basic gneisses which can be solved to give the modal proportions of the eight phases considered:-

$$\text{Biotite} = \frac{Fe^{2} + Mg - Ti - 0.5Fe^{3} - 1.69(2Ca + Na + K - Al)}{5.85} \quad -- (1)$$

$$\text{Hornblende} = \frac{2Ca + Na + K + 0.5\ \text{Biotite} - Al}{2.6} \quad --- (2)$$

$$\text{Ilmenite} = Ti - 0.2\ \text{Hornblende} - 0.4\ \text{Biotite} \quad ----- (3)$$

$$\text{Magnetite} = \frac{Fe^{3}}{2} - (Fe^{3}\ \text{content of mafic silicates}) \quad -- (4)$$

$$\text{Anorthite} = Ca - 1.80\ \text{Hornblende} \quad ---------- (5)$$

$$\text{Albite} = Na - 0.45\ \text{Hornblende} \quad ---------- (6)$$

$$\text{Orthoclase} = K - 1.8\ \text{Biotite} - 0.25\ \text{Hornblende} \quad ---- (7)$$

$$\text{Quartz} = Si - 3\ \text{Albite} - 3\ \text{Orthoclase} - 2\ \text{Anorthite} - 6.65\ \text{Hornblende} - 5.75\ \text{Biotite} \quad ------ (8)$$

A further equation can be added to compute the apatite content if the phosphorous content of the rock is know. One difficulty in the use of this method of paragenesis analysis with the present data is that the minerals and rocks have been analysed by different techniques so that analytical bias between the two methods will cause displacement of mineral fields in multicomponent space in relation to rock compositions. This consideration together

with the neglected variations in the composition of the complex silicates make the relationships at the simplex boundaries in multicomponent space, defined by the various mineral phases, uncertain. Nevertheless the broad relations between rock and mineral compositions and the general form of the paragenesis fields can be assertained.

Normative proportions of the above eight phases can be calculated for the biotite - clinopyroxene gneisses in order to ascertain if the rock composition is incompatible with the amphibolite assemblage. The calculated norms for the six rocks in which the ferric iron contents are known are shown in table 40. The biotite clinopyroxene gneiss 230 which is richer in iron relative to magnesium and poorer in potassium than the other five rocks in table 40, plots outside the eight component symplex by virtue of the negative normative biotite proportion. Similar considerations apply to specimen 1039b and possibly specimen 113a, when allowance is made for an estimated ferric iron content in the computations. Specimen 832a recalculates with both negative normative biotite and negative normative quartz, characteristics which probably also apply to the similar specimen 832b. Specimens 329, 330 and 835, on the other hand, plot within the eight component simplex so that a further factor must be invoked to explain the occurrence of clinopyroxene in these rocks.

Similar normative calculations can be applied to the biotite-hornblende-clinopyroxene gneisses. The calculated norms for the two rocks of this type for which the ferric iron contents have been determined are shown in table 41. Both of these rocks, and also probably specimens 271 and 1040, plot within the quartz, orthoclase amphibolite eight component simplex. The influence of a further factor is therefore necessary to explain the presence of clinopyroxene in these rocks.

Normative mineral proportions of the eight phases calculated for the six pyribolites for which oxidation ratios have been determined are shown in table 42. Of these, specimens 50 and 88b plot just outside the simplex with low negative normative biotite and orthoclase respectively. The other four rocks plot within the seven dimensional field defined by the composition of the eight phases.

The magnesium to ferrous iron ratio is an important compositional variable that has been neglected in the above normative calculations. A direct relationship between the atomic fraction of magnesium in biotite and the rock oxidation ratio is shown in figure 47 for gneisses containing ilmenite and magnetite, and where biotite coexists with one other mafic silicate. A more tentative line can also be drawn on figure 47, connecting biotites from rocks with ilmenite alone or no oxide phase, with a much steeper slope. Wones and Eugster (1965) have found experimentally that the atomic fraction

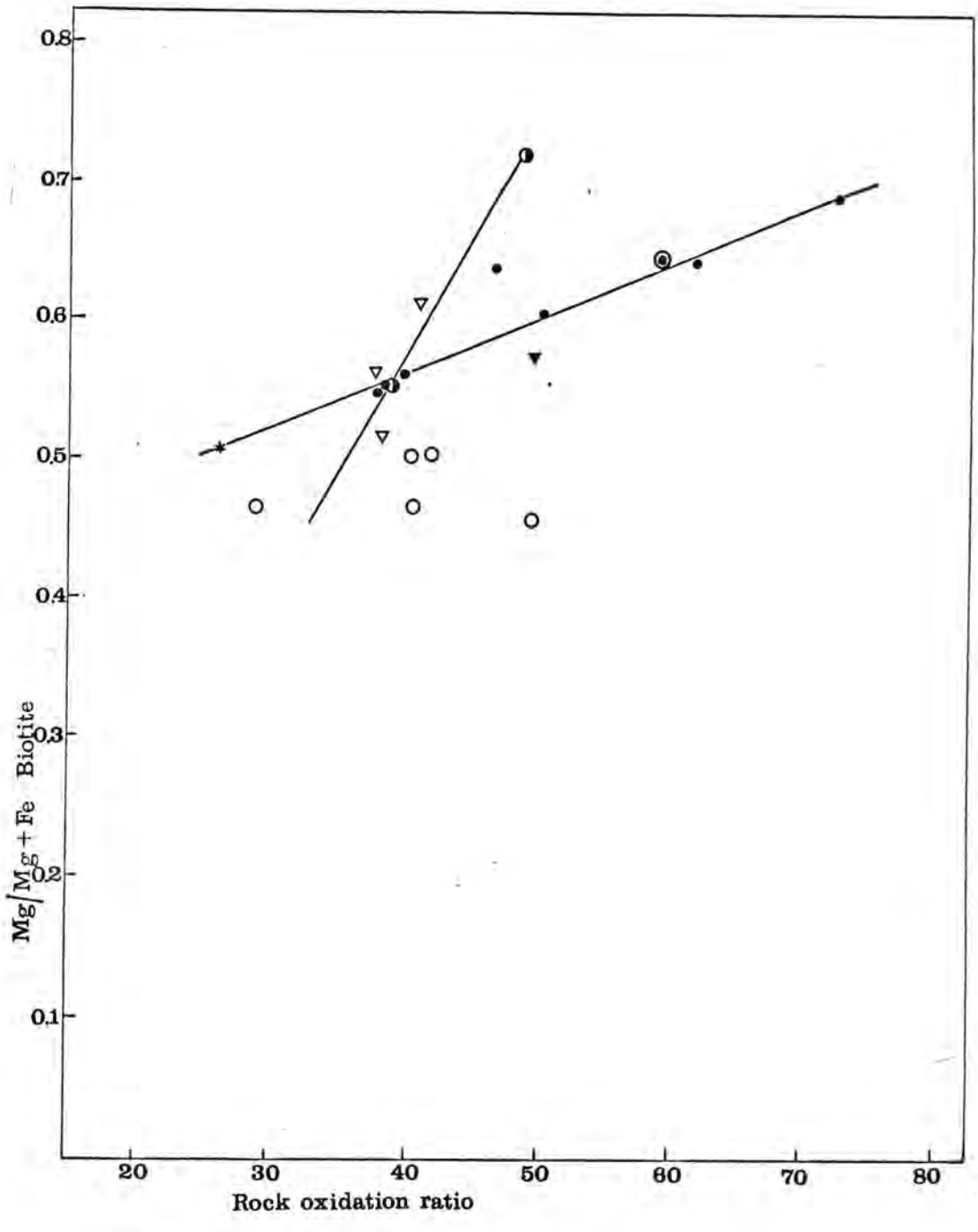

The relationship between magnesium content of biotite and rock oxidation ratio ($2Fe_2O_3$ / $2Fe_2O_3$ + FeO) in o pyribolites, ▼ biotite-hornblende-clinopyroxene gneiss, • amphibolites with magnetite and ilmenite, ▽ amphibolites with ilmenite, ◑ amphibolites with no ore, * biotite garnet gneiss and ◉ biotite clinopyroxene gneiss.

Figure 47.

of biotite along the phlogopite - annite join, coexisting with sanidine and magnetite, is governed by the temperature and the fugacities of water and oxygen. They found that at constant temperature, the biotite becomes more magnesium rich as the oxygen fugacity is increased. They also developed an equation for the estimation of the fugacity of water from the biotite composition and an assumption of the temperature. This equation :-

$$\log fH_2O = \frac{3428 - 4212\ (1 - x_i)^2}{T} + \log x_i = \tfrac{1}{2}\log fO_2 +$$

$$+ 8.23 - \log a\ KAlSi_3O_8 - \log a\ Fe_3O_4$$

where a signifies activity, T is the absolute temperature, fO_2 is the fugacity of oxygen and x_i is the atomic fraction of magnesium in biotite, can be solved after estimation of the oxygen fugacity from the composition of the coexisting magnetite and ilmenite using the date of Buddington and Lindsley (1964). With the assumption of the temperature of metamorphism as 600°C and the oxygen fugacity of 10^{-22} bars for the biotite garnet gneiss 815, substitution in the above equation gives a water fugacity of 0.4 bars. For the most oxidised gneiss, specimen 24m, with an estimated oxygen fugacity of 10^{-17} bars the computed water fugacity is 13 bars. Wones and Eugster (1965) quote a range of 1 to 10 bars for the fugacity of water in the Colton granulite facies rocks of the north - west Adirondacks described by Engel and Engel (1958, 1960 and 1962).

As the magnesium to iron ratio of the biotite is related to the rock oxidation ratio and the distribution of magnesium between biotite and hornblende is subject to compositional constraints, the rock magnesium to iron ratio is also an important factor in the determination of mineral parageneses. Thus the biotite clinopyroxene gneisses 329, 330 and 835 can be shown to lie outside the biotite-hornblende containing compositional space when magnesium and ferrous iron are considered as separate components. When magnesium and iron are assigned to the normative biotite the residual magnesium to ferrous iron ratio is greater than that permitted in coexisting hornblende. A mafic phase which can accommodate more magnesium than the hornblende, ie. clinopyroxene, is therefore favoured. This relationship can be expressed in the form of the equation :-

$$\underset{\text{Hornblende}}{Si_{6.65}Al_{1.70}Ti_{0.12}(Fe+Mg)_{4.60}Ca_{1.80}Na_{0.40}K_{0.25}} + (O) =$$

$$0.4\ \underset{\text{Albite}}{NaAlSi_3O_8} + 0.25\ \underset{\text{Orthoclase}}{KAlSi_3O_8} + 0.53\ \underset{\text{Anorthite}}{CaAl_2Si_2O_8} + 0.33\ \underset{\text{Quartz}}{SiO_2}$$

$$+ 0.12\ \underset{\text{Sphene}}{CaTiSiO_5} + 1.35\ \underset{\text{Clinopyroxene}}{Ca_{0.85}(Fe+Mg)_{1.05}Si_2O_8} + 1.06\ \underset{\text{Magnetite}}{Fe_3O_4}$$

which represents the phases equivalent to hornblende under relatively high oxygen fugacities. Ilmenite may replace sphene as the major titanium phase in many of the rocks. In rocks with both high oxidation ratios and magnesium to iron ratios the crystallisation of hornblende is supressed in favour of the phases on the right of the equation.

Similar reasoning can be employed to explain the occurrence of clinopyroxene in the specimens 280a and 1247 though because of their less extreme composition the above equation becomes reversible so that hornblende coexists with the phases on the right of the equation. In rocks which are relatively poor in potassium, biotite may be the sole potassium-bearing phase.

Similar but more speculative consideration can be applied to the pyribolites. As none of these rocks for which analyses are available contain modal alkali feldspar, the modal biote can be calculated from the rock potassium content. When magnesium and iron are assigned to the normative biotite according to the rock oxidation ratio, the residual magnesium to iron ratio for the pyribolites is less than the biotite clinopyroxene gneisses and all but the most basic amphibolites. It is therefore postulated that the residual magnesium to iron ratio for the pyribolites is less than that acceptable for hornblende coexisting with biotite alone at the oxygen fugacity at which these rocks crystallised. A further mafic phase which can accommodate more iron than the hornblende is therefore favoured. Thus, in the rocks with both relatively low magnesium to ferrous iron ratios and low oxidation ratios, hornblende tends to be replaced by more iron-rich orthopyroxene and clinopyroxene according to the following equation :-

$$Si_{6.65}Al_{1.70}Ti_{0.20}(Fe{=}Mg)_{4.55}Ca_{1.80}Na_{0.40}K_{0.25} + 1.4\ SiO_2$$

Hornblende Quartz

$$= 0.40\ NaAlSi_3O_8 + 0.49\ CaAl_2Si_2O_8 + 0.13\ FeTiO_3$$

Albite Anorthite Ilmenite

$$+ Si_{5.75}Al_{2.30}Ti_{0.50}(FE{+}Mg)_{4.85}K_{1.80} +$$

Biotite

$$1.47\ Ca_{0.85}(Fe{+}Mg)_{1.05}Si_2O_8 + 1.06\ (Fe{+}Mg)_{1.90}Si_2O_6 + (0)$$

Clinopyroxene Orthopyroxene

Though no biotite clinopyroxene orthopyroxene gneisses have been observed except for thin layers within the pyribolites, the assemblage would develop in rocks with sufficiently low magnesium to iron ratios.

The occurrence of pyribolites, amphibolites and biotite clinopyroxene gneisses within the gneiss sequence can therefore be explained in terms of a complex of whole rock compositional factors under essentially constant temperature. It is unnecessary to invoke a period of metamorphism under granulite facies followed by selective retrogression under amphibolite facies, as has been suggested by several authors to explain rock associations similar to those encounted in the present study.

Recently there have been complex mathematical studies of phase equilibria in natural multicomponent systems with the aid of computer techniques eg. by Greenwood (1967) and Saxena (1969c). Greenwood (op. cit.) has postulated

that at least some of the variation in mineral compositions found by Engel and Engel (1958 and 1961) between the amphibolite facies Emeryville rocks and the Colton granulites in the north-west Adirondacks can be interpreted in terms of changes in the bulk composition of the host rocks.

The growing complexity of the facies and subfacies classification of metamorphic rocks has prompted Winkler (1970) to abandon this method in favour of a simpler and broader classification of metamorphism into four stages. In this system the rocks considered above would be assigned to the ' high stage ' of metamorphism, the lower boundary of which is defined by the breakdown of muscovite in the presence of quartz.

16. Summary.

Two series of metamorphic rocks separated by a structural discontinuity have been mapped in the area between Sirdal and Åseral. The structurally lower group of rocks, the Sirdalsvatn Series, is characterised by the presence of an augen gneiss with large alkali feldspar phenoblasts, the Feda augen gneiss, and granitic gneisses containing horizons of alkali feldspar-bearing amphibolite and biotite clinopyroxene gneisses. The Feda augen gneiss originated by a process of extensive potassium feldspar blastesis and homogenisation of a heterogeneous gneiss sequence which may date from an earlier orogenic cycle. The biotite clinopyroxene gneisses of the Sirdalsvatn Series are distinguishable from all other rocks of the area by their relatively high oxidation ratios and high contents of the elements, P, K, Ti, Sr, Zr, Ba, Ce and Pb.

The Flekkefjord Series which occurs structurally above the Sirdalsvatn Series consists of alternations of layered basic, intermediate and granitic gneisses with more uniform granitic gneiss horizons. A few garnetiferous gneisses also occur in the lowest layered basic gneiss-rich horizon, which may be separated from the overlying rocks by a further structural discontinuity. The granitic gneisses of the Flekkefjord Series are either massive or diffusely layered and probably represent nebulitic

migmatite formed from a sedimentary sequence rich in feldspathic greywacke. The more basic horizons contain amphibolite, clinopyroxene amphibolite, pyribolite and biotite-rich gneiss in addition to granitic layers. In some highly deformed parts of the layered basic gneiss agmatitic and phlebitic migmatite is developed. The basic gneisses in the upper Flekkefjord Series show some chemical differences from those in the lower part of the sequence and are without pyribolites. Fine-grain disseminated iron sulphide occurs in thin biotitic gneiss horizons throughout the more heterogeneous parts of the sequence. The major element compositional variation shown by the basic and intermediate rocks of the Flekkefjord Series is comparable to that shown in igneous rock sequences.

The rocks were subjected to intense polyphase deformation, three major phases of which have been recognised within the Flekkefjord Series. Minor fold relics within the Feda augen gneiss indicate that these rocks were subjected to a phase of folding prior to those recognised within the Flekkefjord Series. Two later periods of minor flexuring have also been recognised.

During the climax of orogeny the rocks were metamorphosed to the low pressure granulite-upper amphibolite facies boundary. The mineralogy of the rocks

shows agreement with the sillimanite-cordierite-orthoclase subfacies of the Abukuma-type cordierite amphibolite facies except for the occurrence of orthopyroxene in some basic and feldspathic gneisses.

With the exception of alkali feldspar, magnetite and ilmenite which have undergone unmixing and exsolution while the rocks were cooling, the chemistry of the coexisting phases reflects the original crystallisation compositions. The very restricted compositional range of plagioclase coexisting with alkali feldspar, which is independent of the rock chemistry, indicates a regular relationship determined by environmental parameters and a roughly constant temperature throughout the area. Examination of the biotite analyses reveals that the substitution of ferric iron into the lattice is limited and constant and that an inverse relationship between the ferric to ferrous iron ratio and the titanium content of the biotites exists. Compositional relationships among the hornblendes are more complex. Some chemical features of the hornblendes are intermediate between minerals from established granulite-facies rocks and those from amphibolitefacies rocks.

A temperature of crystallisation of about 600°C and a range of oxygen fugacity from 10^{-21} to 10^{-18} bars during crystallisation can be estimated from the chemistry of the coexisting feldspars and the ilmenite compositions

respectively.

High to moderate positive correlation is apparent in the distribution of titanium and magnesium between the coexisting silicate phases. Much of the scatter in the Roozeboom diagrams is related to rock oxidation ratios, the nature of the coexisting oxide phases and the tetrahedral aluminium content of the hydrous silicates. This is consistent with the crystallisation of the phases under conditions of chemical equilibrium.

The varied parageneses of the gneissic rocks were produced during a single metamorphic event under essentially constant temperature. Rock composition and oxygen fugacity exercised the main constraints on the nature of the coexisting phases.

The gneissic porphyritic adamellite which occupies the core of the Fjotland antiform was formed from pre-existing feldspar-rich gneisses by a process of potassium feldspar blastesis and homogenisation in a region of locally elavated oxygen and water fugacities. This may have resulted from upward migration of water from an upward projection of the Sirdalsvatn Series basement in the core of the fold. The similar rocks in the northern part of the Kvina valley were produced by a less intense phase of the same process.

The widespread molybdenite and chalcopyrite mineralisation, associated with vein quartz, granular leucogranite and pegmatite, originated at depth and was transported in siliceous hydrothermal fluid up basement weakness zones into the overlying heterogeneous gneisses, particularly where the gneissic layering coincided in direction with the basement fracture pattern. The ore metals were fixed as sulphides where the solutions invaded gneisses containing fahlband sulphide. The mineralisation was introduced after the climax of metamorphism and deformation but while the rocks were close to their maximum temperature and still able to deform plastically in response to localised stress. Minor remobilisation of ore occurred subsequently in a phase of cross-cutting pegmatite injection.

An intrusive magmatic event occurred in the waning stages of orogeny with the emplacement of a large volume of quartz monzonite with some discordance. Thermal metamorphic aureoles were developed in the country gneisses with the crystallisation of mineral assemblages indicating a rather higher temperature than that attained at the climax of regional metamorphism.

An early phase of brittle deformation produced faults which were subsequently healed by the slow release of regional strain. Pegmatite and quartz-chalcopyrite veins invaded some of the breaks while they were still open. At a much later time the area was subjected to

further brittle deformation with the formation of mylonites. Hydrous solutions invaded these fractures and the surrounding rocks were retrograded to chlorite, epidote, hematite and piemontite-bearing rocks.

The final event prior to uplift, erosion and finally glaciation was the intrusion of parallel dykes of alkali-rich basic rock.

APPENDIX.

a) Rock chemical analysis.

Rock analysis was carried out by means of the Philips 1212 X-ray spectrometer. The major element analyses were corrected for differences in mass absorption using the method of Holland and Brindle (1966). This method enables large numbers of silicate rocks of the commoner types to be analysed with relative rapidity and fair accuracy. Analyses obtained by this method are satisfactory for comparative studies of related rocks but less so for more rigourous petrological computations, as they are subject to bias and the influence of other factors of which the most important are the mineralogical effects. Variations in the nature of mineral species within a rock give rise to differences in X-ray response which are independent of chemical composition. The importance of these mineralogical effects in the analysis of aluminium has been demonstrated by Leake et. al. (1968). It is impossible to allow adequately for such differences between standards and unknowns in the method of Holland and Brindle, but as material analysed in the present study is relatively close both chemically and mineralogically to the secondary standards employed, some compensation for mineralogical effects has been effected. A further disadvantage of the analytical method employed is that the mathematical procedure adopted for the calculation of

mass absorption corrections requires that the analyses calculated from the initial calibration are normalised on a water free basis, so that the independent check of the oxide total on the reliability of the analyses is impossible.

The total iron contents of 27 rocks were determined chemically be measurement of the intensity of the colour of the orthophenanthroline complex. A graphical comparison of the two sets of iron analyses for these rocks is shown in figure 48. This graph reveals a tendency for the X.R.F. analyses of the iron-rich rocks to be higher than the chemical analyses with a converse relationship for the iron-poor rocks. Ferrous iron was also determined in these rocks using the ammonium metavanadate back titration method described by Wilson (1955). The ferric iron contents were then found by difference and the rock oxidation ratio, ie. 2 Fe_2O_3 x 100/2 Fe_2O_3 + FeO, calculated.

Trace element analysis was carried out by X.R.F. and correction for mass absorption differences for elements with λ less than that the iron K absorption edge effected using the inverse relationship between the height of the tube molybdenum Ka Compton scattering peak and the mass absorption at that wavelength. The initial calibration was in terms of an intermediate rock base spiked with trace elements.

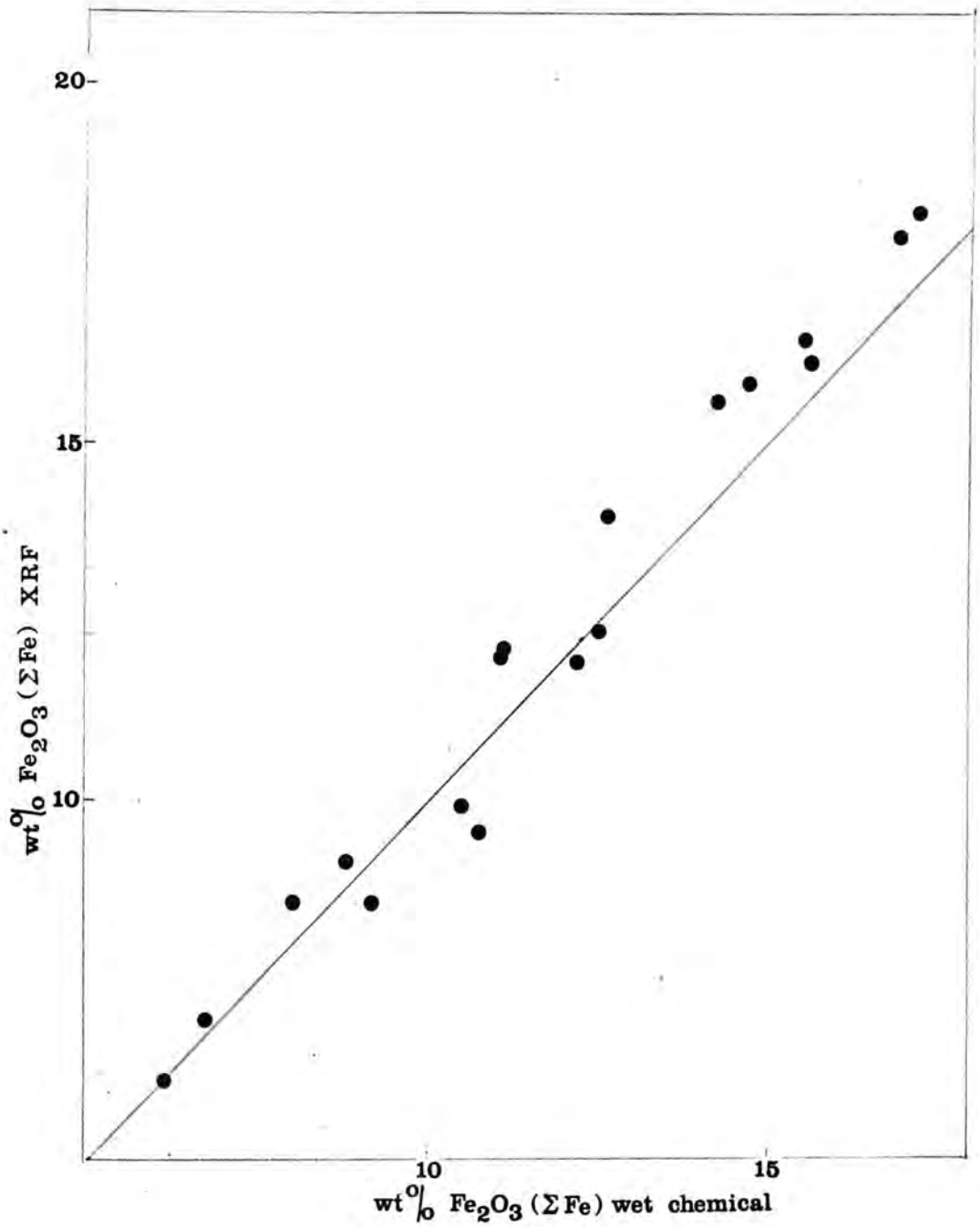

Comparison of wet chemical and X.R.F. analyses of total iron in rocks.

Figure 48.

b) Mineral chemical analysis.

1. Alkali feldspar.

The elements sodium, potassium, barium and calcium were determined in alkali feldspar grains within a polished thin section by means of the Cambridge Instruments Geoscan electron microprobe. In order to avoid volatisation of the alkali elements in surface layers of the minerals an electron excitation potential of 10 kilovolts and an incedent spot defocussed to about 20 microns were used. Standards were made by mounting grains of well analysed natural feldspars, mostly Spenser samples, obtained from the University of Manchester. Calibration was achieved for sodium and potassium by anplot of the peak minus background counts for the standards against the chemically determined results as shown in figures 49 and 50. No atomic number or mass absorption corrections were applied to the experimentally determined compositions using these calibrations because of the close similarity between the standards and unknowns. Calcium and barium were determined in terms of the probe analyses of the standards obtained by Smith and Ribbe (1966) as the chemical determinations of calcium in the bulk samples were considered too high as a result of contamination by small included grains of such minerals as apatite,and those of barium were unreliable.

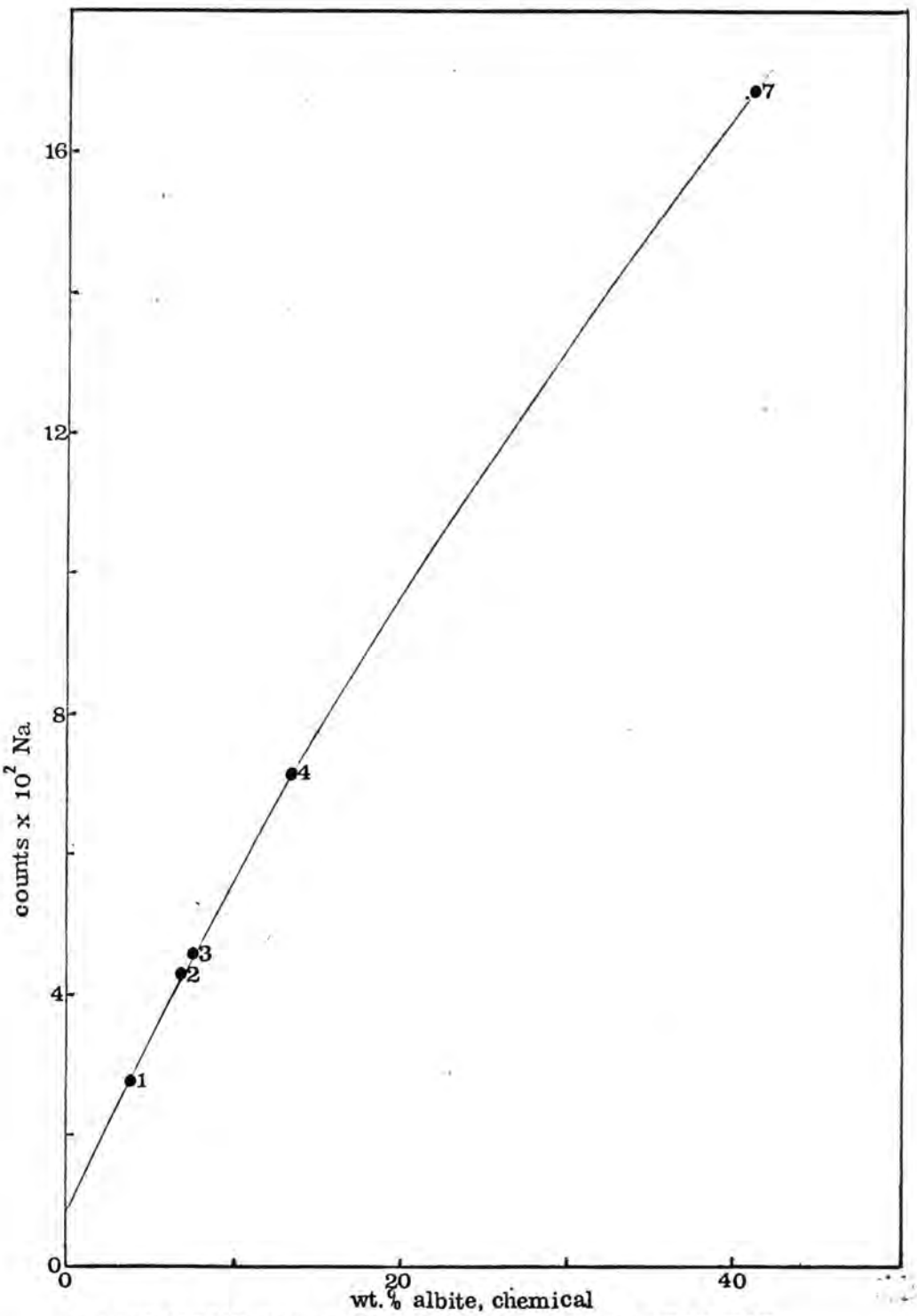

CALIBRATION FOR Na CONTENT OF ALKALI FELDSPAR

Figure 49.

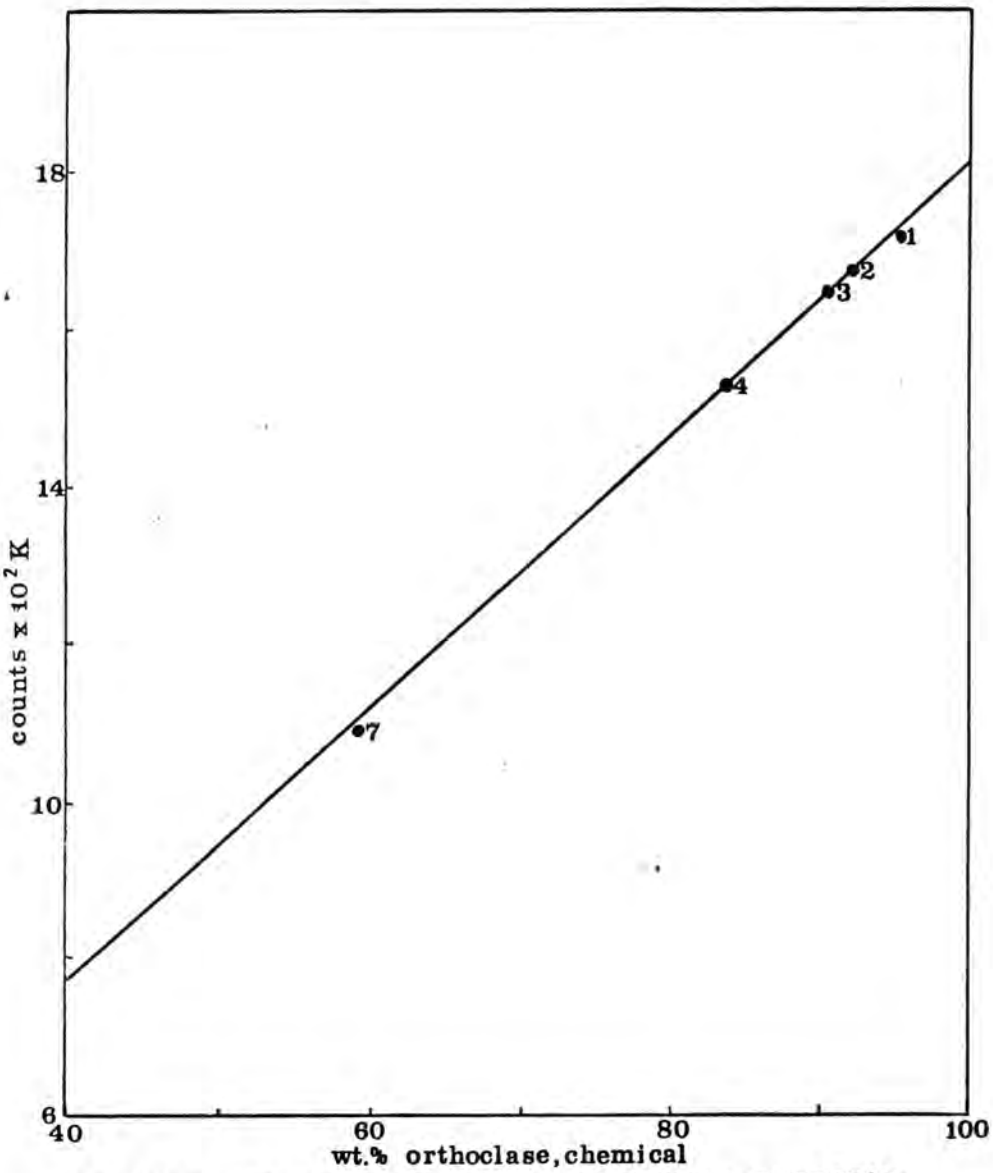

CALIBRATION FOR K CONTENT OF ALKALI FELDSPAR

Figure 50.

2.Plagioclase.

Plagioclase analysis was carried out on the electron microprobe under the same instrumental conditions as for the alkali feldspar analysis. The minerals were analysed for sodium, calcium, aluminium and silicon in terms of a set of calibrations of synthetic plagioclase glasses prepared by D. Lindsley and described by Ribbe and Smith (1966). As Smith (1965) has shown that the X-ray response for a natural plagioclase and a synthetic glass both of composition anorthite 40 wt. % showed agreement to within 1 %, the present minerals were analysed directly in terms of the graphs shown in figures 51 and 52. The pure albite glass was not used in these calibrations as it was unstable, even under the low density of electrons used. As the oxide totals of the minerals analysed for the four major elements were close to the ideal, calcium alone was determined in the other minerals and the results expressed in terms of the weight percentage of the anorthite end-member.

3.Mafic minerals.

The minerals biotite, hornblende, clinopyroxene, orthopyroxene, sphene, garnet and chlorite were analysed on the electron microprobe for the major elements with an electron excitation potential of 15 kilovolts and a focussed beam about 2 microns in diameter. The minerals were

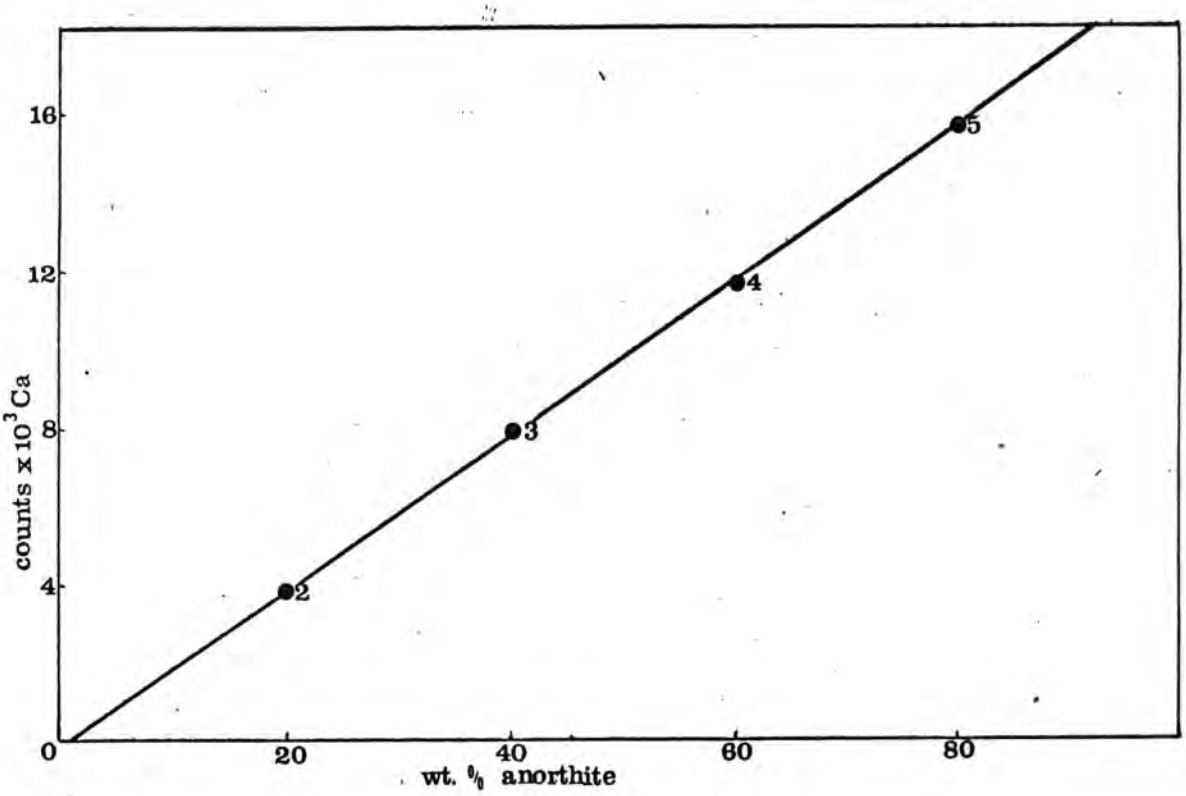

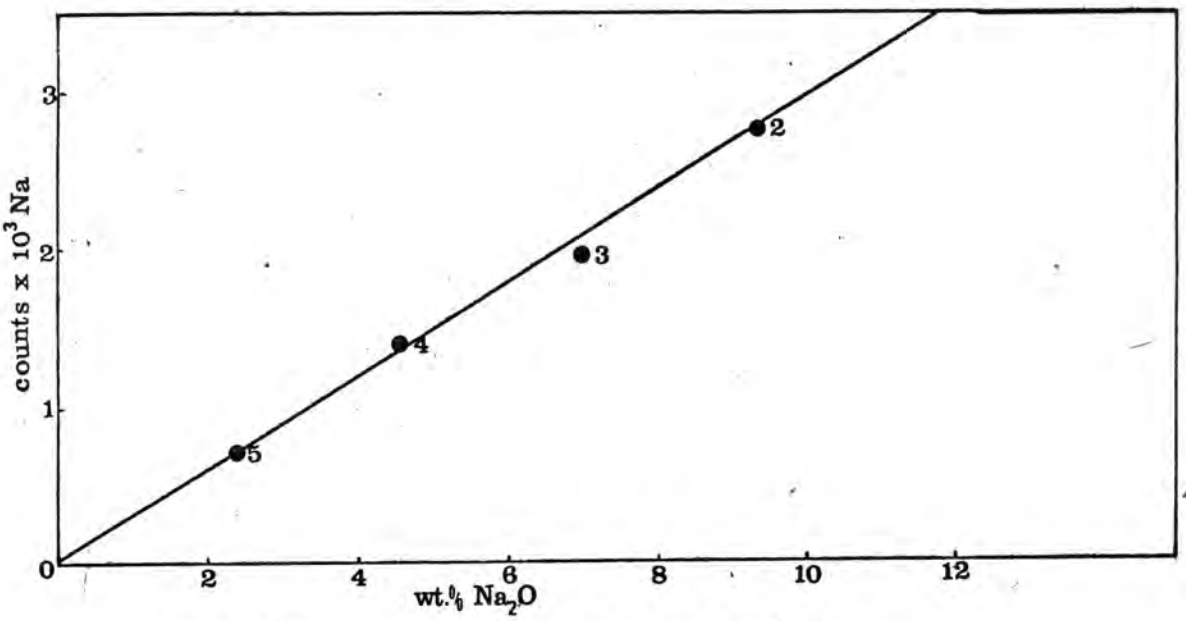

CALIBRATION FOR Ca&Na CONTENT OF PLAGIOCLASE

Figure 51.

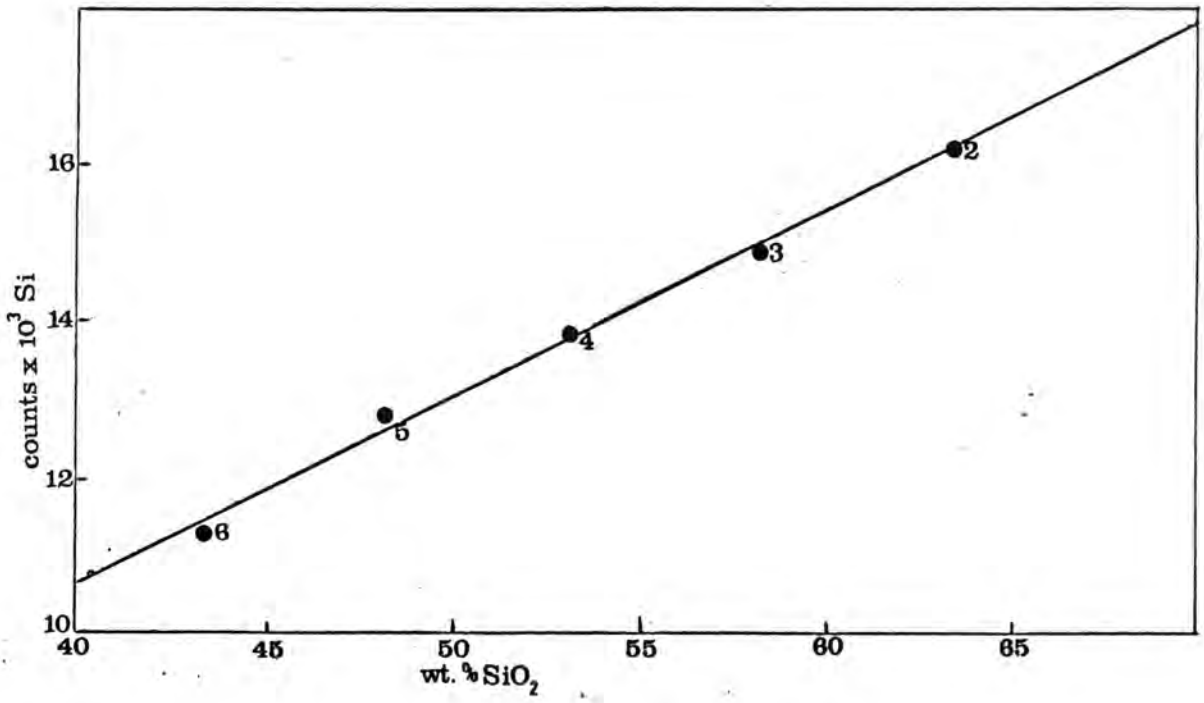

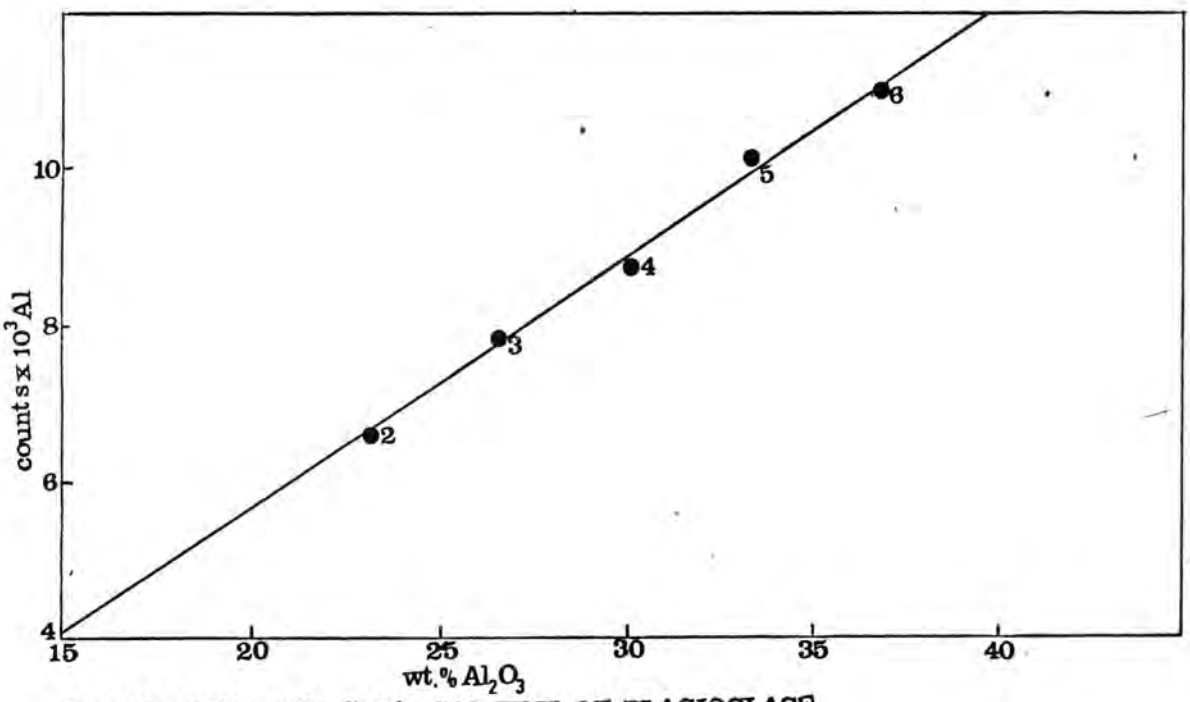

CALIBRATION FOR Si&Al CONTENT OF PLAGIOCLASE

Figure 52.

analysed in terms of a set of five silicate glasses made by Pilkingtons of St. Helens to cover the range of composition of the commoner mafic rock-forming minerals. The chemical composition of these standards used in the calibration was based on an X-ray fluorescence analysis in the same run as the present whole rocks so that both rock and mineral analyses could be as near comparable as possible.

The calculation of the mineral analyses from the raw count data was performed in two computer programmes, the first of which calculated an approximate composition of each mineral by direct ratioing to a single standard for each element after correction of the raw counts for machine drift and counter dead time. In general for each mineral type the glass nearest in composition was used as the standard. The second programme which was based on calculation procedures adopted by Long, corrected the approximate compositions for differences in mean atomic number, mass absorption and fluorescence.

c)The instrumental precision of electron microprobe analysis.

This quantity was estimated by repeated analysis of one spot on the mineral surface. The prolonged bombardment of a single area results in surface damage and pitting, particularly in framework and sheet silicates where selective

volatalisation of elements occurs. Because of this and the fact that the instrument is subject to considerable medium term drift, it is difficult to increase the precision by long counting periods. In this work the usual procedure was to count for three to five consecutive 20 second periods. For the repeated analysis of sodium in an alkali feldspar at about the 1 % level, using a K.A.P. crystal, the coefficient of variation was 8.5% while for potassium in the same mineral it was 1.2%. The coefficient of variation of five determinations of iron in biotite was 0.7%.

d) The variation in composition of minerals within a single rock specimen.

The development of the electron microprobe has made the investigation of variations in composition of individual mineral grains or mineral populations within a rock relatively simple. Prior to this, these investigations relied upon either the measurement of the optical properties of minerals in situ or after bulk separation, or chemical analysis of different fractions of the same mineral produced by heavy liquid separation and the isodynamic magnetic separator. Only in the case of plagioclase is it possible to relate the measured optical properties directly to the chemical composition. The big disadvantage of the direct chemical analysis of mineral fractions is that it is impossible in practice to remove all impurities, particularly those occurring as inclusions.

During the winter of 1965 to 1966 an attempt was made by the present author to separate minerals from a set of representative rock types. This operation was abandoned when it became clear that a satisfactory pure sample in sufficient quantity for chemical analysis of some of the minerals would be almost impossible to obtain in a reasonable time. Hagner, Leung and Denison (1965) separated fractions of biotite, hornblende and orthopyroxene from mafic gneisses which showed significant variations in refractive indices. They correlated these variations with differences in chemical composition that could either be interpreted in terms of microchemical compositional zoning or variation from grain to grain in an apparently homogeneous rock. The formation of equilibrium domains within a homogeneous rock has been postulated both by Korzhinskii (1959b) and Thompson (1959) under a concentration gradient of a mobile component or a temperature gradient. A careful study of the significance of any variation in composition from grain to grain within the various polished thin sections was therefore carried out.

1. Alkali feldspar.

The variation in composition shown from point to point within a single large augen crystal and from grain to grain in the matrix material, illustrated in tables 29 to 31, is considerably greater than that resulting from the analytical

variance. As has been discussed in Chapter 13, these compositional variations result from differences in the amount of leaching of the exsolved sodic phase in the period during which the rocks were cooling. In previous works the chemical analysis of potassium feldspar has been preceded by the crushing of a bulk sample containing the mineral and the separation of the mineral from other phases by means of heavy liquids. Nilssen (1967) has made a critical examination of this technique and has shown that it is possible to separate perthitic feldspars into a series of fractions of steadily decreasing perthite content. Analysis of several fractions of feldspar from the Grimstad granite and the Herefoss granite of southern Norway showed a range of the orthoclase end-member content from 52% to 90% by weight and 71% and 92% by weight respectively. Bulk analyses of perthitic feldspars are therefore of varying significance according to how carefully and precisely the separation has been carried out and to what fraction is selected for analysis. As the fractions at each end of the range will probably contain more impurities than those in the middle of the range, it will be virtually impossible to obtain an unbiased mean composition of the feldspar.

2. Plagioclase.

Hunahashi, Kim, Ohta and Tsuchiya (1968) have shown that the results of the Universal Stage compositional

determination of several plagioclase grains within thin sections of several apparently homogeneous igneous and metamorphic rocks show a considerable range. A histogram of the compositions of 130 plagioclase grains from the older biotite gneiss of the Hida metamorphic belt, Japan, determined on the Universal Stage, is reproduced from Ohta (1969) in figure 53. Ohta (personal communication) also detected similar ranges in plagioclase composition from gneissic rocks from the south Norwegian PreCambrian. Using the Universal Stage method of plagioclase composition estimation employed by Ohta the present author measured the composition of several grains within the amphibolite specimen 56 and found a considerable spread, as illustrated in figure 53.

The composition of several plagioclase grains within a section of the same amphibolite and several other rocks was also determined with the electron microprobe as described above. The range in composition of plagioclase grains from this method for the three rocks with the maximum variation and the amphibolite 56 are also shown in figure 53. The variation in plagioclase composition for specimen 56 obtained from the probe analyses is slightly greater than that which would be expected from the analytical variance but considerably less than the spread of the Universal stage composition determinations. The mode of the probe analyses is at a composition of only 1 % anorthite less than that of the main mode of the optical determinations

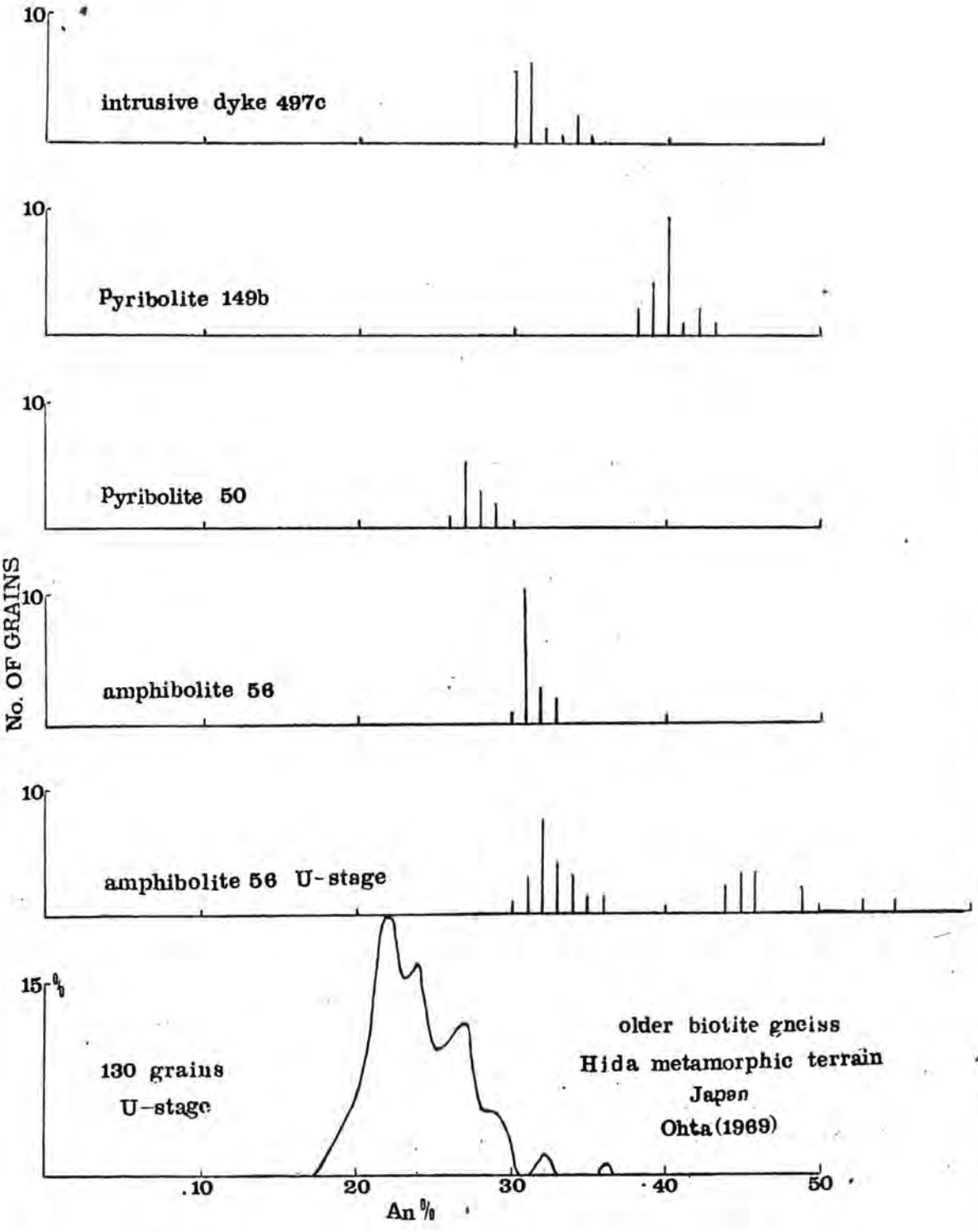

Variation in An content of plagioclase grains

Figure 53.

however. Though the broader distribution of compositions about this maximum can be explained by the lower precision of the optical method no grains with anorthite contents greater than 40 % were detected in the probe analysis.

In the majority of the gneissic rocks that were examined and analysed with the electron microprobe the variation in plagioclase composition detected was close to that which could be predicted as resulting from the precision of the method of analysis used. The greatest compositional variations were shown by the dyke rock 497c which showed some sign of optical zoning in its lath-shaped plagioclase crystals and the two pyribolites 149b and 50 which exhibited diffuse fine scale layering into amphibole-rich and pyroxene-rich components.

3. Mafic minerals.

The procedure adopted for the analysis of the mafic minerals was to count three times on eight to ten spots covering several grains throughout the whole slide. Further spots were analysed if the variation in composition obtained was significantly greater than that expected from the counting statistics. The maximum and mean variation in composition for different grains of the same mineral, as absolute percentages of the oxide, are shown in table 43. In the majority of the mafic mineral analyses the apparent

variation in composition from grain to grain is similar to that expected from the analytical variance. The maximum variations are up to a factor of three greater than this but in most minerals this variation is confined to one element and therefore has little significance in the mineral chemistry of the rock. In the specimen of the Hådeland intrusion, number 306c, both the hornblende and sphene show relatively large variations in the content of several elements, in particular those which occupy similar structural sites. It is therefore deduced that in this rock there are significant differences in the chemistry of separate grains of some of the mineral constituents. For the gneissic rocks the electron microprobe analyses of mineral grains have revealed no significant variations between individual grains with the exception of alkali feldspar. This fact provides strong evidence for chemical equilibrium during the crystallisation of the various parageneses at the climax of metamorphism.

e) Accuracy of mineral analyses.

It is difficult to assess the accuracy of the electron microprobe analyses, both because of the complexity of the factors influencing the X-ray response and because of the lack of another analytical method capable of determining the composition of small single grains of a mineral. The chemical analysis of bulk separated mineral fractions is

subject to serious errors, particularly in the minor element contents of minerals, because of the impossibility of the removal of all impurities.

The errors encounted during the quantitative analysis of minerals with the electron microprobe has been treated at some length by Sweatman and Long (1969). During the present analytical runs with the probe care was excersised in the setting of optimum intrumental conditions for each element and in the alignment of the electron optical column. Machine drift was carefully monitored and the analyses obtained when this was pronounced were rejected. Initially the thickness of the carbon coating on the polished thin sections was standardised to that on the standards visually. According to Sweatman and Long (op. cit.) differences of 50 Å or more could go undetected in visible comparisons, leading to errors of between 1% and 2% in sodium and iron determinations. For the majority of the analyses however, both standards and unknowns were coated with a standard thickness of carbon monitored by its electrical resistance.

The oxide total is often used as a guide to analysis accuracy. Totals well above 100% indicate analytical errors but those below this figure could also mean that a significant component has not been determined. Water has not been determined in the hydrous minerals so that in these minerals the oxide total can only give an indication of accuracy within

very broad limits. As even ideal oxide totals can be misleading, by virtue of cancelling errors in several components, for minerals the best measure of accuracy is the fit of the ideal mineral formula to the recalculated analysis and the balance of charges of the various element groups in the different structural sites. In the complex hydrous silicates these principles are difficult to apply as the ferric iron contents have not been determined.

1. Alkali feldspar.

Smith and Ribbe (1966) have compared chemical analyses of bulk feldspar samples with their probe determinations based on empirical methods of correction. They found some large deviations but close agreement between the flame photometer potassium results of Carmichael and their probe analyses. As the present author's results are based on some of the Spenser potassium feldspars for which Smith and Ribbe (op. cit.) found close agreement it can be concluded that the potassium analyses of the alkali feldspars in this study are comparable to the flame photometer determinations. The calibration for sodium in alkali feldspars used by Smith and Ribbe is also based on the flame photometer analyses of Carmichael. When the analyses of other feldspars were compared however, the probe sodium results were biased higher than the chemical analyses. Nothing can be deduced about the accuracy of the calcium and barium determinations as

the chemical analyses of the standards available were clearly unreliable. A histogram of the molecular totals of the feldspars that have been analysed for all the four elements is shown in figure 54. The distribution is similar to that shown by Smith and Ribbe. Some of the lowest oxide totals were obtained from feldspar grains in specimen 832a which contain the greatest amount of the heavier minor elements calcium and barium and are therefore furthest removed in composition from the standards.

2. Plagioclase.

The seven plagioclases that were analysed for all the major elements have oxide totals from 100.0 to 101.1%, a range comparable to that obtained by Ribbe and Smith (1966) in a series of probe plagioclase analyses, and quoted by Deer, Howie and Zussman (1966) for chemical analyses of bulk material. The recalculations of the present analyses with respect to 32 oxygen atoms show a range of Z-site totals from 15.98 to 16.04 and X-site totals from 3.95 to 4.01 atoms per formula unit. The corresponding ranges of the chemical analyses quoted by Deer, Howie and Zussman (op. cit.) are 15.97 to 16.05 and 3.87 to 4.08 atoms per formula unit for the Z site and X site respectively. Allowance for undetermined iron, Potassium and strontium in the present analyses would produce a closer approach to the ideal formula.

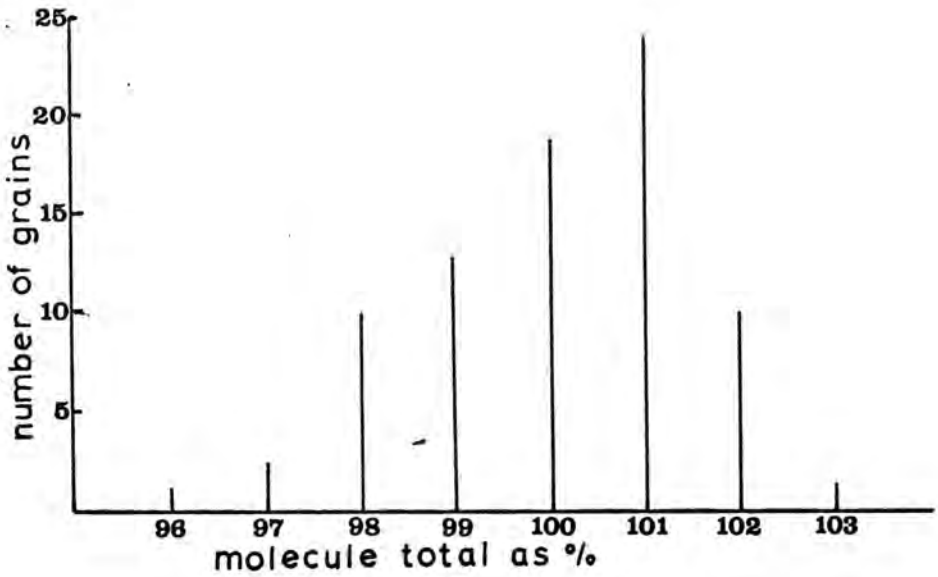

Histogram of alkali feldspar molecule totals.

Figure 54.

3. Orthopyroxene.

Nine orthopyroxenes have been analysed with the electron microprobe for the major elements but manganese, an important minor element, has only been determined in two of the minerals. The oxide totals range from 98.5% to 101.3%, but if allowance is made for manganese most of the totals would probably be in the 100% to 101% range. As orthopyroxenes are relatively simple silicates in which element for element substitutions are limited, it is possible to gauge the analysis accuracy by the closeness of fit of the recalculation of the analysis on the basis of six atoms of oxygen into the ideal mineral formula and the valency balance between the sites. The Z-site totals range from 2.00 to 2.02 atoms per formula unit and the XY site totals range from 1.93 to 2.01 atoms per formula unit. If manganese were included in all the recalculations the Z and XY site totals would be closer to the ideal 2 atoms per formula unit. The corresponding site totals from the empirically corrected probe results of Howie and Smith (1966) range from 1.96 to 2.04 per formula unit and from the best chemical analyses quoted by Deer, Howie and Zussman they range from 1.98 to 2.01 atoms per formula unit. The fact that aluminium replacing silicon in the Z site should be balanced by aluminium and other trivalent elements in the XY site can also be used as a test of accuracy. Only one of the two analyses where manganese is included adheres to

this rule. In many of the best chemical analyses of orthopyroxene the charge in each site in the recalculation does not balance however.

The present probe analyses of orthopyroxenes appears to compare quite favourably with wet chemical analyses of bulk material and are superior in respect to some of the minor elements, in particular calcium. A small amount of clinopyroxene impurity in the bulk sample causes a considerable error in the calcium content. In bulk separation any included clinopyroxene can neither be fully removed nor retained so that the fraction analysed represents an intermediate stage between the original composition and the final orthopyroxene host.

4. Clinopyroxene.

Manganese has only been determined in two of the fifteen analysed clinopyroxenes but as it is less abundant than in the orthopyroxenes its absence from the oxide totals and recalculations is less serious. The oxide totals of the analysed clinopyroxenes range from 97.5% to 100.6% with all but three between 99% and 101%. Smith (1966c) quotes a range of oxide totals from 97.7% to 101.0% in 22 probe analysed minerals. In the recalculations of the present analyses with respect to six oxygen atoms the Z-site totals are all 2.00 atoms per formula unit and the XY site totals

range from 1.97 atoms per formula unit to 2.01 atoms per formula unit. The corresponding XY site totals of the clinopyroxenes analysed by Smith (op. cit.) and the wet chemical analyses of bulk separated minerals quoted by Deer, Howie and Zussman (1966) both range from 1.97 to 2.04 atoms per formula unit. In these respects the present analyses compare favourably with the chemical analyses. The lack of knowledge of the ferric iron content of the minerals makes the valency balance between the two sites impossible to assess.

5. Sphene.

The oxide totals of the eight analysed sphenes range from 92.3% to 98.2% with five between 96.0% and 96.3%. Undetermined water is one contributant to the low oxide totals but, as anything up to one in five of the oxygen atoms of sphene can be replaced by the hydroxyl group, it is difficult to allow for this. Examination of the sphene analyses in Deer, Howie and Zussman (1966) reveals that the water and fluorine content is frequently about 1.5% by weight, which is equivalent to one hydroxyl and fluorine group per 20 oxygen atoms. Using this assumption the present analyses have been recalculated with respect to $19\frac{1}{2}$ oxygen atoms so that these ions can be neglected. On this basis the Z-site totals range from 4.00 to 4.02 atoms per formula unit with a little aluminium entering the site

in the majority of cases. The titanium site totals range from 3.79 to 4.06 atoms per formula unit and the calcium site totals range from 3.69 to 4.07 atoms per formula unit. As neither the rare earth elements nor niobium have been determined, both of which frequently enter the mineral replacing calcium and titanium respectively, it is impossible to attach much significance to the totals. In the case of the rock specimens 20 and 861b however, the niobium and cerium contents are low so that by inference that of the sphenes must also be low. The rare earth content of the intrusion sphene, specimen 306c, is probably greater, as the quartz monzonites are richer in cerium than the majority of the gneissic rocks. Niobium is also enriched in the intrusive rocks compared with the metamorphic rocks. In spite of the corrections applied to the probe analyses the large extrapolation from the titanium content of the standard to that of the sphenes is likely to lead to greater errors in these analyses compared with those of the other silicates.

6. Biotite.

The oxide totals of the 39 analysed biotites range from 92.8% to 98.3% with 18 of these between 95.0% and 96.0%. The majority of the analysed metamorphic biotites included in Deer, Howie and Zussman (1966) have a combined water and fluorine content of around 4% by weight. With this assumption and allowing for manganese where

necessary, the majority of the oxide totals range from 99% to 100%. In the recalculations with respect to 22 oxygen atoms, ten of the biotites have Z site totals of less than 8.00 atoms per formula unit if titanium is excluded from the site. Though some chemical analyses of biotites, mostly from alkali igneous rocks, with vacancies in the Z-site have been reported, the majority of the published better analyses of metamorphic biotite contain rather more aluminium than the present analyses. Biotites from the Swedish PreCambrian, also analysed on the electron microprobe in terms of glass standards and reported by Annersten (1968), are also all relatively low in aluminium compared with chemically analysed metamorphic biotites. It is difficult to decide whether the probe aluminium results are accurate or subject to a bias in relation to chemical analyses as the bulk fractions may contain more aluminous impurities like chlorite. The lack of ferric iron determinations in the present biotite analyses makes the assessment of charge balance between the structural sites impossible but the regular relationship between the titanium content and the apparent negative charge balance in figure 22 suggests that valency balance is fulfilled. Though it is difficult to define the accuracy of the biotite analyses except by extrapolation from that of the simpler pyroxenes analysed in the same manner and other indirect means, the suitability of the data for comparative petrological computations is manefest. The very low calcium content of the minerals

when compared with many chemical analyses of similar material can be explained in terms of contamination of the bulk samples with small grains of calcium-rich phases like apatite which are physically impossible to remove.

7. Hornblende.

The oxide totals of the 31 analysed hornblendes range from 95.4% to 99.5% with 25 of these between 96.5% and 98.0%. Assuming a water plus fluorine content of about 2% by weight and a manganese content of 0.5% by weight in those samples in which the element has not been determined the majority of the oxide totals would then lie in the range of 99.0% to 101.0%. The Z sites in the recalculations on the basis of 23 oxygen atoms all total 8.00 atoms per formula unit. The Y-site totals range from 4.98 to 5.34 atoms per formula unit and the combined X and A-site totals range from 2.12 to 2.68 atoms per formula unit. According to Phillips (1963) a Y-site total of greater than 5.10 atoms per formula unit indicates analytical error. The lack of ferric iron determinations in the present analyses precludes the computation of charge balance between the sites. Nevertheless the site and oxide totals of the majority of the present probe analyses are comparable to many published chemical analyses of metamorphic amphiboles.

8. Chlorite and garnet.

The analysed chlorite has an oxide total of 89.6% which is a little high if a water content of between 11% and 12% is assumed. The recalculation of the analysis on a water free basis on the basis of 24 oxygen atoms shows a very close fit to the ideal formula however. The oxide total of 101.6% for the analysed garnet is also slightly high but the recalculation of the analysis on the basis of 24 oxygen atoms fits very closely into the ideal mineral formula.

X.R.F. Analyses of intrusive quartz monzonites etc.

	Ljosland intrusion					Haddeland		Åseral	
No.	1264	1257	1266	2003	1253	306c	307	1192	1204
SiO_2	72.9	66.5	65.1	65.0	63.2	66.4	62.6	62.4	52.9
Al_2O_3	14.3	16.3	15.8	16.9	16.1	14.0	14.8	16.3	15.3
FeO*	1.9	4.0	5.0	3.8	5.5	6.9	8.1	5.5	12.4
MgO	0.3	1.4	1.2	1.0	1.2	1.0	1.7	1.2	5.3
CaO	1.8	3.1	4.8	4.6	5.3	3.6	5.0	5.0	8.0
Na_2O	3.2	3.2	3.5	3.5	3.3	2.8	2.9	3.6	3.1
K_2O	5.1	4.9	3.6	4.0	3.5	4.7	3.5	3.4	2.4
TiO_2	0.4	0.8	0.9	0.8	1.1	0.4	1.4	1.0	2.4
MnO	-	-	-	0.06	0.09	0.14	-	0.10	-
P_2O_5	-	-	-	0.39	0.72	-	-	1.46	-
BaO	-	-	-	0.21	0.24	0.15	-	0.31	-

FeO* = Total iron expressed as ferrous oxide

Notes.

Specimen 1264 is from an inclusion of alkali feldspar-rich granitic rock within the normal quartz monzonite and is without modal hornblende.

Specimen 1257 is from the pink porphyritic facies of the Ljosland intrusion and contains accessory tourmaline.

Specimen 1204 is from a basic facies of the Åseral intrusion and contains clinopyroxene in addition to hornblende.

Table 1.

X.R.F. Analyses of basic dykes.

	Metamorphosed			Igneous			
No.	374	390a	497c	16	37	370a	1147
SiO_2	50.2	50.2	52.9	50.7	51.4	51.3	49.8
Al_2O_3	18.6	19.7	16.6	17.9	17.8	19.3	19.3
FeO*	11.4	11.1	10.8	12.0	12.2	10.4	10.9
MgO	6.8	4.5	5.1	4.0	4.4	3.8	5.7
CaO	7.3	8.5	6.7	6.7	6.6	7.1	8.0
Na_2O	2.3	3.6	3.3	3.9	3.2	3.9	3.3
K_2O	1.5	0.8	1.9	1.7	1.5	1.7	1.4
TiO_2	2.0	1.9	2.5	3.1	3.1	2.5	2.2
MnO	0.16	0.14	0.15	0.13	0.13	0.11	-
BaO	0.05	0.03	0.08	0.06	0.06	0.06	-

Notes.

Specimens 374 and 390a are from different positions along the metamorphosed dyke to the north of Knaben.

Specimens 16, 37 and 370a were taken from different positions along the length of the igneous dyke which runs just north of Knaben. Specimen 37 is from the most westerly position.

Specimen 1147 is from an olivine-bearing igneous dyke to the north of the Knaben dyke.

Table 2.

Corrected probe analyses of a chlorite and a garnet.

	chlorite 8	garnet 818e
SiO_2	27.7	38.0
Al_2O_3	19.0	21.6
FeO*	23.9	32.7
MgO	17.9	5.5
CaO		1.9
Na_2O		
K_2O		
TiO_2		0.1
MnO	1.1	1.8
	89.6	101.6

Numbers of ions on the basis of 28 oxygens (chlorite) and 24 oxygens (garnet)

Si	5.67	Si	5.97
Al	2.33	Al	4.00
	8.00	Ti	0.01
Al	2.27		4.01
Fe	4.08	Fe	4.20
Mg	5.47	Mg	1.26
Mn	0.20	Ca	0.31
	12.02	Mn	0.23
			6.00

TABLE 3.

Comparison of retrograded and similar, unaltered rocks.

No	52	10	66a	923
SiO_2	72.8	72.5	63.0	68.5
Al_2O_3	14.0	15.2	20.3	16.0
Fe_2O_3	3.1	1.5	3.4	3.4
MgO	1.0	0.3	0.9	0.8
CaO	1.0	1.3	1.0	1.8
Na_2O	5.2	3.5	5.3	3.7
K_2O	2.3	5.5	5.7	4.9
TiO_2	0.5	0.2	0.4	0.1

Total iron as Fe_2O_3

Specimen 52 Retrograded granitic gneiss with piemontite and chlorite.

Specimen 10 Normal granitic gneiss.

Specimen 66a Retrograded adamellitic gneiss with muscovite.

Specimen 923 Normal adamellitic gneiss.

TABLE 4.

Chemical analyses of mineralised rocks.

No.	40d	41c	2000c
S	0.77%	4.61%	0.55%
Ni	17ppm	31ppm	2440ppm
Cu	2820 "	3.59%	40 "
Zn	61 "	125ppm	260 "
As	n.d.	3 "	n.d.
Se	n.d.	6 "	1ppm
Rb	225ppm	155ppm	11ppm
Sr	275ppm	185ppm	255ppm
Zr	37ppm	215ppm	105ppm
Mo	135 "	28 "	5 "
Ag	5 "	33 "	n.d.
Ba	820 "	450 "	95ppm
Ce	30 "	25 "	77 "
Pb	45 "	35 "	16 "
Bi	n.d.	7 "	n.d.
Th	6ppm	9 "	2ppm

n.d. = not detected.

Specimens 40d and 41c are from the Knaben mineralised zone

Specimen 2000c is from the contact of the Ljosland intrusion

Table 5.

Whole-rock chemical composition.

Granitic rocks of the Kvinesdal gneiss.

No.	2011	90	214	10	11	31	26	1642
SiO_2	73.7	73.2	72.6	72.6	72.5	72.3	69.9	68.5
Al_2O_3	14.0	14.5	15.2	15.2	15.4	15.5	16.0	16.3
FeO	1.7	1.9	1.3	1.4	1.4	1.7	2.3	3.0
MgO	0.2	0.5	0.2	0.3	0.4	0.4	0.7	0.7
CaO	1.3	1.7	1.4	1.3	1.4	1.1	1.7	2.2
Na_2O	3.5	3.0	3.6	3.5	3.5	3.7	3.9	3.4
K_2O	5.1	4.8	5.1	5.3	5.3	5.1	5.2	5.2
TiO_2	0.3	0.2	0.2	0.2	0.2	0.4	0.4	0.5
MnO	0.019	-	-	-	-	-	-	0.039
BaO	0.090	-	-	-	-	-	-	0.129
	1							2

Normative minerals.

An	6.4	8.4	7.0	6.4	7.0	5.6	8.4	10.9
Ab	29.6	25.4	30.4	29.6	29.6	31.2	33.0	28.8
Or	29.5	26.7	29.2	29.8	29.8	28.0	28.0	28.1
Qtz	31.0	33.4	28.5	29.9	29.0	28.8	23.6	24.0

1= Composite sample over mineralised zone.

2= From transitional zone with Lande gneiss.

Table 6.

Whole-rock chemical composition.

Granular leucogranites.

No.	76	626a	884	393a	68	38
SiO_2	77.1	75.8	75.6	75.0	74.4	72.6
Al_2O_3	13.7	13.1	13.9	14.1	14.9	15.1
FeO	0.2	1.9	0.8	0.9	0.4	1.4
MgO	0.0	0.1	0.1	0.2	0.1	0.5
CaO	0.4	0.5	0.9	0.9	1.1	1.3
Na_2O	3.0	3.1	3.4	3.6	3.4	3.4
K_2O	5.4	5.3	5.2	5.2	5.6	5.5
TiO_2	0.0	0.2	0.0	0.1	0.0	0.3
MnO	-	0.035	0.014	-	-	-
BaO	-	0.064	0.007	-	-	-

Normative Minerals.

An	1.9	2.5	4.5	4.5	5.6	6.4
Ab	25.4	26.2	28.8	30.4	28.8	28.8
Or	32.0	30.7	30.0	29.7	32.5	30.1
Qtz	37.9	36.2	34.1	32.4	30.8	29.8

Table 7.

Whole-rock chemical composition.

Granitic rocks of the Øie gneiss.

No.	39c	64	885	35	233	923	262	65
SiO_2	74.2	72.3	70.9	70.7	70.7	68.8	67.3	66.2
Al_2O_3	14.4	15.1	14.8	15.8	15.4	16.0	16.2	17.0
FeO	1.3	1.8	2.2	2.2	2.3	3.1	4.2	3.4
MgO	0.3	0.4	0.7	0.7	0.6	0.8	0.9	1.1
CaO	1.0	1.3	2.0	1.4	1.9	1.8	1.9	2.7
Na_2O	3.3	3.7	3.7	3.7	3.2	3.7	3.3	4.1
K_2O	5.2	5.2	4.8	5.1	5.3	5.2	5.5	4.6
TiO_2	0.2	0.2	0.5	0.4	0.4	0.5	0.8	0.6
MnO	-	-	0.042	-	0.032	0.050	0.051	0.062
BaO	-	-	0.121	-	0.120	0.110	0.156	0.097

Normative minerals.

An	5.0	6.4	10.0	7.0	9.4	8.9	9.5	13.3
Ab	27.9	31.2	31.2	31.2	27.0	31.2	27.9	34.6
Or	29.5	29.2	25.3	26.2	28.8	27.8	28.9	23.1
Qtz	32.9	27.6	27.0	27.7	27.8	23.6	22.9	18.6

Table 8.

Whole-rock chemical composition.

Massive and layered Tonstad granitic gneisses.

No	769a	768p	767a	828	125a	785	768d
SiO_2	76.1	74.6	72.9	72.5	70.8	70.8	69.4
Al_2O_3	14.0	14.7	14.6	14.8	16.0	15.6	15.9
FeO	0.3	0.3	1.4	1.5	1.7	2.2	3.1
MgO	0.1	0.1	0.4	0.2	0.3	0.6	0.5
CaO	1.3	1.6	2.0	1.6	1.6	2.0	2.1
Na_2O	2.9	3.7	3.4	3.7	3.5	3.3	3.3
K_2O	5.1	4.6	4.6	5.2	5.3	5.1	4.9
TiO_2	0.0	0.0	0.2	0.2	0.3	0.3	0.5
MnO	0.022	0.018	-	0.037	0.019	0.007	0.003
BaO	0.080	0.073	-	0.090	0.074	0.137	0.080
	1	1	1	2	2	2	1

Normative minerals.

An	6.7	8.1	10.0	7.8	7.8	10.0	10.4
Ab	24.6	31.2	28.8	31.2	29.6	27.9	27.5
Or	29.5	25.8	26.2	29.8	29.8	27.9	27.2
Qtz	37.0	32.1	30.6	27.8	26.9	27.8	26.9

1 = Layered granitic gneiss.

2 = Massive granitic gneiss.

Table 9.

Whole-rock chemical composition.

Assorted granitic rocks.

No	1005	3	177b	170a	115
SiO_2	74.3	74.2	73.1	70.2	66.4
Al_2O_3	14.7	14.4	14.9	17.3	16.7
FeO	1.0	1.3	1.4	1.5	4.7
MgO	0.2	0.2	0.4	0.2	1.4
CaO	1.0	0.8	1.4	1.5	1.8
Na_2O	3.8	2.8	3.6	3.5	3.3
K_2O	4.9	6.1	4.7	5.4	4.8
TiO_2	0.1	0.2	0.2	0.3	0.6
MnO	-	-	0.024	0.020	0.049
BaO	-	-	0.058	0.097	0.048
	1	2	3	3	4

Normative minerals.

An	5.0	3.9	7.0	7.5	8.9
Ab	32.2	23.6	30.4	29.6	27.9
Or	27.8	34.2	26.7	30.9	23.1
Qtz	31.2	33.3	31.0	25.9	24.8

1 = Weakly foliated granite

2 = Microgranite dyke

3 = Granitic layers within Lande gneiss

4 = Granitic layer within Lervig gneiss

Table 10.

Whole-rock chemical composition.

Porphyritic gneissic granites.

No.	188	183	191c	189a	187	1163
SiO_2	72.8	72.1	69.7	69.3	69.0	64.4
Al_2O_3	15.4	15.8	16.5	16.1	16.8	17.0
FeO	1.0	1.5	2.2	2.5	2.3	3.9
MgO	0.1	0.3	0.6	0.7	0.5	1.9
CaO	1.6	1.5	2.3	2.2	1.7	3.6
Na_2O	3.6	3.6	3.6	3.8	3.7	3.9
K_2O	4.8	4.7	4.6	4.7	5.3	4.5
TiO_2	0.1	0.2	0.4	0.4	0.4	0.8
MnO	0.009	0.019	0.023	0.025	0.027	0.069
BaO	0.158	0.084	0.172	0.136	0.102	-
						*

Normative Minerals

An	7.8	7.5	11.4	10.9	8.3	13.9
Ab	30.4	30.4	30.4	32.1	31.2	32.0
Or	27.8	26.4	24.8	25.0	29.5	20.7
Qtz	30.0	30.0	25.8	24.5	23.6	16.1

* = Hornblende-bearing rock.

Table 11.

Whole-rock chemical composition.

Feda augen gneiss.

No.	1246	123a
SiO_2	65.3	63.3
Al_2O_3	15.9	16.2
FeO	4.2	5.0
MgO	1.4	2.9
CaO	4.0	4.4
Na_2O	3.5	3.7
K_2O	4.7	3.0
TiO_2	1.0	0.9
MnO	-	0.077
BaO	-	0.120
P_2O_5	-	0.31

Table 12.

Whole-rock chemical composition.

Intermediate gneisses of the Lervig and Lande gneisses.

No.	336	820	106	69	551c	688	235a	551b
SiO_2	64.6	61.0	58.2	58.2	57.0	55.6	55.4	54.3
Al_2O_3	15.1	20.6	17.4	16.0	15.0	15.4	14.2	15.5
FeO	5.1	3.9	7.8	7.1	8.7	8.4	11.5	10.5
MgO	2.6	0.8	2.3	4.1	5.8	4.8	4.9	4.4
CaO	3.9	2.6	5.0	5.6	6.2	5.9	6.7	6.1
Na_2O	3.3	4.9	3.9	3.6	3.2	3.1	4.0	2.5
K_2O	3.9	5.4	4.0	3.5	2.3	4.5	1.1	4.4
TiO_2	1.1	0.5	1.5	1.8	1.4	2.0	1.6	2.1
MnO	0.075	0.128	-	0.119	0.220	-	-	-
BaO	0.203	0.094	-	0.250	0.057	-	-	-
P_2O_5	-	-	-	-	0.43	-	-	-

All rocks except specimen 235a contain modal alkali feldspar.

Table 13.

Whole-rock chemical composition.

Intermediate gneisses within the Kvinesdal gneiss.

No.	178a	1050	14	24m
SiO_2	67.4	61.8	59.8	56.3
Al_2O_3	16.0	16.4	17.0	15.1
FeO*	3.6	8.1	6.3	1o.7
MgO	1.4	1.7	2.9	4.3
CaO	2.8	3.7	5.0	6.4
Na_2O	3.9	4.2	4.0	3.0
K_2O	4.1	2.8	3.5	1.4
TiO_2	0.7	1.3	1.4	2.2
MnO	0.060	-	0.082	0.138
BaO	0.107	-	0.235	0.097
P_2O_5	-	-	-	0.75

Specimen 24m contains accesory alkali feldspar

Table 14.

Whole-rock chemical composition.

Intermediate gneisses within and adjacent to the Fjotland Granite.

No.	228a	220	280a	271
SiO_2	64.8	56.9	54.5	54.2
Al_2O_3	18.4	12.9	16.4	16.3
FeO	3.3	8.4	9.0	9.9
MgO	1.8	7.7	6.0	5.5
CaO	3.2	4.5	6.1	6.7
Na_2O	3.5	1.7	3.3	3.8
K_2O	4.0	6.0	2.6	1.6
TiO_2	0.6	1.4	1.8	1.9
MnO	0.043	0.194	0.158	0.153
BaO	0.143	0.396	0.066	0.076

Specimens 280a and 271 contain clinopyroxene in addition to biotite and hornblende.

Table 15.

Whole-rock chemical composition.

Intermediate gneisses within the Sirdalsvatn Series.

No.	787	159	1039a	133	830	1040	1247
SiO_2	62.5	60.6	58.6	57.5	56.3	54.1	53.3
Al_2O_3	16.4	15.7	16.2	18.1	16.2	15.8	15.8
FeO	5.2	6.1	6.4	6.2	6.9	9.0	7.1
MgO	2.7	4.3	4.5	2.8	4.7	7.4	6.7
CaO	3.8	5.4	6.1	4.4	5.4	7.1	6.0
Na_2O	3.4	3.9	2.9	3.5	3.7	3.4	2.3
K_2O	5.0	2.4	3.8	5.4	5.1	1.9	5.7
TiO_2	1.0	1.2	1.5	1.4	1.8	1.4	1.8
MnO	0.017	0.115	-	0.084	-	-	0.078
BaO	0.191	0.061	-	0.377	-	-	0.610
P_2O_5	-	-	-	0.66	-	-	1.17

Specimen 1247 contains clinopyroxene in addition to biotite and a little hornblende.

Table 16.

Whole-rock chemical composition.

Biotite-clinopyroxene gneisses.

No.	113a	835	1039	330	230	329	832b	832a
SiO_2	56.5	55.3	54.5	54.5	53.9	53.0	51.2	50.0
Al_2O_3	15.0	13.7	16.4	15.0	14.8	15.7	15.7	16.0
FeO*	10.7	8.2	10.3	8.7	10.5	9.0	7.8	8.2
MgO	3.4	7.2	2.7	5.6	4.6	6.8	7.6	7.6
CaO	5.7	6.6	7.2	5.8	7.5	6.2	7.1	8.4
Na_2O	3.3	2.5	3.9	2.9	2.9	3.4	1.6	1.5
K_2O	2.1	3.5	2.3	4.3	2.8	3.5	6.4	5.9
TiO_2	2.5	1.3	2.0	2.2	2.8	2.1	2.2	2.3
MnO	0.138	0.110	0.125	0.103	0.144	0.122	0.115	0.023
BaO	0.115	0.200	-	0.158	0.226	0.139	0.562	0.599
P_2O_5	0.87	1.12	0.82	-	-	-	-	-
				*	*	*		

* = specimens from adjacent to Fjotland granite.

Specimens 113a, 1039 and 230 contain little alkali feldspar.

Specimens 832b and 832a contain little or no quartz.

Table 17.

Whole-rock chemical composition.

Amphibolites of the Lervig gneiss.

No.	715	5250	1101	582b	579a	139a
SiO_2	51.2	48.5	47.9	47.7	47.4	45.4
Al_2O_3	13.6	16.5	15.8	15.3	16.1	14.4
FeO*	13.7	11.0	13.3	11.9	11.9	16.3
MgO	6.3	8.4	7.3	8.9	7.8	7.6
CaO	9.0	10.0	9.6	12.5	10.6	8.9
Na_2O	3.2	3.0	3.2	1.4	2.2	2.5
K_2O	1.0	1.5	1.1	0.7	2.4	1.4
TiO_2	1.7	1.1	1.9	1.1	1.5	3.2
MnO	0.234	-	-	0.220	0.210	0.235
BaO	0.025	-	-	0.029	0.030	0.021
P_2O_5	-	-	-	0.18	-	0.48

Specimens 715 and 582b contain clinopyroxene in addition to hornblende.

Specimens 5250 and 579a contain clinopyroxene together with biotite and hornblende.

Table 18.

Whole-rock chemical composition.

Amphibolites of the Lande gneiss.

No.	235c	862	243	56	1082	861b	207d	497b
SiO_2	51.5	50.3	50.0	49.0	48.9	48.7	48.4	47.5
Al_2O_3	13.9	15.1	15.2	15.0	15.9	15.7	13.7	17.4
FeO*	10.6	13.4	13.9	12.7	13.1	11.0	14.2	10.8
MgO	9.2	6.1	5.9	7.7	6.2	8.8	7.1	8.3
CaO	9.4	7.8	7.5	10.0	9.8	10.1	10.0	10.8
Na_2O	3.3	2.9	3.5	3.1	3.3	3.0	3.1	2.6
K_2O	1.1	2.1	1.7	1.1	1.0	1.4	1.1	1.6
TiO_2	1.6	2.2	2.3	1.5	1.7	1.0	1.7	0.9
MnO	0.223	-	0.252	0.237	-	0.130	0.324	0.218
BaO	0.024	-	0.032	0.013	-	0.013	0.007	0.033
P_2O_5	0.04	-	-	0.11	-	0.11	0.29	0.06

Specimens 207d and 497b contain clinopyroxene in addition to biotite and hornblende.

Table 19.

Whole-rock chemical composition.

Amphibolites of the Knaben gneiss.

No.	386	370b	430	30	20
SiO_2	47.4	46.8	46.3	45.2	44.4
Al_2O_3	16.7	17.8	16.2	16.0	15.0
FeO*	12.9	12.0	14.4	14.6	16.6
MgO	8.2	8.5	5.6	8.3	7.3
CaO	8.5	9.3	9.9	9.7	8.4
Na_2O	3.1	1.8	3.0	2.6	2.4
K_2O	1.3	2.1	1.8	1.1	2.9
TiO_2	1.8	1.5	2.1	2.4	2.9
MnO	0.211	0.273	0.284	0.235	0.277
BaO	0.020	0.016	0.013	0.022	0.032
P_2O_5	-	-	0.48	0.57	0.55

Table 20.

Whole-rock chemical composition.

Basic gneisses of the Oddevassheii gneiss.

No.	409	359d	359c
SiO_2	48.6	46.0	44.7
Al_2O_3	17.0	17.3	17.9
FeO*	13.4	13.9	13.8
MgO	5.8	6.5	7.6
CaO	9.8	9.2	8.7
Na_2O	3.0	2.2	1.8
K_2O	0.4	2.0	3.1
TiO_2	2.2	2.5	2.6
MnO	-	0.223	0.199
BaO	-	0.034	0.036
P_2O_5	-	0.41	-

Table 21.

Whole-rock chemical composition.

Pyribolites.

No.	1079	798	88b	149b	50	809b	743
SiO_2	56.5	53.1	52.5	50.2	49.8	48.8	46.1
Al_2O_3	14.5	16.1	17.3	16.9	15.7	16.0	16.3
FeO*	11.3	10.5	11.2	10.9	14.2	13.2	15.0
MgO	2.9	4.7	3.9	6.3	3.5	6.7	7.0
CaO	6.8	7.0	7.2	10.1	8.1	7.8	9.2
Na_2O	3.2	3.4	4.2	3.3	3.5	3.0	1.7
K_2O	2.1	1.7	1.2	1.0	1.6	1.8	2.0
TiO_2	2.6	2.5	1.9	1.0	2.5	2.2	2.5
MnO	-	0.090	0.198	0.365	0.219	0.177	0.241
BaO	-	0.120	0.044	0.018	0.093	0.044	0.034
P_2O_5	-	1.00	0.53	0.18	1.05	0.48	0.25

Specimen 1079 was collected 10 kilometres to the west of area surveyed and contains alkali feldspar as a significant phase.

Specimens 798, 809b and 743 are from the Lervig gneiss and the remainder from the Lande gneiss.

Table 22.

Whole-rock chemical composition.

Garnet-bearing gneisses.

No.	1067	1063	818d	615b	818e	511b
SiO_2	77.6	66.8	60.6	60.2	59.8	47.4
Al_2O_3	13.1	14.4	17.0	18.8	17.0	21.8
FeO*	0.6	3.2	7.7	9.6	8.8	15.0
MgO	0.1	6.8	3.6	0.7	4.2	4.5
CaO	1.0	1.6	4.1	3.8	4.0	2.6
Na_2O	3.1	2.9	3.1	4.4	2.4	3.3
K_2O	4.5	3.9	2.6	0.9	2.6	3.9
TiO_2	0.0	0.5	1.1	1.6	1.2	1.6
MnO	-	-	0.111	-	0.171	-
BaO	-	-	0.044	-	0.049	-
P_2O_5	-	-	0.14	-	-	-

Specimen 1067 is without biotite or iron oxide

Specimen 511b is without quartz and contains spinel

Table 23.

Oxidation ratios of intermediate and basic gneisses.

No.	Origin	$^{0}/_{R}$	No.	Origin	$^{0}/_{R}$
20	Kn.	38.0	123a	S.	46.7
24m	Kv.	72.3	133	S.	65.8
30	Kn.	37.5	230	Fj.	63.0
50*	La.	40.1	280a	Fj.	49.5
56	La.	38.7	329	Fj.	49.7
88b*	La.	28.7	330	Fj.	56.9
139	Le.	39.4	832a	S.	66.1
149b*	La.	28.5	835	S.	65.8
207d	La.	30.2	1247	S.	63.8
430	Kn.	40.9			
497b	La.	39.3			
551c	Le.	58.9	Kn. = Knaben gneiss		
582b	Le.	41.4	Kv. = Kvinesdal gneiss		
743*	Le.	49.2	La. = Lande gneiss		
798*	Le.	40.1	Le. = Lervig gneiss		
809b*	Le.	41.8	S. = Sirdalsvatn Series		
815	Le.	26.4	Fj. = Fjotland granite		
861b	La.	48.5	* = pyribolite		

Table 24.

Whole-rock trace element analyses.

Sirdalsvatn Series.

No.	113a	123a	133	835	1039	1247
S	1060	310	2000	2080	1280	1420
Cl	85	30	105	160	115	265
Ci	30	60	46	215	96	195
Cu	24	20	76	58	17	10
Zn	200	105	165	182	200	170
Ga	18	19	20	17	17	17
Rb	77	155	165	220	220	175
Sr	695	1320	2360	1540	1400	3250
Y	54	44	66	53	34	60
Zr	400	345	1430	475	590	860
Ce	105	79	285	165	150	195
Pb	28	48	72	33	40	52
Th	5	11	17	4	6	3

Table 25.

Whole-rock trace element analyses.

Lervig gneiss.

No.	139b	551c	582b	743	798	809b	815
S	1260	240	100	940	1940	640	80
Cl	80	315	40	150	115	120	90
Ni	145	110	76	175	105	155	92
Cu	62	n.d.	7	76	31	14	n.d.
Zn	280	285	125	210	225	235	185
Ga	18	17	11	17	18	17	18
Rb	100	150	10	110	68	205	160
Sr	290	290	410	210	1000	270	235
Y	41	49	15	65	54	47	52
Zr	215	290	74	195	485	230	240
Ce	39	98	23	52	105	62	73
Pb	18	21	21	14	23	18	30
Th	4	6	1	6	3	1	9
				*	*	*	

* = pyribolite

Table 26.

Whole-rock trace element analyses.

Lande gneiss.

No.	50	56	88b	149b	207d	235c	497b	861b
S	1600	270	390	150	850	450	140	240
Cl	50	60	25	35	300	40	160	160
Ni	42	120	83	270	105	85	190	260
Cu	35	8	12	20	9	11	6	24
Zn	230	155	175	385	265	225	150	245
Ga	21	14	17	13	18	11	14	14
Rb	64	36	62	83	21	115	48	94
Sr	390	265	395	485	190	225	300	270
Y	83	21	46	28	72	31	20	2
Zr	735	73	485	90	96	18	41	59
Ce	131	30	81	50	56	34	44	50
Pb	23	22	24	36	23	17	22	34
Th	1	6	3	2	1	1	n.d.	2
	*		*	*				

* = pyribolite

Table 27.

Whole-rock trace element analyses.

Kvinesdal, Knaben and Oddevassheii gneisses.

No.	20	24m	30	359d	430
S	180	160	940	110	1490
Cl	130	65	140	65	520
Ni	105	46	160	165	175
Cu	20	42	42	n.d.	115
Zn	365	230	215	215	315
Ga	19	20	18	20	18
Rb	410	64	165	420	200
Sr	220	805	335	235	335
Y	39	30	51	23	45
Zr	210	410	230	125	215
Ce	48	100	42	66	62
Pb	17	25	20	18	25
Th	n.d.	5	3	n.d.	2
	b	a	b	c	b

a = Kvinesdal gneiss

b = Knaben gneiss

c = Oddevassheii gneiss

Table 28.

Probe Analyses of Potassium Feldspar.

37 points within single large augen in specimen 123a.

%Or	%Ab	%An	%Cn	Sum	%Or	%Ab	%An	%Cn	Sum
80	18			101	75	22			100
76	21			100	80	18			101
73	23			99	79	18			100
80	18			101	82	16			101
87	12			102	74	22			99
79	15			97	84	13			100
80	19			102	79	18			100
77	18	Varies from 0.6% - 1.1%	Varies from 1.7% - 2.5%	98	79	18	Varies from 0.6% - 1.1%	Varies from 1.7% - 2.5%	100
75	20			98	80	18			101
76	22			101	80	17			100
83	15			101	84	15			102
83	15			101	77	21			101
83	15			101	71	27			100
80	18			101	77	20			100
75	23			101	78	20			101
79	21			103	83	15			101
82	17			102	77	21			101
82	17			102	82	17			102
80	18			101					

Analyses recalculated to give Wt. % of the feldspar end members orthoclase, albite, anorthite and celsian.

Table 29.

Probe Analyses of Potassium Feldspar (2)

Matric grains in specimen 123a.

%Or	%Ab	%An	%Cn	Sum	%Or	%Ab	%An	%Cn	Sum
83	12			98	86	9			98
85	10			98	87	10			100
87	10			100	85	13			101
82	12			97	86	13			102
81	14			98	88	11			102
88	7			98	85	13			101
88	8	Varies from 0.6% - 0.8%	Varies from 2.1% - 2.7%	99	80	16	Varies from 0.6% - 0.8%	Varies from 2.1% - 2.7%	99
92	5			100	88	11			102
88	10			101	88	10			100
91	5			99	88	11			102
86	10			99	86	11			100
91	5			99	88	8			99
84	13			100	89	9			101
87	10			100	88	8			99
92	6			101	80	15			98
90	7			100	88	10			101
87	12			101	88	10			101
89	8			100					

Table 30.

Probe Analyses of Potassium feldspars (3).

Variation in composition of the alkali feldspar phase in 9 rocks. Each analysis represents 1 grain.

No.	%Or	%Ab	%An	%Cn
14	86	7	Varies from 0.5% - 0.7%	Not determined
	87	6		
	87	7		
	86	7		
	86	8		
	84	9		
	85	8		
	87	6		
	86	6		
	86	7		
	87	7		
24	86	9	Not determined	=
	83	10		
	85	8		
	83	10		
	82	12		
	82	11		
	83	11		
	82	12		
	84	11		
52	94	3	N.D.	=
	95	2		
	94	2		
	95	2		
	94	3		
220	84	9		
	78	15		
	78	14		
	77	16		
	82	11		
	81	13		
306c	79	16	Not determined	=
	85	9		
	82	12		
	86	8		
	84	9		
	86	10		
	73	21		
	77	17		
	81	13		
330	83	10	Not determined	=
	83	11		
	83	11		
	84	10		
	83	10		
	83	11		
	82	11		
551b	85	11	Not determined	=
	78	16		
	83	11		
	77	16		
	79	12		
	87	9		
	88	8		
	82	11		
	86	9		
	78	15		

Table 31.

Probe analyses of Potassium feldspars (3) continued.

No.	%Or	%Ab	%An	%Cn
	84	9		
	82	10		
	90	4	Not determined	Not determined
688	90	4		
	89	6		
	89	7		
	87	6		
	74	21		
	61	32		
	77	17		
832a	73	21	0.7% - 0.8%	3.9% - 4.9%
	61	30		
	69	24		
	72	22		

Table 31. (continued)

Major element probe analyses of plagioclase.

No.	14	20	30	88b	123a	139a	818e
SiO_2	62.7	60.8	56.9	61.5	62.5	59.5	58.0
Al_2O_3	24.0	25.3	27.7	24.4	24.0	26.1	26.8
Fe_2O_3	0.2	0.1	0.1	-	-	-	-
CaO	5.0	6.8	9.1	5.9	5.1	7.8	8.9
Na_2O	9.0	7.8	6.5	8.2	8.7	7.3	6.4
K_2O	-	0.3	0.1	-	-	-	-
Sum	100.9	101.1	100.4	100.0	100.3	100.7	100.1
An%	23.5	32.5	44.0	28.0	24.0	37.0	41.0

Numbers of ions on the basis of 32 oxygen atoms.

Si	11.02	10.71	10.17	10.92	11.05	10.59	10.38
Al	4.96	5.25	5.81	5.10	4.98	5.45	5.64
Fe	0.03	0.02	0.01	-	-	-	-
	16.01	15.98	15.99	16.02	16.03	16.04	16.02
Ca	0.94	1.29	1.74	1.13	0.97	1.48	1.71
Na	3.06	2.66	2.25	2.83	2.98	2.52	2.24
K		0.06	0.02	-	-	-	-
	4.00	4.01	4.01	3.96	3.95	4.00	3.95

Table 32.

Partial Probe Analyses of Plagioclase

No.	CaO wt.%	An%	Rock Type
8	4.7	22.0	Retrograded granitic gneiss
24	4.5	21.0	Amphibolite K-feldspar
50	5.8	27.5	Pyribolite
56	6.5	31.0	Amphibolite
69	4.8	22.5	Amphibolite + K-feldspar
81	6.5	31.0	Amphibolite + clinopyroxene
96b	7.2	34.0	Amphibolite + orthopyroxene
108a	6.9	32.5	Pyribolite
133	5.0	23.5	Amphibolite + K-feldspar
138a	11.0	52.0	Amphibolite + orthopyroxene
144b	5.1	24.0	Amphibolite + K-feldspar
149b	8.4	40.0	Pyribolite
152	5.1	24.0	Amphibolite + K-feldspar
230	4.9	23.0	Biotite,clinopyr,K-fel gneiss
208a	4.8	22.5	Biot,horn,clinopyr,K-fel gneiss
329	5.1	24.0	Biotite,clinopyr,K-fel gneiss
370b	10.4	49.0	Amphibolite
430	8.8	41.5	Amphibolite
497	6.8	32.0	Amphibolite + clinopyroxene
551b	4.9	23.0	Amphibolite + K-feldspar
551c	4.5	21.0	Amphibolite + K-feldspar
582b	9.3	44.0	Amphibolite + clinopyroxene
688	4.6	21.5	Amphibolite + K-feldspar
743	8.8	41.5	Pyribolite
798	6.4	30.5	Pyribolite
809b	6.2	29.5	Pyribolite
818d	7.0	33.0	Biotite garnet gneiss.

Table 33.

Corrected Probe Analyses of biotites

No	14	20	24	30	50	56	65	69	88b
SiO_2	38.7	38.2	38.8	37.2	37.0	37.8	37.9	38.4	37.3
Al_2O_3	13.3	13.2	13.0	14.7	13.1	12.9	13.3	12.5	12.9
FeO	18.3	20.9	13.9	17.5	21.4	18.2	17.9	14.0	20.6
MgO	15.2	12.5	17.2	12.7	10.4	12.6	13.3	16.6	10.0
CaO	0.0	0.0	0.0	0.0	0.0	0.0	0.0	0.0	0.0
Na_2O	0.2	0.2	0.1	0.2	0.1	0.1	0.1	0.1	0.0
K_2O	9.1	8.8	9.2	8.6	8.9	9.0	9.0	8.9	9.2
TiO_2	2.4	3.1	3.1	4.3	5.2	4.9	3.2	2.5	5.2
MnO	0.5	0.2	0.3	0.5	-	-	0.6	-	-
	97.7	97.1	95.6	95.7	96.1	95.4	95.3	93.0	95.2

Numbers of ions on basis of 22 oxygens.

Si	5.74	5.75	5.75	5.59	5.65	5.71	5.75	5.83	5.72
Al	2.26	2.25	2.25	2.41	2.35	2.29	2.25	2.17	2.28
	8.00	8.00	8.00	8.00	8.00	8.00	8.00	8.00	8.00
Al	0.05	0.07	0.01	0.19			0.12	0.06	0.04
Fe	2.26	2.62	1.72	2.19	2.72	2.29	2.29	1.77	2.64
Mg	3.35	2.79	3.80	2.84	2.38	2.84	3.00	3.76	2.30
Ti	0.27	0.35	0.35	0.49	0.60	0.56	0.36	0.28	0.60
Mn	0.06	0.03	0.04	0.06	-	-	0.08	-	-
	5.99	5.86	5.92	5.77	5.70	5.69	5.85	5.87	5.58
K	1.73	1.69	1.74	1.66	1.74	1.74	1.75	1.73	1.75
Na	0.05	0.05	0.03	0.05	0.03	0.03	0.03	0.03	
Ca									
	1.78	1.74	1.77	1.71	1.77	1.77	1.78	1.76	1.75

Table 34.

Corrected Probe Analyses of biotites (2)

No	114q	123a	133	139a	145	149b	220	230	235c
SiO_2	37.8	38.6	38.4	37.2	36.9	37.2	37.1	38.8	37.7
Al_2O_3	13.2	12.6	12.5	13.1	13.8	12.6	12.8	13.3	12.6
FeO	14.3	15.5	15.6	18.6	21.1	17.4	15.6	14.8	15.0
MgO	14.8	14.8	15.6	12.6	9.7	13.8	16.2	15.5	15.5
CaO	0.0	0.0	0.0	0.0	0.0	0.0	0.0	0.0	0.0
Na_2O	0.2	0.1	0.1	0.1	0.1	0.0	0.1	0.0	0.0
K_2O	9.0	9.2	9.3	9.3	9.1	9.3	9.5	9.1	9.4
TiO_2	4.0	4.8	4.2	4.3	2.6	4.2	3.3	4.1	2.6
MnO	-	-	-	-	-	0.3	-	-	-
	93.3	95.6	95.7	95.2	93.3	94.8	94.6	95.6	92.8

Numbers of ions on basis of 22 oxygens.

Si	5.74	5.76	5.73	5.68	5.79	5.66	5.64	5.76	5.80
Al	2.26	2.22	2.20	2.32	2.21	2.26	2.28	2.24	2.20
	8.00	7.98	7.93	8.00	8.00	7.92	7.92	8.00	8.00
Al	0.09			0.02	0.33			0.05	0.08
Fe	1.82	1.93	1.95	2.36	2.86	2.21	1.97	1.83	1.92
Mg	3.37	3.28	3.47	2.86	2.27	3.13	3.66	3.42	3.55
Ti	0.45	0.54	0.47	0.49	0.31	0.48	0.37	0.45	0.30
Mn	-	-	-	-	-	0.04	-	-	-
	5.73	5.75	5.89	5.73	5.77	5.86	6.00	5.75	5.85
K	1.75	1.75	1.77	1.81	1.82	1.81	1.84	1.72	1.84
Na	0.05	0.03	0.03	0.03	0.03		0.03		
Ca									
	1.80	1.78	1.80	1.84	1.85	1.81	1.87	1.72	1.84

Table 34 (continued)

Corrected Probe Analyses of biotites. (3)

No	243a	271	280a	306c	329	330	359d	370b	386
SiO_2	38.4	38.7	38.0	37.2	38.0	38.3	38.1	37.9	38.4
Al_2O_3	12.8	13.1	13.1	12.7	12.9	13.1	12.7	12.9	12.4
FeO	18.2	14.5	17.4	26.8	16.4	15.4	18.5	16.6	15.2
MgO	12.7	14.8	13.2	7.7	14.2	14.4	13.3	15.1	15.6
CaO	0.1	0.0	0.0	0.0	0.0	0.0	0.1	0.0	0.0
Na_2O	0.0	0.1	0.0	0.0	0.0	0.1	0.0	0.2	0.2
K_2O	9.3	9.5	9.3	8.9	9.3	9.3	9.1	9.1	9.2
TiO_2	5.0	4.8	4.8	2.6	5.3	4.1	5.3	3.4	3.9
MnO	-	-	-	-	-	-	-	-	-
	96.5	95.5	95.8	95.9	96.1	94.7	97.1	95.2	94.9

Numbers of ions on basis of 22 oxygens.

Si	5.75	5.75	5.70	5.84	5.66	5.77	5.67	5.70	5.76
Al	2.25	2.25	2.30	2.16	2.28	2.23	2.22	2.28	2.20
	8.00	8.00	8.00	8.00	7.94	8.00	7.89	7.98	7.96
Al	0.01	0.03	0.01	0.18		0.09			
Fe	2.27	1.79	2.18	3.50	2.04	1.93	2.29	2.09	1.90
Mg	2.83	3.27	2.94	1.80	3.15	3.22	2.94	3.39	3.49
Ti	0.56	0.54	0.54	0.31	0.59	0.46	0.59	0.38	0.43
Mn	-	-	-	-	-	-	-	-	-
	5.67	5.63	5.67	5.79	5.78	5.70	5.82	5.86	5.82
K	1.77	1.80	1.78	1.79	1.77	1.79	1.73	1.75	1.76
Na		0.03				0.03		0.05	0.05
Ca	0.02	—	—	—	—	—	0.02	—	—
	1.79	1.83	1.78	1.79	1.77	1.82	1.75	1.80	1.81

Table 34 (continued)

Corrected Probe Analyses of biotites. (4)

No	430	497c	551b	551c	743	798	809b	818e	818d
SiO_2	38.5	38.7	38.0	38.2	37.5	37.7	38.6	36.7	36.6
Al_2O_3	12.4	12.9	13.4	13.6	13.1	13.5	13.3	15.6	15.1
FeO	17.3	17.6	14.7	15.3	19.7	20.7	19.5	18.9	18.6
MgO	15.3	12.7	16.0	15.7	9.5	11.7	11.2	10.8	10.9
CaO	0.0	0.0	0.0	0.0	0.0	0.0	0.0	0.0	0.0
Na_2O	0.1	0.0	0.1	0.0	0.1	0.1	0.1	0.1	0.1
K_2O	9.2	9.2	9.1	9.0	9.1	9.3	9.3	9.5	9.5
TiO_2	2.4	4.5	3.9	3.8	5.4	5.3	5.3	4.4	3.9
MnO	-	-	-	-	-	-	-	-	-
	95.2	95.6	95.2	95.6	94.4	98.3	97.3	96.0	94.7

Numbers of ions on basis of 22 oxygens.

Si	5.82	5.82	5.67	5.68	5.78	5.61	5.75	5.56	5.59
Al	2.18	2.18	2.33	2.32	2.22	2.37	2.25	2.44	2.41
	8.00	8.00	8.00	8.00	8.00	7.98	8.00	8.00	8.00
Al	0.03	0.10	0.01	0.06	0.16		0.06	0.33	0.31
Fe	2.17	2.21	1.83	1.90	2.54	2.57	2.43	2.38	2.38
Mg	3.44	3.84	3.55	3.47	2.17	2.60	2.49	2.43	2.49
Ti	0.27	0.51	0.44	0.42	0.63	0.59	0.59	0.50	0.45
Mn	-	-	-	-	-	-	-	-	-
	5.91	5.66	5.83	5.85	5.50	5.76	5.57	5.64	5.63
K	1.77	1.77	1.74	1.73	1.80	1.75	1.76	1.83	1.85
Na	0.03		0.03		0.03	0.03	0.03	0.03	0.03
Ca									
	1.80	1.77	1.77	1.73	1.83	1.78	1.79	1.86	1.88

Table 34 (continued)

Corrected Probe Analyses of biotites. (5)

No.	832a	861b	2000
SiO_2	38.1	39.8	38.2
Al_2O_3	12.8	13.0	13.6
FeO	14.1	12.4	12.5
MgO	15.6	17.6	17.2
CaO	0.0	0.0	0.1
Na_2O	0.1	0.1	0.0
K_2O	9.3	9.2	9.2
TiO_2	3.6	1.2	5.4
MnO	-	-	-
	93.6	93.3	96.2

Numbers of ions on basis of 22 oxygens.

Si	5.76	5.95	5.62
Al	2.24	2.05	2.34
	8.00	8.00	7.96
Al	0.04	0.24	
Fe	1.78	1.54	1.53
Mg	3.51	3.92	3.76
Ti	0.41	0.13	0.60
Mn	-	-	-
	5.74	5.83	5.89
K	1.80	1.76	1.73
Na	0.03	0.03	
Ca			0.02
	1.83	1.79	1.75

Table 34 (continued)

Corrected Probe Analyses of hornblendes

No	14	20	24	30	50	56	69	88b	114q
SiO_2	41.8	41.2	44.0	42.4	42.2	44.1	44.0	43.8	46.4
Al_2O_3	9.5	11.0	9.7	12.0	9.9	9.5	9.2	9.6	8.8
FeO	20.0	21.0	15.3	17.4	21.5	17.4	15.7	18.8	13.5
MgO	10.6	8.0	11.6	10.0	7.9	11.1	12.2	9.2	15.1
CaO	11.4	11.6	11.3	10.7	11.0	10.5	11.2	11.5	11.6
Na_2O	1.6	1.6	1.4	1.8	1.4	1.3	1.4	1.2	0.6
K_2O	1.4	1.3	1.2	1.6	1.4	1.0	1.3	1.4	0.7
TiO_2	0.9	1.1	1.6	1.9	2.1	2.0	1.2	2.0	1.4
MnO	0.8	0.5	0.6	-	-	-	-	-	-
	98.0	97.3	96.7	96.8	97.4	96.9	96.2	97.5	98.1

Numbers of ions on basis of 23 oxygens.

Si	6.42	6.37	6.65	6.41	6.50	6.66	6.68	6.65	6.76
Al	1.58	1.63	1.35	1.59	1.50	1.34	1.32	1.35	1.24
	8.00	8.00	8.00	8.00	8.00	8.00	8.00	8.00	8.00
Al	0.15	0.39	0.37	0.55	0.29	0.35	0.32	0.36	0.27
Fe	2.56	2.71	1.92	2.20	2.76	2.19	1.98	2.38	1.64
Mg	2.42	1.86	2.61	2.25	1.79	2.50	2.75	2.08	3.27
Ti	0.10	0.13	0.18	0.22	0.24	0.23	0.14	0.23	0.15
Mn	0.10	0.06	0.07	-	-	-	-	-	-
	5.33	5.15	5.15	5.22	5.08	5.27	5.19	5.05	5.33
Ca	1.88	1.92	1.83	1.74	1.82	1.71	1.82	1.88	1.81
Na	0.48	0.49	0.42	0.52	0.42	0.38	0.42	0.36	0.18
K	0.28	0.27	0.23	0.10	0.28	0.20	0.26	0.27	0.13
	2.64	2.68	2.48	2.36	2.52	2.29	2.50	2.51	2.12

Table 35.

Corrected Probe Analyses of hornblendes (2)

No	123a	133	139a	149b	220	235c	243a	271	280a
SiO_2	44.5	44.1	43.7	43.9	45.2	44.0	44.2	46.1	44.9
Al_2O_3	8.6	8.7	9.6	9.5	8.3	8.5	9.4	8.8	9.3
FeO	14.9	14.7	17.8	16.5	14.5	15.6	17.5	14.1	16.1
MgO	12.9	13.0	10.8	11.6	12.4	13.7	10.6	12.8	12.0
CaO	11.6	11.5	10.8	11.0	11.3	11.2	10.9	11.4	11.2
Na_2O	1.4	1.6	1.3	1.3	1.7	1.4	1.4	1.2	1.2
K_2O	1.1	1.3	1.0	1.1	1.0	1.2	1.4	1.1	1.1
TiO_2	1.9	1.9	2.0	1.8	1.0	1.3	2.0	1.9	1.8
MnO	-	-	-	-	-	-	-	-	-
	96.9	96.8	97.0	96.7	95.4	96.9	97.4	97.4	97.6

Numbers of ions on basis of 23 oxygens.

Si	6.68	6.65	6.63	6.65	6.80	6.64	6.68	6.81	6.70
Al	1.32	1.35	1.37	1.35	1.20	1.36	1.32	1.19	1.30
	8.00	8.00	8.00	8.00	8.00	8.00	8.00	8.00	8.00
Al	0.20	0.20	0.32	0.34	0.27	0.15	0.35	0.34	0.33
Fe	1.87	1.84	2.25	2.08	1.82	1.96	2.20	1.74	2.00
Mg	2.88	2.91	2.44	2.61	2.78	3.08	2.38	2.81	2.66
Ti	0.22	0.22	0.23	0.20	0.11	0.15	0.23	0.21	0.20
Mn	-	-	-	-	-	-	-	-	-
	5.17	5.17	5.24	5.23	4.98	5.34	5.16	5.10	5.19
Ca	1.87	1.85	1.76	1.78	1.82	1.81	1.77	1.81	1.79
Na	0.39	0.47	0.38	0.38	0.49	0.41	0.41	0.35	0.35
K	0.21	0.25	0.22	0.11	0.19	0.24	0.27	0.20	0.21
	2.47	2.57	2.36	2.27	2.50	2.46	2.45	2.36	2.35

Table 35 (continued)

Corrected Probe Analyses of hornblendes (3)

No	306c	359d	370b	386	430	497c	551b	551c	582b
SiO_2	40.3	42.0	44.3	44.1	43.2	44.9	45.0	44.5	44.9
Al_2O_3	10.2	10.5	9.4	9.6	10.0	9.1	9.2	9.6	9.2
FeO	26.3	17.7	16.2	17.1	19.1	16.3	15.1	15.5	14.8
MgO	4.6	10.4	11.5	11.1	10.5	11.4	12.9	12.6	11.4
CaO	10.5	11.4	11.0	11.0	10.8	11.1	11.0	10.9	11.3
Na_2O	1.5	1.2	1.6	2.1	1.6	1.2	1.6	1.5	1.1
K_2O	1.7	1.6	1.5	1.0	1.3	1.4	1.2	1.1	1.4
TiO_2	1.2	2.0	1.8	1.3	1.3	1.7	1.7	1.9	2.2
MnO	-	-	-	-	-	-	-	-	-
	96.3	96.8	97.3	97.3	97.8	97.1	97.7	97.6	96.3

Numbers of ions on basis of 23 oxygens.

Si	6.47	6.42	6.66	6.65	6.55	6.75	6.70	6.63	6.75
Al	1.53	1.58	1.34	1.35	1.45	1.25	1.30	1.37	1.25
	8.00	8.00	8.00	8.00	8.00	8.00	8.00	8.00	8.00
Al	0.40	0.31	0.30	0.35	0.33	0.36	0.31	0.31	0.38
Fe	3.52	2.26	2.03	2.16	2.41	2.04	1.87	1.92	1.85
Mg	1.10	2.37	2.57	2.49	2.36	2.55	2.86	2.80	2.56
Ti	0.14	0.23	0.20	0.14	0.15	0.19	0.19	0.22	0.25
Mn	-	-	-	-	-	-	-	-	-
	5.16	5.17	5.10	5.14	5.25	5.14	5.23	5.25	5.04
Ca	1.81	1.87	1.78	1.78	1.76	1.78	1.76	1.76	1.82
Na	0.46	0.36	0.47	0.62	0.47	0.35	0.46	0.43	0.33
K	0.35	0.31	0.29	0.20	0.25	0.27	0.23	0.22	0.27
	2.62	2.64	2.54	2.60	2.48	2.40	2.45	2.41	2.42

Table 35 (continued)

Corrected Probe Analyses of hornblendes (4)

No	743	798	809b	861b
SiO_2	44.4	45.2	46.0	42.7
Al_2O_3	9.7	9.6	9.9	10.1
FeO	17.7	16.7	19.2	15.2
MgO	9.9	11.5	9.8	12.5
CaO	11.1	11.0	10.0	11.4
Na_2O	1.4	1.0	1.2	1.7
K_2O	1.5	1.3	1.4	1.6
TiO_2	2.0	1.8	2.0	1.1
MnO	-	-	-	0.4
	97.7	98.1	99.5	96.7

Numbers of ions on basis of 23 oxygens.

Si	6.68	6.72	6.80	6.48
Al	1.32	1.28	1.20	1.52
	8.00	8.00	8.00	8.00
Al	0.39	0.38	0.52	0.29
Fe	2.22	2.07	2.37	1.93
Mg	2.22	2.54	2.15	2.82
Ti	0.23	0.20	0.22	0.13
Mn	-	-	-	0.05
	5.06	5.19	5.26	5.22
Ca	1.80	1.76	1.59	1.87
Na	0.41	0.29	0.35	0.50
K	0.30	0.25	0.27	0.31
	2.51	2.30	2.21	2.68

Table 35. (continued)

Corrected Probe Analyses of clinopyroxenes.

No.	50	88b	149b	230	271	280a	329	330	359d
SiO_2	51.3	51.8	52.1	53.2	53.5	53.3	53.4	53.6	51.8
Al_2O_3	1.2	1.2	1.2	1.4	1.5	1.5	1.4	1.3	1.7
FeO	16.3	15.4	12.7	9.5	8.9	10.0	9.8	9.4	13.5
MgO	9.3	10.5	12.8	14.2	14.0	13.3	13.8	13.7	11.6
CaO	20.6	21.2	20.3	21.3	21.4	21.6	21.4	21.8	18.7
Na_2O	0.3	0.4	0.2	0.5	0.5	0.4	0.4	0.5	0.2
K_2O									
TiO_2	0.1	0.1	0.1	0.2	0.2	0.1	0.2	0.2	0.3
MnO	0.5	-	-	-	-	-	-	-	-
	99.6	100.6	99.4	100.3	100.0	100.2	100.4	100.5	97.8

Numbers of ions on basis of 6 oxygens.

Si	1.98	1.97	1.97	1.98	1.98	1.99	1.98	1.99	1.99
Al	0.02	0.03	0.03	0.02	0.02	0.01	0.02	0.01	0.01
	2.00	2.00	2.00	2.00	2.00	2.00	2.00	2.00	2.00
Al	0.04	0.02	0.02	0.04	0.05	0.06	0.04	0.05	0.07
Fe	0.52	0.49	0.40	0.29	0.28	0.31	0.30	0.29	0.44
Mg	0.54	0.60	0.72	0.78	0.77	0.74	0.76	0.76	0.67
Ca	0.85	0.86	0.83	0.85	0.85	0.87	0.85	0.86	0.77
Na	0.03	0.03	0.01	0.04	0.03	0.04	0.03	0.04	0.01
Ti				0.01	0.01		0.01	0.01	0.01
Mn	0.01	-	-	-	-	-	-	-	-
	1.99	2.00	1.98	2.01	2.00	2.01	1.99	2.01	1.97

Table 36.

Corrected Probe Analyses of clinopyroxenes. (2)

No	497c	582b	743	798	809b	832a
SiO_2	51.7	53.2	51.6	52.1	52.0	52.0
Al_2O_3	1.2	1.4	1.2	1.3	1.5	1.5
FeO	12.0	10.4	12.7	12.0	14.9	8.9
MgO	12.7	13.3	13.1	12.8	11.5	13.0
CaO	20.4	21.5	21.0	20.4	19.0	21.3
Na_2O	0.3	0.3	0.4	0.4	0.4	0.6
K_2O						
TiO_2	0.1	0.1	0.2	0.2	0.2	0.2
MnO	-	-	-	-	0.5	-
	98.4	100.2	100.2	99.2	100.0	97.5

Numbers of ions on basis of 6 oxygens.

Si	1.98	1.99	1.95	1.98	1.98	1.98
Al	0.02	0.01	0.05	0.02	0.02	0.02
	2.00	2.00	2.00	2.00	2.00	2.00
Al	0.04	0.05		0.04	0.05	0.05
Fe	0.38	0.32	0.40	0.38	0.47	0.28
Mg	0.72	0.74	0.74	0.72	0.65	0.74
Ca	0.84	0.86	0.85	0.83	0.78	0.87
Na	0.02	0.02	0.03	0.03	0.03	0.04
Ti			0.01	0.01	0.01	0.01
Mn	-	-	-	-	0.01	-
	2.00	1.99	2.03	2.01	2.00	1.99

Table 36 (continued)

Corrected Probe Analyses of orthopyroxenes.

No	50	88b	145	149b	359d	743	798	809b	2000
SiO_2	49.8	50.2	52.1	51.7	50.4	50.1	51.7	51.5	51.0
Al_2O_3	0.6	0.6	1.4	0.7	1.0	0.6	0.6	0.6	1.1
FeO	35.9	33.6	31.5	29.8	32.5	30.5	30.6	31.5	25.6
MgO	11.1	13.8	14.0	16.3	14.9	16.9	15.5	15.1	20.0
CaO	0.9	0.9	0.6	0.8	0.6	0.9	0.9	0.8	0.6
Na_2O							0.1	0.1	
K_2O									
TiO_2	0.1	0.1	0.1	0.1	0.2	0.1	0.1	0.2	0.2
MnO	1.3	-	-	-	-	-	-	1.5	-
	99.7	99.2	99.7	99.4	99.6	99.1	99.6	101.3	98.5

Numbers of ions on basis of 6 oxygens.

Si	2.00	1.99	2.02	2.00	1.98	1.97	2.01	1.98	1.96
Al		0.01			0.02	0.03		0.02	0.04
	2.00	2.00	2.02	2.00	2.00	2.00	2.01	2.00	2.00
Al	0.03	0.02	0.07	0.03	0.03		0.03	0.01	0.01
Fe	1.20	1.12	1.02	0.97	1.06	0.99	0.99	1.04	0.82
Mg	0.66	0.82	0.81	0.94	0.87	0.98	0.90	0.87	1.14
Ca	0.04	0.04	0.03	0.03	0.03	0.04	0.04	0.03	0.03
Na							0.01		
K									
Ti					0.01		0.01	0.01	0.01
Mn	0.04							0.05	
	1.97	2.00	1.93	1.97	2.00	2.01	1.98	2.01	2.01

Table 37.

Corrected Probe Analyses of sphenes

No	8	14	20	69	235c	306c	832a	861b
SiO_2	29.3	29.8	30.3	30.0	30.3	30.2	27.6	30.3
Al_2O_3	2.8	2.3	3.9	2.3	1.9	4.8	1.7	2.5
Fe_2O_3	2.6	2.5	2.9	2.0	1.8	2.5	1.7	1.4
MgO	0.1	0.0	0.0	0.0	0.0	0.0	0.0	0.0
CaO	27.3	27.5	28.3	26.2	28.8	27.3	26.3	28.3
Na_2O	0.0	0.0	0.0	0.0	0.0	0.0	0.1	0.0
K_2O	0.0	0.0	0.0	0.0	0.0	0.0	0.1	0.0
TiO_2	33.8	32.9	32.8	35.6	33.5	31.5	34.8	33.5
MnO	0.2	0.2	-	-	-	-	-	-
	96.1	95.2	98.2	96.1	96.3	96.3	92.3	96.0

Numbers of ions on basis of $19\frac{1}{2}$ oxygens.

Si	3.86	3.98	3.94	3.95	4.00	3.97	3.82	4.02
Al	0.14	0.02	0.06	0.05	___	0.03	0.18	___
	4.00	4.00	4.00	4.00	4.00	4.00	4.00	4.02
Al	0.29	0.35	0.53	0.31	0.29	0.71	0.10	0.37
Fe	0.26	0.26	0.28	0.20	0.18	0.25	0.18	0.15
Mg	0.02							
Ti	3.43	3.30	3.20	3.51	3.32	3.10	3.61	3.33
	4.00	3.91	4.01	4.02	3.79	4.06	3.89	3.85
Ca	3.84	3.93	3.94	3.69	4.07	3.85	3.89	4.02
Mn	0.02	0.02						
Na							0.02	
K	___	___	___	___	___	___	0.01	___
	3.86	3.95	3.94	3.69	4.07	3.85	3.92	4.02

Table 38.

Semiquantitative probe analyses of oxide minerals.

	Magnetite	Ilmenite	
No.	TiO_2	FeO*	TiO_2
30		47.4%	57.3%
50	1.85%	46.9%	55.8%
88b		47.3%	58.3%
139	0.21%	49.4%	57.8%
230	0.20%	53.6%	53.2%
280	0.18%	50.0%	54.8%
329	0.22%	49.1%	54.7%
330	0.25%	47.7%	54.5%

FeO* = Total iron expressed as FeO

Table 39.

Normative mineral proportions in the biotite-hornblende simplex. of biotite clinopyroxene gneisses.

No.	230	329	330	832a	835
Quartz	5.4	4.1	6.5	-2.5	10.7
Albite	18.9	24.2	20.6	5.6	15.5
Orthoclase	23.9	13.3	20.6	36.4	15.9
Anorthite	13.0	11.2	12.6	12.0	9.0
Biotite	-12.4	7.8	4.7	-9.3	2.7
Hornblende	44.0	35.9	29.7	54.1	44.3
Ilmenite	4.7	2.2	2.9	3.3	0.8
Magnetite	5.2	2.6	3.9	3.5	2.7
Sum	102.7	101.3	101.5	103.1	101.6

Table 40.

Normative mineral proportions in the biotite-hornblende simplex of biotite hornblende clinopyroxene gneisses.

No.	280a	1247
Quartz	10.4	3.5
Albite	24.9	14.8
Orthoclase	4.9	29.2
Anorthite	17.5	10.9
Biotite	14.8	2.9
Hornblende	23.3	35.2
Ilmenite	1.7	2.1
Magnetite	3.3	3.4
Sum	100.9	102.0

Table 41.

Normative mineral proportions in the biotite-hornblende simplex of pyribolites.

No.	50	88b	149b	743	798	809b
Quartz	4.0	6.9	2.5	6.2	10.5	5.6
Albite	24.0	31.8	20.7	9.3	25.1	20.7
Orthoclase	8.0	-3.1	0.9	2.2	3.4	-0.2
Anorthite	16.6	19.7	19.9	23.9	18.9	18.4
Biotite	-3.3	14.5	1.3	11.7	7.7	13.8
Hornblende	43.1	27.4	54.8	39.4	28.9	36.7
Ilmenite	3.5	1.7	0.1	2.6	3.2	2.1
Magnetite	3.7	1.7	-	5.9	2.9	3.8
Sum	99.6	100.6	100.2	101.2	100.6	100.9

Table 42.

Variation in composition of mafic minerals within one thin section.

Maximum.

	Na_2O	MgO	Al_2O_3	SiO_2	K_2O	CaO	TiO_2	FeO
Biotite		0.3%	0.2%	0.6%	0.3%		0.3%	0.3%
Hornblende	0.1%	0.3%	0.3%	0.9%	0.1%	0.3%	0.2%	0.7%
Clinopyroxene		0.3%		0.8%		0.6%		0.4%
Orthopyroxene		0.3%		0.5%		0.1%		0.5%
Sphene			0.2%	0.4%		0.3%	0.5%	0.1%

Mean

	Na_2O	MgO	Al_2O_3	SiO_2	K_2O	CaO	TiO_2	FeO
Biotite		0.1%	0.1%	0.3%	0.2%		0.2%	0.2%
Hornblende	<0.1%	0.1%	0.1%	0.4%	<0.1%	0.1%	0.1%	0.2%
Clinopyroxene		0.1%		0.4%		0.3%		0.3%
Orthopyroxene		0.1%		0.4%		0.1%		0.3%
Sphene			0.1%	0.2%		0.2%	0.3%	0.1%

The figures represent variations in absolute amounts of each of the elements.

Table 43.

REFERENCES.

Adams J.B. 1968: Differential solution of plagioclase in supercritical water. Am. Min., 53 pp 1603-1613.

Andersen B.G. 1960: Quaternary, Sørlandet. In Holtedahl O. (Editor). Geology of Norway. Norges Geologiske Undersøkelse, Oslo pp 403-409.

Andersen O. 1928: The genesis of some types of feldspars from granite pegmatites. Norsk Geol.Tids., 10 p 116.

Annersten H. 1968: A mineral chemical study of a metamorphosed iron formation in Northern Sweden. Lithos, 1 pp. 374-397.

Antun P. 1956: Géologie et petrologie des dolerites de la région d'Egersund. Ph.D. Thesis Univ. Liège.

Antun P. 1962: Soggendalite (C.F. Kolderup). A sporophitic dolerite. Norsk Geol. Tids., 42 pp 261-268.

Antun P. 1962: On some Noritic dykes from Ørsdalen. Norsk Geol. Tids., 42 pp 269-274.

Barth T.F.W. 1935: The large Pre-Cambrian intrusive bodies in the southern part of Norway. XVI internat. Geol. Congress Reports, Washington pp 297-310.

Barth T.F.W. 1945: Geological map of Western Sørland. Norsk Geol. Tids., 25 pp 1-10.

Barth T.F.W. 1956: Studies in gneiss and granite. I: Relation between temperature and the composition of the feldspars. II. the feldspar-equilibrium temperature in granitic rocks of the Pre-Cambrian of Southern Norway. Skrifter Norske Videnskaps-Akad, Oslo.1, Mat-Naturv. Kl., No.1.

Barth T.F.W. 1959: Principles of classification and norm calculations of metamorphic rocks. J. of Geol., 67 p 135.

Barth T.F.W. & Sons J.A. 1960: PreCambrian of Southern Norway. In Holtedahl O. (Editor) Geology of Norway. Norges Geologiske Undersøkelse, Oslo pp 6-62.

Barth T.F.W. & Reitan 1963: The PreCambrian of Norway. In Rankama K. (Editor) The PreCambrian, volume 1. Interscience Publishers pp 27-80.

Barth T.F.W. 1968: Additional data for the two-feldspar geothermometer. Lithos 1 pp 305-306.

Binns R.A. 1962: Metamorphic pyroxenes from the Broken Hill district, New South Wales. Min. Mag., 33 pp 320-338.

Borchert H. 1961: Zusammenhänge zwischen Lagerstättenbildung, Magmatismus und Geotektonik Geol. Runds. 50 pp 131-165.

Boyd F.R. & England J.L. 1960: Minerals of the mantle: aluminous enstatite. Rep. Geophys. Lab., Carneg. Instn. 59 p 49.

Broch O.A. 1964: Age determinations of Norwegian minerals and rocks up to March 1964. Norges Geol. Unders., 228 pp 84-113.

Buddington A.F. & Lindsley D.H. 1964: Iron-titanium oxide minerals and their synthetic equivalents. J. Petrol., 5 pp 310-357.

Bugge A. 1963: Norges Molybdenforekomster. Norges Geol. Unders., 217.

Bugge C. 1907: Lidt om molybden og molybdenforekomster i Norge. Tids f. kemi, farmaci og terapi, 16.

Carmichael I.S.E. 1967: The mineralogy and petrology of the volcanic rocks from the Leucite Hills, Wyoming. Contrib. Min. and Pet., 15 pp 24-66.

Carstens H. 1959: Comagmatic lamprophyres and diabases on the south coast of Norway. Beitr. Min. and Petrog., 6 p 299.

Chinner G.A. 1960: Pelitic gneisses with varying ferrous/ ferric ratios from Glen Clova, Angus, Scotland, J. of Petrol., 1 pp 178-217.

Christie O.H.J. 1959: Crystallisation experiments with alkali olivine basaltic glass from Egersund, Norsk Geol. Tids., 39 p 271.

Coombs D.S. and Wilkinson J.F.G. 1969: Lineages and fractionation trends in undersaturated volcanic rocks from the East Otago Province (New Zealand) and related rocks. J. of Petrol., 10 pp 440-501.

Dahl O. 1970: Octahedral titanium and aluminium in biotite. Lithos, 3 pp 161-166.

Davidson L.R. 1969: Fe^{++}-Mg^{++} distribution in coexisting metamorphic pyroxenes. Spec. Publs. Geol. Soc. Austr., 2 pp 333-339.

Deer W.A., Howie R.A. & Zussman M.A. 1962: Rock forming Minerals. Vols. 1,2,3 & 4. Longmans, Green & Co., Ltd., London.

DeVore G.W. 1955: The role of absorption in the fractionation and distribution of elements. J. of Geol. 63 pp 159-190.

Edwards A.B. 1954: Textures of the ore minerals. Australian Institute of Mining and Metallurgy. Melbourne.

Engel A.E.J. & Engel C. (1958, 1960) Progressive metamorphism and granitisation of the major paragneiss, northwest Adirondack Mountains, New York; pt. 1, Total rock; pt.2 Mineralogy. Geol. Soc. Am. Bull., 69 pp 1369-1413 & 71 pp 1-58.

Engel A.E.J. & Engel C. 1962a: Hornblendes formed during progressive metamorphism of amphibolites, northwest Adirondack Mountains, New York. Bull. Geol. Soc. Am., 73 pp 1499-1514.

Engel A.E.J. & Engel C. 1962b: Progressive metamorphism of amphibolite, northwest Adirondack Mountains, New York. Geol. Soc. Am. Petrologic Studies, Buddington Volume, pp 37-82.

Engel A.E.J.,Engel C.E. & Havens R.G. 1964: Mineralogy of amphibolite interlayers in the gneiss complex, N.W. Adirondack mountains, New York. J. of Geol., 72 pp 131-156.

Eskola P. 1939: Die metamorphen Gesteine. In Barth T.F.W. Correns C.W. & Eskola P., Die Entstehung der Gesteine. pp 263-407. Berlin.

Falkenberg O. 1915: Om molybdenmalmer. Deres forekomst, oppberedning, anvendelse o.s.v. Tids. f. Kemi, Farmaci og Terapi Nr., 1-4.

Falkenberg O. 1917: Om molybdenglans. Tids. f. Kemi, Farmaci og Terapi. Nr. 16.

Falkenberg O. 1920: Norske Molybdengruber. Tids. f. Bergv., Nr. 10.

Falkenberg O. 1936: Knabeheiens Molybdenfelter. Tids. f. Kjemi og Bergv. Nr. 3 & 4.

Falkum T. 1966: Geological investigations in the PreCambrian of southern Norway. 1. The complex of metasediments and migmatites at Tveit, Kristiansand. Norsk Geol. Tids., 46 pp 85-110.

Falkum T. 1967: Structural and Petrological investigations of the PreCambrian metamorphic and igneous charnockite and migmatite complex in the Flekkefjord area, southern Norway. Norges Geologiske Undersokelse. Nr. 242 pp 19-25.

Gammon J.B. 1966: Fahlbands in the PreCambrian of southern Norway. Econ Geol., 61 pp 174-188.

Greenwood H.J. 1967: The N-dimensional tie-line problem. Geochim. Cosmochim Acta, 31 pp 465-490.

Hagner A.F., Leung S.S. & Dennison J.M. 1965: Optical and chemical variations in minerals from a single rock specimen. Am. Min., 50 pp 341-355.

Hallimond A.F. 1943: On the graphical representation of the calciferous amphiboles. Am. Min., 28 pp 65-89.

Heier K. 1955: The Ørsdalen tungsten deposit. Norsk Geol. Tids., 35 pp 69-85.

Heier K. 1956: The geology of the Ørsdalen district, Rogaland, S. Norway. Norsk Geol. Tids., 36 pp 167-211.

Hey M.H. 1954: A new review of the chlorites. Min. Mag., 30 pp 277-292.

Himmelberg G.R. & Phinney W.M.C. 1967: Granulite-facies metamorphism, Granite Falls-Montevideo area, Minnesota. J. of Petrol., 8 pp 325-348.

Holland H.D. 1959: Some applications of thermochemical data to problems of ore deposits. 1. Stability relations among the oxides, sulphides, sulphates and carbonates of ore and gangue metals. Econ. Geol., 54 pp 184-233.

Holland J.G. & Brindle D.W. 1966: A self-consistent mass absorption correction for silicate analysis by X-ray fluorescence. Spectrochim. Acta, 22 pp 2083-2093.

Hollander N.B. 1970: Distribution of chemical elements among mineral phases in amphibolites and gneiss. Lithos, 3 pp 93-111.

Holtedahl O. 1960: Features of the geomorphology. In Holtedahl O. (Editor). Geology of Norway. Norges Geologiske Undersøkelse, Oslo pp 507-531.

Hounslow A.W. & Moore J.M. Jr. 1967: Chemical petrology of Grenville schists near Fernleigh, Ontario. J. of Petrol., 8 pp 1.28.

Howie R.A. & Smith J.V. 1966: X-ray emission microanalysis of rock forming minerals; v. Orthopyroxenes. J. of Geol., 74 pp 443-462.

Hunahashi M., Kim C.W., Ohta Y. & Tsuchiya T. 1968: Co-existence of plagioclases of different compositions in some plutonic and metamorphic rocks. Lithos, 1 pp 356-373.

Hutton C.O. 1938: On the nature of withamite from Glen Coe, Scotland. Min. Mag., 25 pp 119-124.

Härme M. 1965: On the K migmatites of south Finland. Bull. Comm. Geol. Finlande, 212 pp 1-43.

Jahns R.H. & Burham C.W. 1957: Preliminary results from experimental melting and crystallisation of the Harding pegmatite. Geol. Soc. Amer. Bull., 68 pp 1751-1752.

Keilhau B.M. 1838, 1844, 1850: Gaea Norvegica. Kristiania.

Kjerulf Th. 1879: Udsigt over det sydlige Norges geologi. Kristiania.

Korzhinskii D.S. 1959a: Physicochemical basis of the analysis of the paragenesis of minerals. Consultants Bureau, Inc. New York.

Korzhinskii D.S. 1959b: The advancing wave of acidic components in ascending solutions and hydrothermal acid-base differentiation. Geochim. Cosmochim. Acta, 17 p 17.

Kostyuk E.A. & Sobolev V.S. 1969: Paragenetic types of calciferous amphiboles of metamorphic rocks. Lithos, 2 pp 67-81.

Krauskopf K.B. 1967: Introduction to Geochemistry. McGraw-Hill, New York.

Kretz R. 1959: Chemical study of garnet, biotite and hornblende from gneisses of south-western Quebec, with emphasis on the distribution of elements in coexisting minerals. J. of Geol., 67 pp 371-402.

Kretz R. 1960: The distribution of certain elements among coexisting calcic pyroxenes, calcic amphiboles and biotites in skarns. Geochim. Cosmechim. Acta, 20 pp 161-191.

Kretz R. 1963: Distribution of magnesium and iron between orthopyroxene and calcic pyroxene in natural mineral assemblages. J. of Geol., 71 p 773.

Leake B.E. 1964: The chemical distinction between ortho- and para-amphibolites. J. of Petrol., 5 pp 238-254.

Leake B.E. 1965a: The relationship between composition of calciferous amphibole and grade of metamorphism. In Pitcher W.S. & Flinn G.W. (Editors). Controls of Metamorphism. Oliver and Boyd. Edinburgh.

Leake B.E. 1965b: The relationship between tetrahedral aluminium and the maximum possible octahedral aluminium in natural calciferous and subcalciferous amphiboles. Am. Min., 50 pp 843-851.

Leake B.E. et al. 1969: The chemical analysis of rock powders by automatic X-ray flourescence. Chem. Geol., 5 pp 7-86.

Leake R.C. 1968: The geology and tectonics of the area between Åseral and Sirdal, Vest Agder, Norway. (abstract) Geol. Fören. i Stockholm forhand. 90 p 463.

MacLean W.H. 1969: Liquidus phase relations in the FeS-FeO-Fe_3O_4-SiO_2 system, and their application in geology. Econ. Geol., 64 pp 865-884.

Magnusson N.H. 1965: The Pre-Cambrian history of Sweden. Quart. J. Geol. Soc. London, 121 pp 1-30.

Mehnert K.R. 1968: Migmatites and the origin of granitic rocks. Elsevier Amsterdam.

Michot J. 1961: The anorthosite-leuconorite para-anatectic and anatectic complex of Håland-Hellern. Norsk Geol. Tidsk. 41 p 157.

Michot J. & Posteels P. 1968: Étude géochronologique du domaine métamorphique du Sud-Ouest de la Norvège (Note preliminaire) Ann. Soc geol. Belgique, 91 pp 93-110.

Michot P. 1957: Phénomenes géologiques dans la catazone profonde. Geol. Rundschau, 46 pp 147-173.

Michot P. 1960: La géologie de la catazone; Le probleme des anorthosites, la palingenese basique et la tectonique catazonale dans le Rogaland méridional, Norvège méridionale. Geol. Congr. Norden Guide g (A.9).

Middlemost E. 1968: The granitic rocks of Farsund, South Norway, Norsk Geol. Tids 48 pp 81-99.

Morton R.D. & Carter N.L. 1963: Contributions to the mineralogy of Norway. no. 21. On the occurrence of Mn-poor Piemontite and Withamite in Norway. Norsk Geol. Tids. 43, pp 445-455.

Miyashiro A. & Seki Y. 1958: Enlargement of the composition field of epidote and piemontite with rising temperature. Am. Jour. Sci., 256 pp 423-430.

Neumann H. 1960: Apparent ages of Norwegian minerals and rocks. Norsk Geol. Tids. 40 p 173.

Nilssen B. 1967: Separation of perthitic microcline by heavy liquid fractionation - A too sensitive method ? Norsk Geol. Tids., 47 pp 149 - 157.

Oftedahl C. 1957: Studies on the igneous rock complex of the Oslo region. Origin of composite dikes. Norske Vid. Akad. Oslo Skr., Mat-Naturv. Kl., no. 2.

Ohta Y. 1966: The tectonics of the Kvinesheii region. Unpublished report Telemark Project.

Ohta Y. 1969: On the formation of augen structure. Lithos 2 pp 109-132.

Perry K. Jr. 1968: Representation of mineral chemical analyses in 11-dimenional space; part 2, amphiboles. Lithos 1, pp 307-321.

Phillips R. 1963: The recalculation of amphibole analyses. Min. Mag. 33 pp 701-711.

Phillips R. 1965: Amphibole compositional space. Min. Mag. 35, pp 945-952.

Poldervaart A. & Hess H.H. 1951: Pyroxenes in the crystallisation of basic magma. J. of Geol., 59 p 472.

Ramberg H. & DeVore G.W. 1951: The distribution of Fe^{2+} and Mg^{2+} in coexisting olivines and pyroxenes. J. of Geol., 59, pp 193-210.

Ribbe P.H. & Smith J.V. 1966: X-ray emission microanalysis of rock-forming minerals ; IV. plagioclase feldspars. J. of Geol., 74 pp 217-233.

San Miguel A. 1969: The aplite-pegmatite association and its petrogenetic interpretation. Lithos, 2 pp 25-37.

Saxena S.K. 1966: Distribution of elements between coexisting biotite and hornblende in metamorphic Caledonides lying to the west and north-west of Trondheim, Norway. N. Jb. Miner., Mb. 3 pp 67-80.

Saxena S.K. 1968: Chemical study of phase equilibria in charnockites, Varberg, Sweden. Am. Min., 53 pp 1674-1695.

Saxena S.K. 1969: A statistical approach to the study of phase equilibria in multicomponent systems. Lithos, 3 pp 25-36.

Schetelig J. 1937: De geologiske forhold i Knabeheia. Norsk Geol. Tids.

Shido F. 1958: Plutonic and metamorphic rocks of the Nakoso and Iritono districts in the central Abukuma plateau. J. Fac. Sci. Univ. Tokyo, sec. 2, 11 pp 131-217.

Shido F. & Miyashiro J. 1959: Hornblendes of basic metamorphic rocks. J. Fac. Sci. Univ. Tokyo, sec. 2, 12 pp 85-102.

Smith J.V. 1965: X-ray emission microanalysis of rock forming minerals; 1. Experimental techniques. J. of Geol., 73 pp 830-864.

Smith J.V. 1966: X-ray emission microanalysis of rock-forming minerals; VI. Clinopyroxenes near the diopside-hedenbergite join. J. of Geol., 74 pp 463-477.

Smith J.V. & Ribbe P.H. 1966: X-ray-emission microanalysis of rock-forming minerals; III. Alkali feldspars. J. of Geol., 74 pp 197-216.

Smithson S.B. 1962: Symmetry relations in alkali feldspars of some amphibolite facies rocks from the southern Norwegian PreCambrian. Norsk Geol. Tids., 42 pp 586-599.

Smithson S.B. & Barth T.F.W. 1967: The PreCambrian Holum granite, South Norway. Norsk Geol. Tids., 47 pp 21-56.

Storetvedt K.M. 1968: The permanent magnetism of some basic intrusions in the Kragerø archipelago, S. Norway, and its geological implications, Norsk Geol. Tids., 48 pp 153-163.

Storetvedt K.M. & Gidskehaug A. 1968: Palaeomagnetism and the origin of the Egersund dolerites, S. Norway, Norsk Geol. Tids., 48 pp 121-125.

Sundius N. 1946: The classification of the hornblendes and the solid solution relations in the amphibole group. Årsbok Sveriges Geol. Undersök., 40 no. 4.

Sweatman T.R. & Long J.V.P. 1969: Quantitative electron probe microanalysis of rock-forming minerals. J. of Petrol., 10 pp 332-379.

Thompson J.B. Jr. 1957: The graphical analysis of mineral assemblages in pelitic schists. Am. Min., 42 pp 842-859.

Thompson J.B. Jr. 1959: Local equilibrian in metasomatic processes. In Abelson P.H. (Editor) Researches in Geochemistry, New York. pp 427-457.

Tobi A.C. 1965: Fieldwork in the charnockitic PreCambrian of Rogaland (S.W. Norway). Geologie en Mijnbouw, 44 pp 208-217.

Touret J. 1967: Les gneiss oeilles de la région de Vegårsheii-Gjerstad (Norvège Méridionale). 1. Étude petrographique. Norsk Geol. Tids., 47 p 131-147.

Touret J. 1967b: Les gneiss oeilles de la région de Vegårsheii-Gjerstad (Norvège Méridionale) 11. L'indice de triclinisme des feldspaths potassique. Norsk Geol. Tids., 47 pp 275-281.

Turner F.J. 1948: Mineralogical and structural evolution of the metamorphic rocks. Geol. Soc. America Mem., 30.

Turner F.J. & Verhoogen J. 1960: Igneous and metamorphic petrology. McGraw-Hill, New York.

Turner F.J. 1968: Metamorphic Petrology. McGraw-Hill, New York.

Wegmann E. 1960: PreCambrian of southern Norway; introductory remarks on the structural relations. In Holtedahl O. (Editor) Geology of Norway. Norges Geologiske Undersøkelse, Oslo pp 6-8.

Wilson A.D. 1955: A new method for the determination of ferrous iron in rocks and minerals. Bull. Geol. Surv. U.K., 9 pp 56-58.

Winkler H.G.F. 1965: Petrogenesis of metamorphic rocks. Springer-Verlag, Berlin.

Winkler H.G.F: 1970 Abolition of metamorphic facies, introduction of the four divisions of metamorphic stage and of a classification based on isograds in common rocks. N. Jahrbh. f. Miner. Mh. pp 189-248.

Wones D.R. & Eugster H.P. 1965: Stability of biotite: Experiment, theory and application. Am. Min. 50 pp 1228-1272.

Zeppernick E. 1966: Geologische Feldbericht zur Flottorp. Unpublished report, Telemark Project.

Winkler H.G.F. & Platen H. von. 1961: Experimentelle Gesteinsmetamorphose-V. Experimentelle anatektische Schmelzen und ihre petrogenetische Bedeutung. Geochim. et Cosmoch. Acta. 24 p 250.

ACKNOWLEDGEMENTS

The author wishes to thank Professors T.F.W. Barth and H. Neuman, and K.C. Dunham and G.M. Brown for making facilities available for this work at the Geologisk-Mineralogisk Museum of the University of Oslo and the Department of Geology of the University of Durham respectively. Supervision and encouragement at different stages of the research by Konservator J.A. Dons, Professor K.C. Dunham and Dr. C.H. Emeleus is gratefully acknowledged. Dr. T. Falkum, Dr. Y. Otha and Professor F.M. Vokes are thanked for invaluable discussion during field work and Dr. J.W. Aucott for computer corrections of electron probe results. Financial support was provided by a N.A.T.O. Research Studentship at the University of Oslo and by N.E.R.C. at the University of Durham.

Key to Geological Map

R – R PROMINENT LINE OF RETROGRADE METAMORPHISM

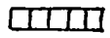
BASIC DYKES (IGNEOUS)


BASIC DYKES (METAMORPHIC)

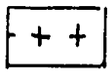
INTRUSIVE QUARTZ MONZONITE (FARSUNDITE TYPE)

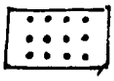
EQUIGRANULAR POORLY FOLIATED "GRANITE"


CONCORDANT COARSE PORPHYRITIC GNEISSIC "GRANITE"


LAYERED GNEISS WITH MUCH BASIC MATERIAL


PROMINENT PELITIC LAYERS WITHIN BASIC GNEISS

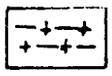
PROMINENT GRANITIC LAYERS WITHIN BASIC GNEISS

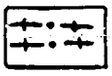
LAYERED BIOTITE FELDSPAR GNEISS

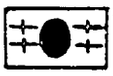
LAYERED BIOTITE FELDSPAR GNEISS INTERSPERSED WITH PORPHYRITIC GNEISSIC "GRANITE"

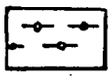
LAYERED FELSIC GNEISS


LAYERED FELSIC GNEISS WITH GARNET


MASSIVE PORPHYRITIC FELSIC GNEISS WITH SOME LAYERING

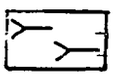
MASSIVE PORPHYRITIC FELSIC GNEISS


LARGE FELDSPAR AUGEN GNEISS


SMALL FELDSPAR AUGEN GNEISS


"GRANITIC" ROCKS ASSOCIATED WITH AUGEN GNEISS

Simplified Geological Section

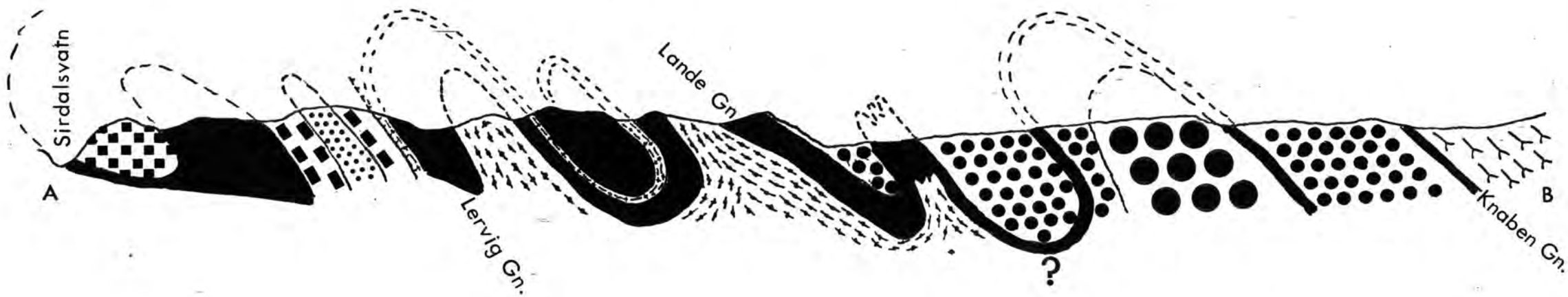

Scale 1;100,000

Plate 1.

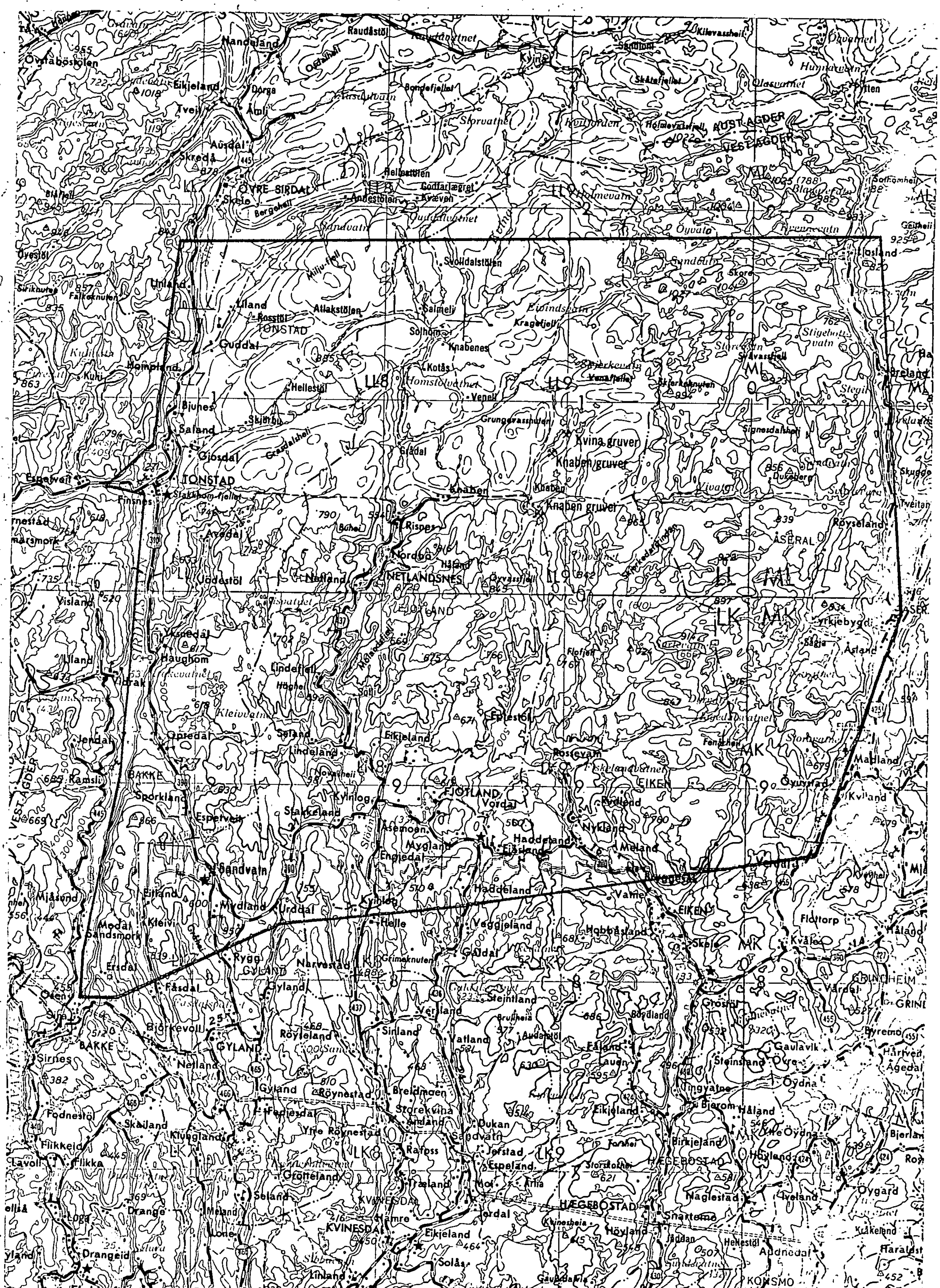

Topographical map, scale 1;250,000 with boundary

of area surveyed.